

T-3114

A CORRELATION FOR CARBON DIOXIDE
MINIMUM MISCIBILITY PRESSURE

by

Kenneth Lee Riedel

ARTHUR LAKES LIBRARY
COLORADO SCHOOL of MINES
GOLDEN, COLORADO 80401

ProQuest Number: 10782740

All rights reserved

INFORMATION TO ALL USERS

The quality of this reproduction is dependent upon the quality of the copy submitted.

In the unlikely event that the author did not send a complete manuscript and there are missing pages, these will be noted. Also, if material had to be removed, a note will indicate the deletion.



ProQuest 10782740

Published by ProQuest LLC (2018). Copyright of the Dissertation is held by the Author.

All rights reserved.

This work is protected against unauthorized copying under Title 17, United States Code
Microform Edition © ProQuest LLC.

ProQuest LLC.
789 East Eisenhower Parkway
P.O. Box 1346
Ann Arbor, MI 48106 – 1346


T-3114

A thesis submitted to the Faculty and the Board of Trustees of the Colorado School of Mines in partial fulfillment of the requirements for the degree of Master of Science (Petroleum Engineering)

Golden, Colorado

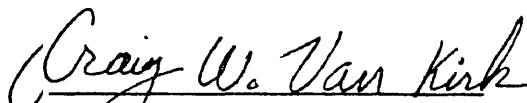
Date 11-15-85

Signed: 
Kenneth Lee Riedel

Approved: 
Dr. Fred H. Poettmann
Thesis Advisor

Golden, Colorado

Date November 20, 1985


Dr. Craig W. Van Kirk
Dr. Craig W. Van Kirk
Head of Department of
Petroleum Engineering

ABSTRACT

There is currently a high level of interest in carbon dioxide (CO₂) flooding as an enhanced oil recovery method. This is largely due to the fact that miscible displacement of reservoir fluids can be achieved by CO₂ injection. Carbon dioxide is not first contact miscible with crude oils at realistically attainable pressures. However, there is a certain minimum pressure level above which multicontact miscibility (also known as dynamic miscibility) can be developed. This pressure is known as the minimum miscibility pressure or MMP. In the design of a CO₂ flood or the screening of candidate reservoirs, it is important that the MMP be accurately known. This thesis presents a correlation for estimating CO₂ MMP which can be used with a standard crude analysis.

Carbon dioxide achieves miscibility by the in situ extraction of hydrocarbons. The pseudoternary diagram has been used to illustrate this process and define the conditions required for dynamic miscibility. In this study, a procedure is developed for calculating pseudoternary diagrams for CO₂-crude oil systems using the Peng-Robinson equation of state. The equation of state is calibrated to predict the phase behavior of four reservoir oils reported

in the literature, and pseudoternary diagrams are calculated at several temperatures and pressures. The miscibility conditions determined from these calculations are used to develop a correlation for MMP using the parameters, temperature, crude C₇₊ concentration, and the molecular weight of the C₆₋ and C₇₊ fractions.

A preliminary test of the correlation is performed by comparing the predicted MMP with the experimental MMP of 17 oils reported in the literature. The correlation appears to be sufficiently accurate to use as a guide for screening candidate reservoirs or designing lab tests. The correlation is also compared to two published correlations and the three are found to perform equally well.

TABLE OF CONTENTS

	<u>Page</u>
ABSTRACT	iii
LIST OF FIGURES	vii
LIST OF TABLES	xiii
ACKNOWLEDGEMENTS	xvi
INTRODUCTION	
Scope	1
Background	5
Approach	15
LITERATURE SURVEY	
Introduction	16
Phase Behavior	17
Measurement of Minimum Miscibility Pressure	39
Minimum Miscibility Pressure Correlations	51
Applications of Equations of State and Simulation	78
PREDICTING CARBON DIOXIDE-CRUDE OIL PHASE BEHAVIOR	
Introduction	90
Peng-Robinson Equation of State	91
Published Data	96
Characterizing Hydrocarbon Fractions	107
Binary Interaction Coefficients	115

	<u>Page</u>
Pseudocomponent Characterization of Reservoir Fluids	123
Comparison of Predicted and Experimental Data	137
PREDICTING MISCIBILITY CONDITIONS	
Introduction	144
Critical Point	145
Limiting Tie Line	157
Calculated Miscibility Conditions	164
DEVELOPMENT OF CORRELATION	188
ACCURACY OF CORRELATION	222
CONCLUSIONS	232
RECOMMENDATIONS	234
NOMENCLATURE	235
REFERENCES CITED	238
APPENDIX A - Sample Calculations	244
APPENDIX B - Summary of EOS Calculations	260

LIST OF FIGURES

<u>Figure</u>		<u>Page</u>
1	Effect of Capillary Number on Residual Oil Saturation	2
2	Displacement of a West Texas Oil from a Sandstone Core by CO ₂	4
3	Hypothetical Pseudoternary Diagram for a CO ₂ -Crude Oil System	6
4	Pressure-Composition Diagram for a CO ₂ -Crude Oil System	9
5	Phase Behavior of a Ternary Mixture Containing CO ₂	10
6	Pseudoternary Diagram for a CO ₂ -Crude Oil System	12
7	Hypothetical Phase Diagrams for Type I Phase Behavior	19
8	Hypothetical Phase Diagrams for Type IIa Phase Behavior	20
9	Hypothetical Phase Diagrams for Type IIb Phase Behavior	23
10	Slim Tube Apparatus Proposed by Yellig and Metcalfe	40
11	Slim Tube Data for CO ₂ Displacement Tests Yellig and Metcalfe	43
12	Effect of Pressure on Oil Recovery by CO ₂	47
13	Measurement of MMP with Rising Bubble Apparatus	48
14	Pseudoternary Illustration of Condensing Gas Drive Mechanism	52

<u>Figure</u>	<u>Page</u>
15	Example of Condensing Gas Drive Miscibility Correlation of Benham et al. 56
16	Example of Condensing Gas Drive MMP Correlation from Data of Benham et al. 57
17	CO ₂ MMP Correlation of Holm and Josendal as Extended by Mungan 59
18	CO ₂ MMP Correlation of Yellig and Metcalfe . . 62
19	CO ₂ MMP Correlation of Holm and Josendal . . . 65
20	CO ₂ MMP Correlation of Alston et al. 69
21	Hydrocarbon Partitioning Coefficient Data of Silva et al. 72
22	CO ₂ MMP Correlation of Enick et al. 75
23	Pseudoternary Diagram Construction Method of Wu et al. 81
24	Determination of MMP from Extrapolation of K-values 84
25	Relationship Between CO ₂ -Hydrocarbon Binary Interaction Coefficients and Hydrocarbon Molecular Weight 118
26	Relationship Between Methane-Hydrocarbon Binary Interaction Coefficients and Hydrocarbon Molecular Weight 120
27	Proportionality Variable S for Determining Intermediate Hydrocarbon Binary Interaction Coefficients 122
28	Predicted Saturation Boundaries and Experimental Bubble Point Data: Maljamar Crude 90°F 129
29	Pressure-Composition Diagram Showing Predicted Isovol Curves and Experimental Volumetric Data: Ford Geraldine Crude 83°F . 138

<u>Figure</u>	<u>Page</u>
30	Pressure-Composition Diagram Showing Predicted Isovol Curves and Experimental Volumetric Data: West Sussex Crude 94°F . . . 139
31	Pressure-Composition Diagram Showing Predicted Isovol Curves and Experimental Volumetric Data: Maljamar Crude 90°F 140
32	Pressure-Composition Diagram Showing Predicted Isovol Curves and Experimental Volumetric Data: Reservoir D Crude 220°F . . . 141
33	Tie Lines Calculated for Ford Geraldine System at 150°F 1500 psia 149
34	Tie Lines Calculated for Ford Geraldine System at 150°F 2500 psia 151
35	Pseudoternary Diagram Shown as a Right Triangle Illustrating Method of Calculating Tie Lines 158
36	Calculated Pseudoternary Diagram for Ford Geraldine System 150°F 2534.9 psia 172
37	Calculated Pseudoternary Diagram for Ford Geraldine System 200°F 2681.3 psia 173
38	Calculated Pseudoternary Diagram for West Sussex System 200°F 3170.5 psia 174
39	Calculated Pseudoternary Diagram for West Sussex System 250°F 3625.3 psia 175
40	Calculated Pseudoternary Diagram for Maljamar System 100°F 3782.9 psia 176
41	Calculated Pseudoternary Diagram for Maljamar System 250°F 4646.5 psia 177
42	Calculated Pseudoternary Diagram for Reservoir D System 100°F 3931.3 psia 178
43	Calculated Pseudoternary Diagram for Reservoir D System 200°F 3897.7 psia 179

<u>Figure</u>	<u>Page</u>
44	MMC Data Calculated for the Ford Geraldine System at 150°F 2534.9 psia 180
45	MMC Data Calculated for the Ford Geraldine System at 200°F 2681.3 psia 181
46	MMC Data Calculated for the West Sussex System at 200°F 3170.5 psia 182
47	MMC Data Calculated for the West Sussex System at 250°F 3625.3 psia 183
48	MMC Data Calculated for the Maljamar System at 100°F 3782.9 psia 184
49	MMC Data Calculated for the Maljamar System at 250°F 4646.5 psia 185
50	MMC Data Calculated for the Reservoir D System at 100°F 3931.3 psia 186
51	MMC Data Calculated for the Reservoir D System at 200°F 3897.7 psia 187
52	Calculated Pseudoternary Diagram for West Sussex System at 100°F 2859.9 psia 189
53	Calculated Pseudoternary Diagram for West Sussex System at 100°F 2134.1 psia 190
54	Calculated Pseudoternary Diagram for West Sussex System at 100°F 1817.0 psia 191
55	Calculated Miscibility Conditions at 100°F for Ford Geraldine, West Sussex, Maljamar, and Reservoir D Systems 194
56	Calculated Miscibility Conditions at 150°F for Ford Geraldine, West Sussex, Maljamar, and Reservoir D Systems 195
57	Calculated Miscibility Conditions at 200°F for Ford Geraldine, West Sussex, Maljamar, and Reservoir D Systems 196

<u>Figure</u>	<u>Page</u>
58	Calculated Miscibility Conditions at 250°F for Ford Geraldine, West Sussex, Maljamar, and Reservoir D Systems 197
59	Calculated Miscibility Conditions for Ford Geraldine System at 100, 150, 200, 250°F . . . 198
60	Calculated Miscibility Conditions for West Sussex System at 100, 150, 200, 250°F. 199
61	Calculated Miscibility Conditions for Maljamar System at 100, 150, 200, 250°F 200
62	Calculated Miscibility Conditions for Reservoir D System at 100, 150, 200, 250°F . . 201
63	Relationship Between MMP and Crude Molecular Weight Ratio at 100°F 202
64	Relationship Between MMP and Crude Molecular Weight Ratio at 150°F 203
65	Relationship Between MMP and Crude Molecular Weight Ratio at 200°F 204
66	Relationship Between MMP and Crude Molecular Weight Ratio at 250°F 205
67	CO ₂ MMP Correlation: Crude C ₆ - MW= 30 Temperature= 100°F 210
68	CO ₂ MMP Correlation: Crude C ₆ - MW= 40 Temperature= 100°F 211
69	CO ₂ MMP Correlation: Crude C ₆ - MW= 50 Temperature= 100°F 212
70	CO ₂ MMP Correlation: Crude C ₆ - MW= 30 Temperature= 150°F 213
71	CO ₂ MMP Correlation: Crude C ₆ - MW= 40 Temperature= 150°F 214
72	CO ₂ MMP Correlation: Crude C ₆ - MW= 50 Temperature= 150°F 215

<u>Figure</u>	<u>Page</u>
73	CO ₂ MMP Correlation: Crude C ₆ - MW= 30 Temperature= 200°F 216
74	CO ₂ MMP Correlation: Crude C ₆ - MW= 40 Temperature= 200°F 217
75	CO ₂ MMP Correlation: Crude C ₆ - MW= 50 Temperature= 200°F 218
76	CO ₂ MMP Correlation: Crude C ₆ - MW= 30 Temperature= 250°F 219
77	CO ₂ MMP Correlation: Crude C ₆ - MW= 40 Temperature= 250°F 220
78	CO ₂ MMP Correlation: Crude C ₆ - MW= 50 Temperature= 250°F 221
79	Accuracy of Proposed Correlation for Predicting CO ₂ MMP of Group A and Group B Oils 224
80	Accuracy of Proposed Correlation for Predicting CO ₂ MMP of Group A Oils 227
81	Accuracy of Aslton et al. Correlation for Predicting CO ₂ MMP of Group A Oils 228
82	Accuracy of Holm and Josendal Correlation for Predicting CO ₂ MMP of Group A Oils 229
A-1	Predicted Saturation Boundary: Ford Geraldine System IOC= 70/30 Temperature= 150°F 246

LIST OF TABLES

<u>Table</u>	<u>Page</u>
1	Summary of GC/MS Data for Recombined Reservoir Fluid: Ford Geraldine Crude 98
2	Summary of GC/MS Data for Recombined Reservoir Fluid: West Sussex Crude 99
3	Summary of GC/MS Data for Recombined Reservoir Fluid: Maljamar Crude 100
4	Summary of GC/MS Data for Recombined Reservoir Fluid: Reservoir D Crude 101
5	Pressure versus Volume Fraction Heavier Phase and Carbon Dioxide Content: Ford Geraldine Crude 83°F 103
6	Pressure versus Volume Fraction Heavier Phase and Carbon Dioxide Content: West Sussex Crude 94°F 104
7	Pressure versus Volume Fraction Heavier Phase and Carbon Dioxide Content: Maljamar Crude 90°F 105
8	Saturation Pressure versus Carbon Dioxide Content: Reservoir D Crude 220°F 106
9	Properties of Single Carbon Number Groups: Ford Geraldine Crude 111
10	Properties of Single Carbon Number Groups: West Sussex Crude 112
11	Properties of Single Carbon Number Groups: Maljamar Crude 113
12	Properties of Single Carbon Number Groups: Reservoir D Crude 114
13	Pseudocomponent Grouping Schemes for Ford Geraldine, West Sussex, and Reservoir D Crudes 127

<u>Table</u>	<u>Page</u>
14 Pseudocomponent Grouping Schemes for Maljamar Crude	128
15 Binary Interaction Coefficients Used in Cases C and D for Maljamar Crude	132
16 Peng-Robinson Equation of State Input Parameters for Ford Geraldine Crude	133
17 Peng-Robinson Equation of State Input Parameters for West Sussex Crude	134
18 Peng-Robinson Equation of State Input Parameters for Maljamar Crude	135
19 Peng-Robinson Equation of State Input Parameters for Reservoir D Crude	136
20 Summary of Calculated Miscibility Conditions for Ford Geraldine System	168
21 Summary of Calculated Miscibility Conditions for West Sussex System.	169
22 Summary of Calculated Miscibility Conditions for Maljamar System	170
23 Summary of Calculated Miscibility Conditions for Reservoir D System.	171
24 Molecular Weight of C ₆₋ and C ₇₊ Fractions and Molecular Weight Ratio of Original Reservoir Fluids	206
25 Critical Temperature and Pressure of Pseudobinary Mixtures of Crude C ₆₋ Fractions With CO ₂	208
26 Properties of Literature Oils and Experimental and Predicted CO ₂ MMP	223
27 Comparison of Accuracy of Proposed Correlation with Correlations of Alston et al. and Holm and Josendal for Group A Oils	226

<u>Table</u>		<u>Page</u>
A-1	Pseudoternary Composition of Mixtures Flashed to define Tie Lines	252
A-2	Tie Line Slopes and Calculated MMC	259

ACKNOWLEDGEMENTS

Many people have been instrumental in the completion of this work. I would like to express my gratitude to Dr. Fred Poettmann for his enthusiasm and assistance throughout the research. I also thank Dr. Ramona Graves, Dr. Dendy Sloan, and Dr. John Wright for serving on my thesis committee, and Dr. Craig Van Kirk for making the software and computer facilities available.

Special thanks are due to my parents for their support and encouragement during my stay at Mines.

INTRODUCTION

Scope

Carbon dioxide flooding is rapidly becoming one of the most attractive enhanced oil recovery techniques. Carbon dioxide increases oil recovery by several mechanisms, including swelling of the crude oil and reducing the viscosity of the oil. Most importantly, however, miscible displacement of crude oil can be achieved by CO₂ injection at pressures above a certain level known as the minimum miscibility pressure (MMP).

When oil is immiscibly displaced in a porous medium, a certain amount of oil is retained behind the flood front. It has long been recognized that the amount of oil retained (the residual oil saturation) is affected by the interfacial tension between the oil and the displacing fluid. Figure 1 from Stalkup⁽¹⁾ illustrates this effect by showing the relationship between capillary number--the product of the Darcy velocity of the displacement front and oil viscosity divided by interfacial tension--and residual oil saturation.

Two fluids are miscible when they can be combined in any proportion and only a single phase results. As there are no interfaces between the fluids there is no interfacial

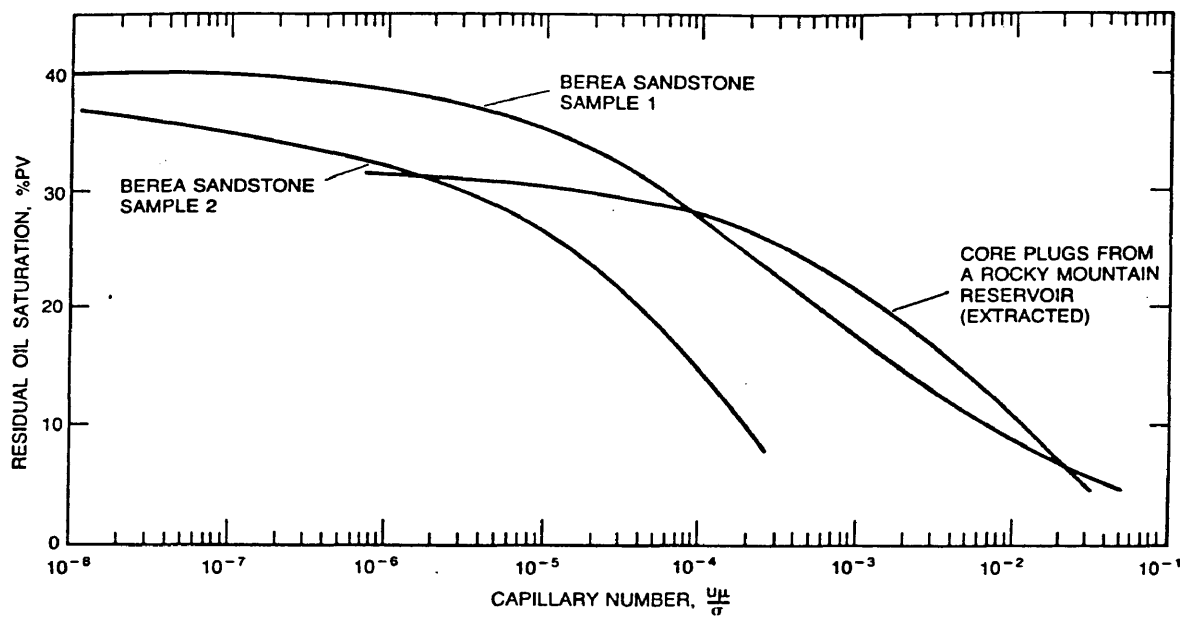


Figure 1. Effect of Capillary Number on Residual Oil Saturation (After Stalkup(1))

tension. As can be seen in Figure 1, if oil is displaced by a completely miscible fluid, corresponding to an infinite capillary number, residual oil saturation is minimized.

In the design of a CO₂ injection project or the screening of candidate reservoirs it is important that the minimum miscibility pressure be accurately known for two reasons. First, the minimum miscibility pressure must be attainable in the reservoir; operation at a lower pressure results in considerably lower oil recovery. Secondly, operation of the project above the minimum miscibility does not result in significantly higher oil recovery but project economics can be adversely affected by higher compression and equipment costs. The effect of pressure on oil recovery above and below the minimum miscibility pressure is illustrated in Figure 2.

Several correlations for estimating CO₂ minimum miscibility pressure have been proposed. Many are highly empirical and most do not fully account for the effect of oil composition and character on MMP. The purpose of this study is to develop an accurate correlation for MMP based on the phase behavior of CO₂-reservoir oil systems as predicted by the Peng-Robinson Equation of State⁽³⁾.

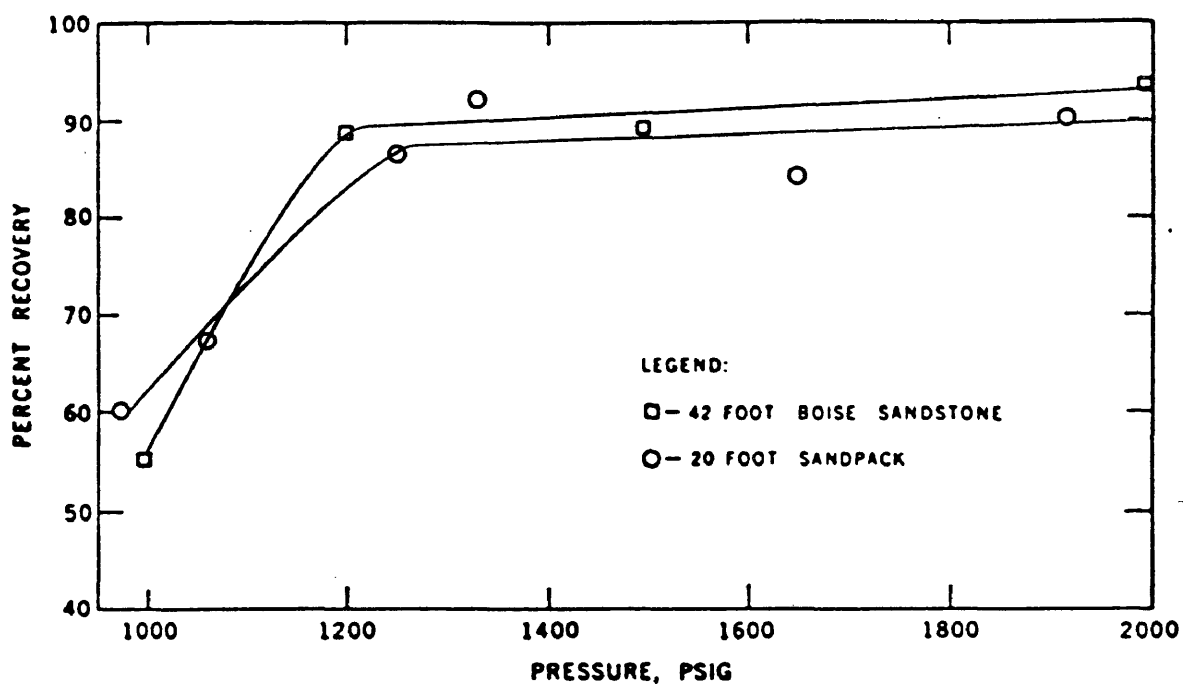


Figure 2. Displacement of a West Texas Oil from a Sandstone Core by CO₂ (After Stalkup⁽²⁾)

Background

Considerable research has recently been directed at the phase behavior relationships of CO₂ and crude oil. Significant works are covered in detail in the next section of this report. At this point, the concepts and methods of representing phase behavior which form the basis of the model used in this study are introduced.

The phase relations of mixtures of three pure components at constant temperature and pressure can be shown exactly on a triangular or ternary diagram. For multicomponent mixtures such as CO₂ with crude oil, the phase behavior can be represented approximately by grouping the components into three pseudocomponents. The diagram is then referred to as a pseudoternary diagram⁽¹⁾. Figure 3 shows a pseudoternary diagram where the crude oil is split into two pseudocomponents; one composed of methane through hexane (C₆₋), and the other composed of heptanes plus (C₇₊). The third component is pure CO₂. Each corner of the diagram corresponds to 100 percent of a given component and the side opposite represents zero percent of that component. Component concentrations between zero and 100 percent lie a proportionate distance between the corner and opposite side. By specifying the concentration of each component, mixtures can be shown on the diagram by a single point.

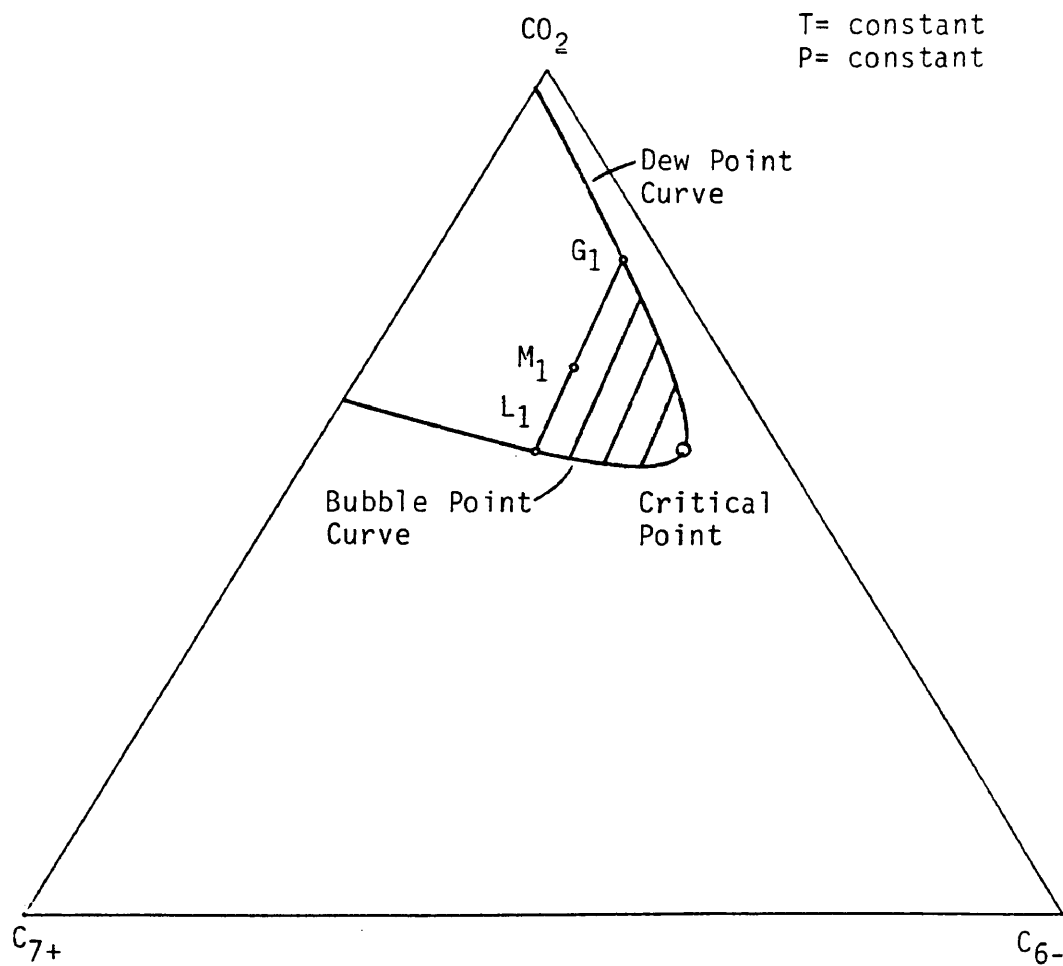


Figure 3. Hypothetical Pseudoternary Diagram for CO₂-Crude Oil System

The phase envelope shown in Figure 3 is made up of the bubble point curve which connects all saturated liquid compositions and the dew point curve which connects all saturated vapor compositions. The two curves meet at the critical point or plait point where the composition and intrinsic properties of the vapor and liquid are identical. All mixtures within the phase envelope form two phases. At the temperature and pressure of the diagram, mixture M_1 would form a liquid of composition L_1 in equilibrium with a gas of composition G_1 . The lines connecting the equilibrium gas and liquid compositions are known as tie lines. All mixtures outside the phase envelope form only one phase. The size of the two phase region is influenced by temperature and pressure. The phase envelope is made larger by an increase in temperature or a decrease in pressure.

It is important to note that the compositions of all possible mixtures of two fluids lie on a line connecting the compositions of the two fluids. This line is sometimes referred to as a dilution line.

Phase relations of reservoir oil and injection fluid at constant temperature can also be shown on pressure-composition (P-X) diagrams. Saturation pressure is plotted against mixture composition expressed as the mole percent of

injection gas in the reservoir fluid. A P-X diagram for CO₂ and crude reported by Simon et al⁽⁴⁾ is shown in Figure 4. A critical point exists where the bubble point curve meets the dewpoint curve. Only a portion of the retrograde dewpoint curve is shown here but the two-phase region is well defined. Lines connecting points of constant volume percent liquid (isovol lines) are shown in this region. Above the phase boundary, mixtures are single phase.

The relationship between ternary diagrams and P-X diagrams can be seen in Figure 5 from Orr and Jensen⁽⁵⁾ which is for a true ternary system. The triangular solid contains all possible mixtures of the three components at constant temperature and over a range of pressures. It can be seen that ternary diagrams are merely horizontal, constant pressure slices through the solid. P-X diagrams are vertical slices along the dilution line connecting pure CO₂ and mixtures of the hydrocarbon components.

For CO₂ to be miscible with a reservoir oil on first contact, all mixtures of CO₂ and oil must be single phase at reservoir temperature. This requires that the dilution line connecting pure CO₂ and the oil on a pseudoternary diagram lie only in the single phase region. For this to be true, the pressure must be above the cricondenbar or maximum

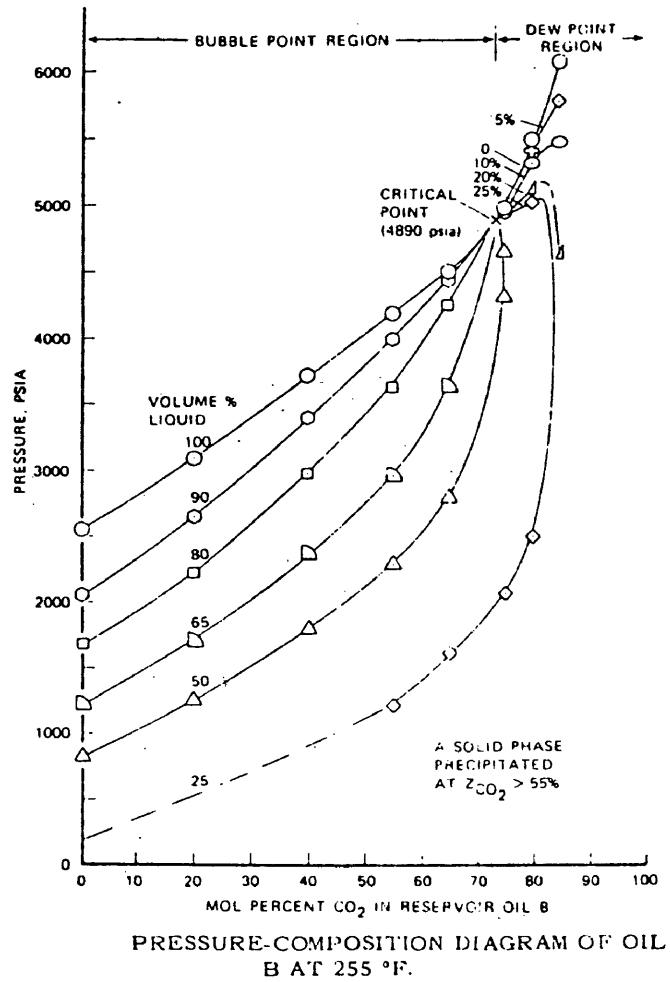


Figure 4. Pressure-Composition Diagram for CO₂-Crude Oil System (After Simon et al. (4))

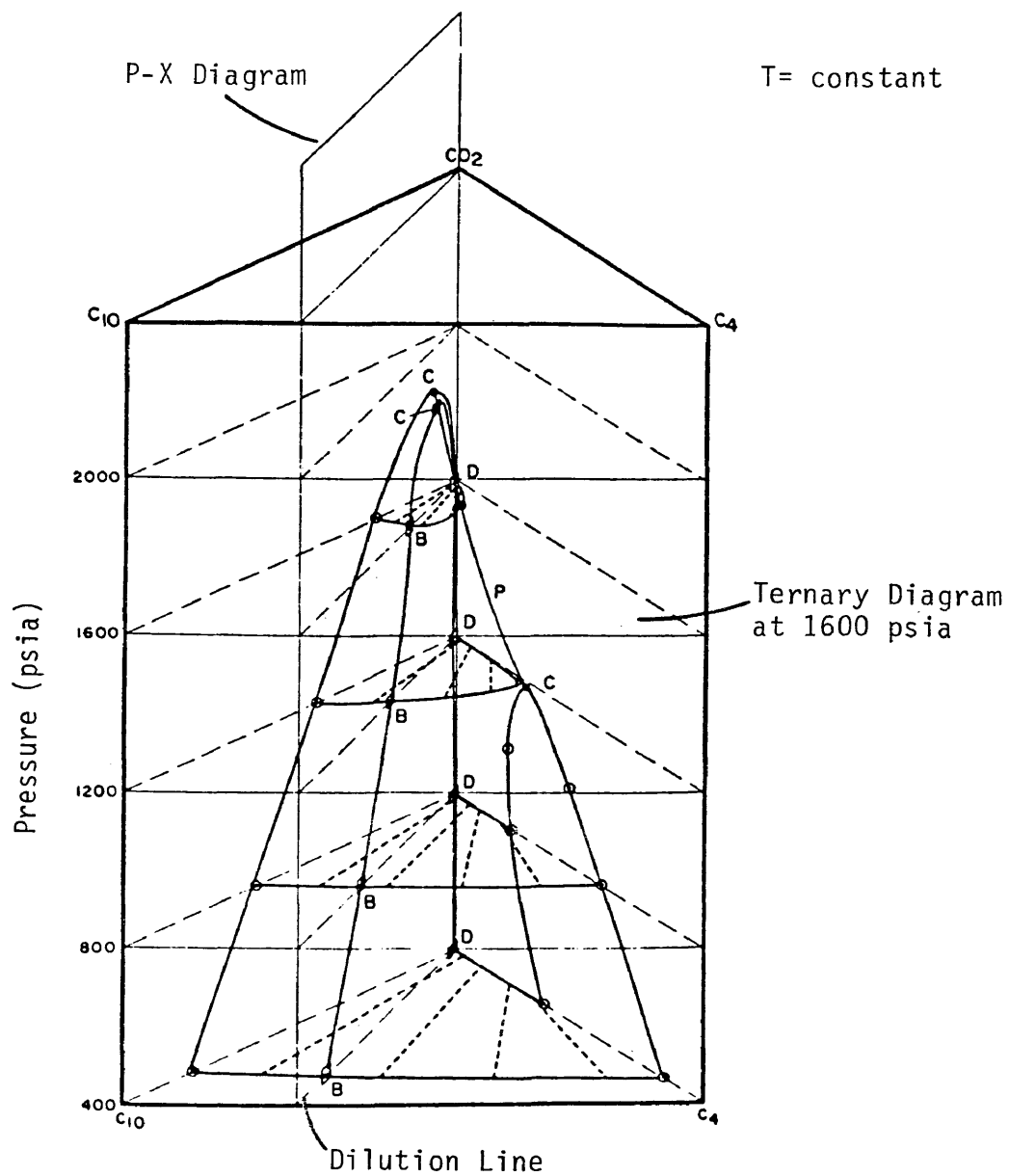


Figure 5. Phase Behavior of a Ternary Mixture Containing CO₂ (After Orr and Jensen⁽⁵⁾)

pressure for multiphase behavior on the P-X diagram. This pressure is too high for practical application. (It is not known if the P-X diagram cricondenbar has actually been measured for a CO₂-crude system. Figure 4, where two-phase behavior is observed above 6000 psia, is typical of the data reported in the literature.) However, by in-situ vaporization of hydrocarbon components by the CO₂, dynamic or multicontact miscibility can be achieved at much lower pressures. This process is known as vaporizing gas drive or high pressure gas drive and was originally illustrated on the pseudoternary diagram by Hutchinson and Braun(6).

Consider a porous medium saturated with Reservoir Oil A whose composition lies on the extension of the limiting tie line through the critical point in Figure 6. This oil is not first contact miscible with injected CO₂ so oil is immiscibly displaced, leaving some oil behind the displacement front in contact with CO₂. Suppose the proportions of CO₂ and residual oil are such that mixture M₁ results. As this mixture is in the two phase region, it separates into a liquid phase L₁ and a gaseous phase G₁ whose compositions are connected by the tie line passing through M₁. Injection of more CO₂ displaces the hydrocarbon enriched gas G₁ further into the reservoir

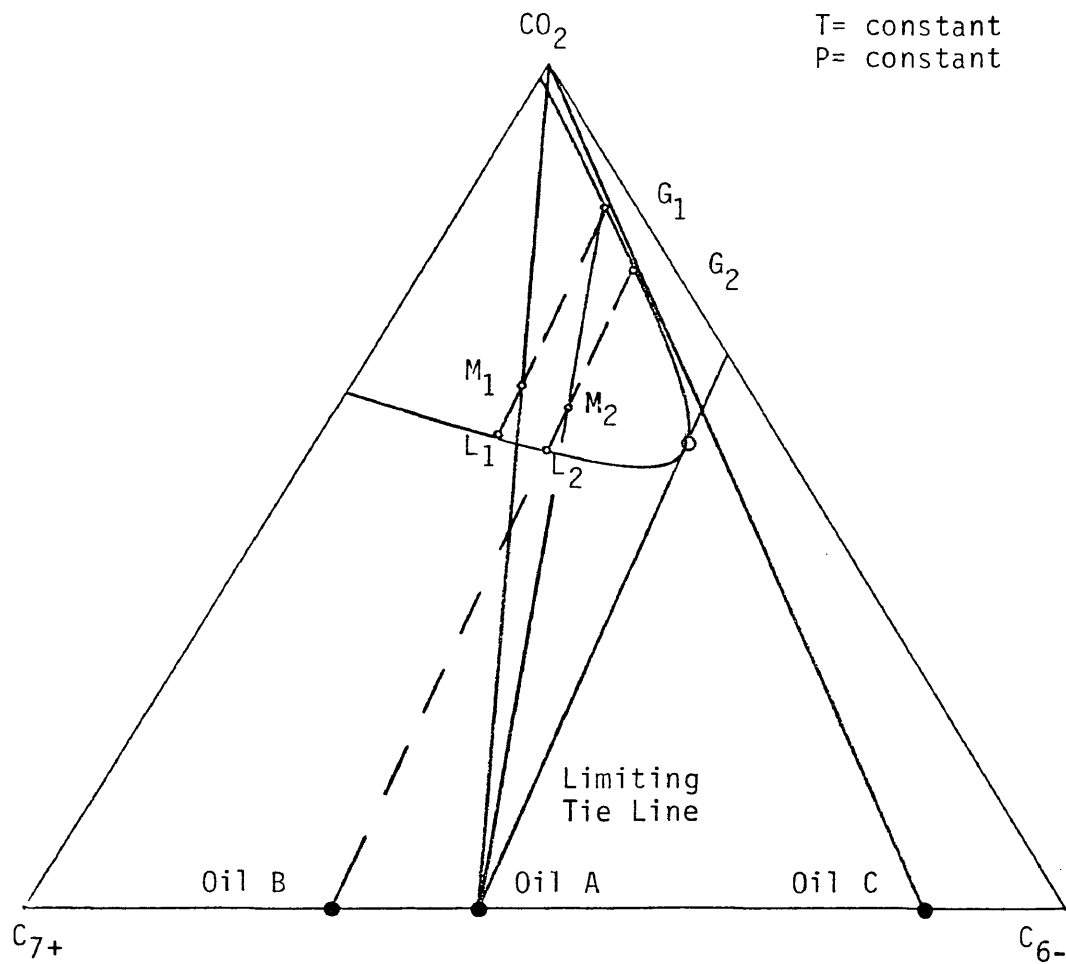


Figure 6. Pseudoternary Diagram for CO₂-Crude Oil System

where it contacts fresh reservoir oil resulting in mixture M_2 which separates into liquid L_2 and gas G_2 . Further injection displaces gas G_2 which contacts fresh reservoir oil and the process is repeated. As the gas at the displacing front continues to be enriched with hydrocarbons, its composition moves along the dewpoint curve until the critical point composition is reached. This fluid is directly miscible with the reservoir oil. It is evident from Figure 6 that for any oil composition between Oil C (which is miscible with CO_2 on first contact) and Oil A, multicontact or dynamic miscibility can be achieved by the vaporizing gas drive process. This is not true for oil compositions to the left of Oil A. With Reservoir Oil B, enrichment cannot proceed past the point of G_2 , as any further contact of Oil B by G_2 would result in mixtures which lie on the tie line connecting G_2 and L_2 . The important items to note are:

1. For Reservoir Oil A, which lies on the extension of the limiting tie line through the critical point on the pseudoternary diagram, the pressure of the diagram is the minimum miscibility pressure or the lowest pressure at which CO_2 can achieve dynamic miscibility with that oil.

2. The concentration of the heavy pseudocomponent (C_{7+}) in Reservoir Oil A is the maximum miscibility composition. This is the highest C_{7+} concentration an oil composed of the two pseudocomponents can have and still achieve dynamic miscibility with CO_2 at the pressure and temperature of the pseudoternary diagram.

The pseudoternary representation for multicomponent systems is not exact. Individual components within a pseudocomponent group have different volatilities and will not be distributed the same way in that group in the gas and liquid phases⁽⁶⁾. Thus, the composition and properties of the pseudocomponent are not the same for all mixtures. Also, the vaporizing gas drive process is a continuous process rather than the multiple-contact batch process described. Hutchinson and Braun⁽⁶⁾ showed that the position of the phase boundary and the slope of the tie lines determined in batch contacts may be different than those determined in flow experiments. Despite the simplifications of the pseudoternary model, it describes the essential phase behavior relating to the CO_2 miscible process and is very useful in studying the effect of such parameters as oil composition and character and temperature.

Approach

In this study, the Peng-Robinson Equation of State⁽³⁾ is calibrated to match published phase behavior data for four crude oils with CO₂ by adjusting pseudocomponent groupings and binary interaction coefficients. Pseudoternary diagrams are generated at several temperatures and pressures with each CO₂-crude system to determine the minimum miscibility pressure and maximum miscibility composition. Minimum miscibility pressure is then correlated as a function of temperature, crude composition in terms of the C₇₊ concentration, and the molecular weight of the C₆₋ and C₇₊ fractions. The accuracy of the proposed correlation is tested and compared to other published correlations.

LITERATURE SURVEY

Introduction

The published material examined in this section is grouped into four subject areas. The first deals with CO₂-crude oil phase behavior, which can be more complicated than was alluded to in the previous section. A discussion of the different types of phase behavior and the factors which lead to their occurrence is presented. Significant works related to the effects of phase behavior and oil composition on the CO₂ miscible process are also discussed. The second section covers the laboratory measurement of minimum miscibility pressure. In the third section, the correlations which are available for predicting minimum miscibility pressure are examined. The last section covers applications of equations of state and numerical simulation towards predicting the conditions required for both hydrocarbon and CO₂ miscibility.

Phase Behavior

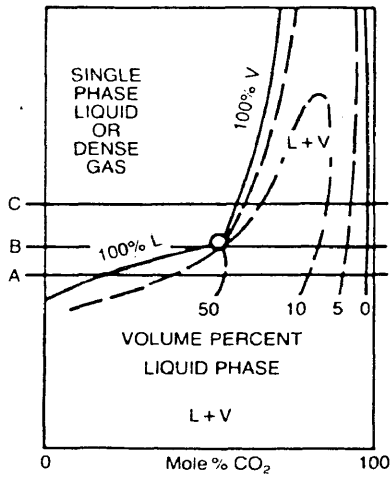
The use of carbon dioxide to increase oil recovery has been studied by the petroleum industry since the early 1950's. The first mechanisms to be recognized by which CO₂ improves recovery were the reduction of oil viscosity and swelling of the oil. In 1959, Holm⁽⁷⁾ reported the potential for miscible displacement by CO₂. It was reasonably assumed that the CO₂ miscible process is greatly affected by phase behavior and extensive research has been done in this area recently. The complex phase behavior of CO₂-crude oil systems is now largely understood.

The phase behavior of CO₂ with crude oil can be classified into two types based on characteristics of the pressure-composition diagram. Type I systems show only liquid and vapor phases existing in the multiphase region of the P-X diagram. Within the multiphase region of Type II systems, there is a region of liquid-vapor separation as well as a region where two equilibrium liquids exist and a region where two liquids and a vapor are in equilibrium. In both Type I and Type II systems a small amount of asphaltine precipitate may form at high CO₂ concentrations. A concise explanation of the two types of CO₂-crude oil phase behavior is presented in Section 2.7 of Stalkup⁽¹⁾ from which some of the following material is adapted.

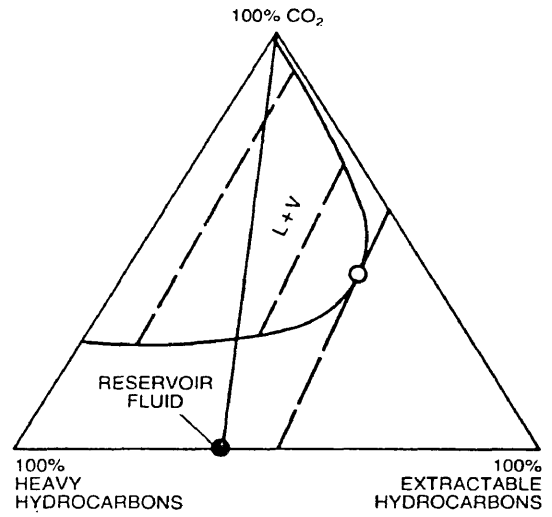
Conceptual P-X and pseudoternary diagrams showing Type I behavior appear in Figure 7. Metcalfe and Yarborough⁽⁸⁾ and Orr, Yu, and Lien⁽⁹⁾ suggest that this type of behavior occurs in systems above approximately 120°F. The bubble point curve joins the dewpoint curve at a vapor-liquid critical point on the P-X diagram and isovol lines show retrograde behavior in the dewpoint region. It is evident from Figures 7b,c,d that as pressure increases, the two-phase region of the pseudoternary diagram becomes smaller. Type I behavior has been documented by other authors^(4,10).

Type II phase behavior occurs in systems below approximately 120°F. The actual temperature for transition from Type I to Type II behavior appears to be related to the composition of the oil. The maximum temperature for Type II behavior can be expected to increase as the average molecular weight of the oil increases⁽⁹⁾. Based upon distinct features of the P-X diagrams, Stalkup⁽¹⁾ has broken Type II systems into three subtypes which he designated Type IIa, IIb, and IIc.

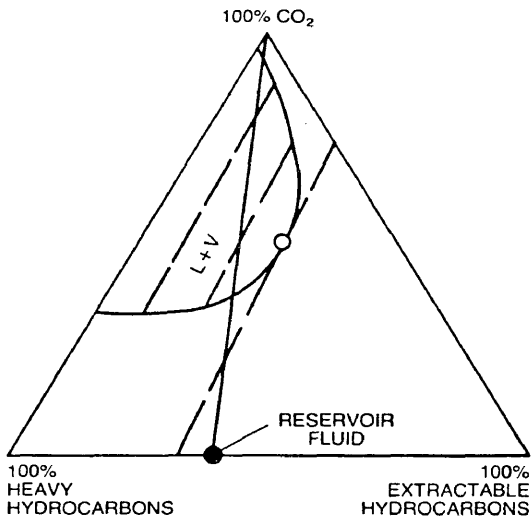
Figure 8 shows hypothetical P-X and pseudoternary diagrams for Type IIa phase behavior. Three phases are shown to exist in the multiphase region: an oil-rich liquid designated LL since it is usually the more dense lower



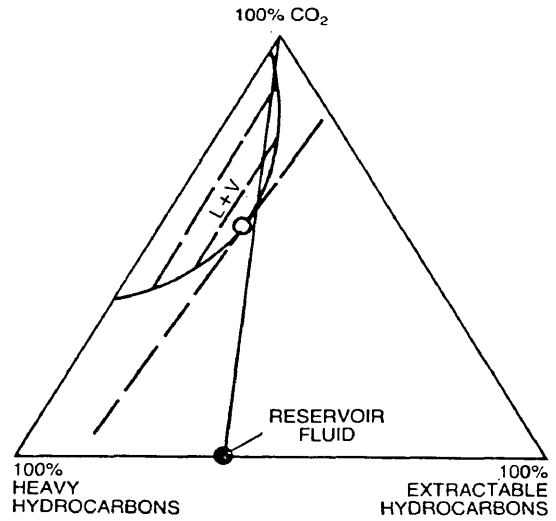
a) PRESSURE-COMPOSITION DIAGRAM



b) PSEUDO TERNARY DIAGRAM AT PRESSURE A



c) PSEUDO TERNARY DIAGRAM AT PRESSURE B



d) PSEUDO TERNARY DIAGRAM AT PRESSURE C

Figure 7. Hypothetical Phase Diagrams for Type I Phase Behavior (After Stalkup⁽¹⁾)

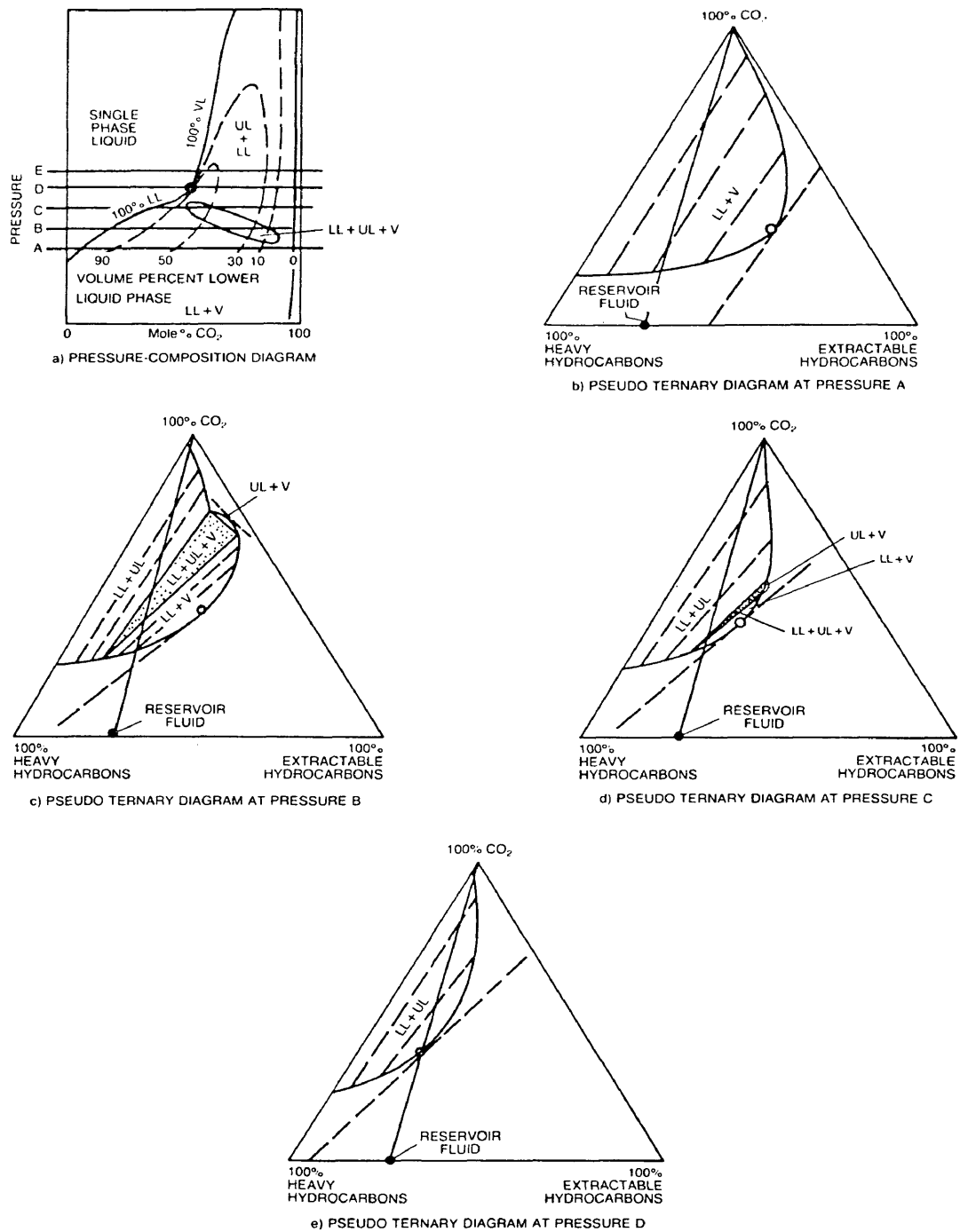


Figure 8. Hypothetical Phase Diagrams for Type IIa Phase Behavior (After Stalkup⁽¹⁾)

liquid in a PVT cell, a CO₂-rich liquid designated UL for upper liquid, and a vapor designated V. Type IIa systems are characterized on a P-X diagram by a three-phase envelope which occurs at lower pressure with increased CO₂ concentration (slopes downward and to the right), and retrograde behavior in the liquid-liquid region. These systems do not generally have a vapor-liquid critical point, however, a liquid-liquid critical point may exist at modest pressures. On pseudoternary diagrams, the three-phase region appears as a triangle. The composition of the three equilibrium phases are defined by the corners of this triangle which are sometimes referred to as invariant points⁽⁵⁾. For any mixture within the triangle, only the amounts of the phases vary. As the pressure of the pseudoternary diagram is increased, the three-phase triangle moves away from the CO₂-heavy hydrocarbon side of the diagram, and at high enough pressure, disappears leaving only liquid-liquid separation (Figures 8c,d,e).

Orr, Yu, and Lien⁽⁹⁾ showed that the features of Type IIa phase diagrams were qualitatively very similar to diagrams depicting the phase behavior of a ternary system containing CO₂, methane, and hexadecane (CO₂-C₁-C₁₆). They speculated that Type IIa phase behavior occurs when the reservoir fluid contains a certain

amount of light hydrocarbons. Further work by Orr and Jensen⁽⁵⁾ demonstrated that a Wasson stock tank crude recombined with solution gas (composed of methane through butane) in the ratio of 602 SCF/BBL did exhibit Type IIa behavior. They also found that there is a maximum temperature at which three phases can form. Above this temperature, liquid-liquid separations still occur at high pressures but as the pressure is reduced, mixtures form a liquid and a vapor phase. The coexistence of all three phases is not observed. This type of phase behavior has been reported by other authors^(11,12).

Figure 9 shows hypothetical phase diagrams for Type IIb phase behavior. Type IIb systems are characterized by a three-phase envelope which exists at higher pressure with increased CO₂ concentration (slopes upward and to the right on a P-X diagram), retrograde behavior is not observed in the liquid-liquid region at pressures of interest, and if a liquid-liquid critical point exists, it is at high pressure. The effect of pressure on the location of the three-phase region on a pseudoternary diagram is illustrated in Figures 9c,d,e,f. As the pressure of the pseudoternary diagram increases, the three-phase triangle moves from the critical point region towards the CO₂-heavy hydrocarbon side of the diagram, eventually disappearing and leaving only liquid-liquid separation.

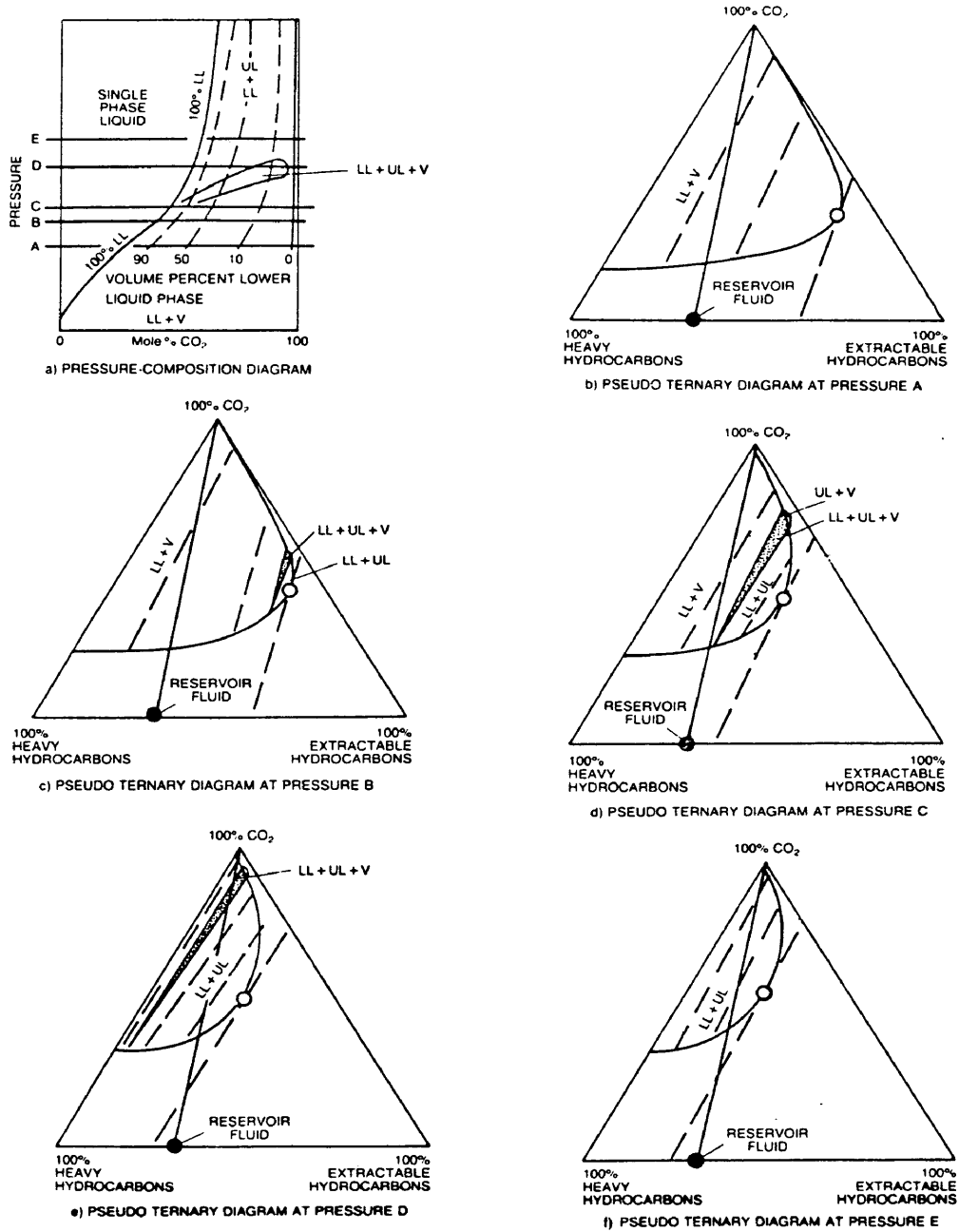


Figure 9. Hypothetical Phase Diagrams for Type IIb Phase Behavior (After Stalkup(1))

Orr, Yu, and Lien⁽⁹⁾ found that the features of Type IIb phase diagrams were qualitatively consistent with the phase behavior of a ternary system composed of CO₂, propane, and hexadecane (CO₂-C₃-C₁₆) and speculated that oils with low concentrations of light hydrocarbons would exhibit Type IIb behavior. This was true for the Wasson separator oil studied by Orr and Jensen⁽⁵⁾ which contained no hydrocarbons lighter than pentane. They also determined that the maximum temperature at which three phases can coexist was higher for the dead oil than the oil recombined with solution gas.

Type IIc phase behavior is similar to Type IIa in that the three-phase envelope slopes downward and to the right on the P-X diagram, however, retrograde behavior is not observed in the liquid-liquid region at pressures of interest. P-X diagrams for the Wasson oil of Orr and Jensen⁽⁵⁾ recombined with solution gas in the ratio of 312 SCF/BBL showed Type IIc characteristics, however, the authors did not refer to this system as another class of Type II phase behavior. This type of behavior appears to have been classified separately only by Stalkup⁽¹⁾.

In conjunction with examining the phase relations of CO₂-crude oil systems, considerable research has been done to determine how phase behavior affects the displacement of

oil by CO₂ and the development of miscibility. In 1971, Rathmel et al.⁽¹³⁾ reasoned that CO₂ achieved miscibility by the vaporizing gas drive mechanism originally described by Hutchinson and Braun⁽⁶⁾. It was known that CO₂ vaporizes hydrocarbons more efficiently than methane, and Rathmel et al.⁽¹³⁾ used pseudoternary diagrams to illustrate that at a given pressure, this leads to a smaller phase envelope and tie line slopes which are more favorable to the development of miscibility when oil is displaced by CO₂ rather than methane. This indicates that miscibility can be achieved at lower pressures with CO₂ which makes this process feasible in a greater number of reservoirs. Displacement tests of three reservoir fluids from sandstone cores verified this. The authors suggested that for a specific reservoir fluid, a higher concentration of intermediate hydrocarbons (C₂-C₆) lowers the pressure required for miscibility while increased methane content raises the miscibility pressure. They stated that the adverse effect of methane is better illustrated with a pseudoquaternary diagram where the crude oil is represented as three components: pure methane, intermediates, and heavy ends. The fourth component is, of course, pure CO₂.

While Rathmel et al.(13) observed liquid-liquid immiscibility for one of their reservoir fluids with CO₂ and speculated on the existence of three phases in equilibrium, in 1974, Huang and Tracht(12) determined the conditions at which liquid-liquid and liquid-liquid-vapor equilibria existed for a CO₂-oil system they studied. They also analyzed a sample of the CO₂-rich liquid and found it to contain an appreciable quantity of extracted hydrocarbons.

In 1974, Holm and Josendal(14) conducted CO₂ displacement tests in slim sand-packed tubes as well as consolidated cores and concluded that CO₂ achieves miscibility by extracting primarily the C₅ through approximately C₃₀ hydrocarbons. Though little extraction of heavier compounds was observed, this is a much deeper extraction than would be possible with methane. They noted that the C₁-C₄ fraction of the oil was vaporized but appeared to be carried ahead of the displacement front. Based on this, they stated that the presence of C₁-C₄ in the reservoir oil did not significantly affect the development of miscibility and in fact, CO₂ could develop miscibility with little or no C₂-C₄ present. However, Alston et al.(15) have presented data which show that in slim tube displacements of an oil, a certain C₂-C₄

content was required to achieve miscibility at a specific pressure. Also, the concentration of methane in the oil had to be below a certain value to achieve miscibility. Their data shows that while miscible displacement is possible with or without methane and intermediates in the oil, both affect the pressure requirement as Rathmel et al.(13) indicated. Regarding the presence of methane in the injected CO₂, Holm and Josendal(14) found that this increases the minimum miscibility pressure. Stalkup(1,2) has also reported this and Graue and Zana(10) found that nitrogen in the CO₂ stream increases the minimum miscibility pressure as well. Metcalfe(16) has shown that the minimum miscibility pressure is increased when the CO₂ stream contains methane, but C₂ and H₂S and--to a greater extent--C₃ and C₄ lower the pressure.

Holm and Josendal(14) also indicated that hydrocarbons can be extracted at low temperatures where CO₂ is a liquid as well as at higher temperatures, however, temperature has a considerable effect on the pressure at which extraction occurs. Higher pressures are required at higher reservoir temperatures. The composition of the oil was also seen to have an effect as high slim tube recoveries were possible at lower pressures for lighter crudes.

Metcalf and Yarborough⁽⁸⁾, in 1979, questioned whether the vaporizing gas drive mechanism proposed by Rathmel et al.⁽¹³⁾ truly described the method by which miscibility was developed at lower temperatures, presumably for systems showing Type II phase behavior. Based on the results of core displacements and static cell phase equilibria for three synthetic oils, the authors concluded that at high temperatures, miscibility is achieved by vaporization but at lower temperatures the process is more accurately described by condensation or absorption of CO₂ into the oil phase. Their low temperature system contained no hydrocarbons heavier than C₁₄, however, and displacement tests were conducted at 120°F which is sufficiently high that only liquid-vapor behavior occurs for mixtures of this oil and CO₂. The P-X diagram for this system is very different from those which other investigators have reported for crude oils (Type I or Type II) and it is questionable whether their conclusions can be extended to actual reservoir fluids which contain significant quantities of hydrocarbons heavier than C₁₄ and may exist at temperatures low enough for liquid-liquid and liquid-liquid-vapor phase behavior.

In 1980, Yellig and Metcalfe⁽¹⁷⁾ presented the results of slim tube tests which further illustrated the effect of temperature on CO₂ minimum miscibility pressure. Contrary to the reports of other investigators, though, they concluded that oil composition had no effect on minimum miscibility pressure in their low temperature tests (95 and 118°F) and what they considered to be only a minor effect at higher temperatures (150 and 192°F). It should be noted that the oils used in this study were prepared by combining the same C₇₊ fraction with varying amounts of light (C₁, N₂, CO₂) and intermediate (C₂-C₆) fractions. Also, the four minimum miscibility pressures measured at 150°F differed by up to 275 psi, and the two measured at 192°F differed by 200 psi. The authors stated that they felt the measurements were accurate within 50 to 100 psi. In view of the similarity of the oil compositions, these differences in MMP may be significant.

In 1979, Gardner et al.⁽¹¹⁾ presented data from single and multiple contact phase experiments for Wasson crude oil and CO₂ at 105°F. The multiple contact data was taken at two pressures: 1350 psia, where conditions of liquid-liquid-vapor equilibria exist, and 2000 psia, where only liquid-liquid behavior occurs. The authors state that at 1350 psia, this data does not indicate the mechanism by

which miscibility is developed. The 2000 psia data indicates that miscibility is achieved by a mechanism analogous to vaporizing gas drive, the two phases both being liquids however. It was also observed that hydrocarbons up to approximately C₂₀ partitioned preferentially into the upper phase, and the oil produced near the end of the experiment contained very little C₃₅₊ material.

The multiple contact data and the single contact data were used to construct pseudoternary diagrams at both pressures. This representation of the phase behavior was used in a simple one-dimensional numerical simulator to calculate the displacement efficiency of a CO₂ flood. The ideal illustration of the vaporizing gas drive process on a pseudoternary diagram holds that as the upper phase is enriched, its composition moves along the dewpoint curve until a composition is reached which is directly miscible with the crude oil. The compositional paths calculated for the Wasson oil displacements follow the upper portion of the phase envelope or dewpoint curve closely at both pressures, albeit within the multiphase region. (Gardner et al.(11) state that only in the limit of zero dispersion will the multiphase region be avoided.) The authors describe the displacement mechanism at both pressures as vaporizing gas drive "for lack of a better term."

In 1981, Orr, Yu, and Lien⁽⁹⁾ used a simulator much like that of Gardner et al.⁽¹¹⁾ to study the effect of phase behavior on the CO₂ displacement efficiency of Maljamar separator oil. Pseudoternary diagrams were used to represent the phase behavior of the CO₂-crude system at 800, 1000, and 1200 psia, and 90°F. In this study, the pseudoternary diagrams were apparently constructed from single contact data only. At 1000 psia a region of three-phase equilibria exists, while at 800 and 1200 psia respectively, only liquid-vapor and liquid-liquid phase separations occur. The results of the simulated displacement at 1200 psia were qualitatively similar to the results Gardner et al.⁽¹¹⁾ obtained for miscible displacements. At the lower pressures, miscibility was not achieved. Enrichment could not proceed past the tie line which, when extended, intersects the original oil composition. As expected though, oil recovery and extraction of hydrocarbons into the upper phase were greater at 1000 psia.

In 1982, a somewhat new approach to defining CO₂ miscibility conditions was taken by Holm and Josendal, who referenced data which shows that the solvent action of CO₂ increases with pressure and reasoned that this can be explained by the corresponding increase in CO₂ density.

The authors studied a variety of oils and found that significant hydrocarbon extraction began when the density of CO₂ was about 0.25 to 0.35 g/cc. The minimum CO₂ density for miscible displacement in slim tube tests appeared to be approximately 0.42 g/cc. The reservoir temperature of the oils examined ranges from 91 to 207°F. The authors argue that temperature only affects extraction by determining the pressure necessary to achieve the required CO₂ density. Orr, Silva, and Lien⁽¹⁹⁾ have shown that CO₂ extracts hydrocarbons more efficiently at higher pressures and that a CO₂ rich liquid phase extracts hydrocarbons more efficiently than a CO₂ rich vapor.

The CO₂ density actually required to achieve dynamic miscibility was found to depend on the amount of C₅-C₃₀ hydrocarbons in the oil and was further affected by the distribution of hydrocarbons (namely C₅-C₁₂ content) within this fraction. In general, higher CO₂ densities are needed for oils low in extractable hydrocarbons or of high molecular weight. Holm and Josendal⁽¹⁸⁾ also found that the required density was affected to a lesser degree by the type of hydrocarbons present, i.e. paraffin, naphthene, or aromatic. They presented data suggesting that when a paraffinic oil was enriched with aromatics, the slim tube minimum miscibility pressure (hence the required CO₂

density) was lowered. They stated that while this may seem contrary to expected behavior since aromatics and naphthenes are known to be less miscible in CO_2 than paraffins, improved oil recovery could possibly be explained by the aromatics and naphthenes which are extracted being better solvents than paraffins for heavy hydrocarbon compounds.

There is some controversy in the literature concerning the effect of hydrocarbon type on minimum miscibility pressure and oil recovery. Monger⁽²⁰⁾ reached the same conclusion as Holm and Josendal⁽¹⁸⁾ based on static cell and coreflood data for synthetic oil systems; that the extraction of heavier hydrocarbons into the CO_2 -rich phase is improved by the presence of aromatics in the oil. Cramer and Swift⁽²¹⁾ used an equation of state to calculate the maximum miscibility composition for ternary mixtures of CO_2 and n-butane with paraffinic (n-decane), naphthenic (n-butylcyclohexane), and aromatic (n-butylbenzene) compounds. They found that changing the heavy hydrocarbon from paraffin to naphthene to aromatic had no substantial effect on the maximum miscibility composition.

The most extensive work in this area appears to have been done by Silva et al⁽²²⁾. These authors reviewed phase composition data for binary CO_2 -hydrocarbon systems which shows that paraffin hydrocarbons are extracted most

efficiently by CO₂, followed in order by naphthenes and aromatics. This data suggested that among the paraffins, highly branched alkanes would be extracted more readily than straight-chain alkanes. These findings were essentially confirmed by the results of phase behavior experiments conducted with CO₂ and four synthetic oils which all contained the same C₃₀ hydrocarbon, squalane.

Hydrocarbons in the iso-alkane mixture partitioned most strongly into the CO₂-rich upper phase followed by the normal alkanes, aromatics, and naphthenes. Comparison of hydrocarbon K-values and estimated limiting tie lines for the four oils indicate that the minimum miscibility pressures would increase in the same order. This is in disagreement with Holm and Josendal's⁽¹⁸⁾ and Monger's⁽²⁰⁾ assertions that aromatics improve the extraction of heavy hydrocarbons. Alkyl side chains on the aromatic compounds of the synthetic oil are apparently responsible for aromatics being extracted more efficiently than naphthenes. For the binary systems this order was reversed.

Experiments with two crude oils, one containing approximately 8 weight percent aromatics (Maljamar) and one containing less than 2 percent aromatics (Rock Creek), showed no significant effects of aromaticity on hydrocarbon

partitioning. Pseudoternary phase envelopes and tie line slopes were similar as were hydrocarbon K-values. Even when the aromatic content of the Rock Creek oil was increased, component partitioning and the total amount of hydrocarbons extracted did not change substantially. The authors reasoned that the aromatic compounds in the crudes may have contained enough alkyl side chains to compensate for the normally adverse effect of the aromatic structure. It is also reported that another investigator determined that although naphthenes and aromatics do not seem to make up a large part of the easily extractable hydrocarbon fraction, those that are present usually contain the alkyl side groups. Based on these results, Silva et al.(22) concluded that the molecular size distribution will have a greater impact on hydrocarbon extraction than molecular type. They also offered an explanation for the apparent effect of aromaticity on minimum miscibility pressure observed by Holm and Josendal(18). The minimum miscibility pressures of the paraffinic and aromatic oils were each estimated from only one slim tube displacement and may not be sufficiently accurate to conclude that aromaticity does actually have an effect. Also, compositional differences not related to aromaticity may be responsible if the minimum miscibility pressures are indeed accurate.

In 1982, Yellig⁽²³⁾ reported the results of CO₂ core floods at two pressures which were above the CO₂ minimum miscibility pressure for a west Texas oil. Liquid-liquid-vapor behavior occurs at the lower pressure (1400 psia), at the higher pressure (1900 psia) the behavior is liquid-liquid. For certain core systems, oil recovery was higher at 1400 psia than at 1900 psia. The authors suggest that a possible explanation is that the effects of three-phase relative permeability may be beneficial to miscibility development. It is possible that certain three-phase relative permeabilities could lead to some type of mobility control which would improve oil recovery. It is not known if this phenomenon occurs in more heterogeneous media or if it has any practical application. Compositional analysis of the effluent indicates that at both pressures miscibility was achieved by vaporization or extraction of light and intermediate hydrocarbons into the CO₂-rich phase.

From the standpoint of semantics, vaporizing gas drive may not provide the best description of the process by which dynamic miscibility with CO₂ is developed at conditions where two liquids or two liquids and a vapor are involved. However, the results of experimental and theoretical work by Yellig⁽²³⁾, Gardner et al.⁽¹¹⁾, and Orr, Yu, and

Lien⁽⁹⁾ show that from the standpoint of phase behavior and in situ mass transfer the description is appropriate. For systems exhibiting Type I phase behavior, the pseudoternary representation of the process and criteria for miscibility are exactly as discussed previously. Any reservoir fluid whose composition lies on or to the right of the extension of the limiting tie line can develop dynamic miscibility with CO₂ at the temperature and pressure of the diagram. The minimum miscibility pressure is defined as the pressure at which the extension of the limiting tie line intersects the reservoir fluid composition. Similarly, the maximum miscibility composition at a specific pressure is defined as the oil composition at the intersection of the limiting tie line and the crude oil base line.

For Type II systems, the process follows the same compositional path though extraction may be a more accurate term for mass transfer between two liquid phases. On the pseudoternary diagram, all reservoir fluids between the first contact miscibility limit and the extension of the limiting tie line can achieve dynamic miscibility and the definitions of minimum miscibility pressure and maximum miscibility composition are as before, but with one added condition. Stalkup⁽¹⁾ states that if the small region where the CO₂-rich liquid (UL) in equilibrium with the

vapor phase (V) exists for the system under consideration (refer to Figure 8c), the extension of its limiting tie line must pass to the left of the 100 percent CO₂ apex.

Of course, the limitations of representing the phase behavior of multicomponent systems on pseudoternary diagrams which were discussed earlier, still hold.

Measurement of Minimum Miscibility Pressure

The preferred method for determining the pressure required for dynamic miscibility with CO₂ is by laboratory displacement tests. Although consolidated cores have been used, the standard experiment is conducted in a long, coiled length of small-diameter steel tubing packed with sand or glass beads and saturated with reservoir fluid. By making the slim tube long enough and of sufficiently small diameter, displacements can be carried out at a fairly high velocity and viscous fingering will be suppressed by transverse dispersion⁽¹⁾. In this highly ideal flow setting, the effects of phase behavior on displacement efficiency can essentially be isolated.

A schematic of the slim tube apparatus recommended by Yellig and Metcalfe⁽¹⁷⁾ is shown in Figure 10. A stainless steel tube, 40 feet long with an outside diameter of one-fourth inch, is packed with 160-200 mesh Ottawa sand and coiled. The coil is attached to a manifold which allows different fluids to be introduced to the sandpack. A capillary-tube sight glass is fitted to the outflow end of the tube for visual observation of the effluent and a backpressure regulator maintains the desired test pressure. This equipment and the movable-piston CO₂ supply cylinder are contained in a constant temperature air bath. Fluids

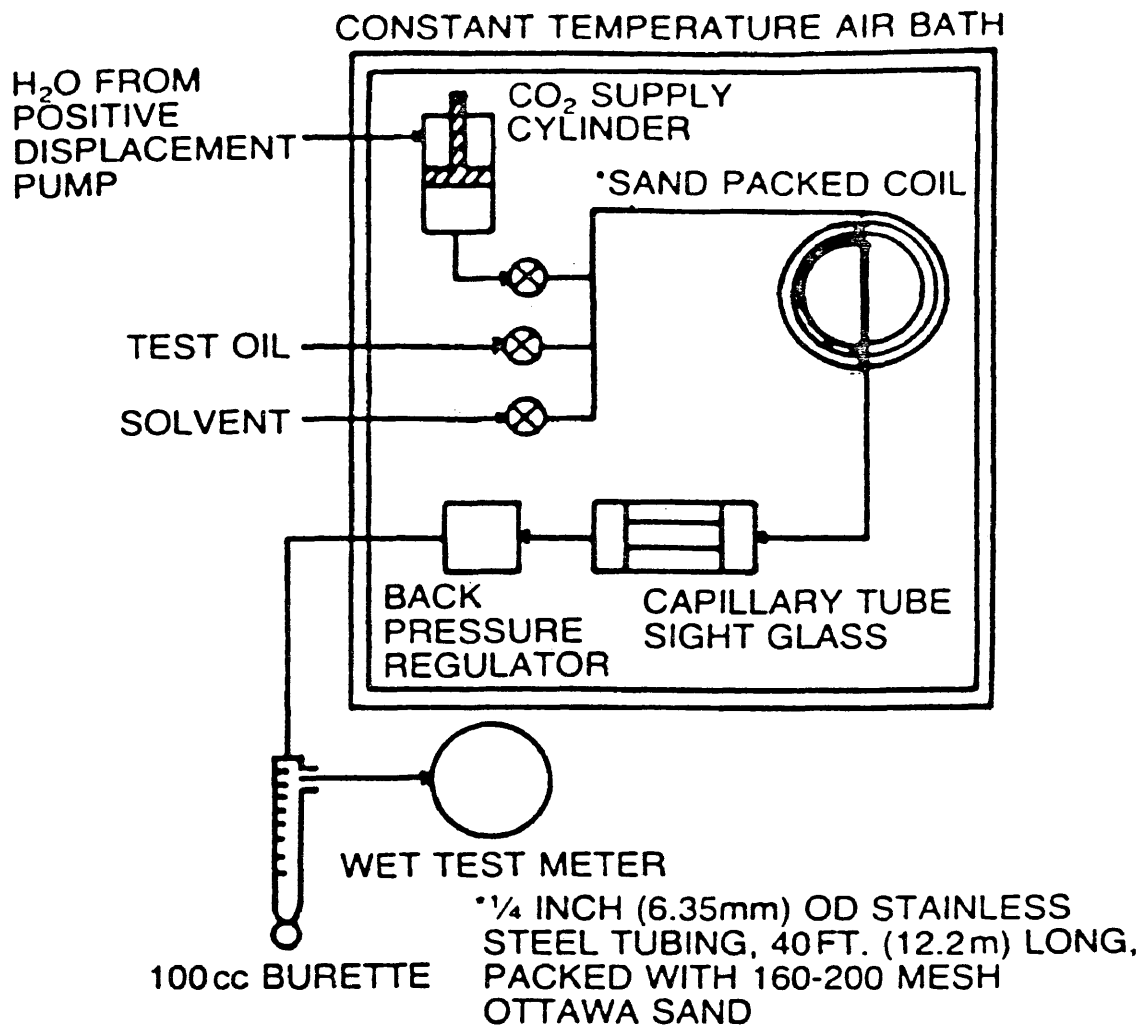


Figure 10. Slim Tube Apparatus Proposed by Yellig and Metcalfe⁽¹⁷⁾

are injected by means of a positive displacement pump. The effluent is continuously flashed to atmospheric conditions where the liquid volume is measured in a burette and the vapor is measured in a wet test meter.

Prior to the displacement tests, the pore volume (PV) of the coil can be determined by measuring the amount of solvent required to fill the evacuated sandpack. For each test, the same sandpack is saturated with oil at the desired test temperature and pressure. The supply cylinder is filled with CO₂ and allowed to equilibrate to the test conditions. Yellig and Metcalfe⁽¹⁷⁾ recommend that the displacement velocity not exceed 40 ft/day until 70 % PV has been injected, at which point, it can be increased to 80 ft/day. The test is terminated after 1.2 PV CO₂ has been injected. The fractional oil recovery can be determined by multiplying the volume of liquid collected in the burette by a predetermined volume factor or by applying this volume factor to the amount of residual liquid extracted from the sandpack by a solvent. Other researchers have had success using different size tubes, different injection rates, and different materials to pack the tube.

Several displacements must be performed at different pressures to determine the minimum miscibility pressure. The percent ultimate oil recovery (after 1.2 PV injection)

for a series of slim tube displacements is plotted versus test pressure in Figure 11. Yellig and Metcalfe⁽¹⁷⁾ judged whether each displacement was miscible based on these criteria: the final oil recovery after the injection of 1.2 PV CO₂ is near the maximum recovery obtained in the series of tests, and visual observation of the transition zone fluids indicates that dynamic miscibility was achieved. The minimum miscibility pressure is then taken as the lowest test pressure at which a miscible displacement occurred or the pressure at the breakover point on the ultimate recovery curve. Yellig and Metcalfe⁽¹⁷⁾ found that with their slim tube apparatus and this interpretation of the experimental results, MMP could be measured within 50 to 100 psi.

Just as there is no industry standard for the slim tube apparatus or the experimental technique, there is no standard definition of minimum miscibility pressure based on the interpretation of slim tube data. The following definitions have also been offered. Prior to Yellig and Metcalfe's⁽¹⁷⁾ paper, Holm and Josendal⁽¹⁴⁾ had defined the MMP as the pressure at which the oil recovery at CO₂ breakthrough is greater than 80 percent and ultimate recovery is greater than 94 percent. Mungan⁽²⁴⁾ proposed a similar definition: the pressure at which the oil recovery at CO₂ breakthrough is at least 85 percent and recovery

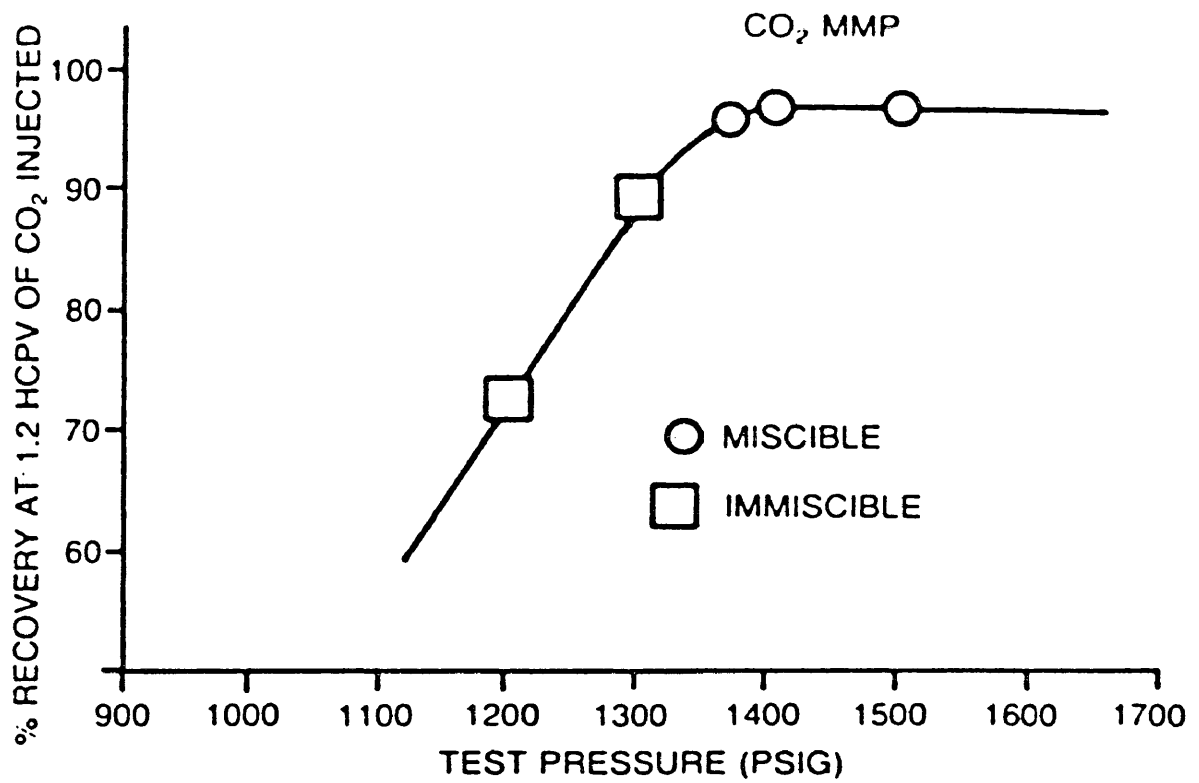


Figure 11. Slim Tube Data for CO₂ Displacement Tests of Yellig and Metcalfe⁽¹⁷⁾

after 1.2 PV injection is 95-98 percent, with no fluid interfaces in the visual cell. Alston et al.(15) attempted to calibrate their slim tube apparatus by comparing the miscibility conditions determined by the limiting tie line concept with slim tube displacements for a true ternary system. The definition they proposed for MMP is the pressure at which oil recovery is 90 percent at CO₂ breakthrough with no two-phase flow in the sight glass. To what extent these different definitions affect the MMP values reported by different researchers is not known.

Johnson and Pollin(25) found the sharpness with which the recovery curve breaks over and the amount of oil ultimately recovered are both affected by such things as the dimensions and packing of the slim tube and the displacement rate. Yellig and Metcalfe(17) reported that the sharpness of the breakover also depends on temperature and that at higher temperatures the maximum recovery is approached more gradually. In essence, the breakover may not always occur at the same recovery level and it may be erroneous to define the MMP in terms of a minimum recovery level at a certain injection volume. The pressure at which the breakover occurs appears to be independent of rate and system effects, as such, Yellig and Metcalfe's(17) criteria for determining MMP from slim tube data has been recommended by

Johnson and Pollin⁽²⁵⁾ and Stalkup⁽¹⁾. Orr, Yu, and Lien⁽⁹⁾ have stated that this criteria for defining minimum miscibility pressure is not as strict as the pseudoternary diagram-limiting tie line definition. The breakover point may indicate a nearly miscible displacement where the phase envelope on the pseudoternary diagram does not get significantly smaller as pressure is increased or the compositional path enters the multiphase region near the critical point. High slim tube recoveries would still be observed because the near-critical fluid does extract hydrocarbons efficiently and interfacial tensions are low. The authors concluded that for operational purposes, the breakover criteria of Yellig and Metcalfe⁽¹⁷⁾ is satisfactory because it indicates the pressure at which phase behavior will be favorable enough to produce a high displacement efficiency which is the chief concern. It is important to note, however, that this displacement may not be strictly miscible, in which case the slim tube MMP could be lower than the MMP determined by the limiting tie line.

Conceivably, miscible displacement could recover 100 percent of the oil from the swept zone. Slim tube recoveries approach this but a small residual oil saturation is still left. One reason for this is that CO₂ is not miscible with crude oil on first contact, consequently oil

is initially displaced immiscibly. Once miscibility has been attained, the vaporization or extraction process stops until dispersion breaks down the miscible front. When this occurs the extraction mechanism begins again and miscibility is re-established. This continual dispersion and rebuilding of the miscible bank also leaves a small amount of residual oil along the displacement path⁽¹⁴⁾. The high oil recoveries obtained in slim tube displacements are not indicative of the amount of oil CO₂ will recover from consolidated media. Figure 12 from Taber⁽²⁶⁾, shows the amount of Maljamar oil recovered by CO₂ from a slim tube and a Berea sandstone core at various pressures. Estimated recoveries for more heterogeneous rocks and the approximate range of recoveries which can be expected in the field are also shown.

Christiansen and Kim⁽²⁷⁾ have recently proposed an alternative method of measuring minimum miscibility pressure which can be performed more rapidly than slim tube displacements. The apparatus consists of a glass tube mounted in a high pressure sight gauge contained in a temperature controlled bath. Bubbles of injection gas are introduced through a hollow needle at the bottom of the tube. A schematic of this equipment is shown in Figure 13a. To perform an experiment, the sight gauge and glass

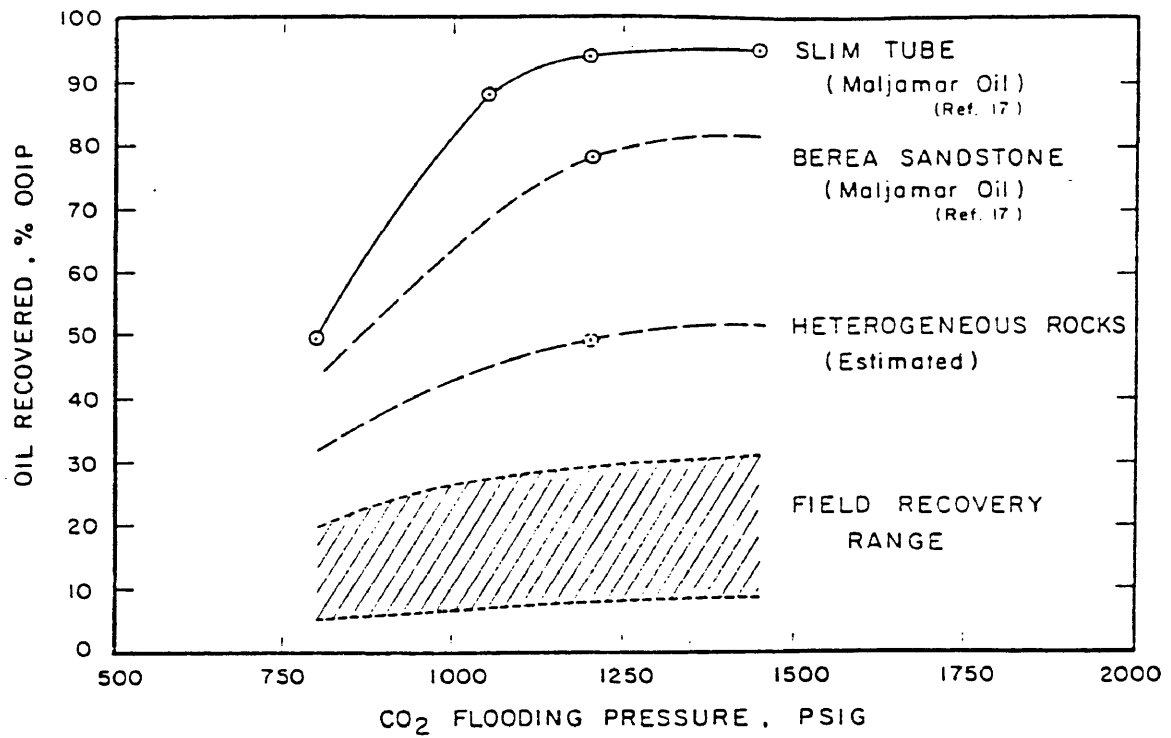
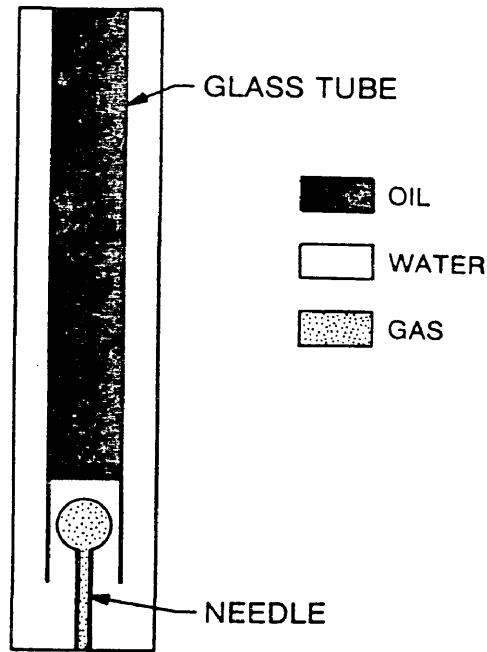
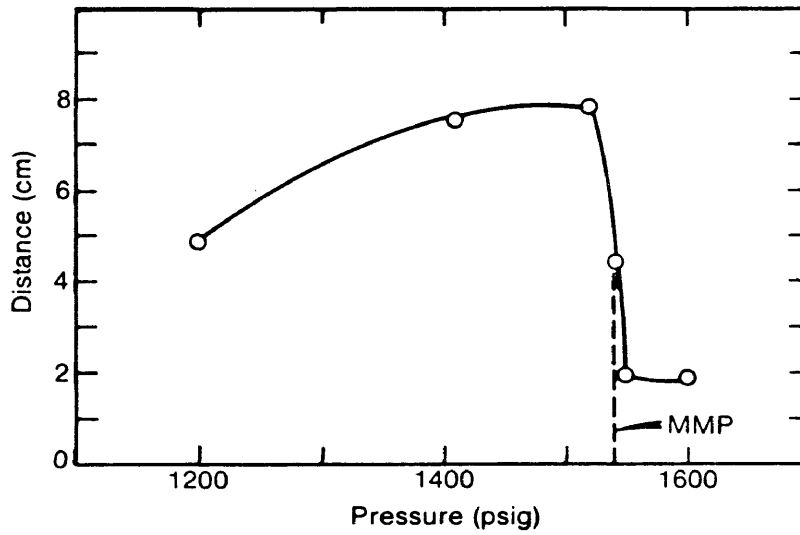


Figure 12. Effect of Pressure on Oil Recovery by CO₂ (After Taber (26))



a) Schematic of Apparatus



b) Effect of Pressure on Bubble Rise Distance

Figure 13. Measurement of MMP by Rising Bubble Apparatus (After Christiansen and Kim⁽²⁷⁾)

tube are first filled with distilled water. Oil is then injected into the glass tube but a short column of water is left at the bottom. Next, a small bubble of injection gas is launched into the water. As the bubble rises its shape and movement are observed and photographed with a motor driven camera. The authors reason that the mass transfer process that occurs as the bubble rises through the oil is very similar to the process that occurs in a slim tube displacement. As the bubble rises it continually contacts fresh oil and as illustrated on a pseudoternary diagram, its composition is progressively altered along the dewpoint curve until it is miscible with the oil.

With this procedure the pressure dependence of bubble behavior and rise distance is determined rather than the pressure dependence of oil recovery. Below the MMP, a rising bubble retains its nearly spherical shape but decreases in size. Near the MMP, a bubble remains almost spherical on top, but the bottom interface becomes flat or wavy. At or slightly above the MMP, the authors report that tail-like features quickly develop on the bottom of the bubble but the top remains spherical. Then, starting at the bottom of the bubble, the interface disappears and the bubble rapidly disperses in the oil. Far above the MMP, a bubble disperses more rapidly, and at the first contact

miscibility pressure, almost immediately. The effect of pressure on the distance travelled by the bubble is shown in Figure 13b which is for CO₂ in a mixture of n-pentane and n-hexadecane.

The authors have tested the rising bubble apparatus (RBA) with several oils and the CO₂ minimum miscibility pressures measured compare favorably with slim tube MMPs. For low temperature CO₂-oil systems (Type II phase behavior) interpretation of the results is more difficult. In some instances, as the CO₂ bubble rose the authors observed the gas-oil interface disintegrate and the contents of the bubble begin to disperse when a second bubble emerged in this region and continued to the top of the glass tube. Due to these complexities, MMP could not be determined as precisely for low temperature systems.

Minimum Miscibility Pressure Correlations

The first published correlation of the conditions required for dynamic miscibility was that of Benham et al.(28) in 1960. This correlation is for the condensing gas drive mechanism and does not directly pertain to CO₂ injection. It is mentioned here because its development was similar in concept to the method used in this study, and because it has been drawn upon by other researchers to correlate CO₂ miscibility conditions.

By means of the condensing or enriched gas drive process, miscibility between an injected hydrocarbon gas and reservoir oil can be developed in situ. Hutchinson and Braun(6) were the first to illustrate this process on a pseudoternary diagram. The phase behavior of a crude oil system is shown conceptually in Figure 14, where the oil is split into three pseudocomponents: methane, ethane through butane (C₂-C₄), and pentanes and heavier (C₅₊). The reservoir oil is not initially miscible with the injection gas B which lies on the extension of the limiting tie line through the critical point. Suppose the first contact of oil and injection gas results in mixture M₁ which is within the two-phase region. The tie line through M₁ indicates that gas G₁ and liquid L₁ are in equilibrium at this point. Further injection of gas B drives the more

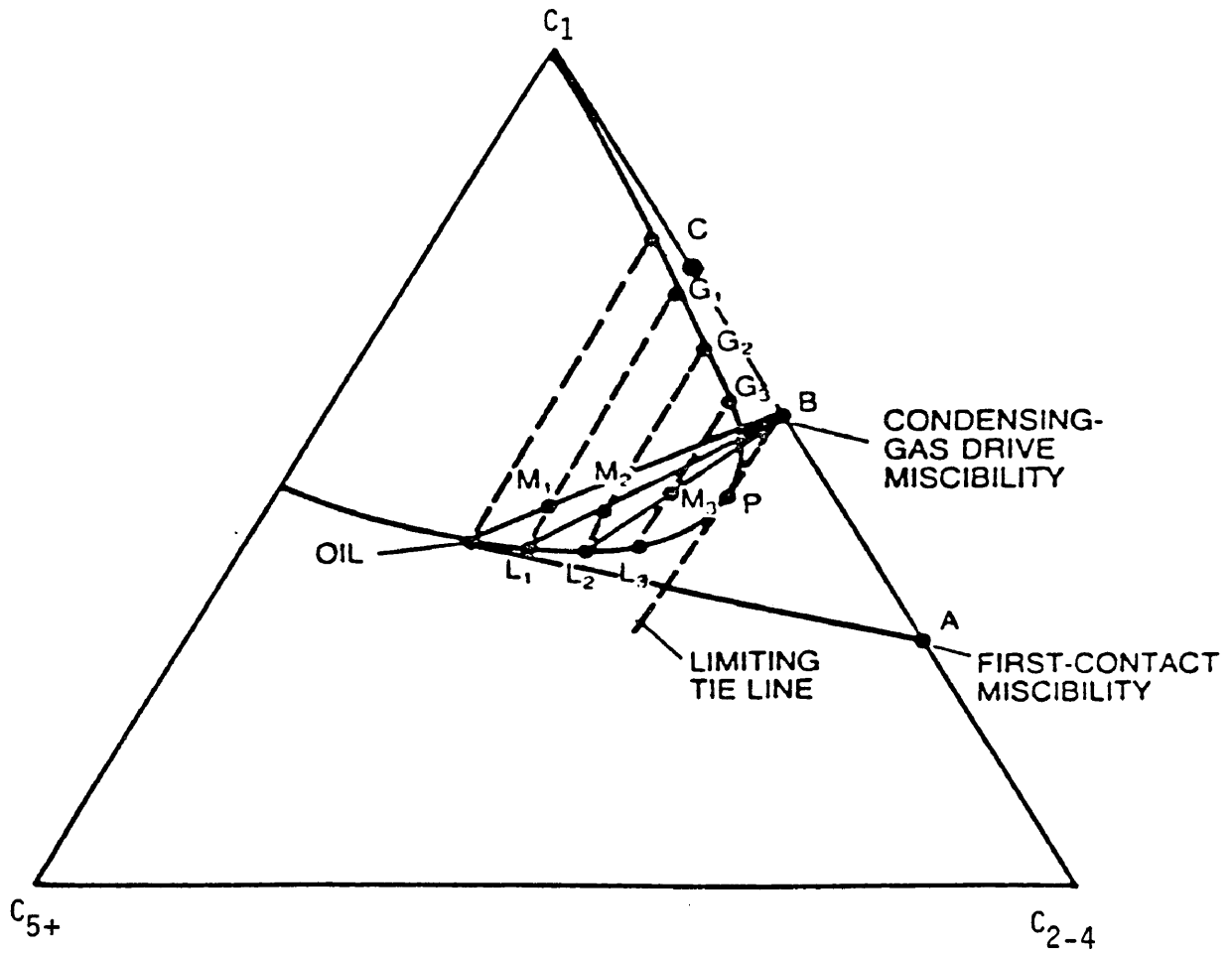


Figure 14. Pseudoternary Illustration of Condensing Gas Drive Mechanism (After Stalkup⁽¹⁾)

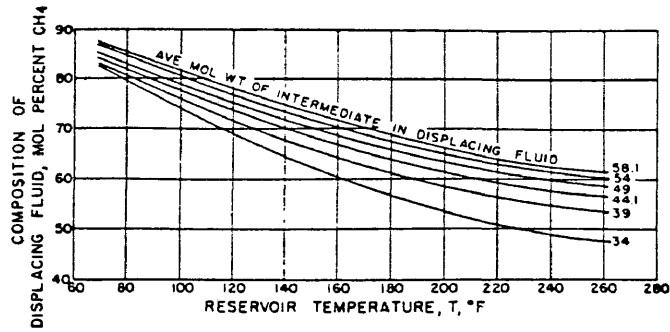
mobile phase G_1 ahead in the reservoir and gas B contacts liquid L_1 . This forms mixture M_2 which separates into liquid L_2 and gas G_2 . Subsequent injection displaces gas G_2 and the process is repeated. In this manner, the composition of the liquid near the injection point is enriched with intermediates (C_2-C_4) and proceeds along the bubble point curve until the critical point composition is reached. This fluid is directly miscible with injection gas B.

An injection gas containing fewer intermediates than gas B cannot develop dynamic miscibility with the same reservoir oil. For example, if gas C were injected, enrichment could not proceed past the point of L_1 since further contacts would only result in mixtures which lie on the tie line connecting L_1 and G_1 . Any injection gas between B and A can achieve dynamic miscibility, and of course, gas A or any richer gas is first contact miscible. Thus, gas B is the leanest gas which can develop dynamic miscibility with the reservoir oil at the temperature and pressure of the pseudoternary diagram. Similarly, the pressure of the diagram is the minimum miscibility pressure for gas B with this reservoir oil.

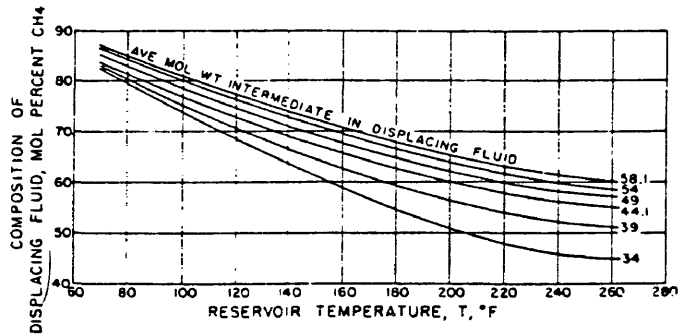
Benham et al.(28) were interested in developing a correlation to predict the leanest injection fluid which could achieve dynamic miscibility with a given reservoir oil at reservoir conditions. The authors selected five reservoir fluids of different compositions and six injection fluids composed of ethane through butane. These oils and injection fluids were mathematically combined in various proportions with methane. The critical temperature and pressure of the mixtures were calculated using the method of Kurata and Katz. On a pseudoternary diagram such as Figure 14, the point at which the limiting tie line extended through one of these compositions intersects the methane-intermediates side of the diagram defines the maximum amount of methane which could be added to the C₂-C₄ injection fluid (or conversely, the minimum amount of C₂-C₄ which could be added to methane) and still achieve miscibility at the calculated critical temperature and pressure. The limiting tie line was assumed to be parallel to the methane-C₅₊ side of the pseudoternary diagram. This simplified the calculational procedure but it is a serious assumption. The authors reasoned that it would lead to a conservative estimate of the maximum methane content, however, for some systems the opposite is true.

Data calculated in this manner was crossplotted to determine the miscibility conditions at specific pressure levels. In the final form of the correlation, the maximum allowable methane content of the injection fluid is correlated with the molecular weight of the C₅₊ fraction of the reservoir fluid, the C₂₊ molecular weight of the injection fluid, and reservoir temperature and pressure. In all, 12 charts were published to cover a range of pressures, C₅₊ molecular weights, C₂₊ molecular weights, and temperatures. Some of these charts at 3000 psia are shown in Figure 15. This data was later replotted as a correlation for the minimum miscibility pressure, given the C₂₊ and C₅₊ molecular weights and reservoir temperature as shown in Figure 16.

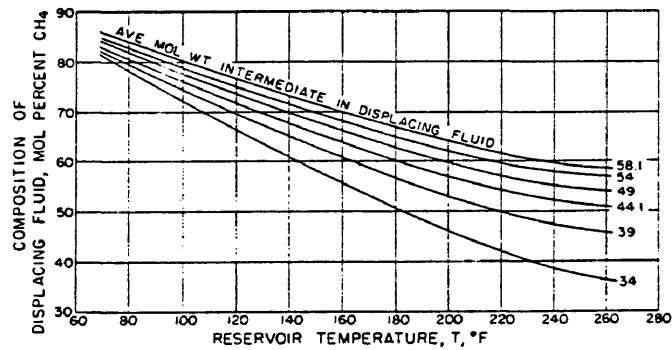
In 1974, Holm and Josendal⁽¹⁴⁾ proposed a correlation for CO₂ minimum miscibility pressure which is based on the correlation of Benham et al⁽²⁸⁾. The authors conducted CO₂ slim tube displacements of several crude oils and found that MMPs predicted by the Benham correlation for an injection fluid composed of 59 percent methane and 41 percent propane were close to the CO₂ MMPs they had measured in the laboratory. Data points for this mixture taken from the 12 original charts of Benham et al. were used to correlate CO₂ minimum miscibility pressure with



-PREDICTED PHASE CONDITIONS AT 3,000 PSIA FOR A MISCIBLE DISPLACEMENT OF A RESERVOIR FLUID CHARACTERIZED BY A C_6+ MOLECULAR WEIGHT OF 180.



-PREDICTED PHASE CONDITIONS AT 3,000 PSIA FOR A MISCIBLE DISPLACEMENT OF A RESERVOIR FLUID CHARACTERIZED BY A C_6+ MOLECULAR WEIGHT OF 200.



-PREDICTED PHASE CONDITIONS AT 3,000 PSIA FOR A MISCIBLE DISPLACEMENT OF A RESERVOIR FLUID CHARACTERIZED BY A C_6+ MOLECULAR WEIGHT OF 220.

Figure 15. Example of Condensing Gas Drive Miscibility Correlation of Benham et al. (28)

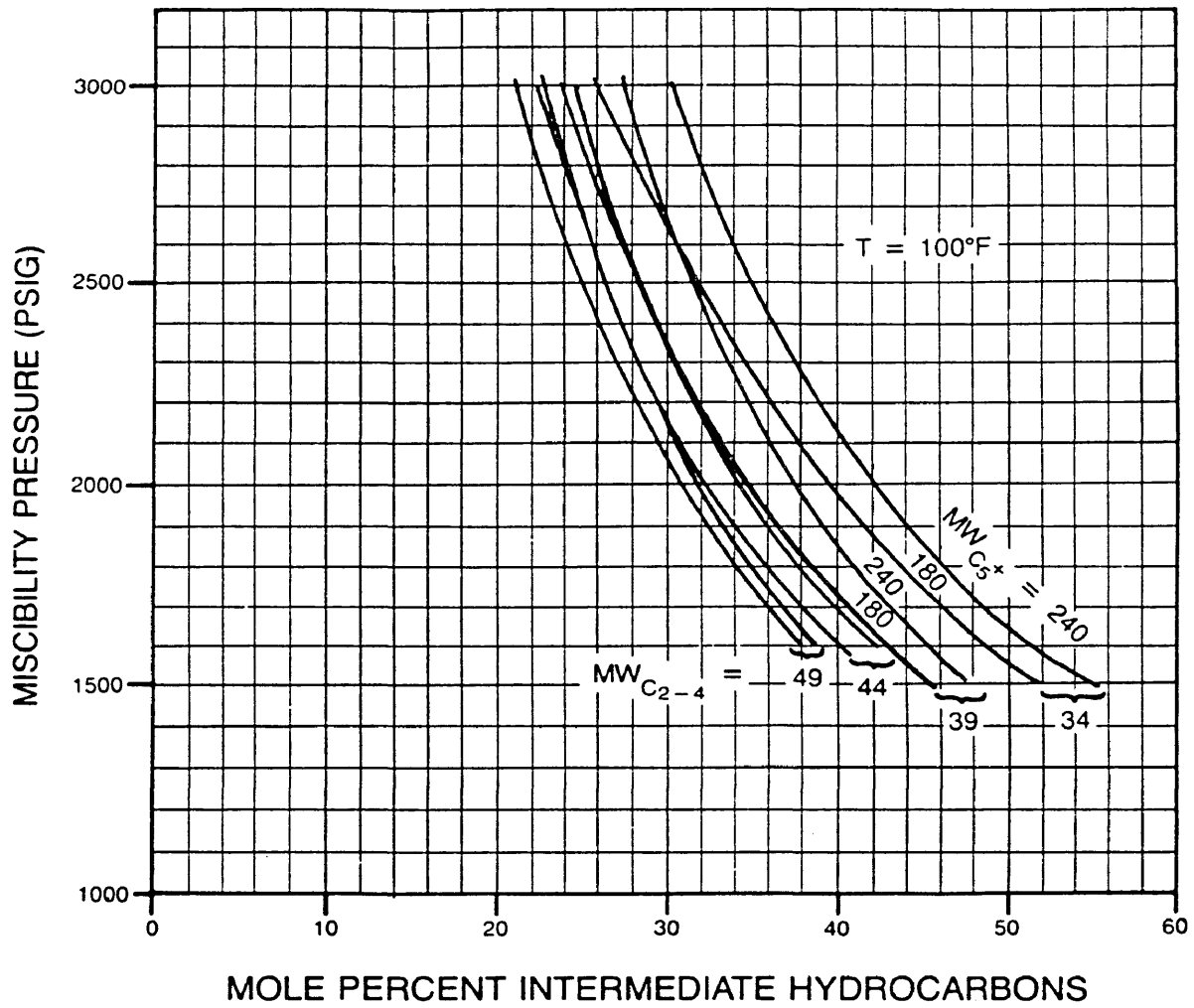


Figure 16. Example of Condensing Gas Drive MMP Correlation from Data of Benham et al. (28)

temperature and the C₅₊ molecular weight of the reservoir oil. Holm and Josendal had already concluded that the C₁-C₄ fraction of the oil did not affect MMP. In 1981, Mungan⁽²⁴⁾ extended the correlation to higher molecular weights. It should be noted that the data calculated by Benham et al.⁽²⁸⁾ did not include CO₂. The correlation is shown in Figure 17.

In 1976, the National Petroleum Council⁽²⁹⁾ presented an empirical correlation which estimates CO₂ minimum miscibility pressure from the API gravity of a crude oil and reservoir temperature. The form of this correlation is shown below.

Miscibility Pressure vs Gravity

Gravity (°API)	Miscibility Pressure (psia)
<27	4000
27 - 30	3000
>30	1200

Correction for Reservoir Temperature

Temperature (°F)	Additional Pressure Required (psi)
<120	None
120 - 150	+200
150 - 200	+350
200 - 250	+500

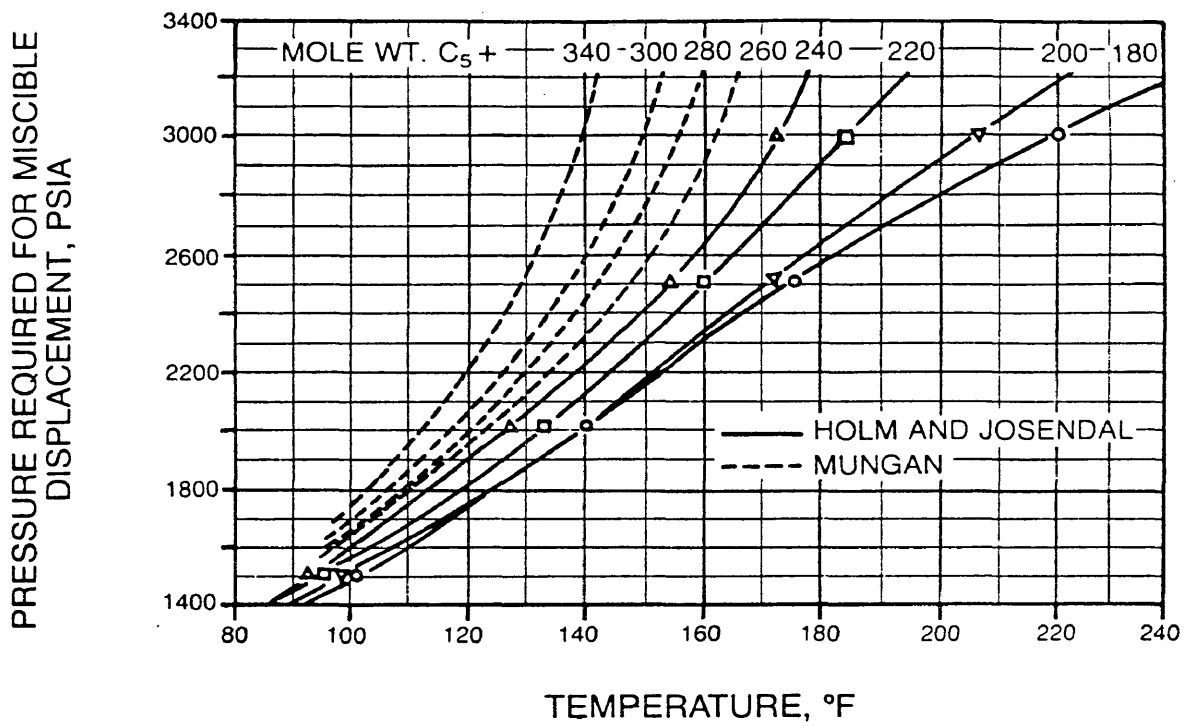


Figure 17. CO₂ MMP Correlation of Holm and Josendal(14) as Extended by Mungan(24)

In 1978, an empirical correlation based on 58 experimental minimum miscibility pressures from various sources was proposed by Cronquist⁽³⁰⁾. The reservoir oil is characterized by the molecular weight of the C₅₊ fraction and the adverse effect of methane and nitrogen in the oil is accounted for. The equation form of the correlation given below was reported in Section 8.2 of Stalkup⁽¹⁾.

$$\text{MMP} = 15.988(T)^{0.7442} + 0.001104(\text{MWC}_{5+}) + 0.001528(\text{MPCl})$$

where:

T= reservoir temperature, °F

MWC₅₊= molecular weight of the C₅₊ fraction

MPCl= mole percent methane and nitrogen in oil

In 1980, Yellig and Metcalfe⁽¹⁷⁾ performed slim tube displacements of four oil samples prepared by combining the same C₇₊ fraction with varying amounts of light and intermediate components. They concluded that oil composition had little or no effect on the minimum miscibility pressure. They proposed a correlation where reservoir temperature is the only parameter. Because it is not known if high oil recoveries can be obtained at pressures below the bubble point pressure of the oil, a

correction is applied if the predicted MMP is below the saturation pressure. In this event, the bubble point pressure is taken as the minimum miscibility pressure. The correlation is shown in Figure 18.

In 1981, Johnson and Pollin⁽²⁵⁾ proposed a rather complicated empirical correlation based on 25 minimum miscibility pressures measured in their laboratory. The correlation parameters are the reservoir temperature, average molecular weight of the oil, and an oil characterization index which is itself a function of oil density and average molecular weight. For CO₂ streams containing methane or nitrogen, the critical temperature, critical pressure, and average molecular weight of the injection gas are included as parameters. The correlation is given below.

$$\text{MMP} = \alpha_{inj}(T_{res} - T_{c,inj}) + I(0.285M - M_{inj})^2 + P_{c,inj}$$

where:

T_{res} = reservoir temperature, °K

M = average molecular weight of the oil

$T_{c,inj}$ = critical temperature of the injection gas

$P_{c,inj}$ = critical pressure of the injection gas

M_{inj} = molecular weight of the injection gas

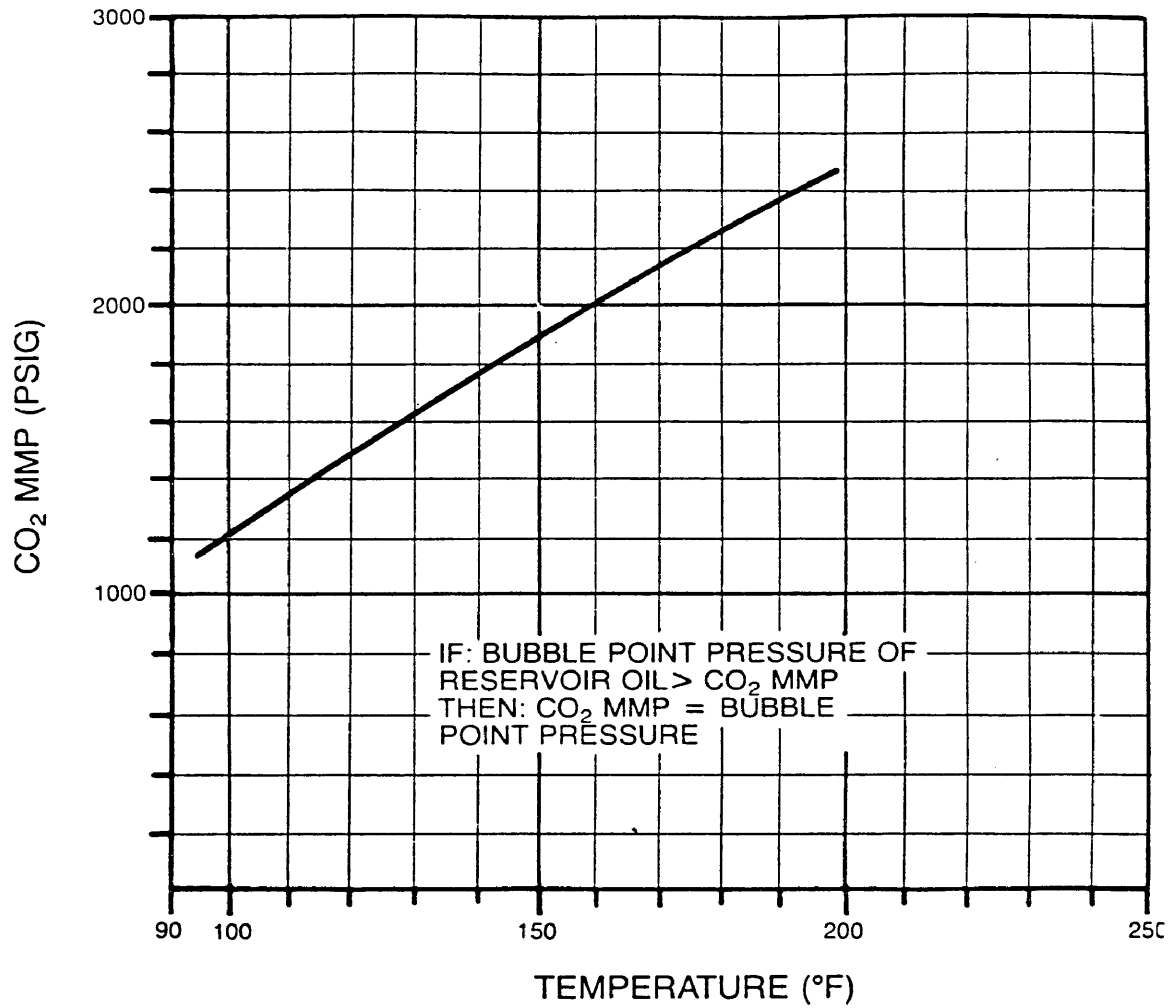


Figure 18. CO₂ MMP Correlation of Yellig and Metcalfe(17)

for pure CO₂ injection gas:

$$\alpha_{inj} = 18.9 \text{ psia/K}$$

for injection gas containing nitrogen:

$$\alpha_{inj} = 10.5 \left(1.8 + \frac{10^3 y_2}{T_{res} - T_{c,inj}} \right)$$

for injection gas containing methane:

$$\alpha_{inj} = 10.5 \left(1.8 + \frac{10^2 y_2}{T_{res} - T_{c,inj}} \right)$$

where y_2 is the mole fraction of nitrogen or methane

The oil characterization index I is given by:

$$I = C_{11} + C_{21}M + C_{31}M^2 + C_{41}M^3 + (C_{12} + C_{22}M)\rho + C_{13}\rho^2$$

where:

$\rho =$ oil density

$$C_{11} = -11.73$$

$$C_{12} = 0.1362$$

$$C_{13} = -7.222 \times 10^{-5}$$

$$C_{21} = 6.313 \times 10^{-2}$$

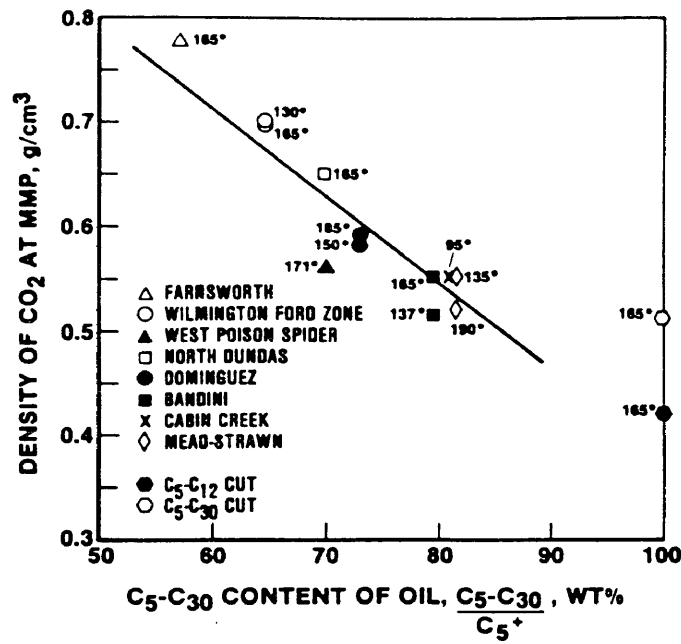
$$C_{22} = 1.138 \times 10^{-5}$$

$$C_{31} = -1.195 \times 10^{-4}$$

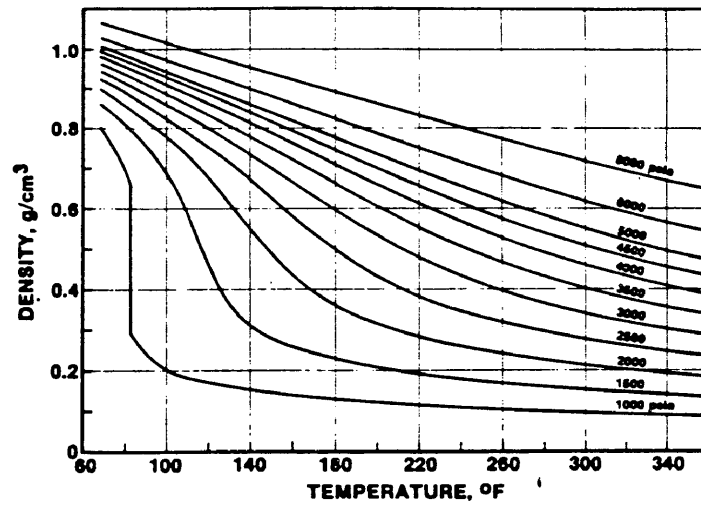
$$C_{41} = 2.502 \times 10^{-7}$$

In 1982, Holm and Josendal⁽¹⁸⁾ proposed a second correlation for CO₂ minimum miscibility pressure. Based on their assertion that the solvent action of CO₂ is a function of density, the authors have empirically correlated the CO₂ density required to achieve dynamic miscibility with the amount of extractable hydrocarbons in the reservoir oil. The correlation is shown in Figure 19a where the required CO₂ density is a linear function of the weight percent of C₅ through C₃₀ in the C₅₊ fraction of the crude. The MMP is the pressure which yields this density at reservoir temperature. Figure 19b provides a suitable means for determining this pressure. The correction of Yellig and Metcalfe⁽¹⁷⁾ is applied if the correlation predicts a value below the bubble point pressure, i.e. the MMP is set equal to the bubble point pressure.

In 1982, Orr and Jensen⁽⁵⁾ suggested that the extrapolated vapor pressure (EVP) of CO₂ could be used to estimate the minimum miscibility pressure for reservoir temperatures below approximately 120°F. The authors showed that for oils exhibiting Type II phase behavior, the EVP provides a good estimate of the pressure above which liquid-liquid behavior will occur. Under these conditions, the CO₂-rich phase should be dense and relatively incompressible and able to extract hydrocarbons



a) Required CO₂ Density



b) CO₂ Density Data

Figure 19. CO₂ MMP Correlation of Holm and Josendal(18)

efficiently. For live oils (Type IIa behavior) a 200–300 psi safety margin should be added, while for dead oils (Type IIb behavior) the estimated MMP should be fairly accurate. The EVP can be calculated from the following equation.

$$\text{EVP} = 101.3 \exp\left(-\frac{2015}{T} + 10.91\right)$$

where:

EVP= vapor pressure, kPa

T= temperature, °K

In 1983, Alston et al.(15) presented an empirical correlation which accounts for the effects of volatile and intermediate components in the reservoir oil and the injected CO₂. The volatile components are considered to be methane and nitrogen and the intermediates are comprised of CO₂, H₂S, and C₂ through C₄. The minimum miscibility pressure of an oil which is essentially devoid of volatile and intermediate components is given by:

$$\text{MMP}_{\text{sto}} = 8.78 \times 10^{-4} (T)^{1.06} (\text{MWC}_{5+})^{1.78}$$

for a live oil, a correction factor is applied:

$$MMP_{live} = MMP_{sto} \times (vol/int)^{0.136}$$

where:

MMP= minimum miscibility pressure, psia

T= reservoir temperature, °F

MWC₅₊= molecular weight of the C₅₊ fraction

vol/int= the ratio of the mole fractions of volatile
and intermediate components in the oil

for CO₂ streams containing N₂, H₂S, or C₁-C₄, the pseudo-critical temperature of the injection gas is calculated using a weight fraction mixing rule:

$$T_{cm} = \sum w_i T_{ci} - 459.7$$

where:

w_i= weight fraction of contaminant in CO₂ stream

T_{cm}= pseudo-critical temperature, °F

T_{ci}= critical temperature of contaminant, °R

Note: for C₂, and H₂S use apparent value of 585 °R

the correction factor for the impure stream is given by:

$$F_{impure} = (87.8/T_{cm})^{(1.935 \times 87.8/T_{cm})}$$

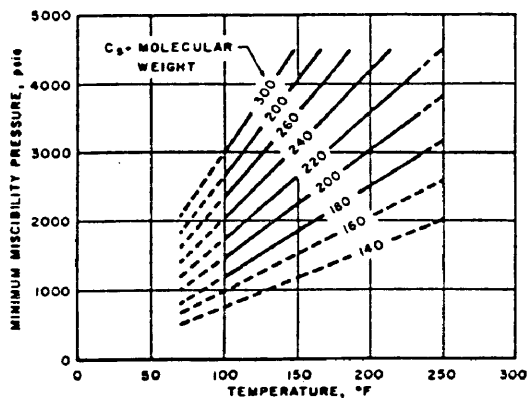
the corrected minimum miscibility pressure is given by:

$$MMP_{\text{impure}} = MMP_{\text{sto or live}} \times F_{\text{impure}}$$

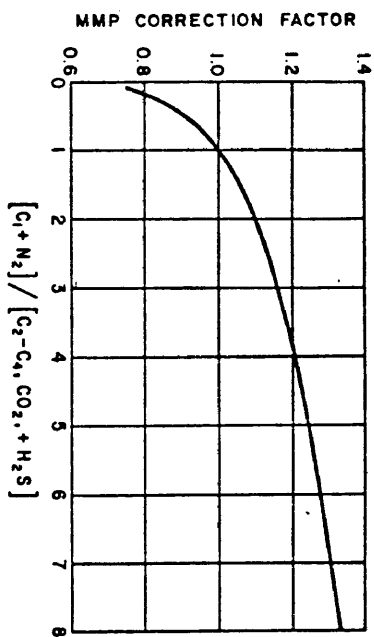
If the calculated MMP is below the bubble point pressure, the MMP is taken as the bubble point. The correlation is also shown in graphical form in Figure 20. The minimum miscibility pressure for a dead oil is given by Figure 20a, the live oil correction by Figure 20b, and the correction for an impure CO₂ stream by Figure 20c.

In 1984, Sebastian et al.⁽³¹⁾ presented a correction factor for impure CO₂ streams which is similar to that of Alston et al.⁽¹⁵⁾. It is also based on the pseudo-critical temperature of the injection gas although the mole fraction mixing rule is used rather than the weight fraction rule. The minimum miscibility pressure for pure CO₂ is simply multiplied by the appropriate correction factor to predict the MMP for a contaminated CO₂ stream. This work does not address the prediction of MMP for pure CO₂ streams, however.

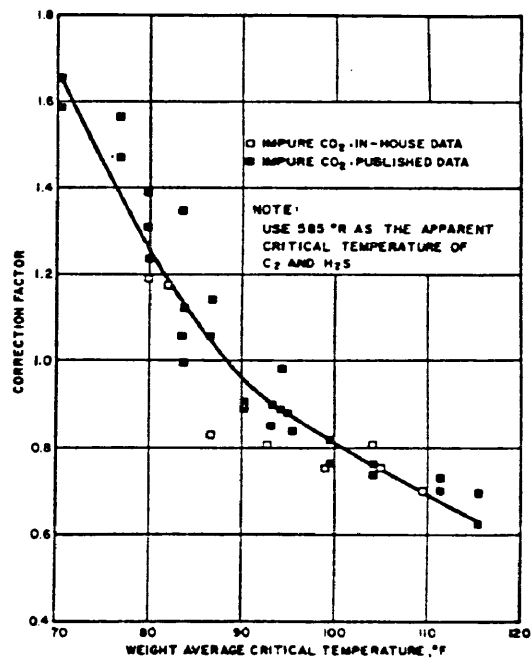
In 1984, Glaso⁽³²⁾ proposed a correlation for CO₂ minimum miscibility pressure which is based on the condensing gas drive data of Benham et al.⁽²⁸⁾. It appears that the author has fit equations to the Benham curves and



a) Dead Oil MMP



b) Live Oil Correction



c) Impure CO₂ Stream Correction

Figure 20. CO₂ MMP Correlation of Alston et al. (15)

has assumed CO₂ to be equivalent to a mixture of 58 percent methane and 42 percent propane. The author presents an equation for calculating CO₂ MMP from the reservoir temperature and the molecular weight of the C₇₊ fraction of the stock tank oil. An equation is also presented which reportedly accounts for the presence of C₂-C₆ in the oil. This equation has as an added parameter the mole percent C₂-C₄ in the reservoir oil. In the charts published by Benham et al. (28) C₅₊ is used as the crude oil heavy fraction. This may account for a "corrected C₇₊ molecular weight" term which appears in the development of the Glaso correlation but is not explained. No justification is given for the use of the C₂-C₄ content to account for the presence of C₂-C₆ in the reservoir oil. The Glaso correlation does not appear to be well grounded and is not shown in this report.

A modification of Holm and Josendal's (18) second correlation was proposed by Silva et al. (22) in 1984. Holm and Josendal (18) correlated the CO₂ density required for miscibility with the amount of extractable hydrocarbons in the crude expressed as the weight fraction (C₅-C₃₀)/C₅₊. Silva et al. (22) have replaced this parameter with a more detailed compositional parameter which also accounts for the fact that CO₂ extracts smaller

hydrocarbon molecules more efficiently than it extracts larger molecules. Partition coefficients--defined as the weight fraction of a hydrocarbon group in the CO₂-rich phase divided by the weight fraction in the oil-rich phase--for single carbon number groups were determined experimentally for mixtures of Maljamar crude with CO₂. This data is shown in Figure 21 along with the straight line relationship between carbon number and partition coefficient used in the correlation. The authors assume that near the MMP, the partition coefficients are independent of temperature, pressure, and composition. The proposed correlating parameter is calculated for the C₂₊ fraction of the oil from a weight fraction mixing rule and the partition coefficients as follows.

$$F = \sum_{i=2}^{37} k_i w_i$$

where:

i = carbon number from C₂ to C₃₇₊

w_i = weight fraction of single carbon number group

and

$$k_i = 10[-0.041(i) + 0.477]$$

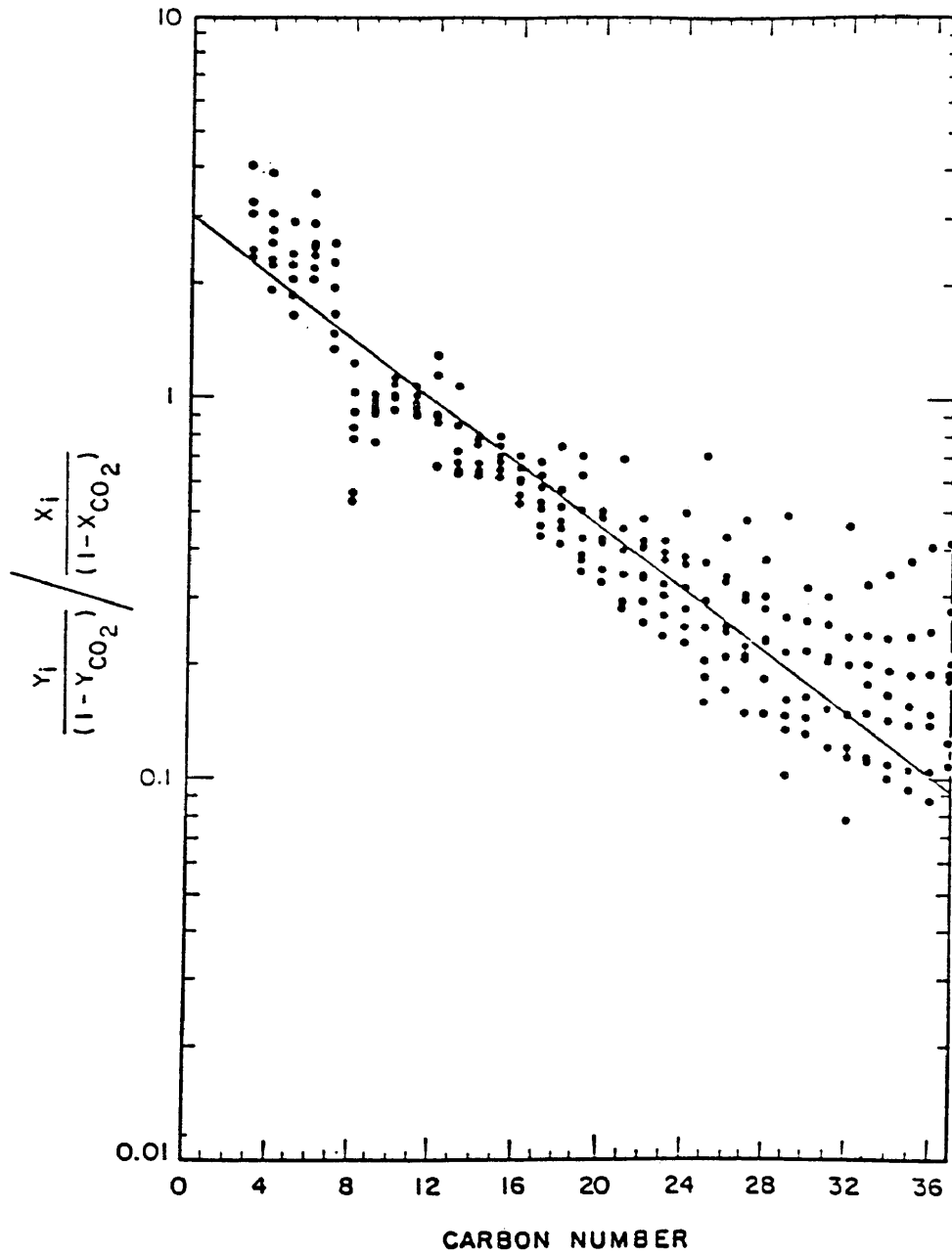


Figure 21. Hydrocarbon Partitioning Coefficient Data of Silva et al. (22)

the empirical relationship between F and the CO_2 density at the minimum miscibility pressure is:

$$\rho_{\text{MMP}} = -0.986(F) + 1.194 \quad \text{for } F < 0.785$$

$$\rho_{\text{MMP}} = 0.42 \quad \text{for } F \geq 0.785$$

The MMP is the pressure required to obtain this CO_2 density at reservoir temperature and can be determined from data such as that in Figure 19b. If this pressure is below the bubble point, the MMP is set equal to the bubble point pressure.

In 1985, Enick et al.⁽³³⁾ proposed a correlation based on modeling a CO_2 -crude system with a binary composed of CO_2 and a normal alkane of the same molecular weight as the C_{5+} fraction of the crude oil. The authors equate the minimum miscibility pressure of the crude oil with the critical pressure of the CO_2 /n-alkane binary. It is correctly stated that for the binary system, the cricondenbar on the P-X diagram is the first contact miscibility pressure for CO_2 with that alkane. (Note: the terms critical pressure and cricondenbar are used interchangeably in this reference which leads to some confusion. The term cricondenbar is usually used to denote the maximum pressure at which two phases can exist on a pressure-temperature diagram. The authors do not make it

clear that they are referring to the maximum pressure on a P-X diagram where, for binary systems which show only vapor-liquid behavior, the cricondenbar and critical pressure are equal. The only phase diagrams shown in this reference are P-T diagrams. There is only one binary composition for which the cricondenbar is equal to the critical pressure on such a diagram.) However, one of the most important concepts regarding multicontact or dynamic miscibility is that by in situ mass transfer between phases, miscibility can be developed at pressures far below the first contact miscibility pressure. Enick et al.⁽³³⁾ even state that the model used is not analogous to the mechanism by which CO₂ achieves miscibility. There does not, then, appear to be a good theoretical basis for predicting the MMP of a crude oil from the critical pressure of an equivalent molecular weight n-alkane/CO₂ binary.

The Peng-Robinson equation of state⁽³⁾ was used to calculate the critical loci for binary systems of CO₂ with the normal alkanes C₁₁ to C₁₈. This gives the correlation, shown in Figure 22, a range of C₅₊ molecular weights of 156 to 256. The authors found the accuracy of the proposed correlation to be poor for oils with an equivalent molecular weight above 190 at temperatures from approximately 77 to 122°F. This is not surprising since

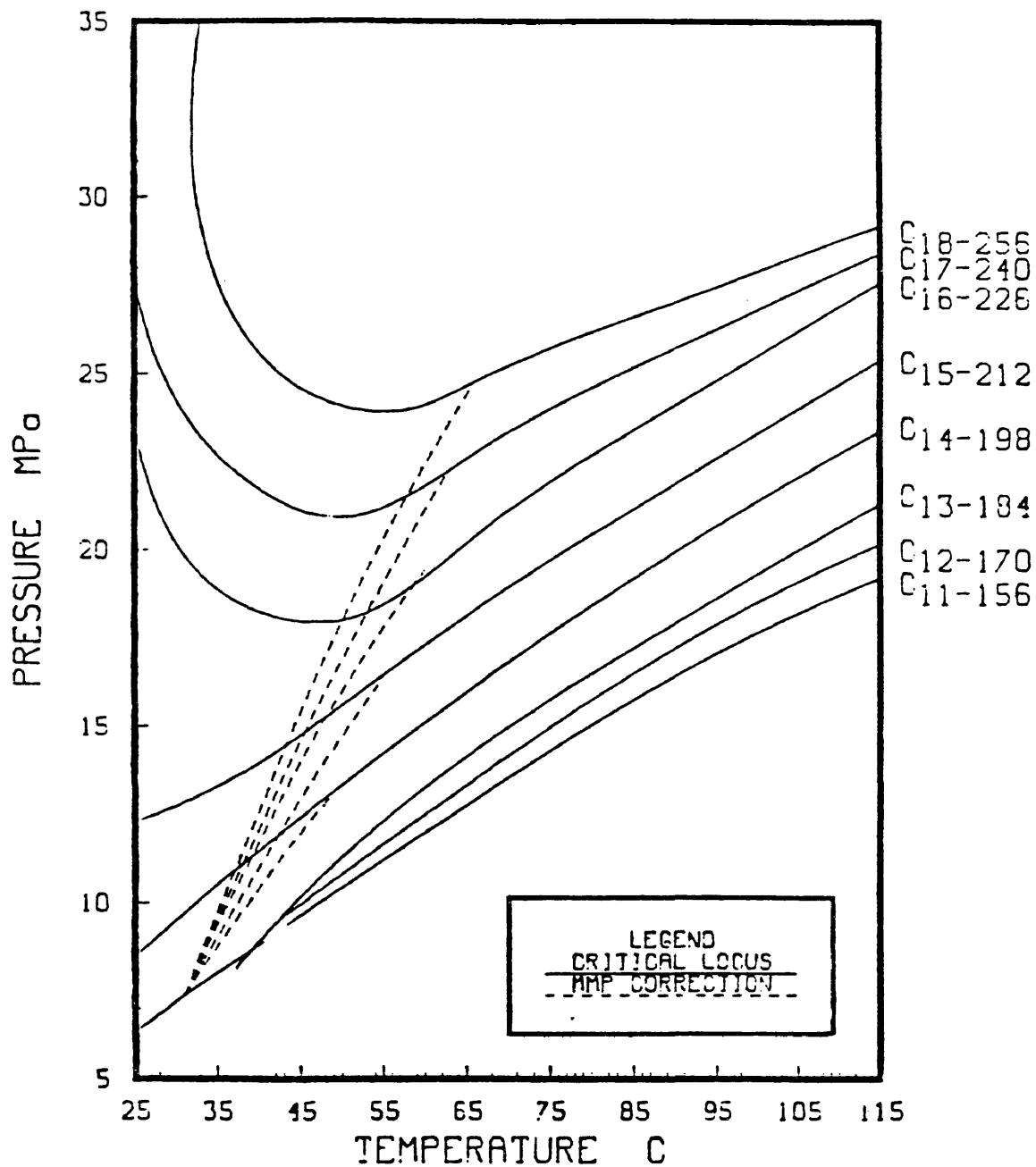


Figure 22. CO₂ MMP Correlation of Enick et al.(33)

this molecular weight corresponds to C_{14} and heavier hydrocarbons. The P-X diagrams for these hydrocarbons with CO_2 show liquid-liquid phase behavior at temperatures within this range⁽⁵⁾ and under these conditions the critical pressure and the P-X cricondenbar are not equal. To correct for this, the critical loci for these hydrocarbons were extrapolated to the critical temperature and pressure of CO_2 . Additional charts were presented which correct the MMP for impurities in the CO_2 stream and volatile and intermediate components in the oil, however, they are not included here.

Four minimum miscibility pressure correlations are described in Reference 33 which were not examined for this report. A correlation by Dumyuskin and Namiot⁽³⁴⁾ was proposed in 1978 which also equates the MMP with the critical pressure of a binary system of CO_2 with a normal alkane having the same molecular weight as the C_{5+} fraction of the crude. Two correlations were proposed by the Petroleum Recovery Institute⁽³⁵⁾ in 1979, one is an empirical correlation of MMP with reservoir temperature, the other estimates MMP from the extrapolated vapor pressure of CO_2 . A modification of the second Holm and Josendal⁽¹⁸⁾ correlation was also proposed by Orr and Jensen⁽³⁶⁾ in 1983, wherein the Peng-Robinson equation of state was used

to calculate the pressure necessary to obtain the specified densities for CO₂ which contains impurities.

Clearly, there is no shortage of correlations for estimating CO₂ minimum miscibility pressure. A credible correlation must adhere to the basic definition of MMP which is the lowest pressure at which dynamic miscibility with CO₂ can be generated. Many of the proposed correlations fail in this respect by equating MMP with the vapor pressure of CO₂ or the critical pressure of a CO₂-alkane binary, or considering "equivalent" hydrocarbon solvents in place of CO₂. Ideally, a correlation should also account for each parameter which affects MMP, but many do not even fully account for the effect of oil composition, or use an inadequate method of characterizing the crude such as API gravity. The correlations which do account for essentially all parameters are not based on the phase behavior principles of the miscible process, but are rather regression analyses of slim tube data. This is not to say that none of the proposed correlations should be used, on the contrary, many have proven to be fairly accurate and can be valuable tools. Even the simplest correlations may serve a purpose when high quality data is not available. It is important, however, that the user of a correlation understand its basis and limitations since it is never known beforehand how accurate the correlation will be.

Applications of Equations of State and Simulation

The practice of predicting the phase behavior of hydrocarbon systems with an equation of state (EOS) is rapidly gaining acceptance by the petroleum industry. EOS based computer programs are often used to predict data which would be costly and time consuming to obtain in the lab. An early application of this technology towards predicting miscibility conditions was the multiple-cell model used by Metcalfe et al.⁽³⁷⁾ in 1973. The condensing gas drive process was simulated by a series of batch contacts where the compositions of the equilibrium gas and liquid phases were determined by flash calculations utilizing the Redlich-Kwong EOS. The authors obtained good results with this model, however they stated it was not known whether the model could be used for the vaporizing gas drive process.

In 1985, Firoozabadi and Aziz⁽³⁸⁾ used the Peng-Robinson EOS in what appears to be a similar model (it is not described in detail) to calculate the vaporizing gas drive MMP for three reservoir fluids when the injection gas is primarily methane. The calculated MMPs were substantially higher than the experimental values for two of the fluids, and the authors concluded that this appears to be a limitation of equations of state of this type. The oils used were only analyzed up to C₁₀₊, although the

analysis was extended by the technique of Katz and Firoozabadi⁽³⁹⁾ to C₁₅₊, and it is not indicated if the EOS was calibrated to match experimental PVT data. Therefore, it seems that rather than an inherent fault in the Peng-Robinson EOS, the overprediction of MMP could just as easily be due to an improperly calibrated EOS.

In 1980, Williams et al.⁽⁴⁰⁾ used the Peng-Robinson equation of state to predict pseudoternary phase diagrams and the associated tie lines for a reservoir fluid. A mixture of the three pseudocomponents was arbitrarily selected on the triangular diagram and a detailed composition was calculated using the correct proportions of individual hydrocarbons within the pseudocomponent groups. The EOS was used to perform a flash calculation for this mixture at the temperature and pressure of interest. The equilibrium gas and liquid compositions were then reduced to the pseudocomponent compositions for display on the triangular diagram. This procedure was repeated until the phase envelope was suitably defined. From the extension of the limiting tie line, the composition of an injection gas for which condensing gas drive miscibility should be possible was defined, along with two gases which should not develop miscibility. Slim tube displacements were conducted and, as predicted, oil recovery indicative of miscibility

was obtained with the first gas while poor recoveries were obtained with the other two. The procedure was only tested for the condensing gas drive mechanism and with just one reservoir fluid, however, the authors state that application to the CO₂ or N₂ vaporizing gas drive process may be possible.

A slightly different technique for calculating pseudoternary phase envelopes was proposed by Wu et al.⁽⁴¹⁾ for the design of enriched gas drive injection fluids. Rather than arbitrarily selecting the mixtures to be flashed, these authors recommend choosing mixtures which lie on a line parallel to the methane-intermediates side of the pseudoternary diagram (A-A' in Figure 23). Such a line can be thought of as representing fixed mole fraction combinations of reservoir oil and solvent, where the solvent varies from lean to rich. In order to define the region near the critical point, this line of compositions should pass through the critical point or fairly near it, and it is suggested that oil mole fractions between 0.05 and 0.15 be tried initially. The actual location of the critical point is found graphically by intersecting the tie line bisector with the phase boundary, and the limiting tie line is obtained graphically also. This technique was used with the Peng-Robinson EOS to predict the injection fluid

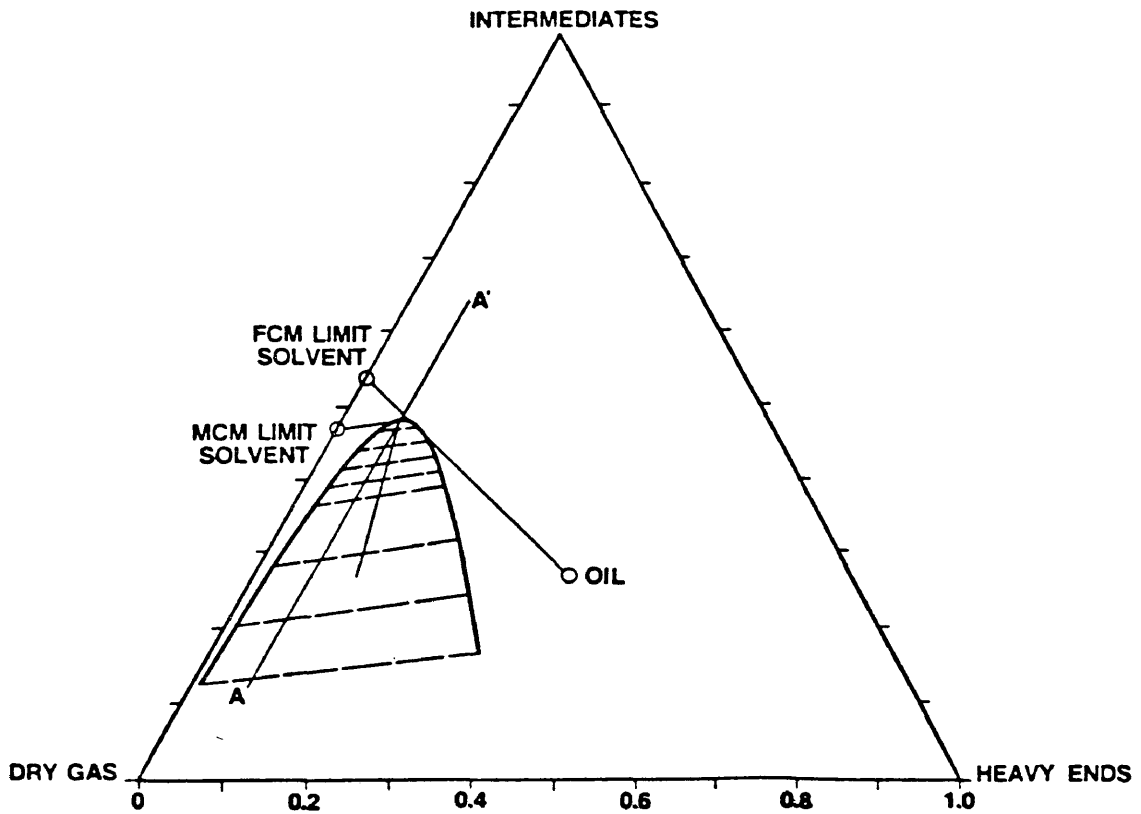


Figure 23. Pseudoternary Diagram Construction Method of Wu et al. (41)

compositions which would yield first contact miscibility for three reservoir fluids at specified design pressures. The minimum pressure for dynamic miscibility with these injection fluids was also estimated. Solvents having these compositions were prepared and used in slim tube displacements of the three oils. For first contact miscibility, the predictions are in excellent agreement with the slim tube results. The estimated MMPs (dynamic miscibility) are in poorer agreement. However, because of the criteria used to define miscibility (90% recovery at 1.2 PV injected) the MMP reported for two of the oils was found by extrapolation and was below the bubble point pressure. The validity of this interpretation is not known, but Yellig and Metcalfe⁽¹⁷⁾ have cautioned against defining miscibility by an arbitrary recovery level.

Hagoort and Dumore⁽⁴²⁾ have proposed a different calculational procedure for determining MMP with an equation of state. On a pseudoternary diagram at pressures below the MMP, a tie line exists which intersects the reservoir oil composition for a vaporizing gas drive or the injection gas composition for a condensing gas drive. The proposed method is based on the premise that as the pressure is increased, the K-values associated with this tie line approach unity and finally converge at the MMP. This is illustrated in

Figure 24 where the solid lines represent the pseudocomponent K-values. In the algorithm given by the authors, an initial pressure is selected which is below the MMP. A flash calculation is made with the EOS for a composition which is on the tie line that intersects the reservoir fluid (vaporizing gas drive) or the injection gas (condensing gas drive) which yields a set of K-values. The pressure is then incremented and the flash calculation is repeated which yields another set of K-values. For the component with a K-value closest to unity, the pressure at unity is found by linear extrapolation (dashed line in Figure 24). The pressure is incremented again, another flash calculation is made, and the extrapolation is repeated. When the incremented pressure and the extrapolated pressure are equal or within a specified tolerance, that pressure is taken as the MMP. What is not explained is how the mixture to be flashed at each pressure is selected so that it lies on the tie line which passes through the reservoir fluid (or injection gas). A mixture cannot be arbitrarily chosen and expected to lie on the correct tie line, nor can the same mixture be flashed at each pressure.

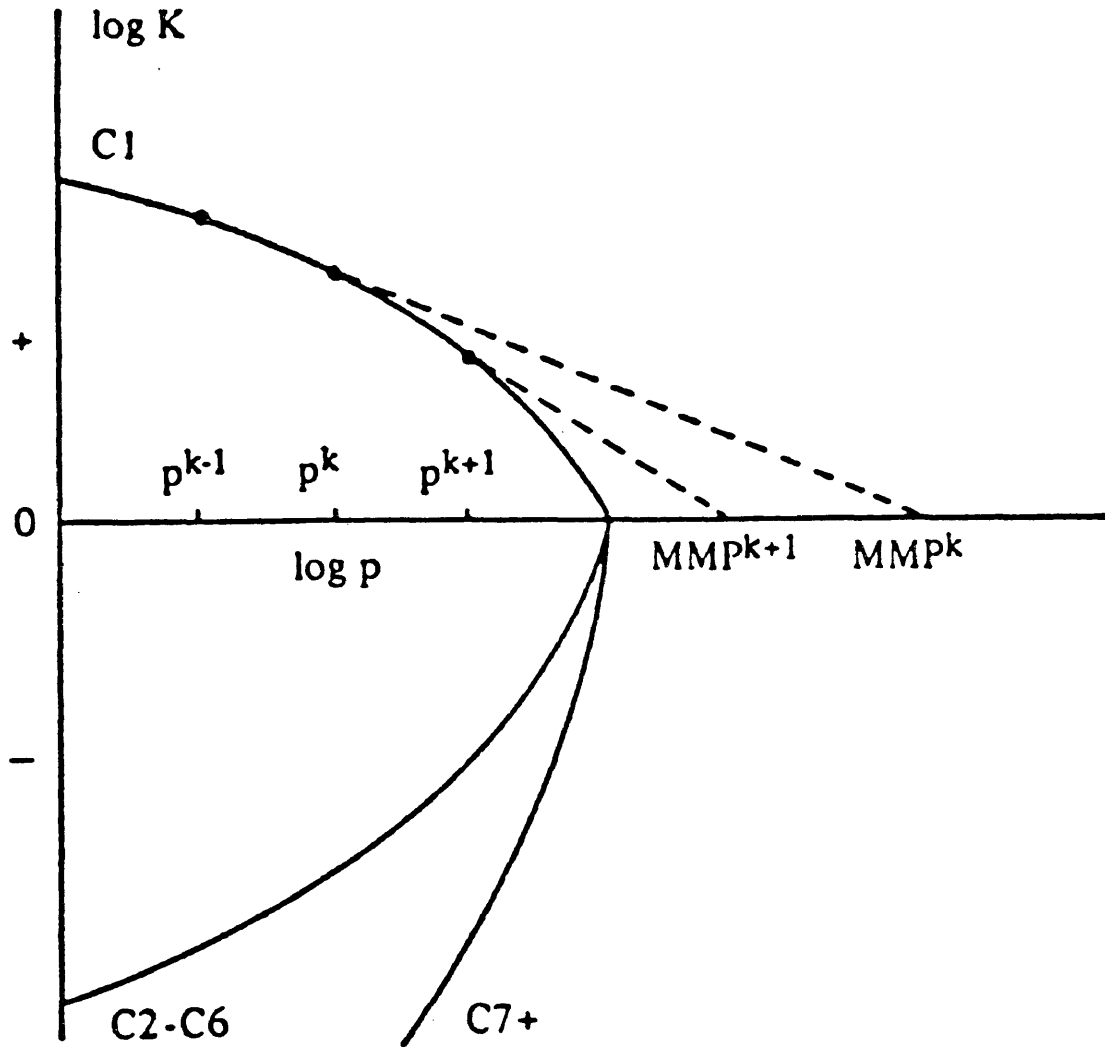


Figure 24. Determination of MMP from Extrapolation of K-values (After Hagoort and Dumore⁽⁴²⁾)

Researchers at the University of Kansas⁽⁴³⁾ used the Soave-Redlich-Kwong equation of state to generate pseudoternary phase diagrams for five crudes with CO₂. Three of the oils were Kansas crudes while the other two were from the literature. The exact procedure by which the phase boundary, tie lines, and critical point were calculated as well as the procedure for obtaining the limiting tie line and maximum miscibility composition is not discussed. It appears that a computer program was developed which performs all of these tasks. The slim tube MMP was known for each of the crudes and for all five, the MMP could be predicted accurately from calculated pseudoternary diagrams. It was necessary to adjust the binary interaction coefficients used in the EOS for different crudes, however. A single set of interaction coefficients which would correctly predict the MMPs for all five oils was not found. This is not surprising since the input parameters for all five crudes were calculated in basically the same way. The boiling point range, average boiling point, specific gravity, and molecular weight for the single carbon number groups were determined from the generalized properties of Katz and Firoozabadi as modified by Whitson⁽⁴⁴⁾. This data was used with the Lee-Kesler⁽⁴⁵⁾ correlations to calculate the critical temperature, critical pressure, and

acentric factor for each group. Also, PVT data was only available for one of the literature crudes (a P-X diagram bubble point curve) to calibrate the EOS before calculating pseudoternary diagrams.

Kuo⁽⁴⁶⁾ used the Peng-Robinson EOS to calculate condensing gas drive MMP by simulating the process with a series of flash calculations. Injection gas of a specified composition is combined with reservoir oil and the mixture is flashed at a given temperature and pressure. The liquid phase from the flash calculation is combined with additional injection gas and this mixture is flashed. The process is repeated until enrichment of the liquid phase ceases. At this point, if the composition of the liquid phase and vapor phase are identical the critical point composition has been reached and the pressure of the flash calculations is the MMP. If the compositions are different, they define a tie line which intersects the injection gas composition and the pressure is below the MMP. In this case, the pressure is increased and the entire process is repeated. The author calculated miscibility conditions for four reservoir fluids and several injection gases with this procedure and used the data to develop a correlation for determining the maximum allowable methane content in an injection fluid. A limited test showed that the correlation performs slightly better than the correlation of Benham et al.⁽²⁸⁾

Another technique which could prove to be a very useful tool in studying the effect of phase behavior on the miscible process is numerical simulation. In fact, Gardner et al.(11) stated that a quantitative interpretation of the effect of phase behavior requires the use of a simulator. These authors obtained very good results when a simple one-dimensional simulator was used to calculate the displacement efficiency of CO₂. Pseudoternary diagrams constructed from experimental data were used to represent CO₂-crude phase behavior at two pressures. Second degree polynomials were fit to the phase boundaries and it was assumed that the tie lines in any region all intersect at one point. Gravity and capillary pressure are neglected, relative permeabilities are a function of saturation only, and physical dispersion is modeled by numerical dispersion. The level of dispersion can be controlled by adjusting the size of the grid blocks and time steps. With a low dispersion level, characteristic of slim tube displacements, the calculated oil recovery as a function of CO₂ injection volume was in excellent agreement with slim tube data. This is very impressive when it is considered that liquid-liquid and liquid-liquid-vapor phase behavior occur at the two pressures considered.

A similar model was used by Orr, Yu, and Lien⁽⁹⁾ to simulate the displacement of a different crude by CO₂. It is explained that the model follows the convection of CO₂ and two hydrocarbon pseudocomponents which can be distributed in three hydrocarbon phases (two liquids and a vapor) and water. The minimum miscibility pressure determined from the calculated oil recovery versus pressure curve is in good agreement with the experimental value.

The University of Kansas researchers⁽⁴³⁾ used this model--modified to allow different CO₂ densities in the different phases--to simulate slim tube displacements for five crudes. Pseudoternary diagrams which were calculated with an equation of state rather than determined experimentally were used to represent the phase behavior of four of these systems. The pseudoternary diagram for the fifth oil is from the literature. The authors compared calculated oil recovery as a function of CO₂ injection volume and as a function of pressure to the actual slim tube data. The results are generally quite good, however, when oil recovery as a function of pressure is considered there is some uncertainty. In this comparison the recoveries must all be referenced to the same point in the displacement, which for certain slim tube data was CO₂ breakthrough. The authors stated that the point corresponding to breakthrough was not known precisely for the calculated

displacements. It is reported that the modification which allows for the variation in CO₂ density between the different phases significantly improved the accuracy of the calculated displacements. The CO₂ density in the liquid phase was also used as a history matching parameter.

One of the more encouraging aspects of the results obtained by Gardner et al.⁽¹¹⁾, Orr, Yu, and Lien⁽⁹⁾, and the group at the University of Kansas⁽⁴³⁾ is the good quantitative agreement between simulated and actual displacements in view of the simple phase behavior representations used. Good results were obtained even with calculated pseudoternary diagrams. At the least, this seems to indicate that the pseudoternary representation, while not thermodynamically rigorous, adequately describes the phase behavior of the multiple contact CO₂ miscible process.

Although miscibility conditions which are sufficiently accurate for design purposes have been calculated with equations of state or numerical simulation, a considerable amount of experimental phase behavior data is required to apply these techniques. Miscibility conditions can generally be determined with less effort through laboratory displacement tests, therefore, this method is preferred over calculations. Nevertheless, calculational techniques provide a valuable means of studying the relationship between dynamic miscibility and phase behavior.

PREDICTING CARBON DIOXIDE-CRUDE OIL PHASE BEHAVIOR

Introduction

In this section, the Peng-Robinson equation of state⁽³⁾ is explained in some detail. The four crudes from the literature which are used in this study are then examined, and the published compositional and PVT data for each is presented. The development of pseudocomponent representations of the crudes for equation of state calculations is explained, along with the procedure for determining the required component properties and interaction coefficients. Finally, the experimental phase behavior of each CO₂-crude system is compared with equation of state predictions.

All equation of state calculations in this study were made with the microcomputer version of the Peng-Robinson equation of state program marketed under the name EQUIPHASE by D.B. Robinson and Associates.

Peng-Robinson Equation of State

Many semi-empirical equations of state are based on the premise that pressure P is the result of a repulsion pressure P_r and an attraction pressure P_a , such that:

$$P = P_r - P_a$$

The form of the equation proposed by Peng and Robinson⁽³⁾ is:

$$P = \frac{RT}{v-b} - \frac{a(T)}{v(v+b) + b(v-b)}$$

The parameter b corrects the system volume for the space occupied by the molecules. The parameter a is related to the attractive force between molecules and is temperature dependent. These parameters are determined empirically. For pure components, the values chosen by Peng and Robinson⁽³⁾ are:

$$b = 0.07780(RT_c/P_c)$$

$$a(T) = 0.45724(R^2T_c^2/P_c)\alpha$$

where:

$$\alpha^{1/2} = 1 + m(1 - T_r^{1/2})$$

$$m = 0.37464 + 1.54226\omega - 0.26992\omega^2$$

for mixtures, the following mixing rules are used:

$$b = \sum_i^n x_i b_i$$

$$a = \sum_i^n \sum_j^n x_i x_j (1 - \delta_{ij}) (a_i a_j)^{1/2}$$

the binary interaction coefficient δ_{ij} is an empirically determined parameter which characterizes the binary formed by component i and component j .

in all previous expressions:

P = pressure

T = temperature

v = molar volume

R = gas constant

P_c = critical pressure

T_c = critical temperature

T_r = reduced temperature

ω = Pitzer acentric factor

n = number of components

x = mole fraction (not specifically liquid phase)

i, j = component identifications

The Peng-Robinson equation of state (PR EOS) is expressed in terms of pressure, however, this is not convenient because molar volume is generally unknown. The equation can be rewritten in terms of the compressibility factor Z and appears as:

$$Z^3 - (1-B)Z^2 + (A-3B^2-2B)Z - (AB-B^2-B^3) = 0$$

where:

$$A = \frac{aP}{R^2T^2}$$

$$B = \frac{bP}{RT}$$

$$Z = \frac{Pv}{RT}$$

The cubic equation in Z may yield one or three real roots depending on the number of phases in the system. In the two-phase region, the largest root is taken as the compressibility factor of the vapor and the smallest as the compressibility factor of the liquid.

A criterion for two phases to be in equilibrium is that the fugacity (f) of each component must be equal in both phases.

The fugacity coefficient (ϕ) of component i in a mixture can be calculated from the following equation:

$$\ln \phi_i = \ln \frac{f_i}{x_i P} = \frac{b_i}{b} (Z-1) - \ln(Z-B) - \frac{A}{2.828B} \left(\frac{2 \sum x_i a_i b_i}{a b} \right) \\ \times \ln \left(\frac{Z+2.414B}{Z-0.414B} \right)$$

Vapor-liquid equilibrium calculations can be made for a system of known composition if the equilibrium ratios or K-values can be determined. For each component, the K-value is merely the ratio of the liquid and vapor fugacity coefficients:

$$K_i = \frac{\phi_{iL}}{\phi_{iV}}$$

The actual computational procedure depends on the specific type of equilibrium calculation, however, an iterative solution is required. In general, the procedure is as follows:

1. From the specified mixture composition and component properties (P_C , T_C , ω) the cubic equation is solved for Z .
2. An initial set of K-values is assumed.

3. The appropriate equilibrium calculation is made.
4. The fugacity of each component in both phases is calculated.
5. The fugacities are compared to determine if they are equal in both phases for each component.
6. If the fugacities are not equal, the K-values (and any other variables being iterated on such as temperature or pressure) are adjusted in a logical manner and the process is repeated from Step 3.

If the fugacities are equal, the correct solution has been obtained.

Published Data

The literature was searched for reservoir fluid systems suitable for use in this study. In order to calibrate the Peng-Robinson equation of state⁽³⁾ (PR EOS), it was deemed necessary for the data published on each system to include an extended analysis of the crude, preferably with measured properties of the C₇₊ fractions, and experimental PVT data for mixtures of the crude with CO₂. Such data is understandably rare, nevertheless, five crudes which fit the requirements were located. Four crudes from the same source were selected for use in this study. They are from Grigg and Lingane⁽⁴⁷⁾ whose work specifically dealt with predicting CO₂-crude phase behavior with the PR EOS. The fifth crude was from Hong⁽⁴⁸⁾ whose work was also in this area. This crude was not used for two reasons. The analysis of the crude is not as complete as the others, consequently it could not be characterized in the same manner. Although Hong⁽⁴⁸⁾ presents "tuned" input parameters, it is not explained how these values were obtained. Also, the molecular weight of the C₆₋ and C₇₊ fractions of this crude are close in value to one of the crudes from Grigg and Lingane⁽⁴⁷⁾, thus the range of the proposed MMP correlation would not be extended.

The oils Grigg and Lingane⁽⁴⁷⁾ studied are the Ford Geraldine, West Sussex, and Maljamar crudes, and an oil referred to as Reservoir D crude. The respective reservoir temperatures are 83, 84, 90, and 220°F. Grigg and Lingane⁽⁴⁷⁾ report that samples of the four dead oils were analyzed by distillation and gas chromatography/mass spectrometry (GC/MS). Twelve cuts resulting from the distillation were divided into single carbon number groups by the gas chromatograph which separates hydrocarbons approximately in boiling point order. From the mass spectrometer, the amount of paraffinic, naphthenic, and aromatic (PNA) compounds in each fraction was identified. Accurate molecular weights were also calculated from the GC/MS data. The compositions of the recombined reservoir fluids were determined by combining solution gas and dead oil in the proper ratios. The compositions of the four recombined fluids along with the molecular weight and PNA analysis of each cut are given in Tables 1-4.

Table 1. Summary of GC/MS Data for Recombined Reservoir Fluid: Ford Geraldine Crude

Carbon No.	Mole Fraction	Molecular Weight	Fraction of Cut		
			Paraffin	Naphthene	Aromatic
1	0.1004	16.0	1.0	0.0	0.0
2	0.0791	30.0	1.0	0.0	0.0
3	0.1136	44.0	1.0	0.0	0.0
4	0.0736	58.0	1.0	0.0	0.0
5	0.0185	72.0	1.0	0.0	0.0
6	0.0452	85.6	0.820	0.180	0.0
7	0.0924	98.2	0.360	0.550	0.090
8	0.0812	111.8	0.390	0.450	0.160
9	0.0539	125.8	0.390	0.440	0.170
10	0.0485	139.8	0.420	0.400	0.180
11	0.0370	153.7	0.470	0.320	0.210
12	0.0341	166.8	0.340	0.340	0.320
13	0.0255	180.5	0.400	0.220	0.380
14	0.0236	195.0	0.460	0.220	0.320
15	0.0162	209.8	0.590	0.180	0.230
16	0.0151	224.4	0.710	0.120	0.170
18	0.0268	252.7	0.750	0.110	0.140
20	0.0202	281.0	0.790	0.120	0.090
22	0.0148	309.8	0.920	0.070	0.010
24	0.0136	337.8	0.920	0.080	0.0
26	0.0093	365.9	0.940	0.060	0.0
28	0.0086	393.9	0.950	0.050	0.0
30	0.0080	421.9	0.970	0.030	0.0
32	0.0051	449.9	0.970	0.030	0.0
34	0.0048	477.9	0.960	0.040	0.0
36	0.0045	505.9	0.970	0.030	0.0
38	0.0043	534.0	1.0	0.0	0.0
40	0.0019	562.0	1.0	0.0	0.0
42	0.0018	590.0	1.0	0.0	0.0
44	0.0018	618.0	1.0	0.0	0.0
45+	0.0164	692.0	1.0	0.0	0.0

Table 2. Summary of GC/MS Data for Recombined Reservoir Fluid: West Sussex Crude

Carbon No.	Mole Fraction	Molecular Weight	Fraction of Cut		
			Paraffin	Naphtthene	Aromatic
1	0.1217	16.0	1.0	0.0	0.0
2	0.0479	30.0	1.0	0.0	0.0
3	0.0487	44.0	1.0	0.0	0.0
4	0.0219	58.0	1.0	0.0	0.0
5	0.0227	72.0	1.0	0.0	0.0
6	0.0730	85.6	0.820	0.180	0.0
7	0.0970	98.2	0.130	0.860	0.010
8	0.0853	111.7	0.200	0.690	0.110
9	0.0766	126.3	0.470	0.730	0.100
10	0.0563	140.2	0.510	0.360	0.130
11	0.0446	153.6	0.470	0.300	0.230
12	0.0304	166.8	0.400	0.260	0.340
13	0.0247	180.9	0.490	0.170	0.340
14	0.0189	196.6	0.760	0.080	0.160
15	0.0211	211.6	0.930	0.030	0.040
16	0.0165	225.3	0.900	0.020	0.080
18	0.0294	253.1	0.880	0.010	0.110
20	0.0238	281.0	0.840	0.040	0.120
22	0.0216	309.9	0.980	0.010	0.010
24	0.0154	337.7	0.920	0.050	0.030
26	0.0142	366.0	0.980	0.020	0.0
28	0.0113	394.0	1.0	0.0	0.0
30	0.0134	422.0	1.0	0.0	0.0
32	0.0099	450.0	1.0	0.0	0.0
34	0.0053	478.0	1.0	0.0	0.0
36	0.0044	506.0	1.0	0.0	0.0
38	0.0042	534.0	1.0	0.0	0.0
40	0.0050	562.0	1.0	0.0	0.0
42	0.0038	590.0	1.0	0.0	0.0
44	0.0048	618.0	1.0	0.0	0.0
45+	0.0258	692.0	1.0	0.0	0.0

Table 3. Summary of GC/MS Data for Recombined Reservoir Fluid: Maljamar Crude

Carbon No.	Mole Fraction	Molecular Weight	Fraction of Cut		
			Paraffin	Naphthene	Aromatic
1	0.3025	16.0	1.0	0.0	0.0
2	0.1077	30.0	1.0	0.0	0.0
3	0.0915	44.0	1.0	0.0	0.0
4	0.0527	58.0	1.0	0.0	0.0
5	0.0247	72.0	1.0	0.0	0.0
6	0.0392	86.0	1.0	0.0	0.0
7	0.0496	98.4	0.420	0.500	0.080
8	0.0475	112.2	0.480	0.400	0.120
9	0.0495	125.6	0.450	0.340	0.210
10	0.0256	138.9	0.350	0.350	0.300
11	0.0267	152.7	0.380	0.280	0.340
12	0.0182	166.2	0.320	0.270	0.410
13	0.0149	179.0	0.230	0.190	0.580
14	0.0115	192.9	0.210	0.200	0.590
15	0.0128	207.4	0.290	0.180	0.530
16	0.0100	221.4	0.330	0.130	0.540
18	0.0178	249.6	0.400	0.060	0.540
20	0.0144	277.7	0.460	0.0	0.540
22	0.0131	305.7	0.460	0.0	0.540
24	0.0093	335.4	0.670	0.0	0.330
26	0.0085	365.2	0.900	0.0	0.100
28	0.0068	393.9	0.990	0.0	0.010
30	0.0080	422.0	1.0	0.0	0.0
32	0.0059	450.0	1.0	0.0	0.0
34	0.0032	478.0	1.0	0.0	0.0
36	0.0026	506.0	1.0	0.0	0.0
38	0.0025	534.0	1.0	0.0	0.0
40	0.0032	562.0	1.0	0.0	0.0
42	0.0021	590.0	1.0	0.0	0.0
44	0.0029	618.0	1.0	0.0	0.0
45+	0.0154	692.0	1.0	0.0	0.0

Table 4. Summary of GC/MS Data for Recombined Reservoir Fluid: Reservoir D Crude

Carbon No.	Mole Fraction	Molecular Weight	Fraction of Cut		
			Paraffin	Napththene	Aromatic
1	0.2268	16.0	1.0	0.0	0.0
2	0.0883	30.0	1.0	0.0	0.0
3	0.0792	44.0	1.0	0.0	0.0
4	0.0499	58.0	1.0	0.0	0.0
5	0.0334	72.0	1.0	0.0	0.0
6	0.0395	86.0	0.943	0.057	0.0
7	0.0321	98.1	0.480	0.370	0.150
8	0.0396	111.5	0.470	0.290	0.240
9	0.0401	125.6	0.490	0.280	0.230
10	0.0316	139.6	0.540	0.210	0.250
11	0.0248	152.6	0.440	0.180	0.380
12	0.0289	165.8	0.360	0.160	0.480
13	0.0281	179.7	0.360	0.130	0.510
14	0.0209	193.3	0.310	0.130	0.560
15	0.0213	207.1	0.300	0.110	0.590
16	0.0181	222.7	0.530	0.070	0.400
18	0.0317	250.2	0.470	0.070	0.460
20	0.0250	277.5	0.390	0.060	0.550
22	0.0213	307.9	0.710	0.030	0.260
24	0.0180	336.2	0.740	0.040	0.220
26	0.0121	364.1	0.740	0.030	0.230
28	0.0132	392.2	0.780	0.0	0.220
30	0.0111	419.4	0.670	0.0	0.330
32	0.0083	442.0	0.0	0.0	1.0
34	0.0051	470.0	0.0	0.0	1.0
36	0.0061	498.0	0.0	0.0	1.0
38	0.0060	526.0	0.0	0.0	1.0
40	0.0034	554.0	0.0	0.0	1.0
42	0.0022	582.0	0.0	0.0	1.0
44	0.0031	610.0	0.0	0.0	1.0
45+	0.0310	692.0	0.0	0.0	1.0

Single-contact (static) phase behavior experiments were also performed with the four recombined fluids. In a typical experiment, measured amounts of CO₂ and crude oil are charged to a high-pressure, variable volume, windowed cell which is maintained at reservoir temperature⁽¹²⁾. The pressure of the cell is increased until the mixture forms only one phase. The pressure is then reduced in small increments with volume measurements taken after each step. When more than one phase forms, the volume of each phase is determined by visual observation. The bubble point pressure is determined by a discontinuity on the pressure versus volume plot. More CO₂ is metered into the cell and the process is repeated. Using this technique, Grigg and Lingane⁽⁴⁷⁾ measured bubble points, dewpoints, and phase volumes for the Ford Geraldine, West Sussex, and Maljamar crudes up to approximately 90 mole percent CO₂. For the experiments with the Reservoir D fluid a blind PVT cell was used and the only data measured was bubble point pressure up to 65 mole percent CO₂. The smoothed experimental data appear in Tables 5-8.

Table 5. Pressure versus Volume Fraction Heavier Phase and Carbon Dioxide Content: Ford Geraldine Crude 83°F

XC02	Volume Fraction Lower Phase												
	0.00	0.10	0.15	0.20	0.30	0.35	0.40	0.50	0.60	0.70	0.80	0.90	1.00
0.0													440
0.12													580
0.25													721
0.34													815
0.39													865
0.44													906
0.48													935
0.51													955
0.57													972
0.70													1450
0.78				880	910		930	950	980	2340	2520	2620	2700
0.80				930	940								
0.80R	3440	2990		2400	1680	1290							
0.90								950					
0.90R								2200					
0.90R								4600					

Note: R Denotes Retrograde Data

Table 6. Pressure versus Volume Fraction Heavier Phase and Carbon Dioxide Content: West Sussex Crude 940F

XCO ₂	Volume Fraction Lower Phase									
	0.00	0.25	0.40	0.50	0.55	0.60	0.70	0.80	0.90	1.00
0.0										440
0.20										794
0.40										1184
0.50										1244
0.55										1319
0.60										1574
0.65										1734
0.70										2034
0.75			966	1060		1120	1300	2540	2860	
0.80			1190	1240	1280					
0.80R					4000					
0.90		2430								
0.90R		3000								
0.90R		5000								

Note: R Denotes Retrograde Data

Table 7. Pressure versus Volume Fraction Heavier Phase and Carbon Dioxide
 Content: Maljamar Crude 94°F

XC02	Volume Fraction Lower Phase										
	0.00	0.10	0.20	0.30	0.40	0.50	0.60	0.70	0.80	0.90	1.00
0.0								880	1030	1230	1583
0.25						980	920	1035	1192	1386	1748
0.40					880	880	1100	1250	1394	1539	1830
0.54					973	1091	1202	1338	1498	1705	2020
0.61				880	1043	1161	1278	1394	1577	2115	2340
0.62				920	1083	1210	1318	1448	2382	2446	2478
0.70				970	1135	1260	1375				
0.70R	3552	3265	3080	2930	2798	2692					
0.72				1010	1170	1330					
0.72R				3015	2120						
0.84											
0.84R	4330	4175	2820	1095							

Note: R Denotes Retrograde Data

Table 8. Saturation Pressure versus CO₂ Content:
Reservoir D Crude 220°F

Mole Fraction CO ₂	Saturation Pressure (psia)
0.0	1484
0.18	1908
0.32	2449
0.50	3088
0.59	3625
0.65	4060

Characterizing Hydrocarbon Fractions

The Peng-Robinson equation of state⁽³⁾ requires that the critical pressure, critical temperature, acentric factor, and molecular weight of each component in a system be specified. These properties have been measured for many pure compounds and are incorporated into the program library. Reservoir fluids, however, are composed of hundreds of different hydrocarbons. The heptanes and heavier components are generally lumped together into the C₇₊ fraction. This fraction is sometimes analyzed by distillation or chromatography, but all of the properties required for EOS predictions are not determined. It is necessary, then, to estimate certain properties of these heavy fractions. Several correlations which can be used for this purpose exist, although the choice of which correlation to use is somewhat limited by the type of data available i.e. distillation or chromatography. A good review of the subject is contained in a paper by Whitson⁽⁴⁴⁾.

The characterization procedure used in this study was proposed by Peng and Robinson⁽⁴⁹⁾ in 1978 and is the same procedure that was used by Grigg and Lingane⁽⁴⁷⁾. It is assumed that each fraction represents a single carbon number group and is composed of paraffins, naphthenes, and aromatics. It is further assumed that in each fraction the

naphthenes and aromatics have one less carbon atom than the paraffins. For each fraction, the properties of the three hydrocarbon types (PNA) are calculated individually using the following equations, then the overall properties of the fraction are calculated using the appropriate mixing rule.

Note: the assumption that naphthenes and aromatics have carbon numbers one less than paraffins is already accounted for in these equations.

Normal Boiling Point Temperature

The normal boiling point temperature T_b in $^{\circ}\text{K}$ is calculated for each hydrocarbon type from the following equations where n is the carbon number of the fraction.

$$\text{P: } \ln T_b = \sum_{i=1}^6 a_i (n-6)^{i-1}$$

$$\text{N: } \ln T_b = \sum_{i=1}^6 a_i (n-7)^{i-1}$$

$$\text{A: } \ln T_b = \sum_{i=1}^6 a_i (n-7)^{i-1}$$

where:

	<u>Paraffin</u>	<u>Naphthene</u>	<u>Aromatic</u>
$a_1 =$	5.83451830	5.85793320	5.86717600
$a_2 =$	$0.84909035 \times 10^{-1}$	$0.79805995 \times 10^{-1}$	$0.80436947 \times 10^{-1}$
$a_3 =$	$-0.52635428 \times 10^{-2}$	$-0.43098101 \times 10^{-2}$	$-0.47136506 \times 10^{-2}$
$a_4 =$	$0.21252908 \times 10^{-3}$	$0.14783123 \times 10^{-3}$	$0.18233365 \times 10^{-3}$
$a_5 =$	$-0.44933363 \times 10^{-5}$	$-0.27095216 \times 10^{-5}$	$-0.38327239 \times 10^{-5}$
$a_6 =$	$0.37285365 \times 10^{-7}$	$0.19907794 \times 10^{-7}$	$0.32550576 \times 10^{-7}$

Critical Pressure

The critical pressure P_C in atmospheres is calculated from a correlation proposed by Lydersen(50):

$$P: P_C = \frac{14.026n + 2.016}{(0.227n + 0.340)^2}$$

$$N: P_C = \frac{14.026n - 14.026}{(0.227n - 0.137)^2}$$

$$A: P_C = \frac{14.026n - 20.074}{(0.227n - 0.325)^2}$$

Acentric Factor

The acentric factor is calculated from the following linear equations:

$$P: \omega = 0.0432n + 0.0457$$

$$N: \omega = 0.0432n - 0.0880$$

$$A: \omega = 0.0445n - 0.0995$$

Critical Temperature

The critical temperature T_C in °K is calculated from the following equation where a correction factor S is applied to an equation originally proposed by Edmister(51):

$$T_C = S \times T_b \left(1 + \frac{3 \log P_C}{7(1+\omega)} \right)$$

where:

$$P: S = 0.996704 + 0.00043155n$$

$$N: S = 0.996704 + 0.00043155(n-1)$$

$$A: S = 0.996704 + 0.00043155(n-1)$$

Overall Properties

The following mixing rules are used to calculate the overall properties of each fraction from the properties of the three hydrocarbon types. The subscript i denotes paraffin, naphthene, and aromatic.

$$T_c = \sum x_i T_{ci}$$

$$P_c = \sum x_i P_{ci}$$

$$\omega = -\log\left[\frac{x_i P_{ci} 10^{-(1+\omega_i)}}{P_c}\right] - 1$$

This procedure was used to calculate the critical pressure, critical temperature, and acentric factor of the single carbon number groups C_7 and heavier in the four crudes used in this study. The properties of C_1 , C_2 , and C_3 were taken from the GPSA Engineering Data Book⁽⁵²⁾. The properties of C_4 , C_5 , and C_6 are as reported by Grigg and Lingane⁽⁴⁷⁾. This data, in the units required for input into the PR EOS, is shown in Tables 9-12.

Table 9. Properties of Single Carbon Number Groups
Ford Geraldine Crude

Carbon No.	Mole Fraction	Critical Values		Acentric Factor	Molecular Weight
		Pressure (atm)	Temp (°K)		
1	0.1004	45.4	190.5	0.013	16.0
2	0.0791	48.2	305.4	0.098	30.0
3	0.1136	41.9	369.8	0.154	44.0
4	0.0736	37.5	425.2	0.201	58.0
5	0.0185	33.2	473.4	0.262	72.0
6	0.0452	32.8	509.1	0.266	85.6
7	0.0924	36.0	545.8	0.246	98.2
8	0.0812	31.9	575.2	0.293	111.8
9	0.0539	28.5	601.8	0.338	125.8
10	0.0485	25.6	626.2	0.386	139.8
11	0.0370	23.2	648.5	0.436	153.7
12	0.0341	22.2	671.4	0.465	166.8
13	0.0255	20.4	689.7	0.516	180.5
14	0.0236	18.6	705.1	0.568	195.0
15	0.0162	16.9	717.7	0.628	209.8
16	0.0151	15.4	729.1	0.689	224.4
18	0.0268	13.7	752.4	0.783	252.7
20	0.0202	12.3	772.6	0.875	281.0
22	0.0148	11.0	789.2	0.982	309.8
24	0.0136	10.2	807.2	1.069	337.8
26	0.0093	9.5	823.9	1.159	365.9
28	0.0086	8.9	840.2	1.247	393.9
30	0.0080	8.3	855.3	1.337	421.9
32	0.0051	7.8	869.5	1.423	449.9
34	0.0048	7.4	882.4	1.508	477.9
36	0.0045	7.0	893.2	1.596	505.9
38	0.0043	6.7	902.0	1.687	534.0
40	0.0019	6.3	910.2	1.774	562.0
42	0.0018	6.1	918.3	1.860	590.0
44	0.0018	5.8	928.2	1.946	618.0
45+	0.0164	5.7	934.5	1.990	692.0

Table 10. Properties of Single Carbon Number Groups
West Sussex Crude

Carbon No.	Mole Fraction	Critical Values		Acentric Factor	Molecular Weight
		Pressure (atm)	Temp (°K)		
1	0.1217	45.4	190.5	0.013	16.0
2	0.0479	48.2	305.4	0.098	30.0
3	0.0487	41.9	369.8	0.154	44.0
4	0.0219	37.5	425.2	0.201	58.0
5	0.0227	33.2	473.4	0.262	72.0
6	0.0730	32.8	509.1	0.266	85.6
7	0.0970	38.3	546.5	0.225	98.2
8	0.0853	33.5	575.9	0.275	111.7
9	0.0766	27.5	600.2	0.348	126.3
10	0.0563	24.8	624.8	0.397	140.2
11	0.0446	23.2	648.7	0.436	153.6
12	0.0304	22.0	670.9	0.472	166.8
13	0.0247	20.0	688.2	0.527	180.9
14	0.0189	17.2	699.6	0.609	196.6
15	0.0211	15.4	711.2	0.681	211.6
16	0.0165	14.8	725.4	0.719	225.3
18	0.0294	13.4	749.8	0.803	253.1
20	0.0238	12.3	771.5	0.884	281.0
22	0.0216	11.0	787.9	0.993	309.9
24	0.0154	10.2	807.1	1.069	337.7
26	0.0142	9.4	823.2	1.165	366.0
28	0.0113	8.8	839.3	1.255	394.0
30	0.0134	8.3	854.8	1.342	422.0
32	0.0099	7.8	869.0	1.428	450.0
34	0.0053	7.4	881.7	1.514	478.0
36	0.0044	7.0	892.7	1.601	506.0
38	0.0042	6.7	902.0	1.687	534.0
40	0.0050	6.3	910.2	1.774	562.0
42	0.0038	6.1	918.3	1.860	590.0
44	0.0048	5.8	928.2	1.946	618.0
45+	0.0258	5.7	934.5	1.990	692.0

Table 11. Properties of Single Carbon Number Groups
Maljamar Crude

Carbon No.	Mole Fraction	Critical Values		Acentric Factor	Molecular Weight
		Pressure (atm)	Temp (°K)		
1	0.3025	45.4	190.5	0.013	16.0
2	0.1077	48.2	305.4	0.098	30.0
3	0.0915	41.9	369.8	0.154	44.0
4	0.0527	37.5	425.2	0.201	58.0
5	0.0247	33.2	473.4	0.262	72.0
6	0.0392	29.7	507.2	0.305	86.0
7	0.0496	35.2	545.1	0.253	98.4
8	0.0475	30.7	573.8	0.304	112.2
9	0.0495	28.2	601.9	0.344	125.6
10	0.0256	26.6	628.4	0.377	138.9
11	0.0267	24.1	650.9	0.425	152.7
12	0.0182	22.6	672.5	0.463	166.2
13	0.0149	21.6	693.6	0.499	179.0
14	0.0115	20.1	710.6	0.541	192.9
15	0.0128	18.3	724.1	0.593	207.4
16	0.0100	17.1	737.2	0.642	221.4
18	0.0178	15.0	759.9	0.739	249.6
20	0.0144	13.4	779.2	0.835	277.7
22	0.0131	12.2	797.6	0.924	305.7
24	0.0093	10.8	811.0	1.037	335.4
26	0.0085	9.6	824.2	1.154	365.2
28	0.0068	8.8	839.4	1.254	393.9
30	0.0080	8.3	854.8	1.342	422.0
32	0.0059	7.8	869.0	1.428	450.0
34	0.0032	7.4	881.7	1.514	478.0
36	0.0026	7.0	892.7	1.601	506.0
38	0.0025	6.7	902.0	1.687	534.0
40	0.0032	6.3	910.2	1.774	562.0
42	0.0021	6.1	918.3	1.860	590.0
44	0.0029	5.8	928.2	1.946	618.0
45+	0.0154	5.7	934.5	1.990	692.0

Table 12. Properties of Single Carbon Number Groups
Reservoir D Crude

Carbon No.	Mole Fraction	Critical Values		Acentric Factor	Molecular Weight
		Pressure (atm)	Temp (°K)		
1	0.2268	45.4	190.5	0.013	16.0
2	0.0883	48.2	305.4	0.098	30.0
3	0.0792	41.9	369.8	0.154	44.0
4	0.0499	37.5	425.2	0.201	58.0
5	0.0334	33.2	473.4	0.262	72.0
6	0.0395	30.7	507.8	0.291	86.0
7	0.0321	35.0	545.7	0.259	98.1
8	0.0396	31.6	575.8	0.301	111.5
9	0.0401	28.0	601.9	0.349	125.6
10	0.0316	25.0	626.1	0.400	139.6
11	0.0248	23.9	650.7	0.432	152.6
12	0.0289	22.6	672.8	0.467	165.8
13	0.0281	20.9	691.3	0.512	179.7
14	0.0209	19.7	708.9	0.551	193.3
15	0.0213	18.4	724.2	0.595	207.1
16	0.0181	16.3	733.1	0.665	222.7
18	0.0317	14.7	758.4	0.747	250.2
20	0.0250	13.5	780.7	0.827	277.5
22	0.0213	11.6	793.0	0.953	307.9
24	0.0180	10.6	810.0	1.045	336.2
26	0.0121	9.8	826.6	1.133	364.1
28	0.0132	9.1	841.6	1.226	392.2
30	0.0111	8.7	857.2	1.300	419.4
32	0.0083	8.9	873.2	1.324	442.0
34	0.0051	8.4	882.8	1.413	470.0
36	0.0061	7.9	891.2	1.502	498.0
38	0.0060	7.4	898.5	1.591	526.0
40	0.0034	7.1	905.2	1.680	554.0
42	0.0022	6.7	912.5	1.769	582.0
44	0.0031	6.4	922.0	1.858	610.0
45+	0.0310	6.2	928.2	1.903	692.0

Binary Interaction Coefficients

The binary interaction coefficient δ_{ij} is an empirical parameter which is generally determined by minimizing the deviation between calculated and experimental PVT data. The interaction coefficients between hydrocarbons of similar molecular structure and weight are near zero. For pairs of dissimilar hydrocarbons or hydrocarbons with non-hydrocarbons such as CO₂, nonzero interaction coefficients are required for accurate EOS predictions.

Several researchers have attempted to define optimum values for the binary interaction coefficients of the Peng-Robinson EOS. Kato et al.⁽⁵³⁾ proposed an empirical correlation where CO₂-n-paraffin interaction coefficients are a function of temperature and hydrocarbon acentric factor. Hong⁽⁴⁸⁾ also used interaction coefficients which were related to the hydrocarbon acentric factor. Whitson⁽⁴⁴⁾ compared PR EOS predictions when both the Kato⁽⁵³⁾ correlation and the Hong⁽⁴⁸⁾ guidelines were used to characterize the coefficients for the CO₂-reservoir oil system reported by Hong⁽⁴⁸⁾. The Kato⁽⁵³⁾ coefficients caused the saturation pressure to be seriously underestimated. Predictions using the Hong⁽⁴⁸⁾ coefficients were better, yet similar results were obtained when a constant value coefficient of 0.145 was used.

Whitson⁽⁴⁴⁾ concluded that there appears to be little advantage to using coefficients which are a function of molecular size, but that this may not be true if predictions are to be made near the critical point. In an extensive study of binary systems, Lin⁽⁵⁴⁾ determined interaction coefficients between CO₂ and a variety of hydrocarbons over a wide range of temperature and pressure. Although the coefficients varied from 0.089 for a system of CO₂ with propane to 0.180 for CO₂ with tetralin, it was found that a constant value of 0.125 represented the majority of the experimental data. Lin⁽⁵⁴⁾ also conceded that calculations in the critical region are more sensitive to the values of the interaction coefficients. Varotsis et al.⁽⁵⁵⁾ proposed empirical correlations for both CO₂-hydrocarbon interaction coefficients and methane-hydrocarbon coefficients. The CO₂ coefficients are correlated as a function of hydrocarbon acentric factor, temperature, and pressure while the methane coefficients are a function of only acentric factor and temperature.

Clearly there is no consensus on the factors which affect binary interaction coefficients, nor on the best values for these coefficients. Since they are basically an EOS parameter which is adjusted to bring predictions more in

line with experimental data, it is possible that evidence of a dependence on temperature, pressure, or even composition may be seen in some multicomponent systems. However, in addition to involving a considerable amount of extra work, it does not seem prudent to use interaction coefficients which vary with temperature or pressure unless experimental data is available to judge how this affects the accuracy of EOS predictions for the specific systems of interest.

Grigg and Lingane⁽⁴⁷⁾ determined interaction coefficients for a limited number of binary systems reported in the literature and used these values to develop a set of coefficients which was used for all four reservoir fluids. From this data, generalized relationships were developed as a part of this study to obtain interaction coefficients for pseudocomponent groupings which, for reasons which will be explained, are different from those used by Grigg and Lingane⁽⁴⁷⁾. These authors found that the CO₂ coefficients start at approximately 0.1 for methane and rise to 0.135 for propane, then decrease gradually to 0.1 for n-decane. These values are plotted against hydrocarbon molecular weight in Figure 25. The additional data points are from the common set of coefficients used by Grigg and Lingane⁽⁴⁷⁾ and are plotted at the average molecular weight of the appropriate hydrocarbon fraction. The methane

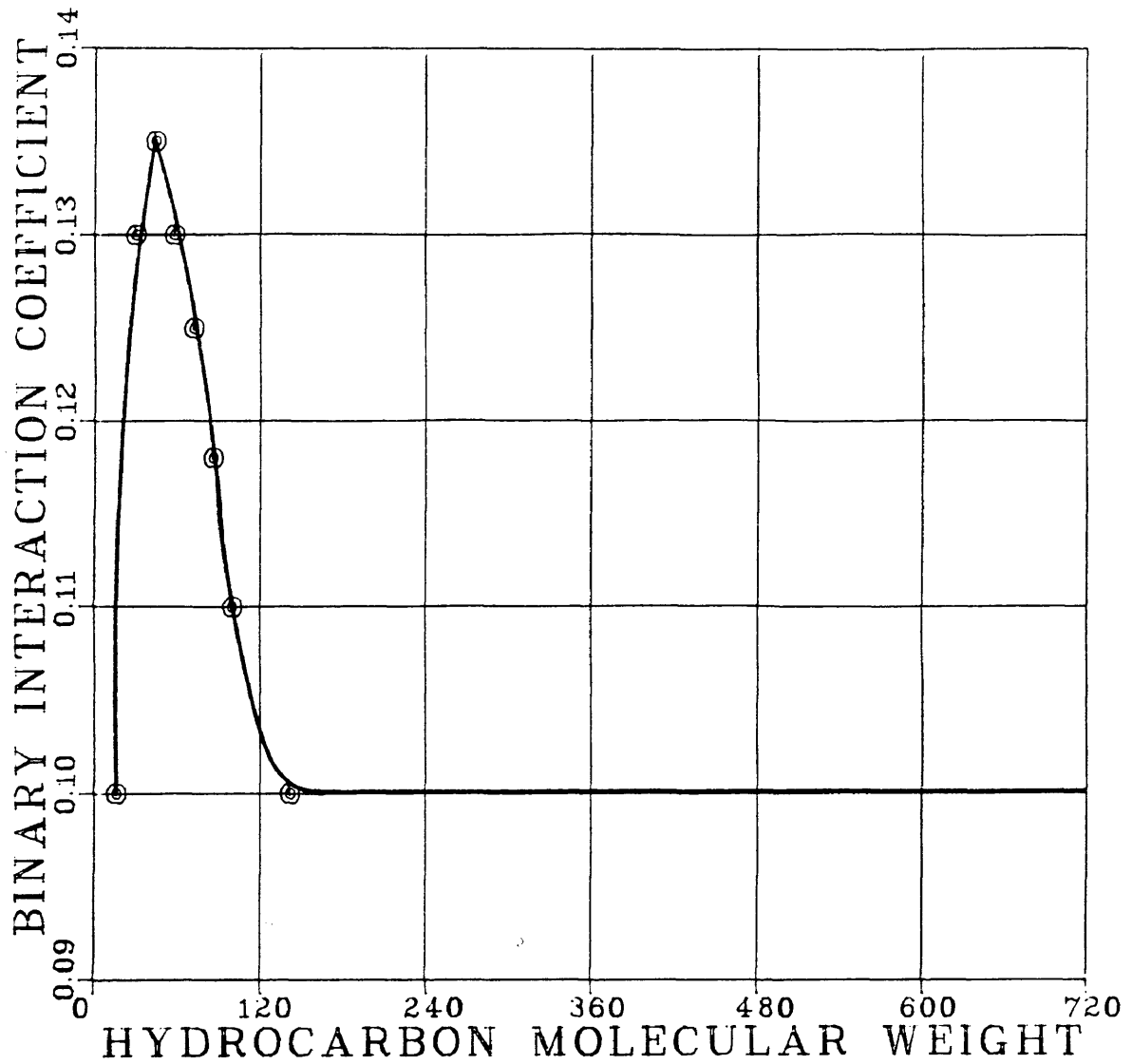


Figure 25. Relationship Between CO₂-Hydrocarbon Binary Interaction Coefficients and Hydrocarbon Molecular Weight

interaction coefficients were found to be approximately zero for hydrocarbons through C₁₀ and increase gradually to a maximum of 0.2 for C₂₂₊ components. The values used by Grigg and Lingane⁽⁴⁷⁾ are plotted in Figure 26 against the average molecular weight of the hydrocarbon fraction.

In many EOS applications the remaining hydrocarbon interaction coefficients (for example, between ethane or propane and the heavier hydrocarbons) are assumed to be zero. A current practice, however, is to assign nonzero values to these coefficients. Grigg and Lingane⁽⁴⁷⁾ found that this was necessary if the phase behavior in the retrograde region and near the critical point is to be predicted accurately. They report that literature data indicates the interaction coefficients for the other hydrocarbon pairs are approximately inversely proportional to the product of the carbon number of the lighter component and the interaction coefficient between the heavier hydrocarbon and methane. In equation form this appears as:

$$\delta_{C_n,H} = \frac{S}{n(\delta_{C_1,H})}$$

where:

$\delta_{C_n,H}$ = interaction coefficient between the light and heavy hydrocarbon

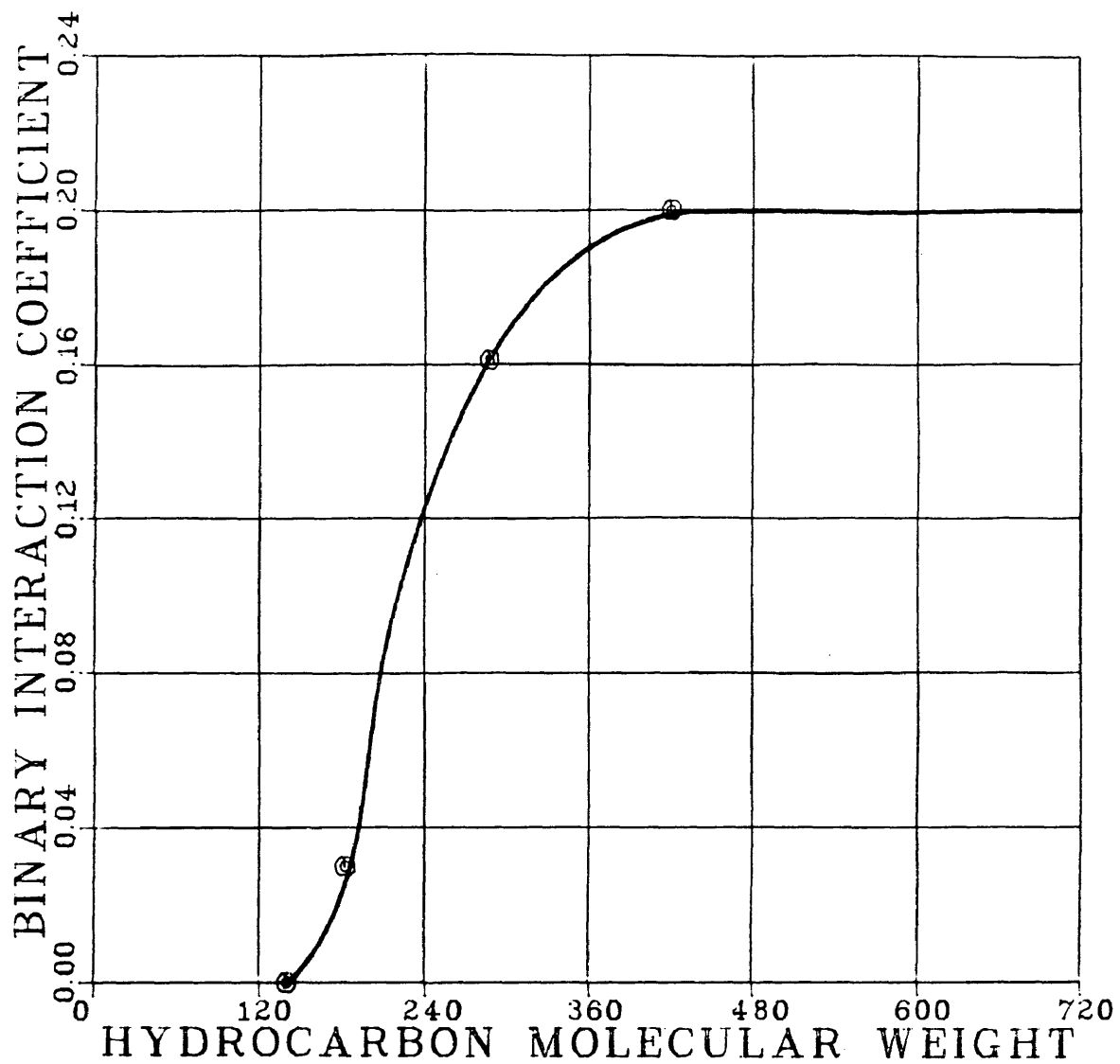


Figure 26. Relationship Between Methane-Hydrocarbon Binary Interaction Coefficients and Hydrocarbon Molecular Weight

$\delta_{C1,H}$ = interaction coefficient between methane and
the heavy hydrocarbon

n = carbon number of the light component

S = proportionality variable

The proportionality variable S is related to the molecular weight of the heavy hydrocarbon. The nature of this relationship was determined from the coefficients used by Grigg and Lingane⁽⁴⁷⁾ and is shown in Figure 27.

The binary interaction coefficients used in this study were obtained from the relationships of Figures 25-27. It will be shown that this proved adequate for three of the four CO₂-crude systems, but that some adjustment of the coefficients was required for the Maljamar crude. The decision to use interaction coefficients derived from the values reported by Grigg and Lingane⁽⁴⁷⁾ is not meant to imply that their work was more extensive than that of other investigators or is more definitive. The decision was largely based on the success these authors had with the four CO₂-crude systems used in this study and a desire to use a consistent method to determine the complete set of interaction coefficients. It is not known if the relationships used here can be applied to other systems.

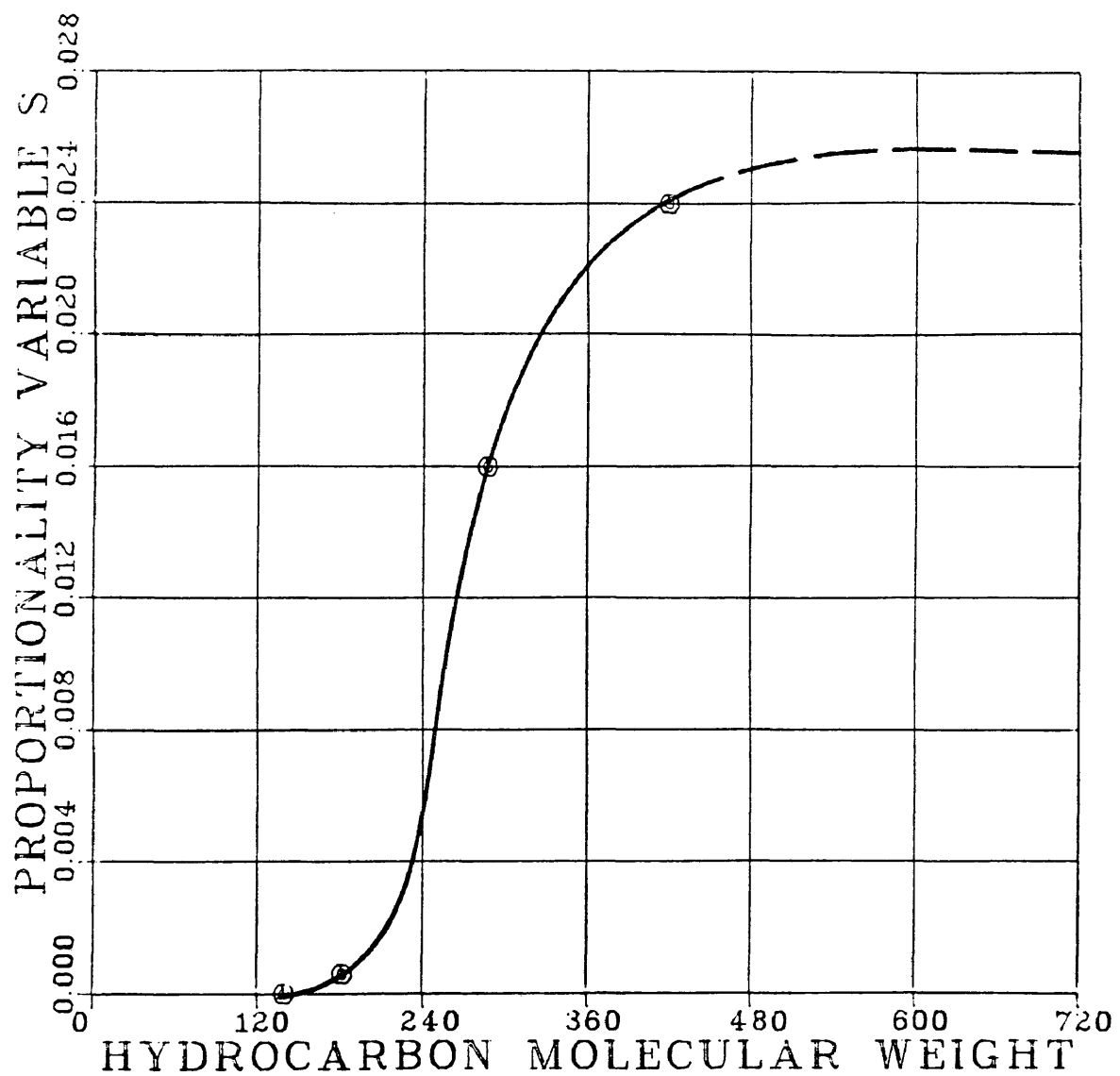


Figure 27. Proportionality Variable S for Determining Intermediate Hydrocarbon Binary Interaction Coefficients

Pseudocomponent Characterization of Reservoir Fluids

This study required many EOS calculations and since the particular computer program used made it impossible to automate the procedure, a great deal of hand calculations and manual bookkeeping were also necessary. The time required for these computations increases considerably with the number of components used to characterize the reservoir fluid, therefore it was desired to represent each crude with a minimum number of pseudocomponents. This practice is common in EOS applications, however it is important to maintain the accuracy of the phase behavior predictions.

Several techniques have been proposed for combining single carbon number groups from an extended analysis into a small number of pseudocomponents and also for calculating the properties of these pseudocomponents. Hong⁽⁴⁸⁾ proposed a trial and error procedure wherein the crude is initially characterized by as few as three pseudocomponents (C_1 , C_2-C_6 , and C_{7+}). The number of components is systematically increased until a satisfactory match is obtained between the calculated and experimental phase diagrams. Weight-fraction averages of the individual component properties are recommended for characterization of the pseudocomponents. Mehra et al.⁽⁵⁶⁾ proposed a statistical procedure to determine which components to

combine. The method partially depends on the anticipated reservoir conditions. The Lee-Kessler⁽⁴⁵⁾ mixing rules are recommended for calculating the pseudocomponent properties, and a fairly complex mixing rule is presented for the interaction coefficients. Whitson⁽⁵⁷⁾ proposed a method which estimates the number of pseudocomponent groups needed to characterize a reservoir fluid and the molecular weight range of each group. This method is based on a probability model for the molar distribution of the crude constituents. Two sets of mixing rules for calculating pseudocomponent properties were also evaluated. One was the simple molar-average or Kay's mixing rule, the other a more complicated set of equations involving average boiling points. There was little difference in the pseudocomponent properties calculated with each method, consequently EOS predictions were not greatly affected by the choice of mixing rule. Li et al.⁽⁵⁸⁾ proposed a scheme wherein the K-value range of the components on a logarithmic scale is divided into equal intervals and the components which fall into the same interval are combined. The K-values are obtained from a flash calculation at the expected operating conditions. The pseudocomponent properties are calculated from the Lee-Kessler⁽⁴⁵⁾ mixing rules, and interaction

coefficients are computed from a correlation involving the critical volumes of the pseudocomponents and an adjustable parameter.

One objective of Grigg and Lingane's work was to determine what effect the number of pseudocomponents and the specific component grouping has on PR EOS predictions for the four reservoir fluids. These authors used a trial and error procedure, but unlike that of Hong⁽⁴⁸⁾, the crudes were initially characterized by a large number of pseudocomponents and it was then attempted to reduce this number while maintaining a suitable match of the experimental phase data. The pseudocomponents were characterized by the molar-average properties of the individual components. Their results provided a good basis for developing the pseudocomponent representations used in this study.

Grigg and Lingane⁽⁴⁷⁾ recommended the same five-pseudocomponent grouping scheme for the Ford Geraldine, West Sussex, and Maljamar crudes, and a three-pseudocomponent representation of the Reservoir D crude. These recommendations were followed closely for the most part. For the Ford Geraldine and West Sussex crudes a six-pseudocomponent representation is used which differs only in that the C₂-C₆ hydrocarbons are lumped into two pseudocomponents rather than one. This provides a slightly better match of

the saturation boundaries. The three-pseudocomponent representation of the Reservoir D crude is used without change. The three and six-pseudocomponent groupings used for these three crudes along with the five-pseudocomponent grouping proposed by Grigg and Lingane⁽⁴⁷⁾ are given in Table 13.

The five-pseudocomponent representation recommended by Grigg and Lingane⁽⁴⁷⁾ proved wholly inadequate for the Maljamar crude. It would seem that the accuracy of EOS predictions could be increased by representing the reservoir fluid with a greater number of pseudocomponents, and in general this is true. However, Whitson⁽⁵⁷⁾ has stated that it is not only the number of pseudocomponents used but which components are lumped together that affects EOS accuracy. This was certainly the case in attempting to obtain a better match of the Maljamar phase diagram. Several different characterizations of this crude were investigated. The pseudocomponent groupings which were tested are given in Table 14. The predicted saturation boundaries are shown in Figure 28 along with the experimental bubble point data. Case A is for the five-pseudocomponent representation of Grigg and Lingane⁽⁴⁷⁾. The bubble point pressures at low CO₂ concentrations are reproduced fairly well, but clearly the

Table 13. Pseudocomponent Grouping Schemes for Ford
Geraldine, West Sussex, and Reservoir D Crudes

Six Components	Three Components	Five Components
C ₁	C ₁	C ₁
C ₂₋₃	C ₂₋₆	C ₂₋₆
C ₄₋₆	C ₇₊	C ₇₋₁₀
C ₇₋₁₀		C ₁₁₋₂₄
C ₁₁₋₂₄		C ₂₆₊
C ₂₆₊		

Table 14. Pseudocomponent Grouping Schemes for Maljamar Crude (See Figure 28)

Case A	Case B	Case C	Case D*
C ₁	C ₁	C ₁	C ₁
C ₂₋₆	C ₂	C ₂₋₃	C ₂₋₃
C ₇₋₁₀	C ₃	C ₄₋₆	C ₄₋₆
C ₁₁₋₂₄	C ₄	C ₇₋₁₀	C ₇₋₁₀
C ₂₆₊	C ₅₋₆	C ₁₁₊	C ₁₁₊
	C ₇₋₈		
	C ₉₋₁₀		
	C ₁₁₋₁₆		
	C ₁₈₋₂₄		
	C ₂₆₋₃₆		
	C ₃₈₊		

* Binary interaction coefficients adjusted

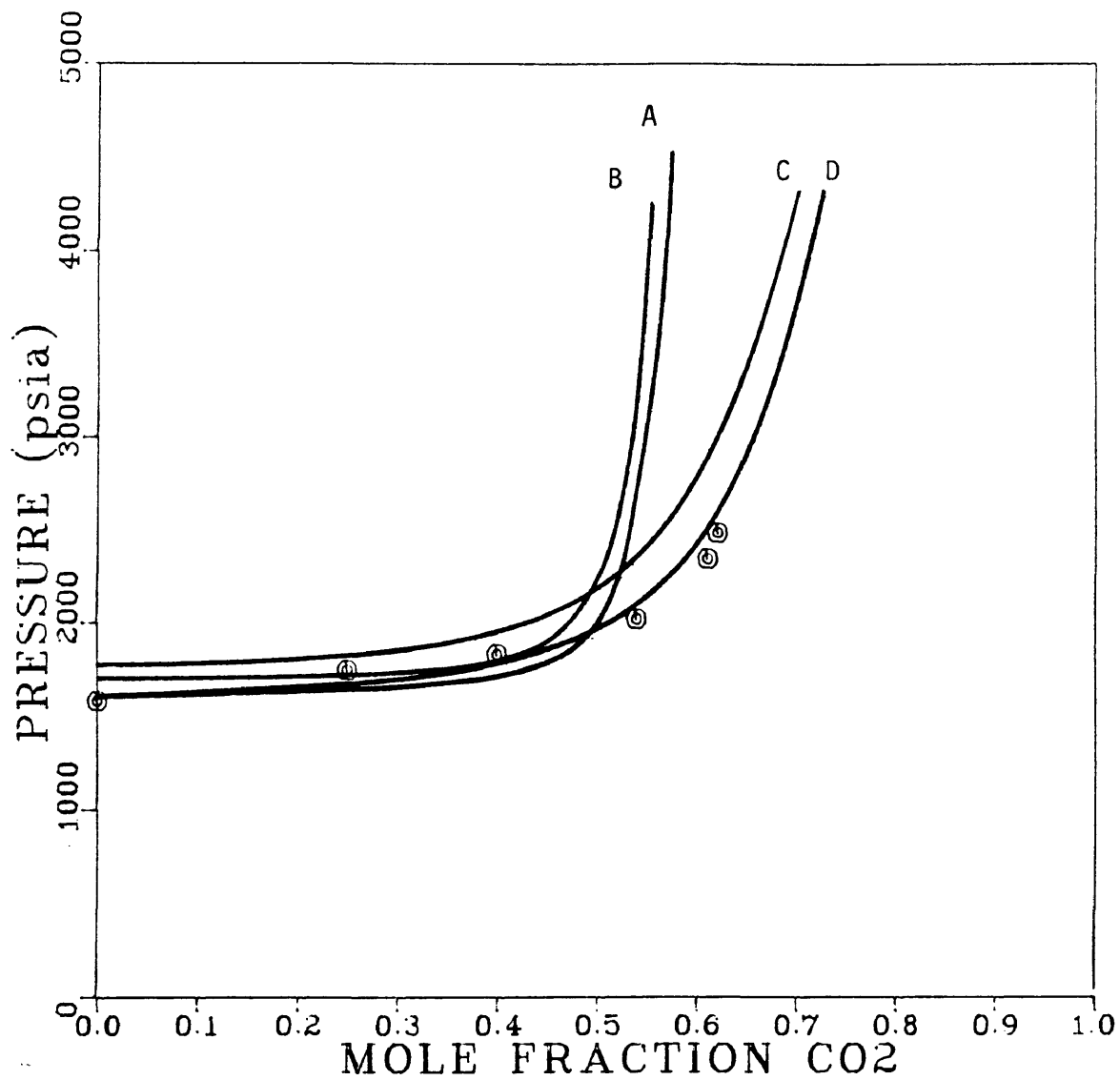


Figure 28. Predicted Saturation Boundaries and Experimental Bubble Point Data: Maljamar Crude 90°F

steeply rising portion of the phase boundary occurs at CO₂ concentrations which are too low. The effect of representing the crude with more pseudocomponents was investigated first. Case B is an 11-pseudocomponent representation which was also used by Grigg and Lingane⁽⁴⁷⁾. It, in fact, leads to an even poorer prediction of the saturation boundary. Since better results were obtained with case A where the heaviest pseudocomponent is C₂₆₊ than with case B where the heaviest is C₃₈₊, it was decided to try a representation where the heavy pseudocomponent was even lighter than C₂₆₊. Case C utilizes five pseudocomponents, the heaviest of which is C₁₁₊. The bubble point pressures at low CO₂ concentrations are overpredicted with this representation, but an improvement is shown where the phase boundary rises steeply. In cases A, B, and C the properties of the pseudocomponents are given by the molar-average of the individual component properties and the binary interaction coefficients used are as reported by Grigg and Lingane⁽⁴⁷⁾ or determined from Figures 25-27. It can be seen in Figure 28 that the saturation boundary predicted for case D matches the experimental data quite well. Case D uses the same pseudocomponent grouping as case C, and the properties of the pseudocomponents (P_C , T_C , ω , and MW) are identical.

However, the binary interaction coefficients between C_{11+} and other hydrocarbon pseudocomponents are lower in case D. The values of the C_{11+} -hydrocarbon interaction coefficients were arrived at by trial and error, but it is generally recognized that reducing the coefficients lowers the predicted saturation pressures. For comparison, the complete sets of interaction coefficients for cases C and D are shown in Table 15.

The final characterizations of the four crudes and the necessary input parameters for the PR EOS are shown in Tables 16-19. Again, the values of critical pressure, critical temperature, acentric factor, and molecular weight for the pseudocomponents are the molar-averages of the respective single carbon number group properties which are given in Tables 9-12. The binary interaction coefficients are generally all from Figures 25-27, however certain coefficients for the Maljamar crude were adjusted. The properties of CO_2 are from the GPSA Engineering Data Book(52).

Table 15. Binary Interaction Coefficients Used in Cases C and D for Maljamar Crude

Case C:

	CO ₂	C ₁	C ₂₋₃	C ₄₋₆	C ₇₋₁₀	C ₁₁₊
CO ₂	-					
C ₁	0.100	-				
C ₂₋₃	0.133	0.0	-			
C ₄₋₆	0.126	0.0	0.0	-		
C ₇₋₁₀	0.114	0.0	0.0	0.0	-	
C ₁₁₊	0.100	0.113	0.050	0.026	0.010	-

Case D:

	CO ₂	C ₁	C ₂₋₃	C ₄₋₆	C ₇₋₁₀	C ₁₁₊
CO ₂	-					
C ₁	0.100	-				
C ₂₋₃	0.133	0.0	-			
C ₄₋₆	0.126	0.0	0.0	-		
C ₇₋₁₀	0.114	0.0	0.0	0.0	-	
C ₁₁₊	0.100	0.078	0.033	0.014	0.009	-

Table 16. Peng-Robinson EOS Input Parameters
Ford Geraldine Crude

Pseudocomponent Properties

Comp. ID	Mole Fraction	Critical Values			
		Pressure (atm)	Temp (°K)	Acentric Factor	Molecular Weight
CO ₂		72.89	304.19	0.225	44.0
C ₁	0.1004	45.8	190.6	0.013	16.0
C ₂₋₃	0.1927	44.5	343.4	0.130	38.3
C ₄₋₆	0.1373	35.4	459.3	0.231	69.0
C ₇₋₁₀	0.2760	31.5	579.5	0.302	114.9
C ₁₁₋₂₄	0.2269	17.6	714.8	0.647	216.0
C ₂₆₊	0.0667	7.4	882.4	1.564	510.2

Binary Interaction Coefficients

	CO ₂	C ₁	C ₂₋₃	C ₄₋₆	C ₇₋₁₀	C ₁₁₋₂₄	C ₂₆₊
CO ₂	-						
C ₁	0.100	-					
C ₂₋₃	0.133	0.0	-				
C ₄₋₆	0.126	0.0	0.0	-			
C ₇₋₁₀	0.114	0.0	0.0	0.0	-		
C ₁₁₋₂₄	0.100	0.078	0.045	0.018	0.010	-	
C ₂₆₊	0.100	0.200	0.063	0.025	0.015	0.010	-

Table 17. Peng-Robinson EOS Input Parameters
West Sussex Crude

Pseudocomponent Properties

Comp. ID	Mole Fraction	Critical Values			
		Pressure (atm)	Temp (°K)	Acentric Factor	Molecular Weight
CO ₂		72.89	304.19	0.225	44.0
C ₁	0.1217	45.8	190.6	0.013	16.0
C ₂₋₃	0.0966	45.1	337.9	0.126	37.1
C ₄₋₆	0.1177	33.8	486.6	0.253	77.8
C ₇₋₁₀	0.3152	32.0	581.5	0.299	116.2
C ₁₁₋₂₄	0.2465	16.9	715.9	0.678	220.4
C ₂₆₊	0.1023	7.3	883.7	1.583	515.4

Binary Interaction Coefficients

	CO ₂	C ₁	C ₂₋₃	C ₄₋₆	C ₇₋₁₀	C ₁₁₋₂₄	C ₂₆₊
CO ₂	-						
C ₁	0.100	-					
C ₂₋₃	0.133	0.0	-				
C ₄₋₆	0.126	0.0	0.0	-			
C ₇₋₁₀	0.114	0.0	0.0	0.0	-		
C ₁₁₋₂₄	0.100	0.078	0.045	0.018	0.010	-	
C ₂₆₊	0.100	0.200	0.063	0.025	0.015	0.010	-

Table 18. Peng-Robinson EOS Input Parameters
Maljamar Crude

Pseudocomponent Properties

Comp. ID	Mole Fraction	Critical Values			
		Pressure (atm)	Temp (°K)	Acentric Factor	Molecular Weight
CO ₂		72.89	304.19	0.225	44.0
C ₁	0.3025	45.8	190.6	0.013	16.0
C ₂₋₃	0.1992	45.4	335.0	0.123	36.4
C ₄₋₆	0.1165	34.0	463.0	0.249	70.4
C ₇₋₁₀	0.1721	30.7	581.7	0.312	116.0
C ₁₁₊	0.2097	15.2	769.7	0.910	304.4

Binary Interaction Coefficients

	CO ₂	C ₁	C ₂₋₃	C ₄₋₆	C ₇₋₁₀	C ₁₁₊
CO ₂	-					
C ₁	0.100	-				
C ₂₋₃	0.133	0.0	-			
C ₄₋₆	0.126	0.0	0.0	-		
C ₇₋₁₀	0.114	0.0	0.0	0.0	-	
C ₁₁₊	0.100	0.078	0.033	0.014	0.009	-

Table 19. Peng-Robinson EOS Input Parameters
Reservoir D Crude

Pseudocomponent Properties

Comp. ID	Mole Fraction	Critical Values			
		Pressure (atm)	Temp (°K)	Acentric Factor	Molecular Weight
CO ₂		72.89	304.19	0.225	44.0
C ₁	0.2268	45.8	190.6	0.013	16.0
C ₂₋₆	0.2902	40.6	390.5	0.176	51.1
C ₇₊	0.4830	19.2	719.7	0.747	255.8

Binary Interaction Coefficients

	CO ₂	C ₁	C ₂₋₆	C ₇₊
CO ₂	-			
C ₁	0.100	-		
C ₂₋₆	0.130	0.0	-	
C ₇₊	0.104	0.084	0.0	-

Comparison of Predicted and Experimental Data

The characterization of the four reservoir fluids was primarily evaluated by comparing the predicted saturation boundary and the experimental bubble point pressure data. However, for the final characterizations given in Tables 16-19, full P-X diagrams including isovol lines were generated and compared with the volumetric data of Tables 5-8. These phase diagrams appear in Figures 29-32. The overall accuracy of the predictions appear to be quite good, especially in view of the experimental error associated with the volumetric data. Grigg and Lingane⁽⁴⁷⁾ stated that the error was approximately "a few percent in the CO₂ mole fraction scale."

As would be expected from the reservoir temperatures of the four crudes, the Reservoir D system exhibits Type I phase behavior while the Ford Geraldine, West Sussex, and Maljamar systems exhibit Type II phase behavior. Regions where three phases exist in equilibrium were observed by Grigg and Lingane⁽⁴⁷⁾ for the Type II systems, but detailed data was not reported. Attempts to define the three phase envelopes for these systems using the PR EOS and the characterizations of Tables 16-19 were unsuccessful. The three-phase bubble point pressure and dewpoint pressure calculations require an initial estimate of the pressure,

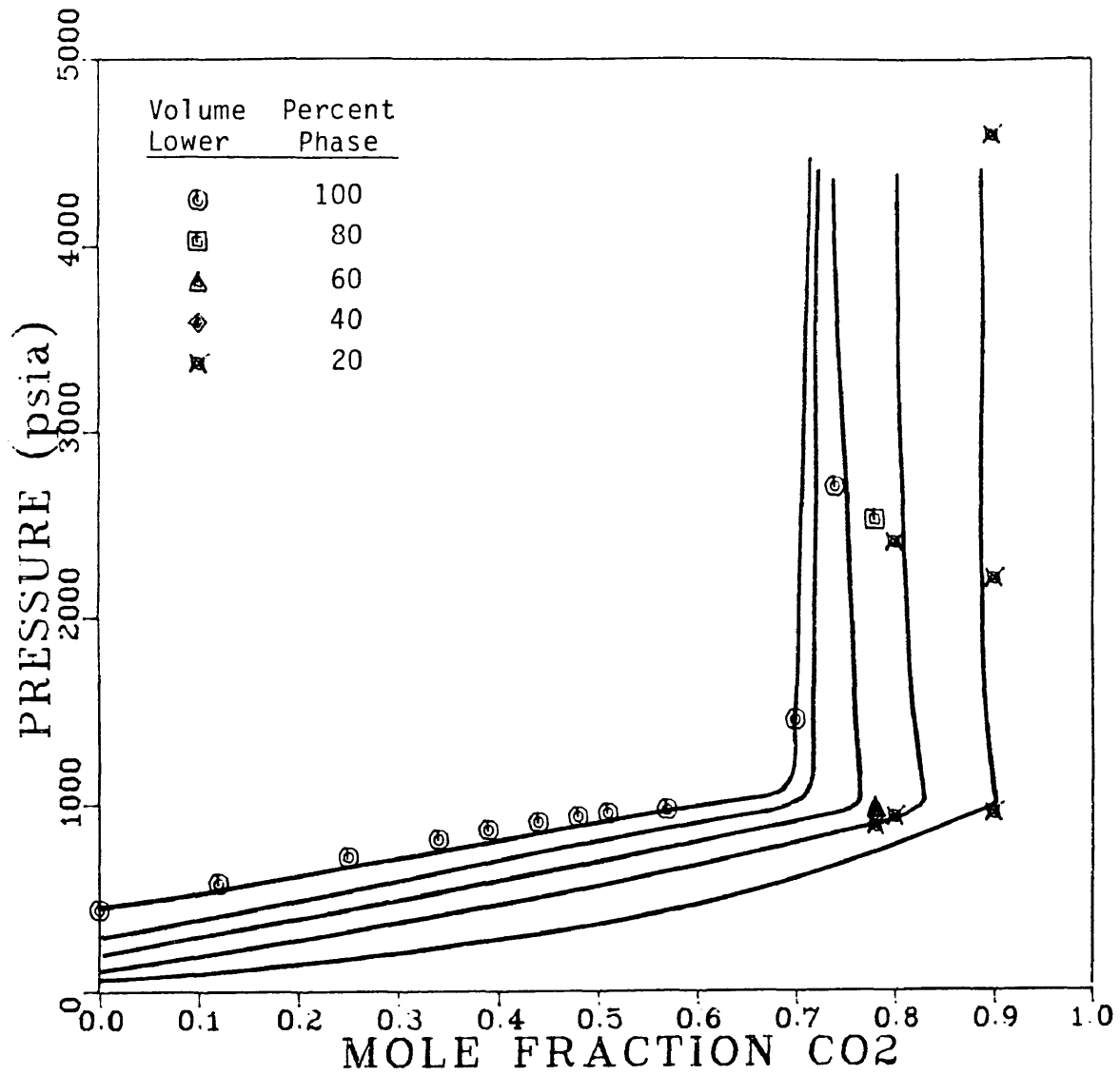


Figure 29. Pressure-Composition Diagram Showing Predicted Isovol Curves and Experimental Volumetric Data: Ford Geraldine Crude 83°F

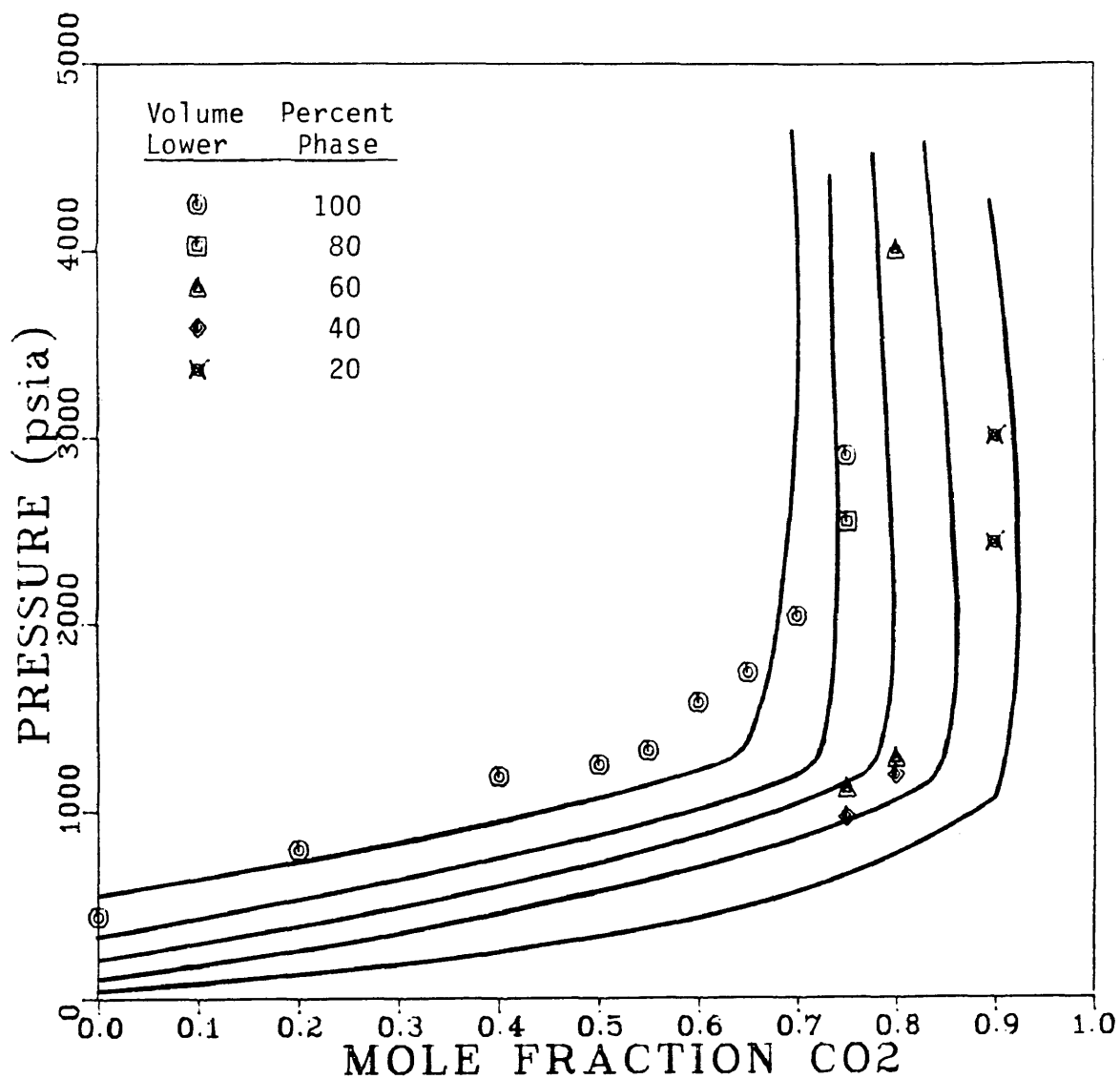


Figure 30. Pressure-Composition Diagram Showing Predicted Isovol Curves and Experimental Volumetric Data: West Sussex Crude 94°F

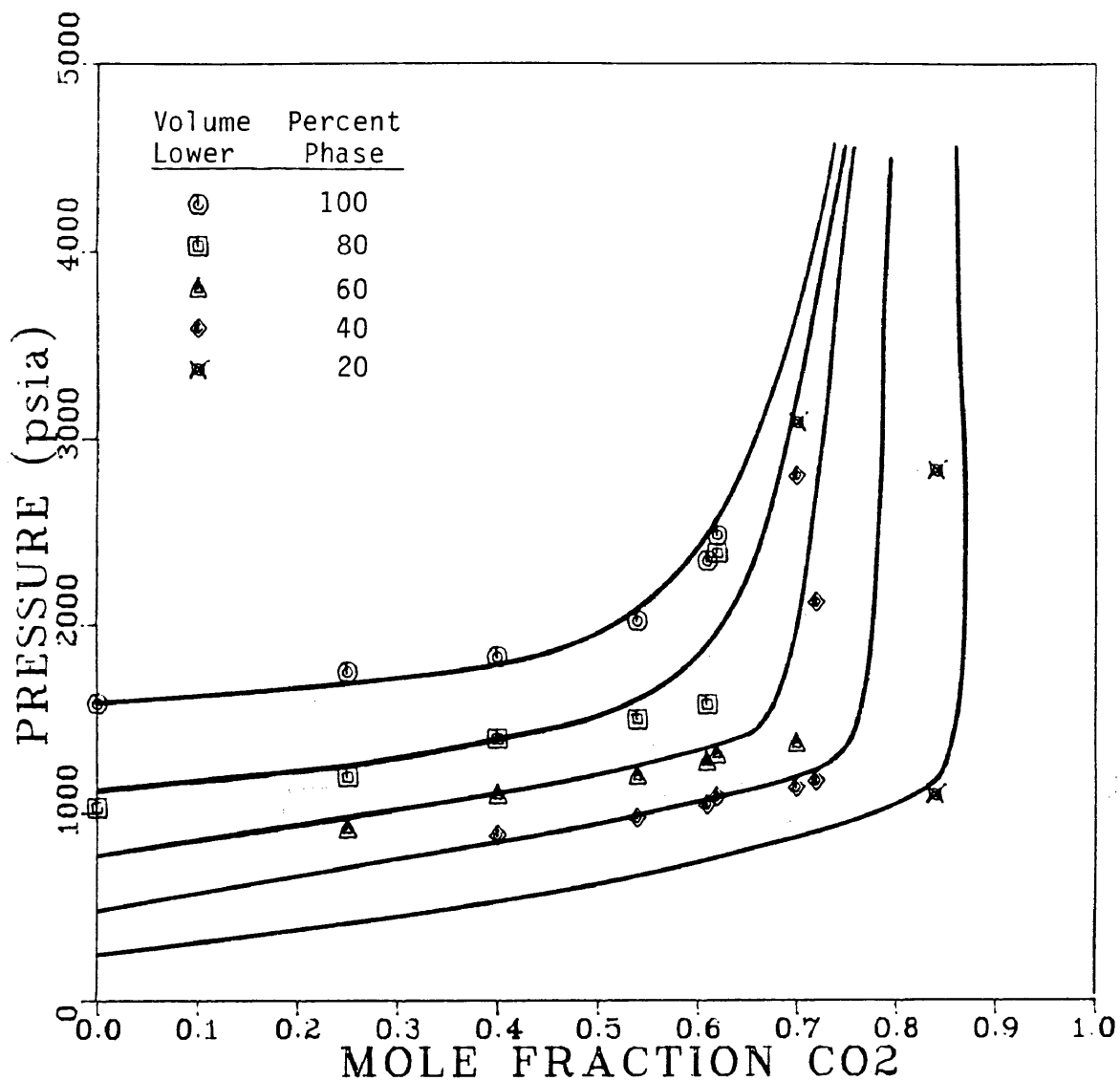


Figure 31. Pressure-Composition Diagram Showing Predicted Isovol Curves and Experimental Volumetric Data: Maljamar Crude 90°F

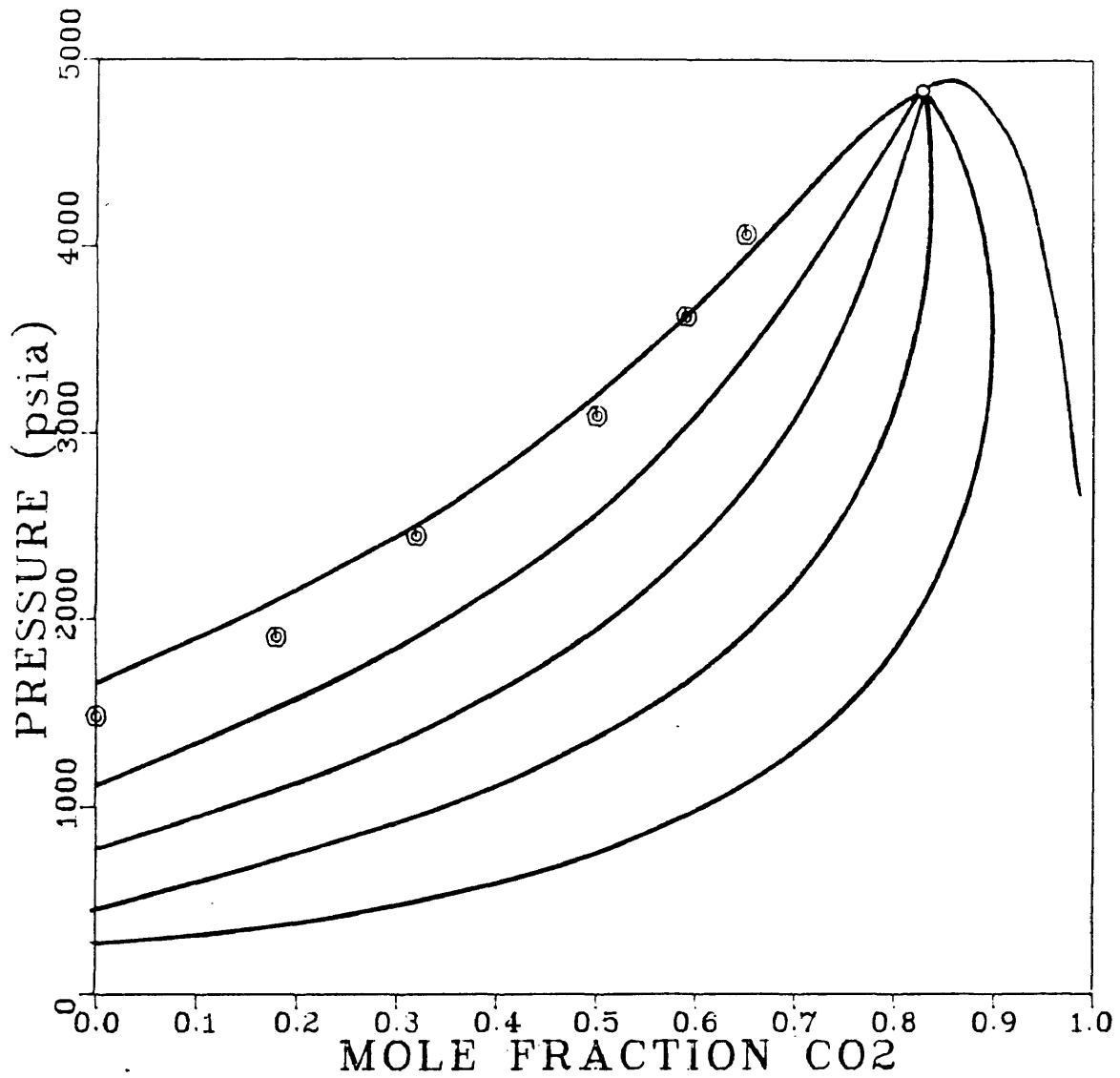


Figure 32. Pressure-Composition Diagram Showing Predicted Isovol Curves and Experimental Volumetric Data: Reservoir D Crude 220°F

and appear to be very sensitive to this value. The program did not always converge to unique solutions and the predicted bubble point pressure in particular, was greatly affected by the initial pressure estimate. The failure of three-phase calculations with the PR EOS to converge for CO₂-hydrocarbon systems has also been reported by Orr, Lien, and Pelletier⁽⁵⁹⁾.

It is felt that these characterizations are about the best that can be obtained with a trial and error procedure for grouping components and adjusting input parameters. The other proposed procedures do not offer much hope for improvement because in general, they appear to be as empirical as the procedure used here. Significant improvement of the characterizations would likely require some type of regression based EOS procedure such as that proposed by Coats and Smart⁽⁶⁰⁾.

The most serious shortcoming of this work is not being able to verify the predictions at the critical point. Experimental evidence of a critical point was reported at approximately 2600 psia and 63 mole percent CO₂ for the Maljamar crude and at approximately 3000 psia and 78 mole percent CO₂ for the Ford Geraldine crude. It was attempted to predict the critical point of both systems with the PR EOS, however, the calculations did not converge.

(More will be said about the calculation of critical points in the next section.) A critical point was predicted for the Reservoir D crude at 4844 psia and 82.7 mole percent CO₂ but no experimental data was taken in this region. No experimental critical point was observed for the West Sussex crude, and similarly, attempts to calculate a critical point with the PR EOS did not converge.

PREDICTING MISCIBILITY CONDITIONS

Introduction

To predict miscibility conditions from a pseudoternary diagram the critical point region must be well defined. It is often difficult to obtain EOS solutions near the critical point, however. This section explains how pseudoternary diagrams--particularly the critical point and limiting tie line-- are calculated with the Peng-Robinson equation of state.

The pseudoternary diagrams generated in this study have the crude oil split into two pseudocomponents: C_{6-} and C_{7+} . This grouping is used so that a generalized CO_2 MMP correlation can be developed from the calculated miscibility conditions which is compatible with a standard crude analysis. A representative sample of the pseudoternary diagrams calculated for the Ford Geraldine, West Sussex, Maljamar, and Reservoir D systems is presented along with a summary of the calculated miscibility conditions.

Critical Point

Three methods of calculating critical points with the PR EOS were evaluated as part of this study. The first method investigated was the subroutine included in current PR EOS computer programs which calculates critical points directly. The other two methods are indirect procedures where the critical point is determined from phase envelopes predicted with the PR EOS.

The theoretical basis for the direct calculation of critical points is found in thermodynamic criteria established by Gibbs in 1876, and first extended to multicomponent systems by Peng and Robinson⁽⁶¹⁾. The calculational procedure used in the PR subroutine is based on material instability criterion proposed by Heidemann and Khalil⁽⁶²⁾. Temperature, specific volume, and composition (component mole fractions) are treated as independent variables. For a specified composition, the procedure involves locating temperature-volume values which satisfy the critical point conditions expressed in terms of Helmholtz free energy. The pressure corresponding to this temperature and volume is then calculated. The procedure is complicated by the fact that for most systems there is more than one volume which satisfies the critical point conditions for a given temperature, and for many systems

there is more than one temperature which satisfies the conditions for a given volume. In fact, Heidemann and Khalil⁽⁶²⁾ found that three critical points could be calculated for a single mixture of CO₂ and n-hexadecane (C₁₆). For some systems the higher density critical points correspond to negative pressures and have no physical significance. However, for systems which can form two liquid phases, the high density solutions may be liquid-liquid critical points.

Since three of the four crudes used in this study exhibit Type II phase behavior with CO₂, any technique used to calculate critical points must be capable of calculating liquid-liquid criticals. Unfortunately, the PR subroutine is designed to calculate liquid-vapor critical points only. This is accomplished by starting the iterative solution with sufficiently high values of volume and temperature. This causes the calculations to converge to the highest temperature which satisfies the critical point conditions for a given volume. It was attempted to calculate the critical point of several mixtures of CO₂ with each of the four reservoir fluids with the direct calculation subroutine. In all cases the calculations either did not converge or the calculated critical temperature was unrealistically high, often greater than

300°F. It is likely that the critical point criteria were also satisfied at lower temperatures, however, this could not be verified. Without some control over the temperature range searched or modifications that allow all possible critical points to be evaluated, this method does not meet the requirements of this work.

The two indirect methods for calculating critical points which were investigated are simple in concept but fairly time consuming. One of the methods is similar to a procedure described by Williams et al.⁽⁴⁰⁾ A series of flash calculations is used to construct the phase envelope of a CO₂-crude system on a pseudoternary diagram. The critical point composition can then be determined graphically by intersecting the tie line bisector with the phase boundary. To begin, a mixture of the three pseudocomponents used in the pseudoternary representation (CO₂, C₆₋, and C₇₊) is arbitrarily selected. The composition of this mixture in terms of the pseudocomponents used in the EOS characterization is then calculated. This mixture is flashed at a temperature and pressure of interest, and the detailed compositions of the upper and lower phases are reduced to the pseudoternary compositions for display on the triangular diagram. This process is repeated until the phase envelope is suitably defined.

On the surface this method appears to have some distinct advantages. For example, in the process of locating the critical point, necessary tie line data is calculated. Also, the ability to fix temperature and pressure may be viewed as an advantage from the standpoint of correlating the calculated data. Several drawbacks associated with this procedure became apparent, though, when it was used in an attempt to calculate critical points for the Ford Geraldine crude with CO₂. The first is that a critical composition may not even exist unless the temperature and pressure are chosen judiciously; the two-phase region can appear as a band across the pseudoternary diagram. If a critical point does exist within the diagram at the specified conditions, flash calculations simply do not provide an efficient means of locating it. A large number of flash calculations may be required, and even for mixture compositions which are several mole percent away from the critical point these calculations converge very slowly. Figure 33 shows the equilibrium phase compositions calculated for the Ford Geraldine system at 150°F and 1500 psia. Eleven flash calculations were made yet the location of the critical point is not obvious. Also, there is large degree of scatter in the data, particularly the lower phase

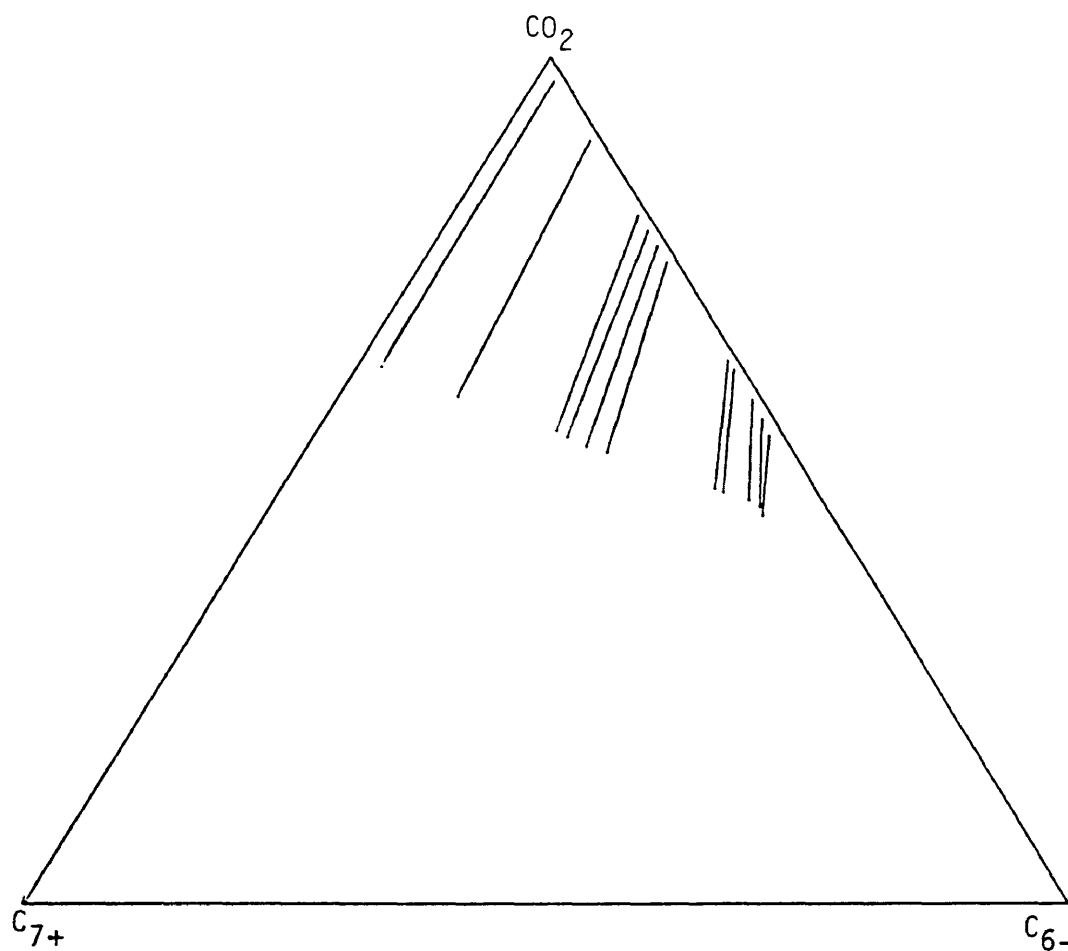


Figure 33. Tie Lines Calculated for Ford Geraldine System
at 150 °F 1500 psia

compositions. This is likely due to the somewhat random selection of the mixture compositions to be flashed. More serious problems were also experienced. Figure 34 shows the results of calculations for the Ford Geraldine system at 150°F and 2500 psia. As the critical region is approached the phase envelope does not close and, although the flash calculations all converge, some of the predictions appear to be outside the two-phase region. This may also be due to the way mixture compositions were selected. Without knowledge of the critical composition, it is impossible to approach the critical point in a logical or consistent manner. Similar problems were reported by Williams et al.(40) in their attempts to predict condensing gas drive miscibility. Finally, the method gives up some precision because the critical point must be determined graphically and there is a wide degree of latitude for extrapolating the near-critical portion of the phase boundary and the tie line bisector.

The procedure that is actually used to calculate critical points in this study was developed in response to the problems encountered with the flash calculation method. In this procedure, bubble point pressure and dewpoint pressure predictions are used to define the phase boundary on a P-X diagram. Oil composition and temperature are

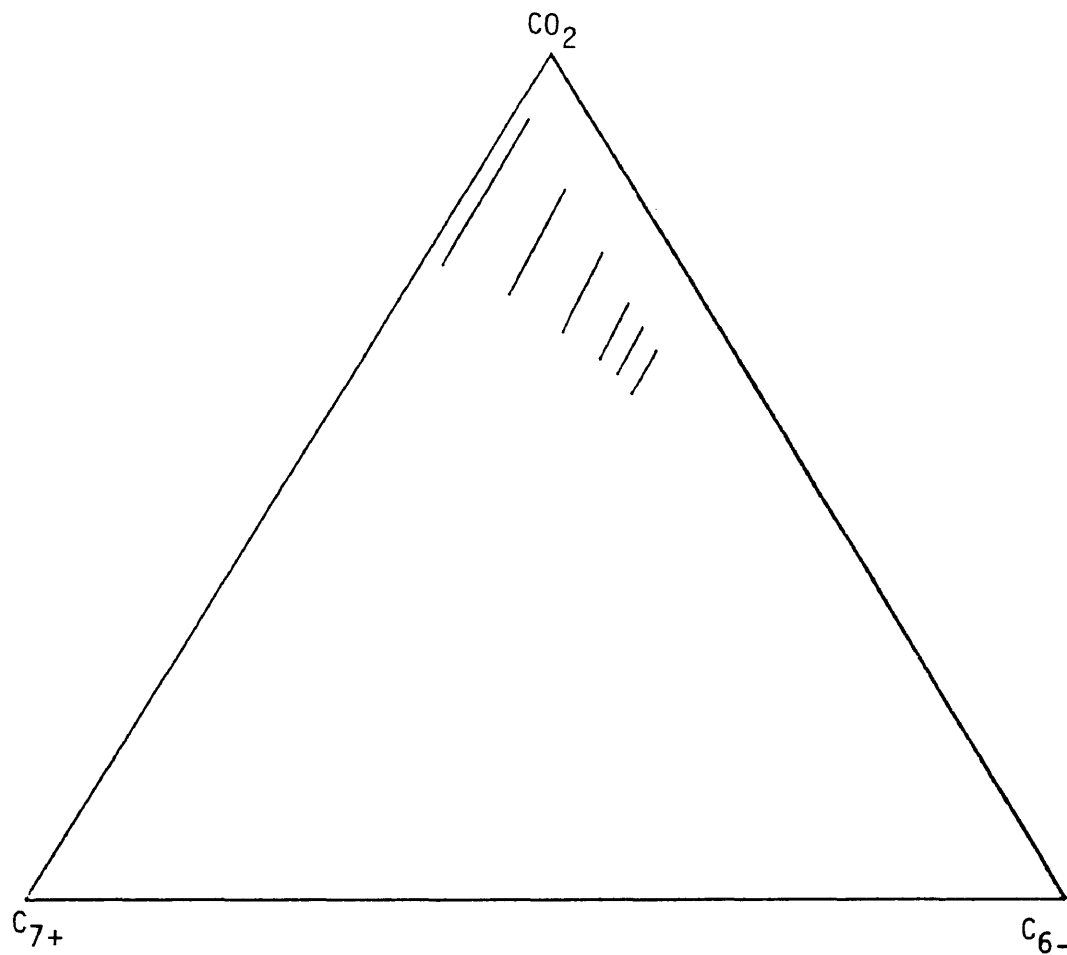


Figure 34. Tie Lines Calculated for Ford Geraldine System
at 150 °F 2500 psia

specified and the calculations are performed for various CO₂ concentrations. The critical point is defined where the calculated bubble point pressure and dewpoint pressure are equal. To visualize the process on a pseudoternary diagram, recall that the oil composition is shown as a mixture of the two hydrocarbon pseudocomponents (C₆₋ and C₇₊) and that the abscissa or composition axis of the P-X diagram coincides with the dilution line connecting the oil and pure CO₂. Thus, the composition of all mixtures on the P-X diagram, including the critical point, lie on this dilution line.

The first step in this procedure is to select a mixture of the two hydrocarbon pseudocomponents used in the pseudoternary representation of the oil (C₆₋ and C₇₊). This mixture is referred to here as the initial oil composition (IOC) and should not be confused with the composition of the original reservoir fluid. The detailed composition of this mixture in terms of the EOS pseudocomponents is then calculated. An arbitrary amount of CO₂ is mathematically added to the IOC, the mixture composition is normalized, and the saturation pressure is calculated at the temperature of interest. The procedure is repeated as the CO₂ concentration is systematically varied. The process can be started at either end of the CO₂ mole fraction scale but

it is advantageous to begin in the bubble point region with a mixture that contains a small amount of CO_2 . The bubble point and dewpoint calculations both require an estimate of the saturation pressure, but the solution is not overly sensitive to the quality of the estimate at low CO_2 concentrations. The CO_2 concentration is then gradually increased, and to aid convergence the bubble point pressure from the previous calculation is used as the pressure estimate for the new calculation. This becomes very important where the saturation boundary is rising steeply because in this region the calculations may not converge unless a very accurate pressure estimate is supplied. In fact, the solution in this region is so sensitive to the initial pressure value that it may be necessary to increase the CO_2 concentration in increments of 0.1 mole percent or less.

If the PR program output is observed, it is apparent when the CO_2 concentration is near the critical concentration. In the critical region, the calculated composition and intrinsic properties of the equilibrium vapor are very near those of the saturated liquid. When this is observed, the bubble point pressure and the dewpoint pressure are calculated for each mixture and compared. (It is the upper dewpoint that is of interest, therefore

retrograde dewpoint pressure calculations are made.) When the two pressures are equal or within an acceptable limit, the critical CO₂ concentration has been located. A suitable criterion is that at the critical point the retrograde dewpoint pressure is within 0.5 psi of the bubble point pressure.

This method was used in an attempt to calculate the critical points of the four original reservoir fluids at reservoir temperature. The predicted saturation boundaries for all four systems are in good agreement with the experimental data (refer to Figures 29-32), however, only the critical point of the Reservoir D system was calculated. Unfortunately, the critical point for this system was not determined experimentally. Experimental critical points were reported for the Ford Geraldine and Maljamar crudes, but could not be positively located with the proposed procedure. For these systems, the saturation boundary becomes nearly vertical, and while the EOS calculations do converge in this region, the CO₂ concentration at which the bubble point pressure and retrograde dewpoint pressure are equal could not be located. Minute changes in the CO₂ concentration induce such large changes in the saturation pressure that the method is not accurate enough to pinpoint the critical CO₂

concentration for these oils. It was not possible to locate the critical point of the West Sussex system with this procedure, however, experimental data indicates that this system does not have a critical point at pressures of interest.

Although this method was not able to locate the critical points of the original Ford Geraldine, West Sussex, or Maljamar crudes at reservoir temperature, it has been applied successfully in many other instances. Saturation boundaries predicted at higher temperatures and for initial oil compositions which lie slightly to the right of the three original reservoir fluids on the pseudoternary diagram generally do not break as sharply or rise as steeply. Under these circumstances, the critical CO₂ concentration can be located without difficulty.

There are many advantages to calculating critical points with this method. Bubble point pressure and dewpoint pressure calculations converge much faster than flash calculations, and the calculations work equally well for liquid-vapor and liquid-liquid saturation boundaries. The procedure allows the temperature to be fixed, but since a search is performed for both the composition and pressure corresponding to a critical state, it is much more likely that the critical point will be located. Also, critical

points are located more precisely and in less time because no extrapolation or graphical techniques are required. The most important advantage, however, is that this method appears to be more reliable than the other indirect procedure. This may be due to the fact that there is only one compositional variable in this procedure, as opposed to three in the flash calculation method.

Limiting Tie Line

Once the critical point composition has been calculated, the slope of the limiting tie line must be determined. There is no tie line which actually passes through the critical point so the limiting slope must be estimated from tie lines in the vicinity of the critical point. Tie lines can be predicted with the PR EOS by simply performing flash calculations for mixtures in the two-phase region. Cases were presented which show that when flash calculations are performed with near-critical mixtures, scatter in the calculated data and erroneous solutions can result. These problems, however, were attributed to the manner in which mixture compositions were selected. A simple procedure was developed where the critical point composition is approached in a smooth, methodical fashion. Tie line data calculated in this manner is consistent and reliable and can be extrapolated to the critical point to define the limiting tie line.

At this point an alternate form of the pseudoternary diagram is introduced. Although the diagram is most frequently shown as an equilateral triangle, it is just as correct to show mixtures of three components on a right triangle diagram such as Figure 35. Each corner of the diagram still corresponds to 100 percent of a given

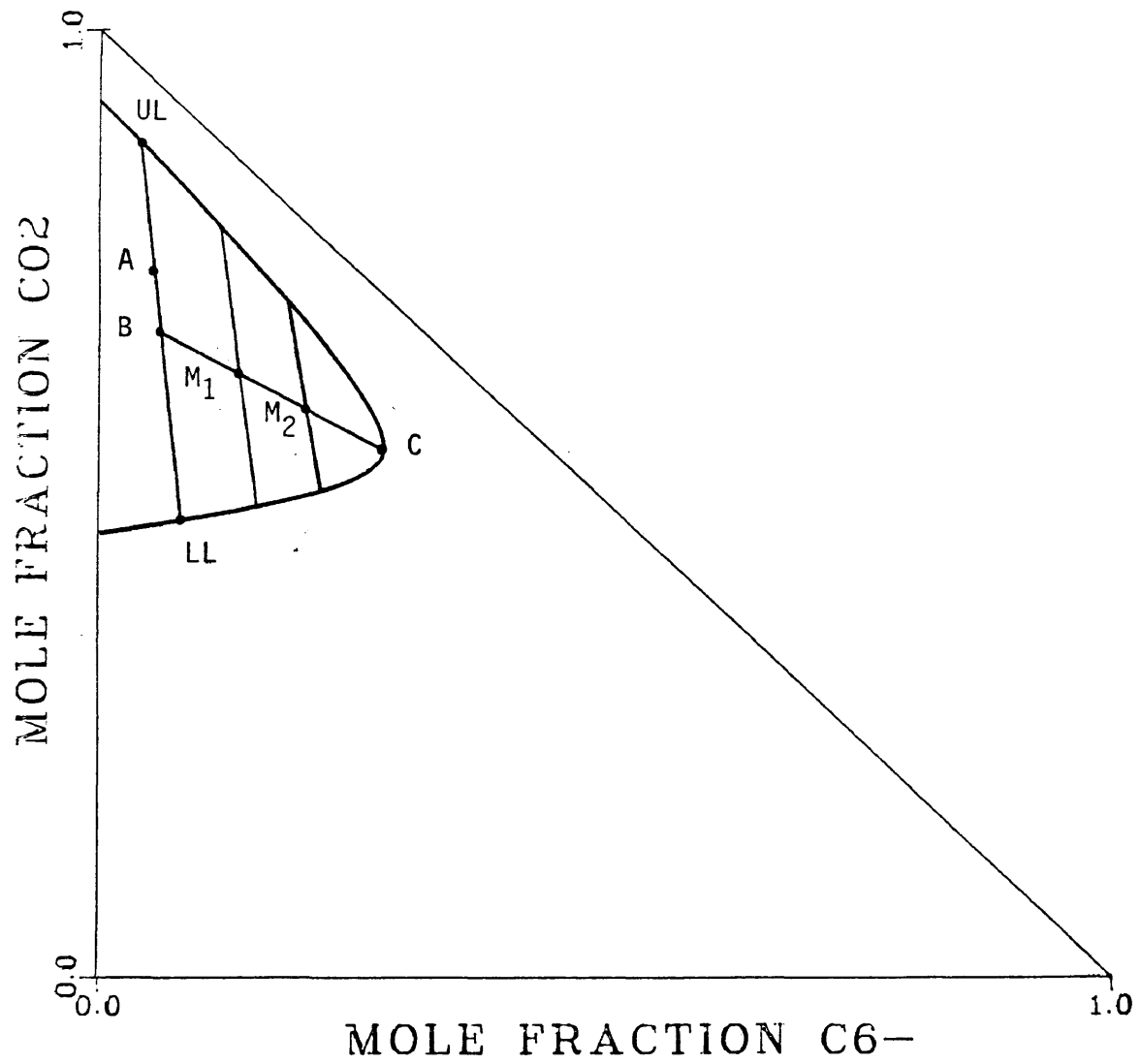


Figure 35. Pseudoternary Diagram Shown as a Right Triangle Illustrating Method of Calculating Tie Lines

component, however, in this form it is easy to see how mixture compositions can be treated as simple (x,y) coordinate pairs where the x coordinate is the mole fraction C_6 and the y coordinate is the mole fraction CO_2 . Since mixture compositions can be described by (x,y) coordinates, tie line slopes can be calculated, equations can be written for dilution lines, the intersection of two lines can be calculated, etc. A right triangle diagram is not required for these applications, but it does make them easier to visualize.

The procedure used to calculate tie line data is illustrated conceptually in Figure 35. Mixture C is a previously calculated critical point. The temperature and pressure of this diagram are equal to the critical temperature and pressure of mixture C. The first step in the procedure is to arbitrarily select a mixture within the two-phase region such as mixture A. This mixture is flashed, resulting in the two equilibrium phases UL and LL. Point B bisects the tie line connecting UL and LL. The tie lines which will be used to estimate the slope of the limiting tie line are obtained by flashing mixtures along the line connecting point B with the critical point C. Thus, the mixtures that are flashed are within a few mole percent of being tie line bisectors themselves. This method

of calculating tie lines appears to eliminate the problem of calculations converging outside the phase envelope or the phase envelope not closing, as well as the scatter observed when tie lines are calculated randomly. Also, since it is assured that mixtures on the line BC are in the two-phase region, it is easier to calculate tie lines very near the critical point.

The following expressions can be used to calculate the pseudoternary composition of any mixture M on line BC if the CO₂ concentration $X_{CO_2,M}$ is specified. They follow directly from the equation of line BC in terms of mole fraction C₆₋ and CO₂, and the fact that for any mixture the sum of the mole fractions X_{CO_2} , X_{C6-} , and X_{C7+} equals one.

$$X_{C6-,M} = \frac{X_{CO_2,M} - X_{CO_2,B}}{m_{BC}} + X_{C6-,B}$$

and:

$$X_{C7+,M} = 1 - X_{CO_2,M} - X_{C6-,M}$$

where:

$$X_{CO_2,B} = \frac{X_{CO_2,UL} + X_{CO_2,LL}}{2}$$

$$X_{C6-,B} = \frac{X_{C6-,UL} + X_{C6-,LL}}{2}$$

$$m_{BC} = \frac{X_{CO_2,B} - X_{CO_2,C}}{X_{C6-,B} - X_{C6-,C}}$$

with the definitions:

m_{BC} = slope of line BC

X_{CO_2} = mole fraction CO_2

X_{C6-} = mole fraction C_{6-}

X_{C7+} = mole fraction C_{7+}

M denotes a mixture M on line BC

B denotes point B which bisects initial tie line

UL denotes upper phase from initial flash

LL denotes lower phase from initial flash

C denotes critical point

In addition to yielding dependable tie line data, flashing mixtures along the line BC provides an effective means of extrapolating this data to the critical point to determine the limiting tie line. The slope of each tie line is dependent on the composition of the mixture used in the flash calculation. Because the mixtures are chosen in a consistent manner the tie line slope tends to vary uniformly as the critical point composition is approached. The tie line slope can therefore be considered a function of the departure of the mixture from the critical composition. This departure can conveniently be measured in terms of mole

fraction CO_2 and is referred to here as ΔX_{CO_2} . For each calculated tie line it is given by:

$$\Delta X_{\text{CO}_2} = X_{\text{CO}_2, \text{M}} - X_{\text{CO}_2, \text{C}}$$

The slope of the limiting tie line can be determined by plotting the slopes of the calculated tie lines against ΔX_{CO_2} and extrapolating the relationship to $\Delta X_{\text{CO}_2} = 0$ which corresponds to the critical point. The slope of each calculated tie line is given by:

$$m_{\text{tie line}} = \frac{X_{\text{CO}_2, \text{UL}} - X_{\text{CO}_2, \text{LL}}}{X_{\text{C6-}, \text{UL}} - X_{\text{C6-}, \text{LL}}}$$

where UL and LL now denote the upper and lower phases that define this particular tie line

Very similar results are obtained if ΔX_{CO_2} is considered to be the difference in CO_2 concentration between the upper and lower phases for each tie line. However, there is no particular advantage to this technique since the CO_2 concentration in each phase is dependent on the composition of the mixture flashed.

The objective of all of these calculations is to determine the maximum miscibility composition. The MMC can be calculated from the critical point composition and the

slope of the limiting tie line with the following equation:

$$\text{MMC} = 1 - X_{C6-,C} + \frac{X_{CO2,C}}{m_{LTL}}$$

where:

MMC= maximum miscibility composition (X_{C7+})

m_{LTL} = slope of the limiting tie line

There is an alternative to determining the slope of the limiting tie line by extrapolation and then calculating the MMC. For each calculated tie line, the MMC that would result if this tie line were extended through the critical point can be calculated. These values can then be plotted against ΔX_{CO2} and extrapolated to $\Delta X_{CO2}=0$ to find the true MMC. Since the only variable in the MMC equation is tie line slope, identical results are obtained with both procedures. There is a slight advantage to extrapolating the resulting MMCs, however, as this data is generally more well behaved. Near the critical point, tie line slopes often vary from very large negative values to very large positive values, and occasionally a tie line of infinite slope will be encountered. The MMCs, on the other hand, are always positive values and do not vary by more than a few mole percent which is convenient whether the extrapolation is done graphically or by regression.

Calculated Miscibility Conditions

The following steps summarize the procedure used to calculate miscibility conditions with the PR EOS for a reservoir fluid system at a given temperature:

1. Select an initial oil composition (IOC) which is a mixture of the two hydrocarbon pseudocomponents used to represent the reservoir fluid on the pseudoternary diagram (C_{6-} and C_{7+} in this study). Calculate the detailed composition of this mixture in terms of the EOS pseudocomponents.
2. Determine the critical point composition and critical pressure at the specified temperature by generating the P-X diagram saturation boundary for the IOC- CO_2 system. This is done by making a series of bubble point pressure and retrograde dewpoint pressure predictions with the PR EOS. Reduce the detailed critical point composition to the pseudoternary composition.
3. Arbitrarily select a mixture of the pseudoternary components (CO_2 , C_{6-} , and C_{7+}) which lies in the two-phase region. Calculate the detailed composition of this mixture and perform a flash calculation at the previously determined critical temperature and pressure

to define an initial tie line. Reduce the detailed compositions of the two equilibrium phases to the pseudoternary compositions.

4. Calculate the pseudoternary composition of several mixtures which lie on the line connecting the bisector of the initial tie line and the critical point composition. Calculate the detailed compositions of these mixtures and perform flash calculations to define tie lines in the vicinity of the critical point. Reduce the detailed compositions of the calculated equilibrium phases to the pseudoternary compositions.
5. Calculate the MMC (X_{C7+}) that would result from extending each of the tie lines calculated in the previous step through the critical point.
6. Determine the true MMC by extrapolating the data calculated in the previous step to $\Delta X_{CO_2} = 0$. For the oil composition defined by the MMC, the CO_2 MMP at the specified temperature is the critical pressure determined in Step 2.

This procedure was used to calculate several sets of miscibility conditions for component mixtures of the Ford Geraldine, West Sussex, Maljamar, and Reservoir D crudes.

Calculations were made at four temperatures: 100, 150, 200, and 250°F. Critical points were calculated for initial oil compositions (IOCs) that ranged from 55 mole percent C₆₋ and 45 mole percent C₇₊ to 95 mole percent C₆₋ and 5 mole percent C₇₊. This is the overall range. The range over which it was possible to locate critical points at pressures of interest varied for each reservoir fluid and temperature.

For each critical point, tie lines were calculated at five values of ΔX_{CO_2} : 0.08, 0.06, 0.04, 0.02, 0.01. Again, these values measure the departure of the mixture that is flashed from the critical point composition in mole fraction CO₂. To define the whole pseudoternary phase envelope, an arbitrarily selected CO₂-C₇₊ mixture was also flashed. For virtually all of the tie line calculations it was necessary to perform liquid-liquid flash calculations. This does not necessarily mean that liquid-liquid behavior persists to temperatures as high as 250°F. Rather, it appears that the liquid-vapor flash calculation subroutine of the Peng-Robinson program simply cannot distinguish between the two equilibrium phases near the critical point of the mixtures under consideration. However, for mixtures which can be flashed with the liquid-vapor subroutine, the liquid-liquid subroutine converges to the same solution.

The MMC corresponding to each temperature-pressure pair was determined by fitting a second degree polynomial to the MMC versus ΔX_{CO_2} data calculated from the five tie lines. In general, an excellent fit of the data was obtained with a quadratic and this expression was used to calculate the MMC at $\Delta X_{CO_2} = 0$.

The calculated miscibility data for each of the four crude systems is summarized in Tables 20-23. The pseudo-ternary diagrams for eight representative systems are shown in Figures 36-43. Figures 44-51 show the MMC versus ΔX_{CO_2} data for these systems and the polynomial fit to the data.

A sample calculation which details each step of the calculational procedure and shows the output generated by the PR EOS program is contained in Appendix A. Appendix B contains data sheets which summarize the calculations performed for each pseudoternary system. Included in these data sheets is the IOC, the critical CO_2 concentration and critical point composition, the pseudoternary composition of all mixtures flashed and the resulting equilibrium phases, and the MMC data calculated from the tie lines.

Table 20. Summary of Calculated Miscibility Conditions:
Ford Geraldine System

Temp (°F)	MMP (psia)	MMC (X _{C7+})
100	1414.3	0.7038
100	1610.1	0.7154
100	2251.6	0.7599
100	2964.5	0.7809
150	1705.2	0.6016
150	1881.7	0.6298
150	2046.7	0.6569
150	2534.9	0.7179
150	3023.5	0.7728
200	1727.0	0.3945
200	2187.8	0.5904
200	2475.1	0.6270
200	2681.3	0.6496
200	3182.8	0.7261
200	3567.4	0.7878
250	2199.7	0.5762
250	2491.2	0.6056
250	3076.7	0.6653
250	3580.0	0.7425
250	3963.3	0.8017

Table 21. Summary of Calculated Miscibility Conditions:
West Sussex System

Temp (°F)	MMP (psia)	MMC (X _{C7+})
100	1817.0	0.7957
100	2134.1	0.7864
100	2859.9	0.7838
150	2214.7	0.7525
150	2413.7	0.7306
150	3172.1	0.7544
200	2703.9	0.6743
200	3170.5	0.7013
200	3791.2	0.7543
250	3178.8	0.6605
250	3625.3	0.6944
250	4177.2	0.7601

Table 22. Summary of Calculated Miscibility Conditions:
Maljamar System

Temp (°F)	MMP (psia)	MMC (X _{C7+})
100	2618.9	0.7685
100	3003.9	0.7087
100	3782.9	0.7306
150	3232.2	0.7763
150	3615.9	0.7477
150	3989.3	0.7814
200	3626.2	0.7789
200	4077.2	0.7782
200	4361.0	0.8130
250	3823.4	0.7697
250	4370.9	0.7925
250	4646.5	0.8321

Table 23. Summary of Calculated Miscibility Conditions:
Reservoir D System

Temp (°F)	MMP (psia)	MMC (X _{C7+})
100	1893.5	0.4947
100	2281.7	0.5803
100	2889.6	0.6495
100	3931.3	0.6993
150	2399.4	0.5046
150	2925.6	0.6072
150	3450.0	0.6921
150	3927.8	0.7514
200	2631.7	0.5053
200	3335.1	0.6208
200	3897.7	0.7211
200	4257.4	0.7831
250	2900.1	0.5378
250	3273.2	0.5963
250	3528.5	0.6324
250	4176.9	0.7363
250	4517.0	0.8033

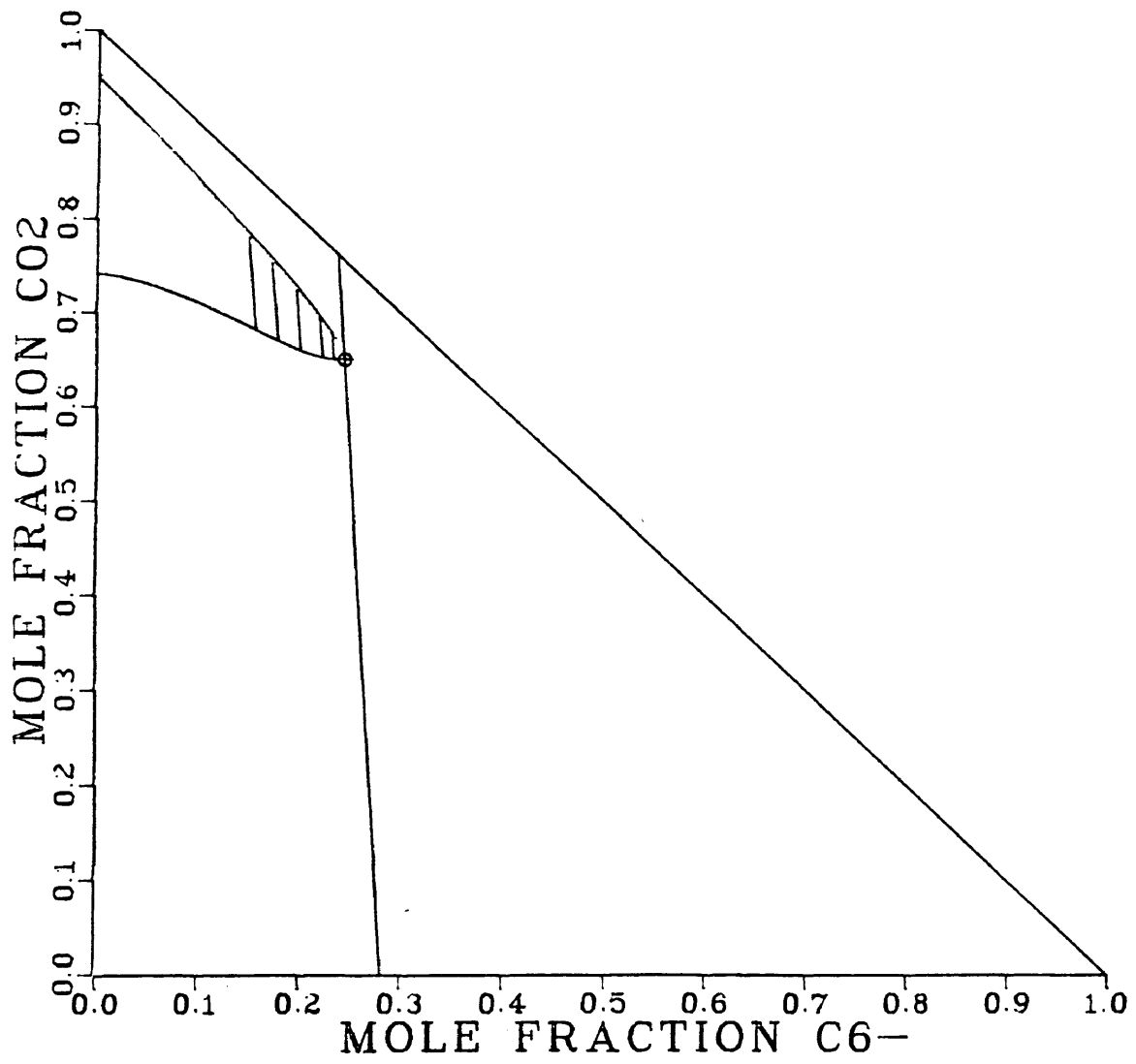


Figure 36. Calculated Pseudoternary Diagram for Ford Geraldine System: 150°F 2534.9 psia

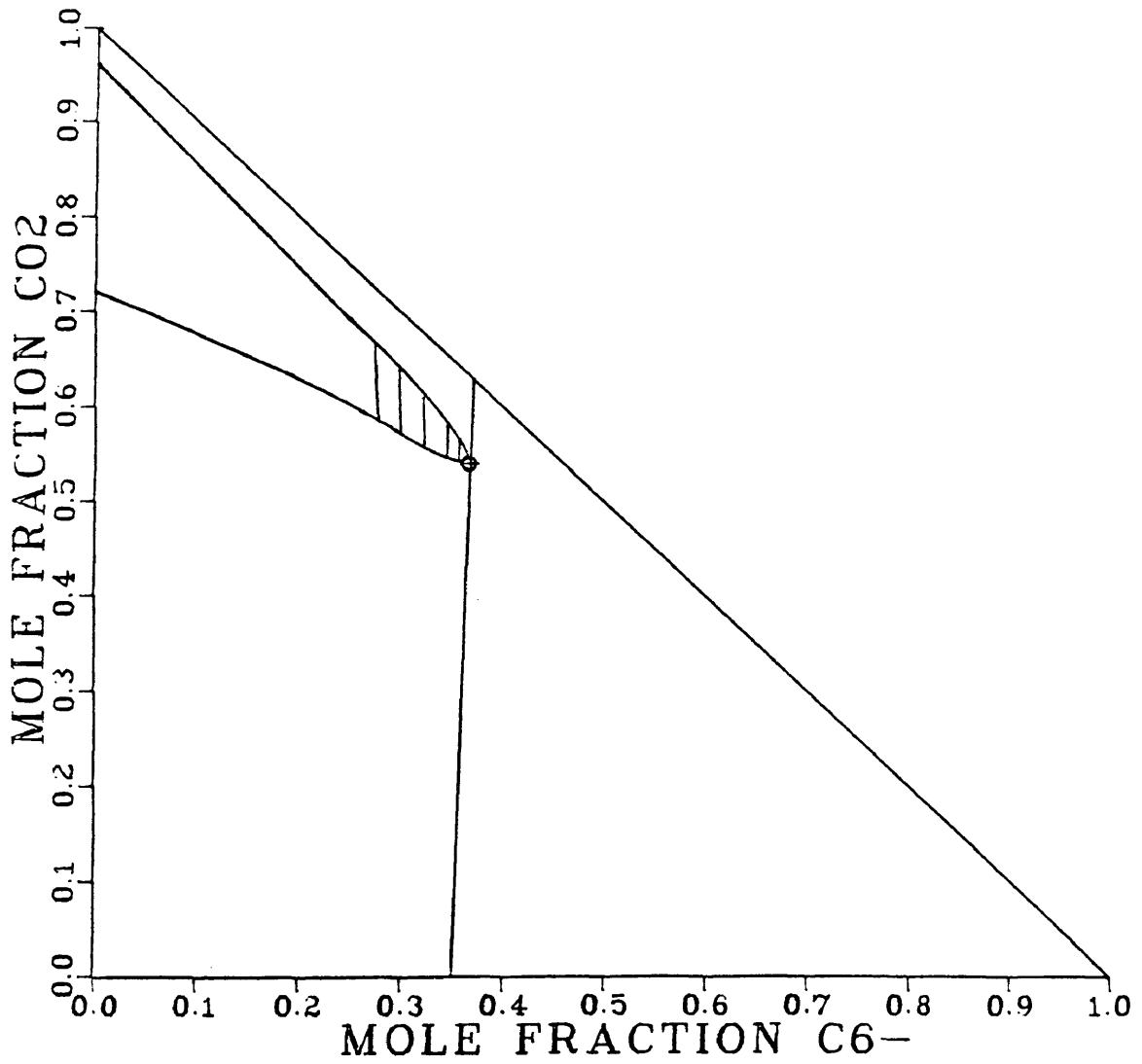


Figure 37. Calculated Pseudoternary Diagram for Ford Geraldine System: 200°F 2681.3 psia

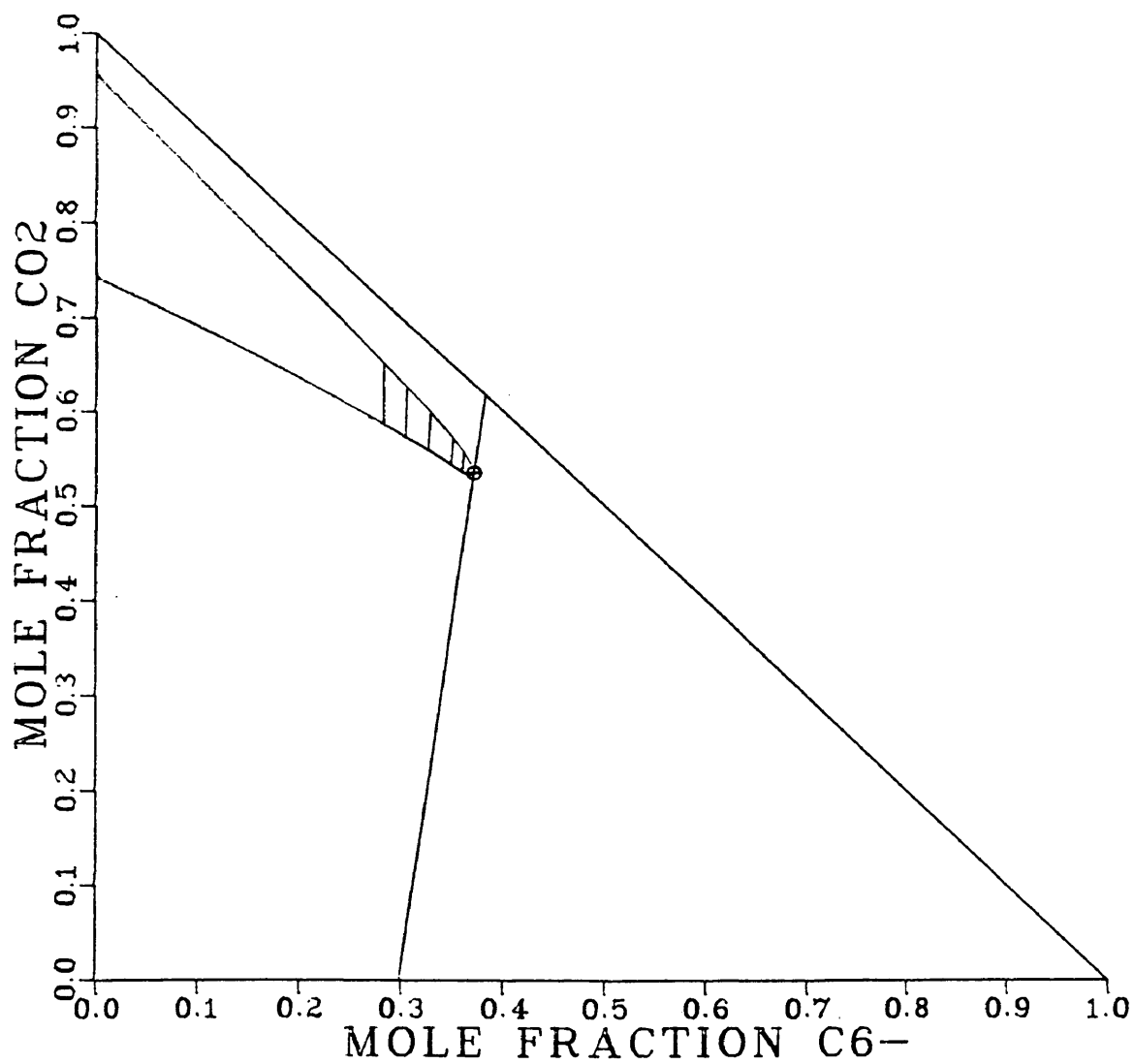


Figure 38. Calculated Pseudoternary Diagram for West Sussex System: 200°F 3170.5 psia

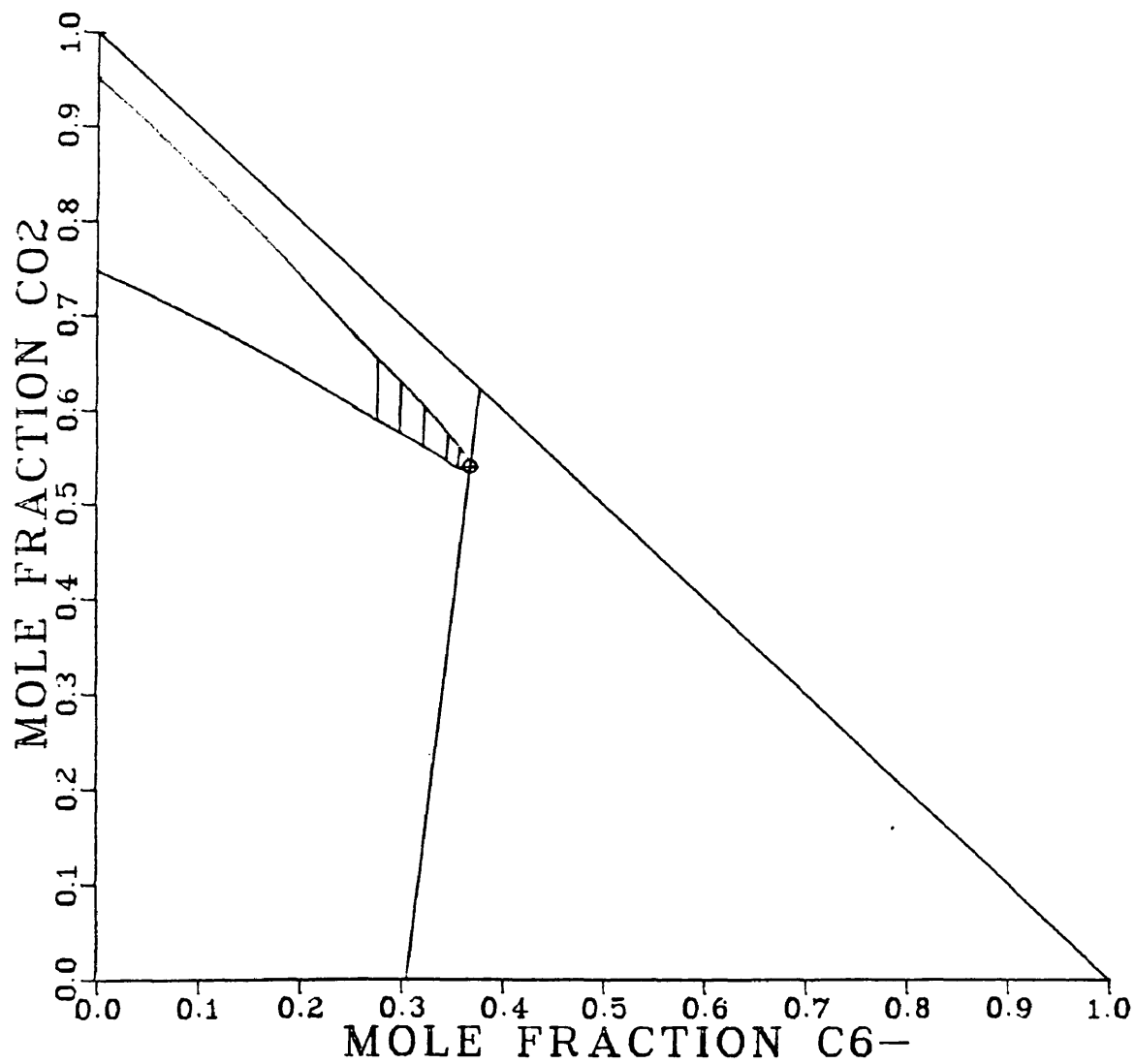


Figure 39. Calculated Pseudoternary Diagram for West Sussex System: 250°F 3625.3 psia

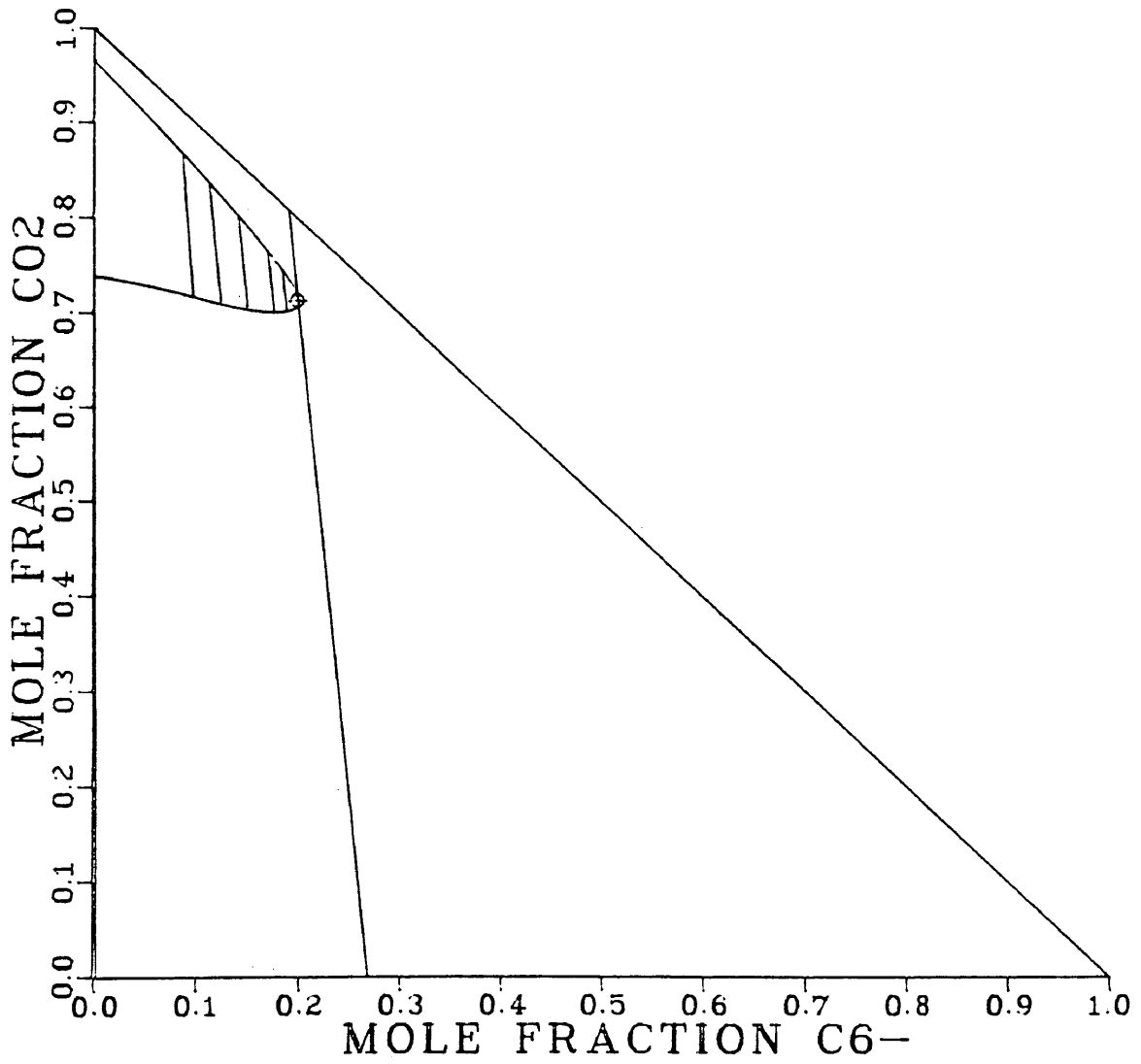


Figure 40. Calculated Pseudoternary Diagram for Maljamar System: 100°F 3782.9 psia

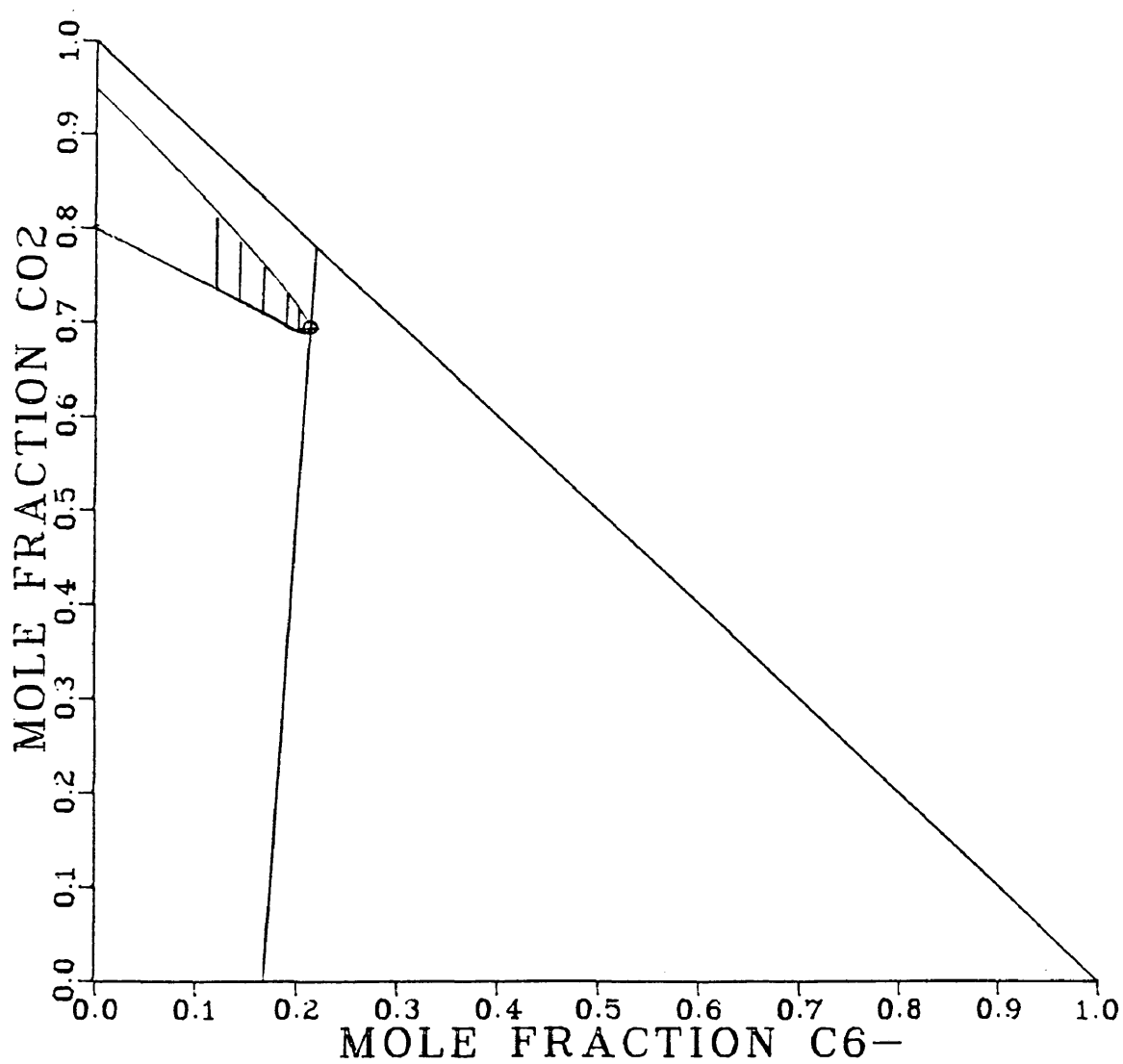


Figure 41. Calculated Pseudoternary Diagram for Maljamar System: 250°F 4646.5 psia

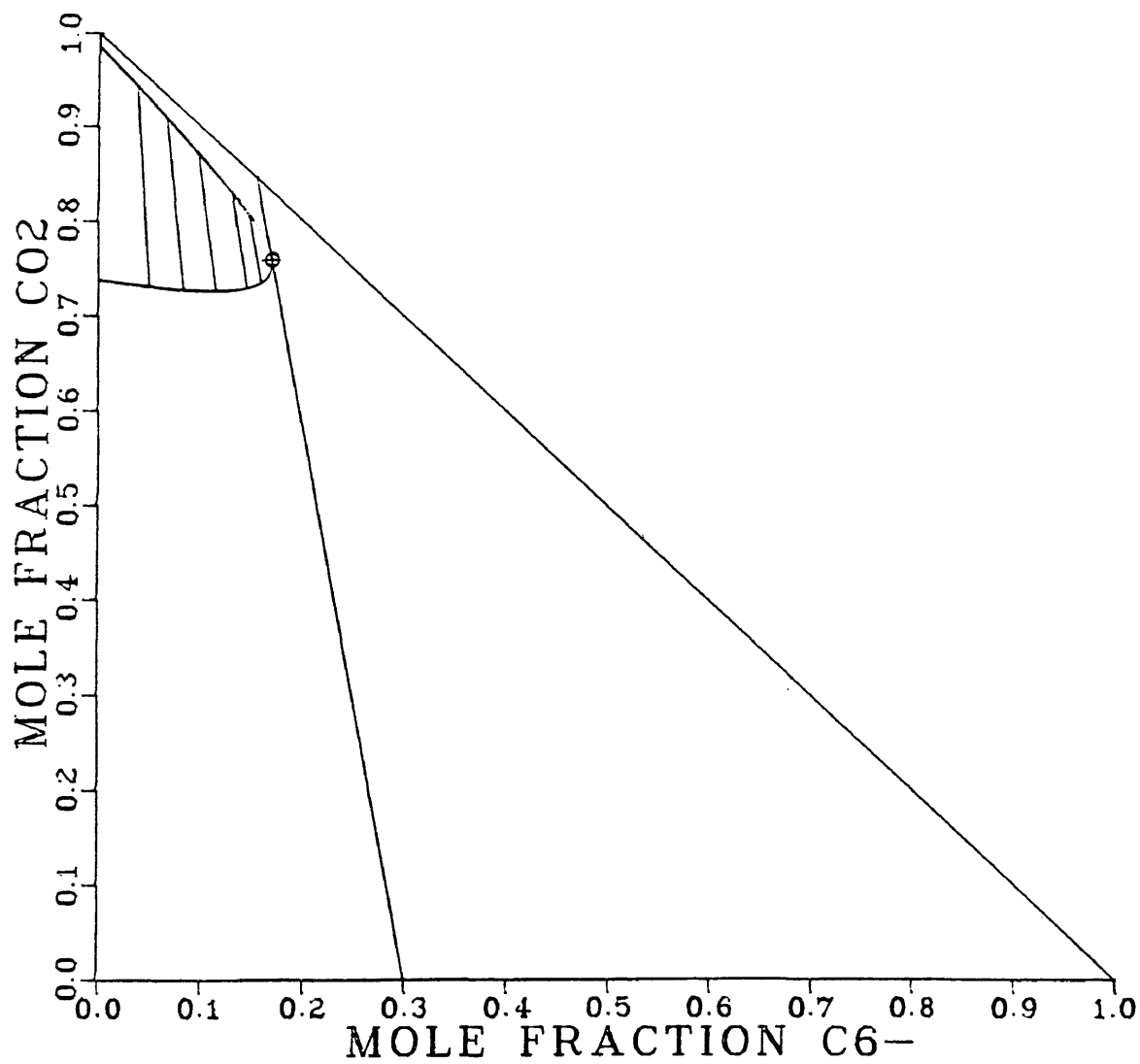


Figure 42. Calculated Pseudoternary Diagram for Reservoir D
System: 100°F 3931.3 psia

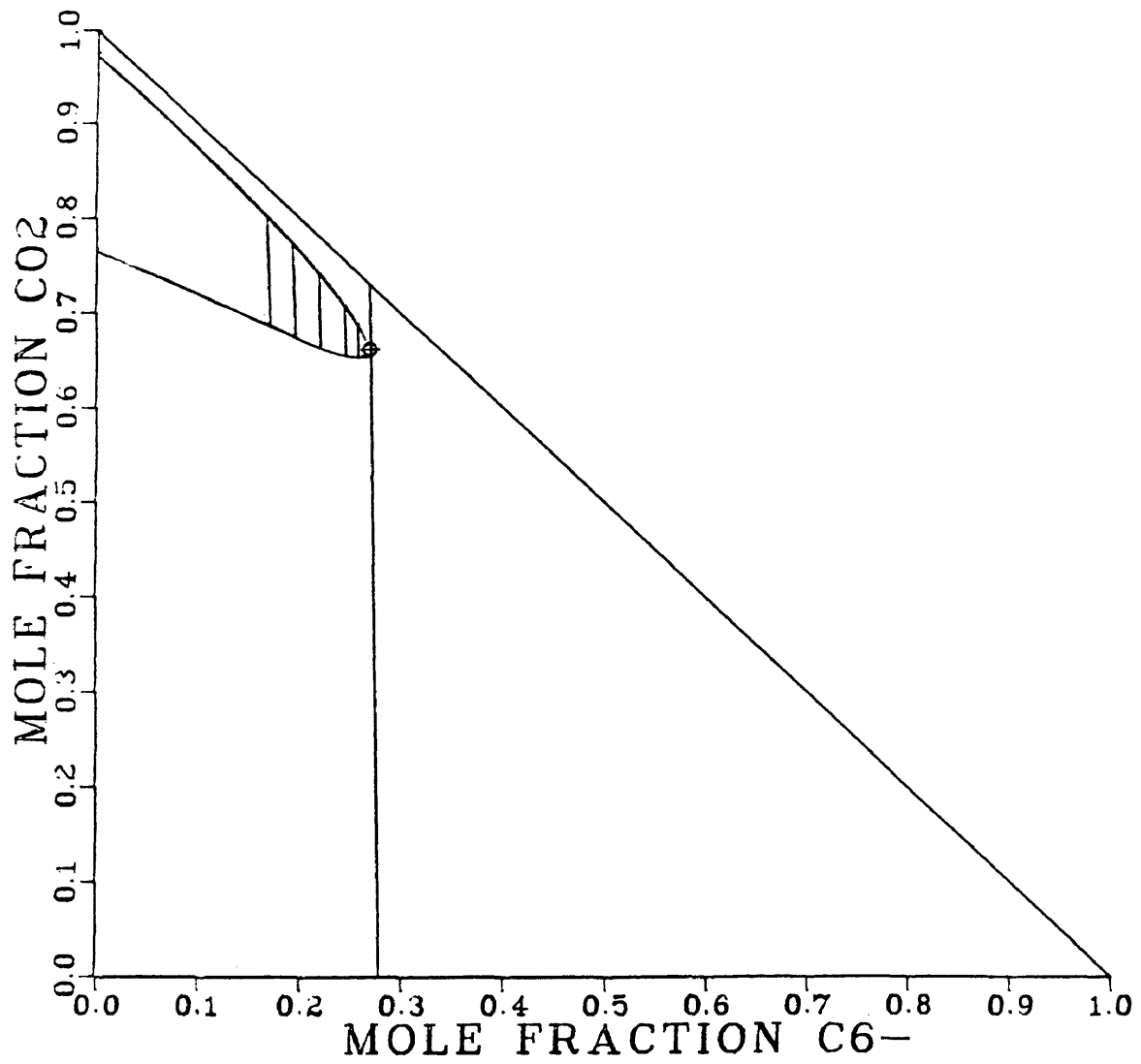


Figure 43. Calculated Pseudoternary Diagram for Reservoir D
System: 200°F 3897.7 psia

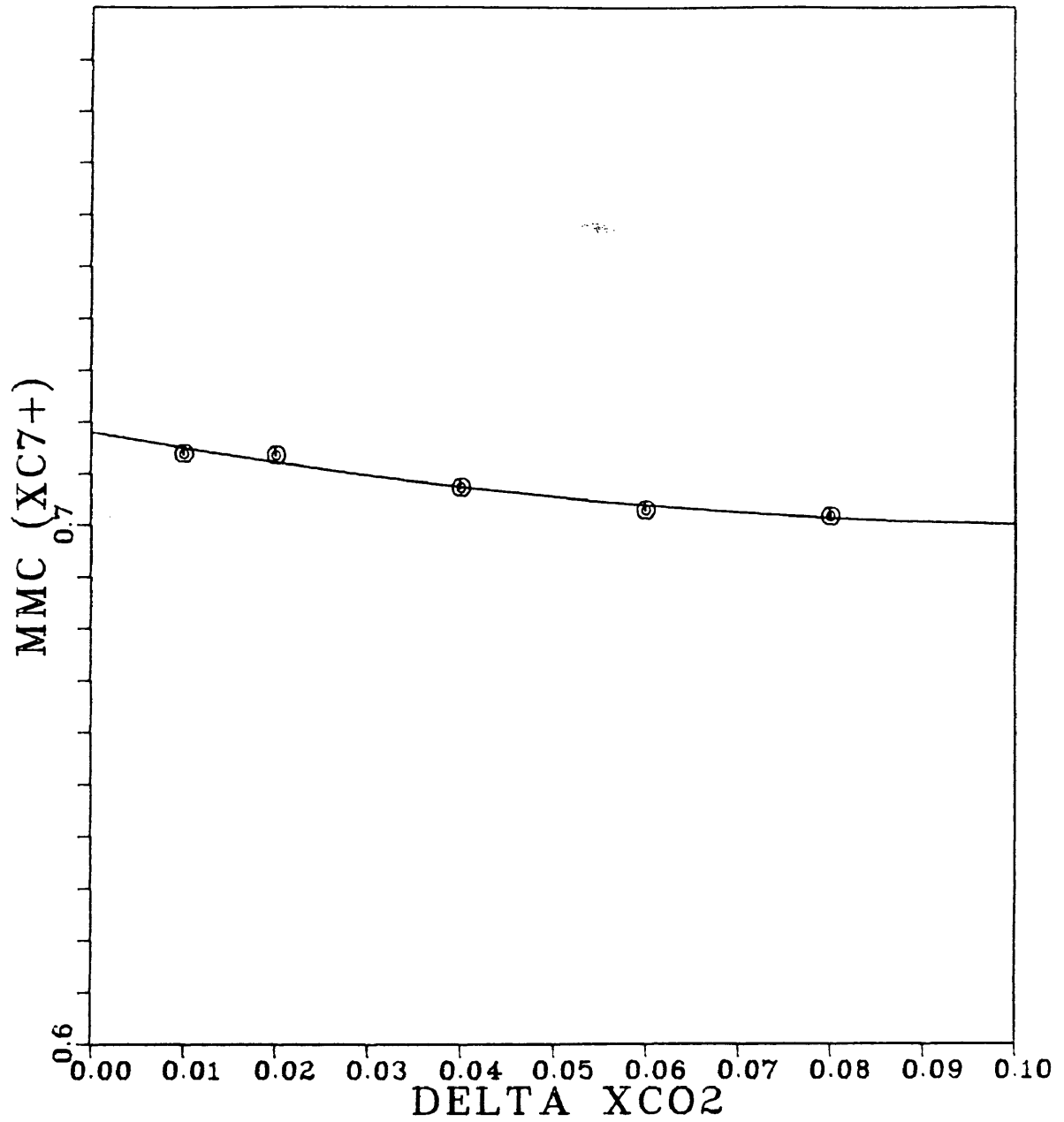


Figure 44. MMC Data Calculated for the Ford Geraldine System: 150°F 2534.9 psia

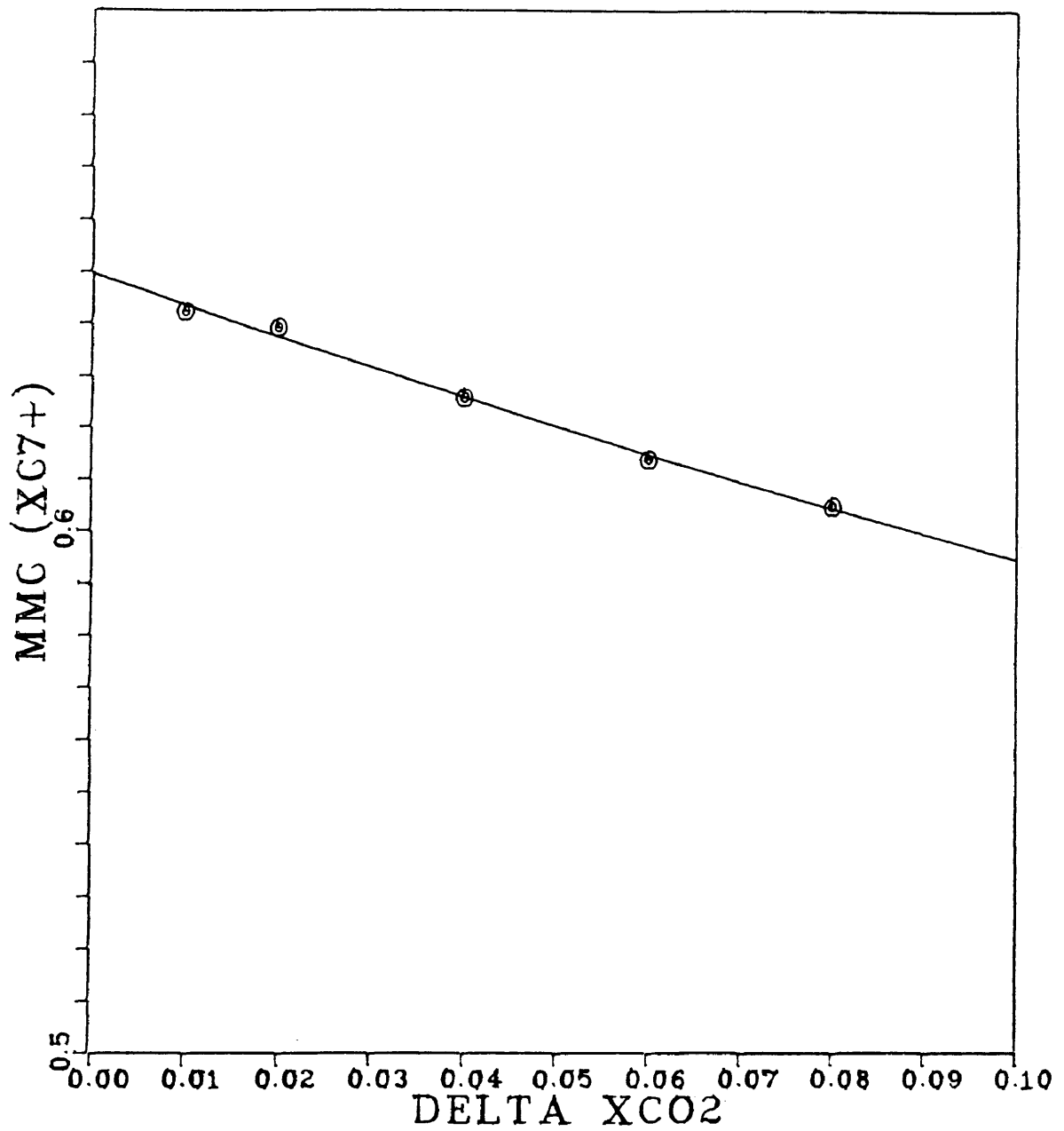


Figure 45. MMC Data Calculated for the Ford Geraldine System: 200°F 2681.3 psia

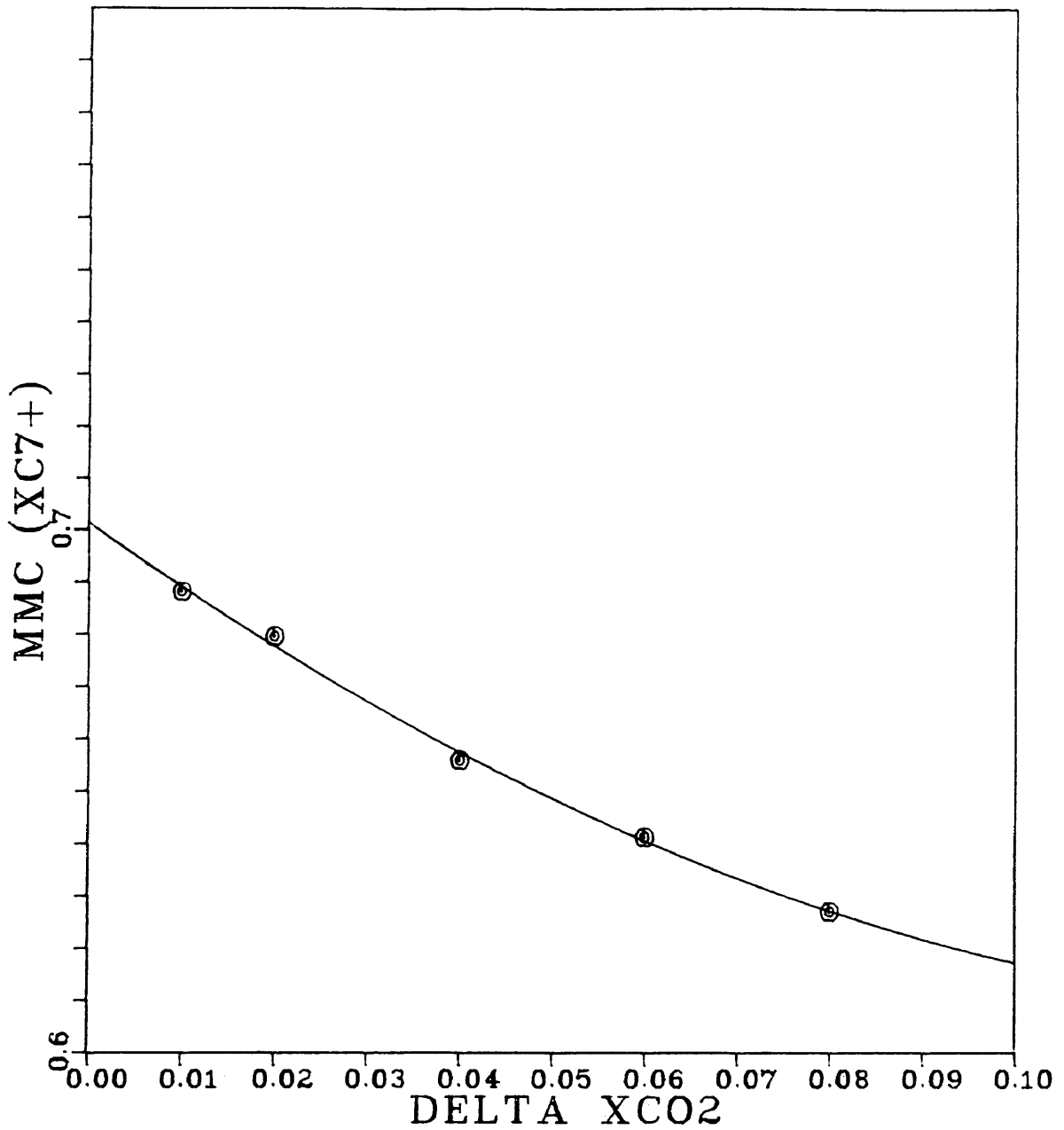


Figure 46. MMC Data Calculated for the West Sussex System:
200°F 3170.5 psia

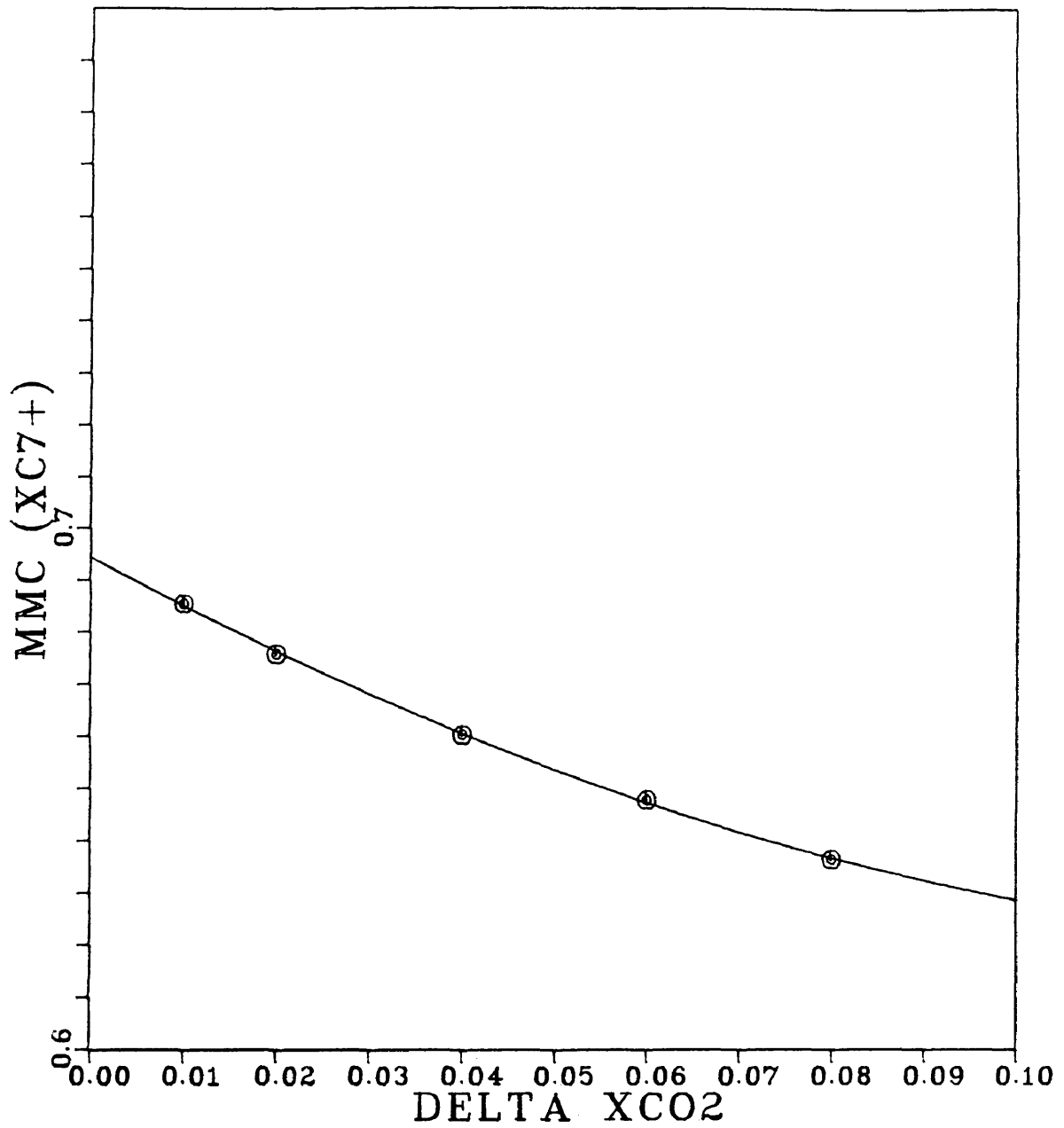


Figure 47. MMC Data Calculated for the West Sussex System:
250°F 3625.3 psia

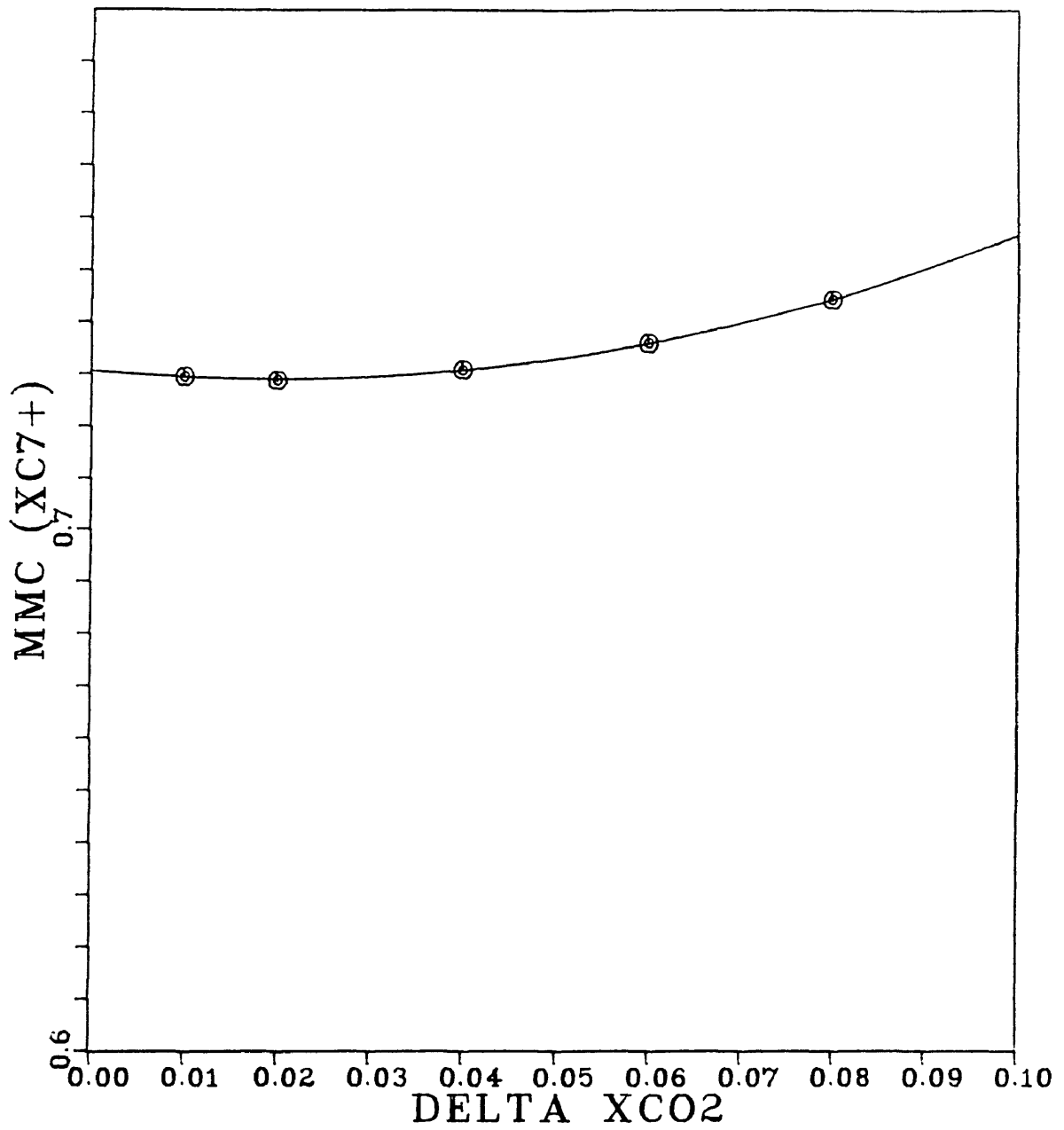


Figure 48. MMC Data Calculated for the Maljamar System:
100°F 3782.9 psia

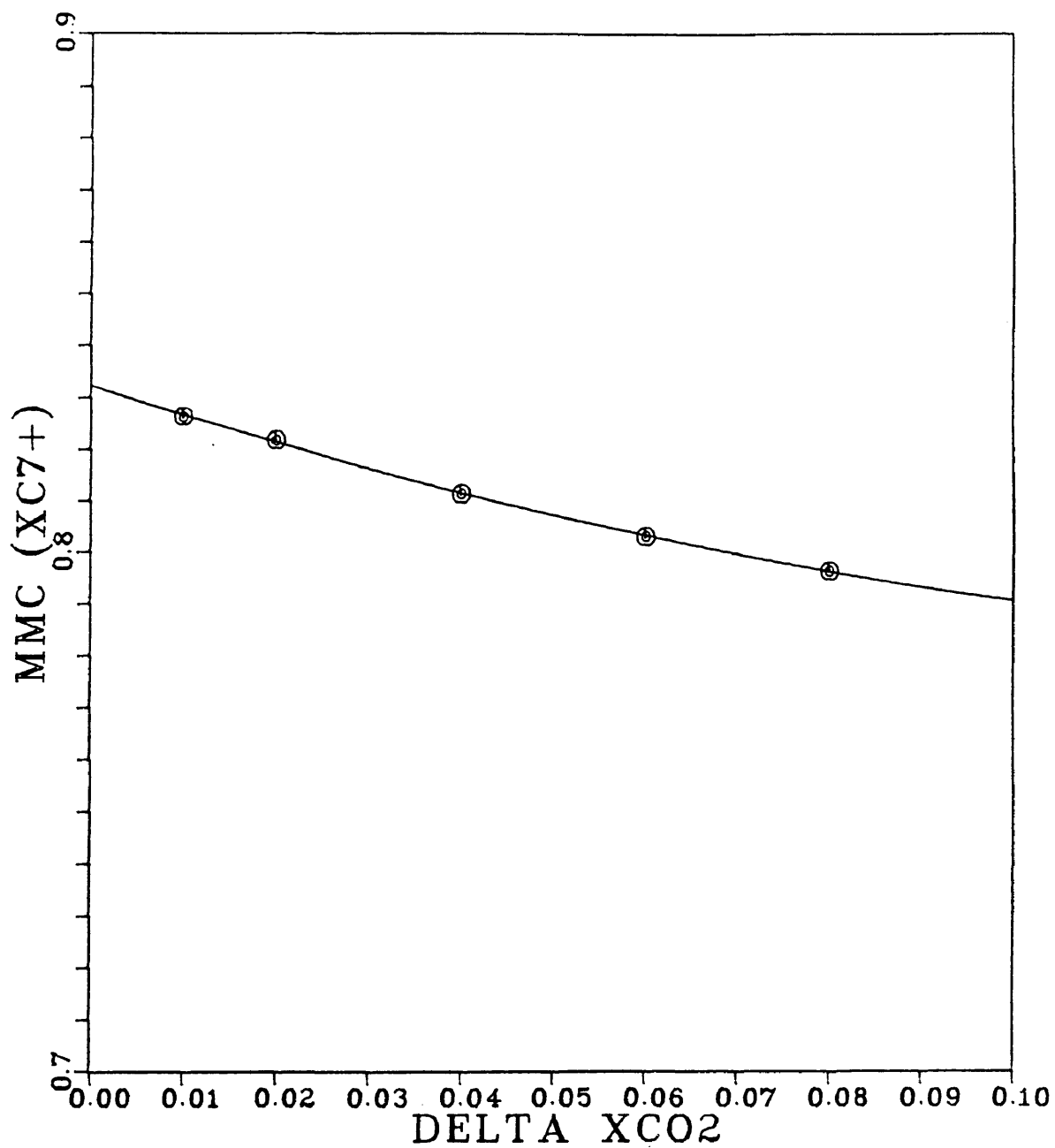


Figure 49. MMC Data Calculated for the Maljamar System:
250°F 4646.5 psia

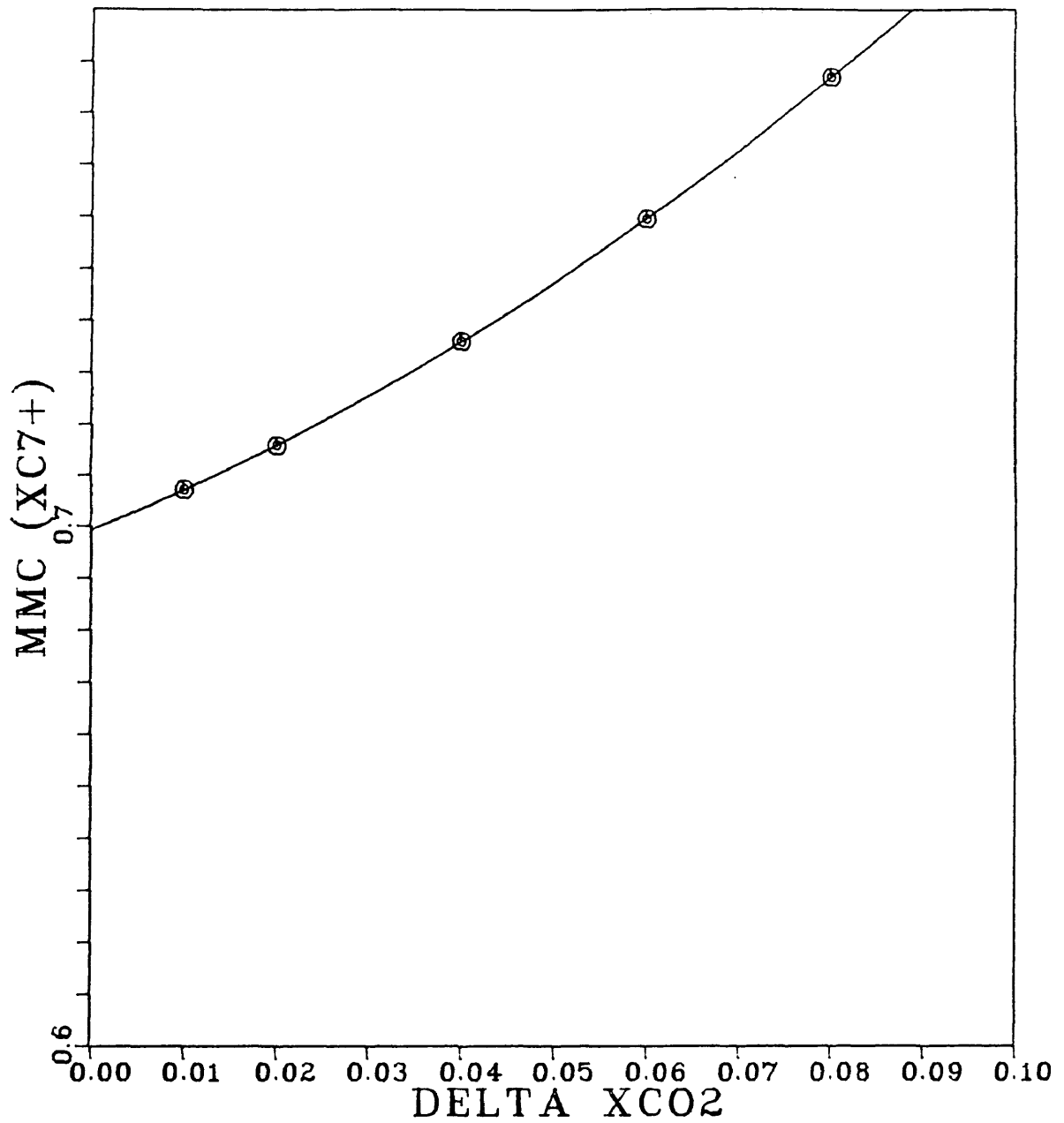


Figure 50. MMC Data Calculated for the Reservoir D System:
100°F 3931.3 psia

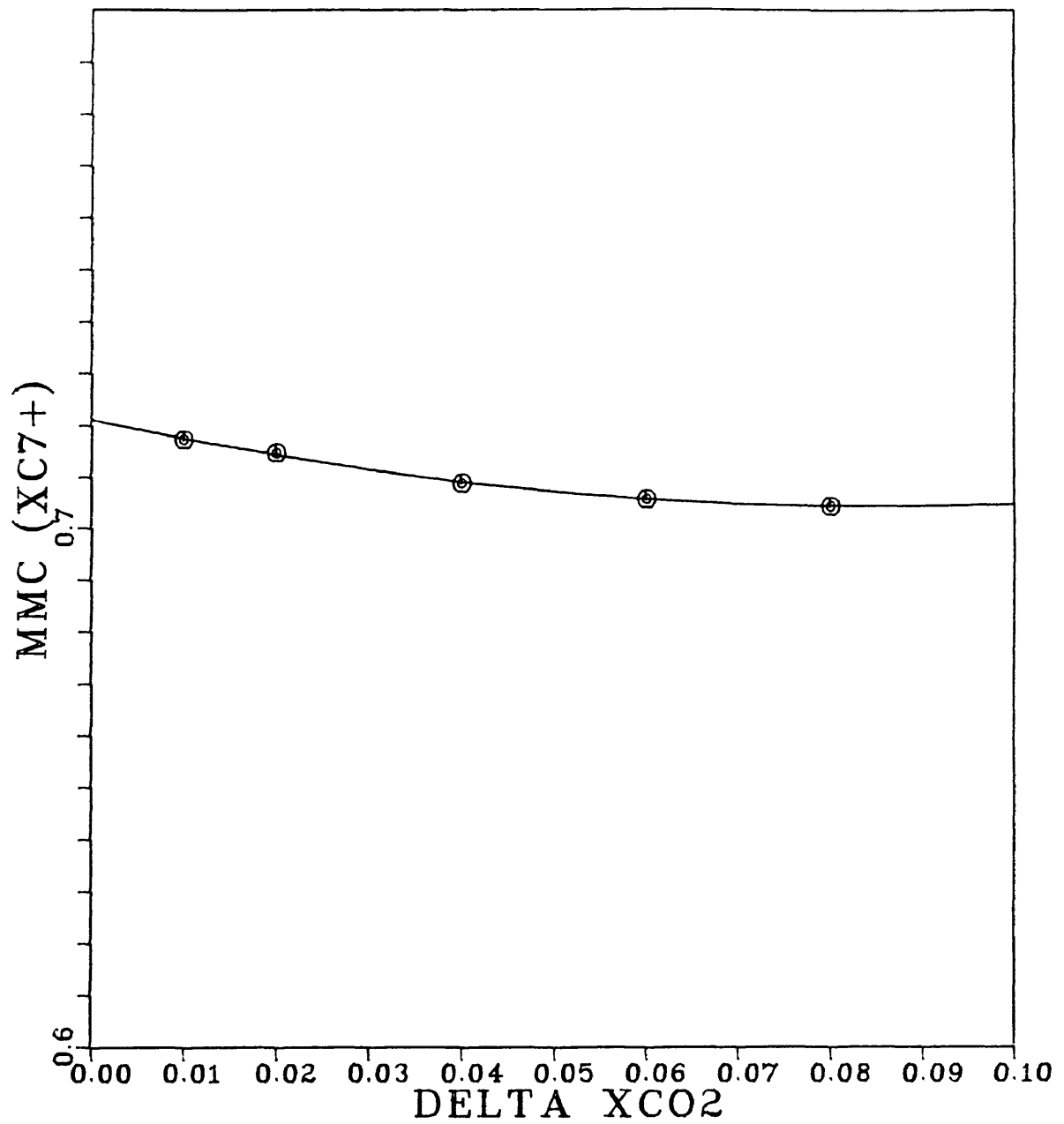


Figure 51. MMC Data Calculated for the Reservoir D System:
200°F 3897.7 psia

DEVELOPMENT OF CORRELATION

An examination of the calculated miscibility conditions in Tables 20-23 revealed that the Ford Geraldine and Reservoir D systems correlate quite well but that the majority of the West Sussex data and several of the Maljamar points are not consistent. For a given system at constant temperature, as the pressure is decreased the two-phase region on the pseudoternary diagram becomes larger, thus as the MMP decreases the MMC should also decrease. These trends are evident for the Ford Geraldine and Reservoir D systems, but with the West Sussex system as the MMP decreases there is very little change in the MMC at the higher temperatures and the MMC actually increases at the lower temperatures. The same behavior is observed with the Maljamar system, but fewer points are involved.

This behavior appears to be due to the calculated tie lines rather than the critical points. Figures 52-54 show the calculated pseudoternary diagrams for the West Sussex system at 100°F. The phase envelopes and the location of the critical points appear normal. The two-phase region becomes larger as the pressure is decreased, however, the slope of the limiting tie line becomes more positive and as a result the calculated MMC is higher at 1817 psia than at

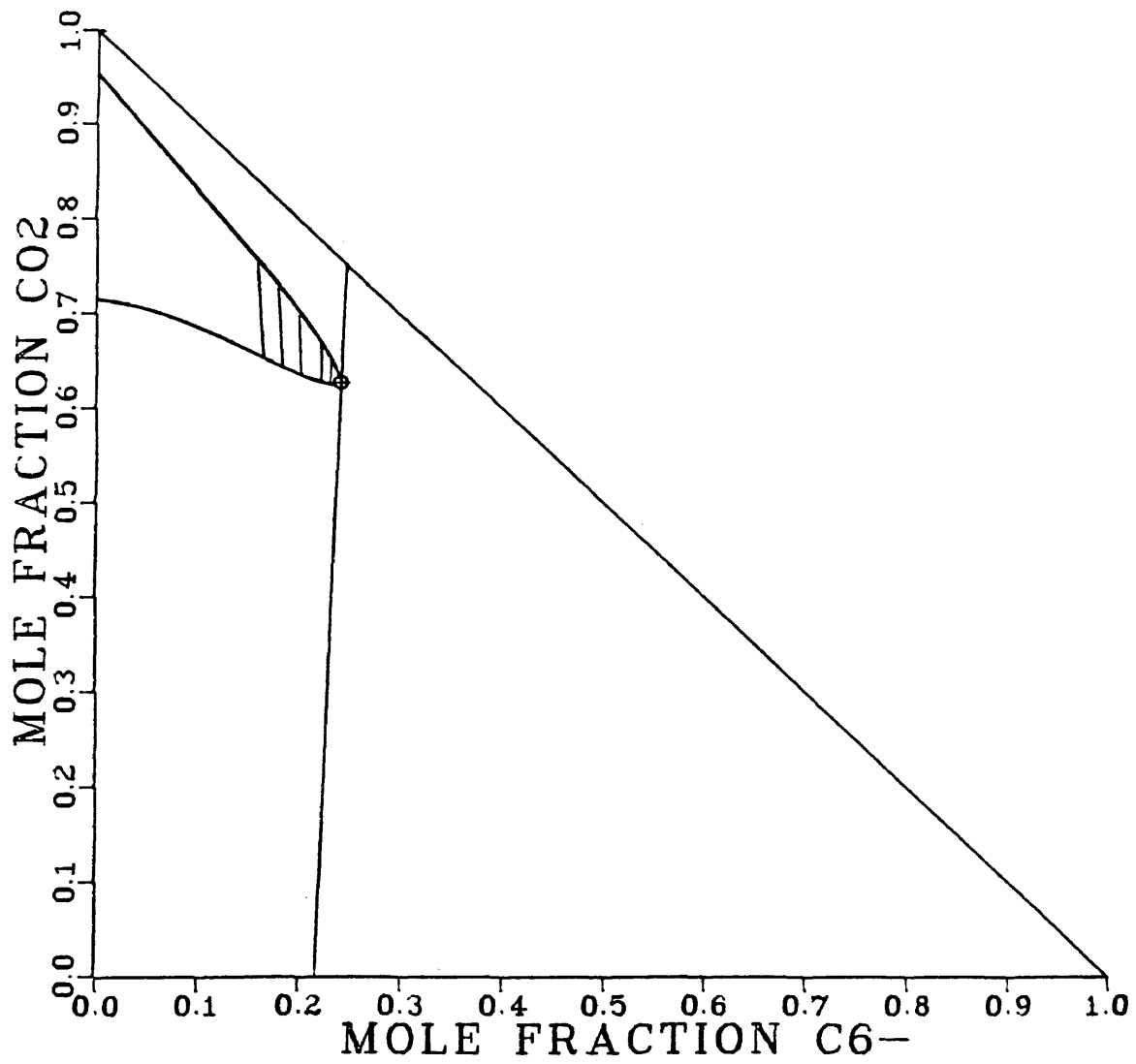


Figure 52. Calculated Pseudoternary Diagram for West Sussex System: 100°F 2859.9 psia

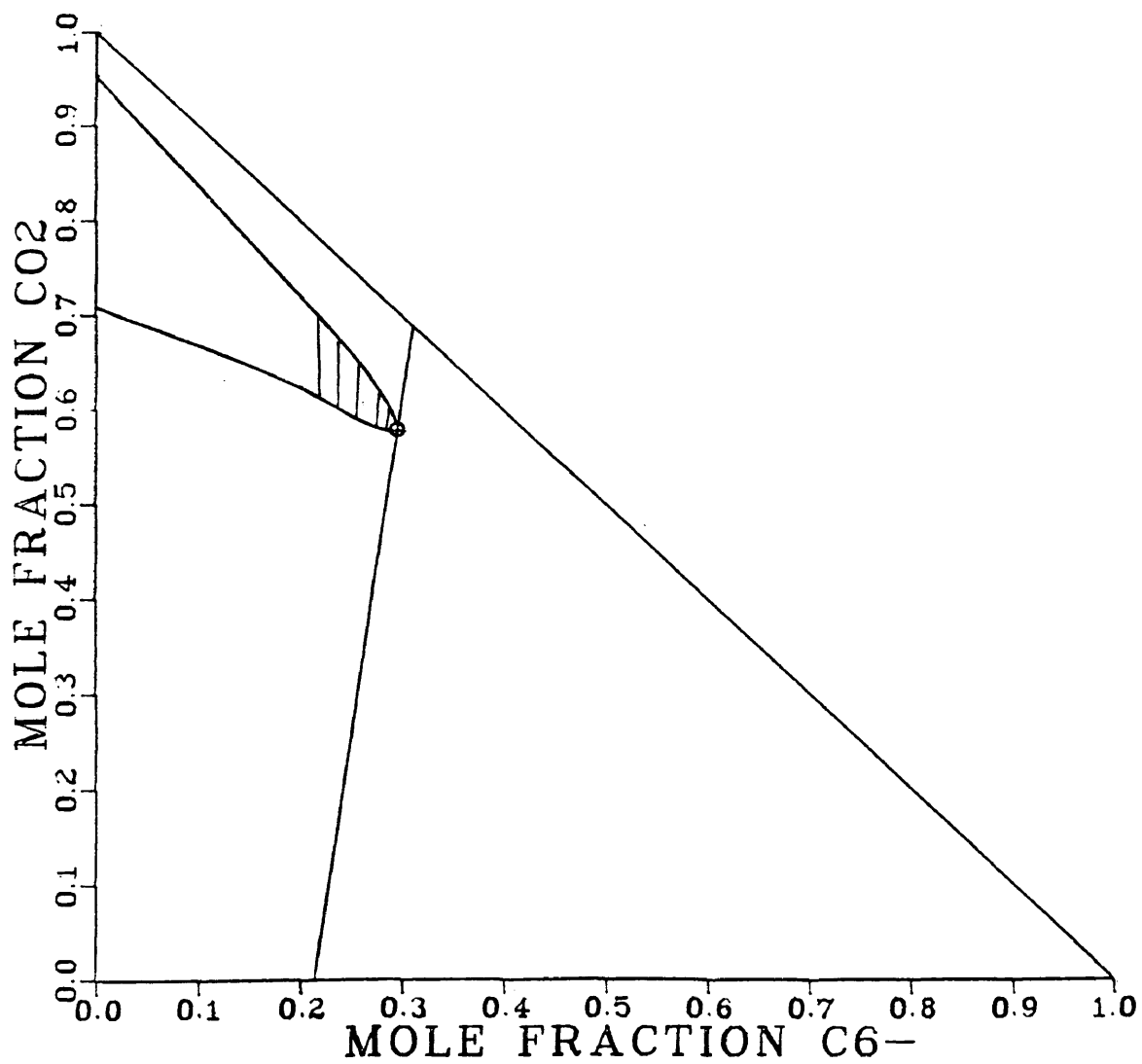


Figure 53. Calculated Pseudoternary Diagram for West Sussex System: 100°F 2134.1 psia

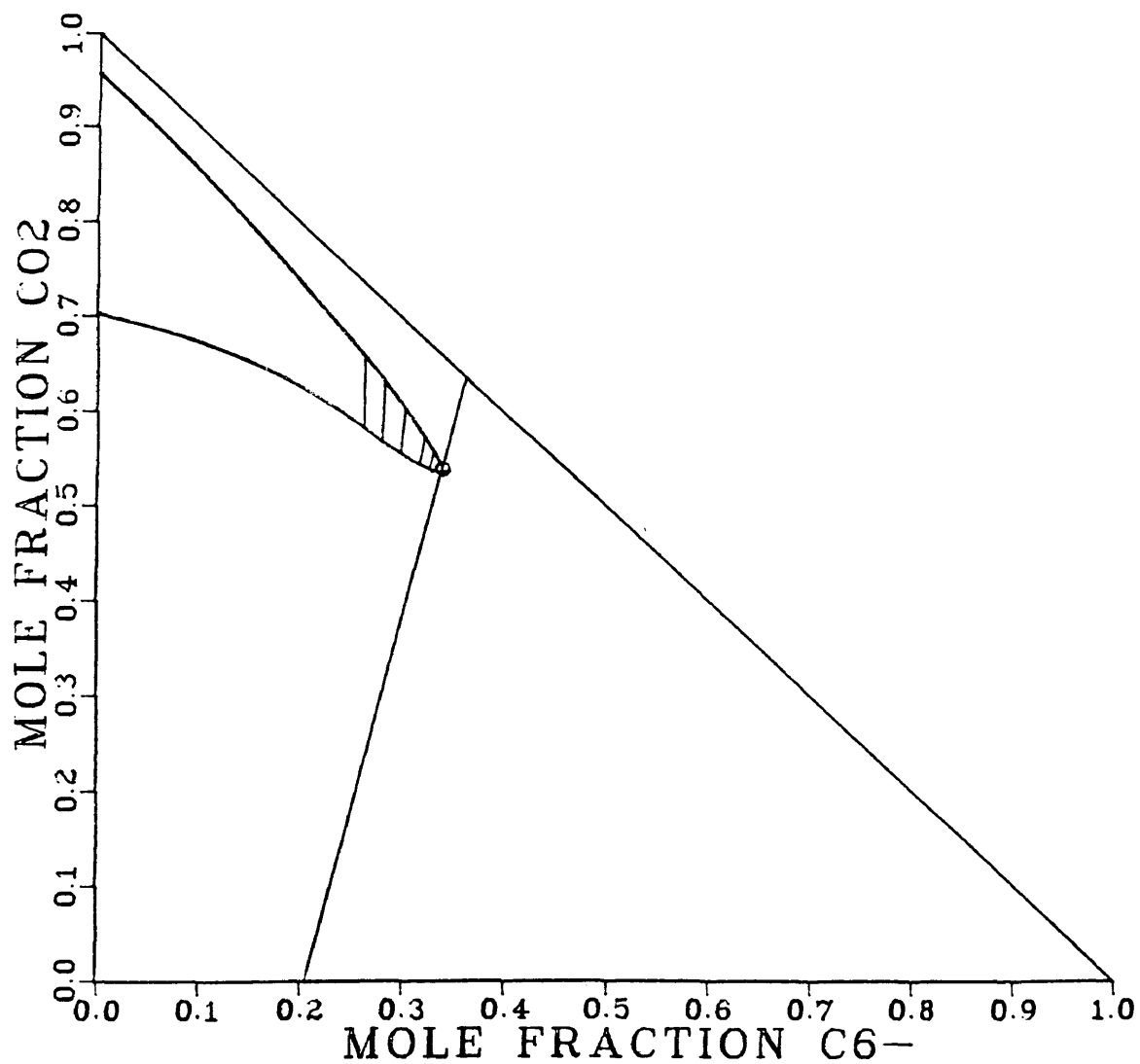


Figure 54. Calculated Pseudoternary Diagram for West Sussex System: 100°F 1817.0 psia

2860 psia. The reason the tie line slopes change so drastically with pressure is not known. It could simply be a characteristic of the West Sussex and Maljamar systems. It is also possible that the EOS characterizations of these systems, particularly the West Sussex, are not accurate enough. In this study--as with most EOS applications--predictions are made well outside the range of temperature, pressure, and composition for which the EOS was originally calibrated and there is no way of knowing how accurate the predictions are under these circumstances.

Because of the inconsistencies in the West Sussex data, it was not used in the development of the generalized correlation for CO₂ MMP. For the same reason, four of the 12 Maljamar points were omitted.

The remaining miscibility data was smoothed to obtain internally consistent relationships between MMP, temperature, and oil composition. It was also necessary to extend the relationships where calculated data did not exist or had been discarded. This was accomplished by plotting the data in two sets and also working with crossplots of the data. By working back and forth between the three types of plots, it was possible to draw smooth curves through the points and extrapolate to fill in any gaps. Figures 55-58 each show the calculated MMP plotted against mole fraction C₇₊ (MMC)

for all four crude systems at one temperature, whereas Figures 59-62 each show the data at all four temperatures for an individual system. Initially, approximate curves were drawn through the points and adjusted so that they were consistent on both the constant temperature plots and the plots for each individual system. These curves were further refined by crossplotting the points at constant temperature and constant mole fraction C_{7+} . Minimum miscibility pressure was plotted against the ratio of the molecular weights of the C_{7+} and C_{6-} fractions. Good results were obtained by making MMP a linear function of this ratio. The crossplots showing the linear relationships are illustrated in Figures 63-66. No data points are shown in these figures because the curves shown in Figures 55-62 are taken directly from the crossplots and better illustrate the fit of the calculated miscibility conditions. The C_{6-} and C_{7+} molecular weights and the molecular weight ratio R of the four original reservoir fluids are shown in Table 24.

The smoothing and extrapolation process was aided by the fact that the Maljamar system is bounded by the Ford Geraldine and Reservoir D systems which are relatively well defined. In addition, for each system mixtures of CO_2 and the C_{6-} fraction were treated as pseudobinaries and the critical point locus calculated with the PR EOS. At the

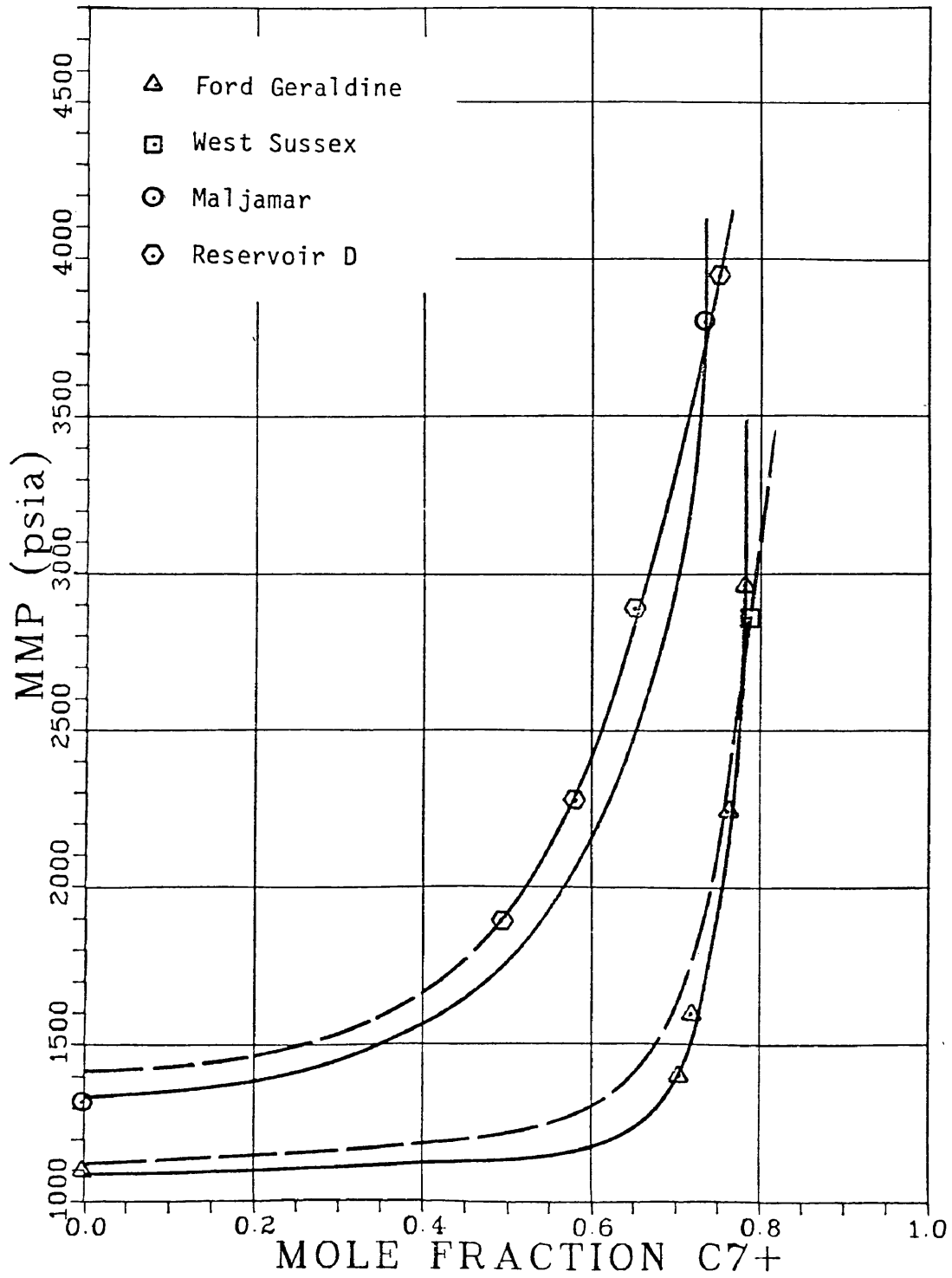


Figure 55. Calculated Miscibility Conditions at 100°F: Ford Geraldine, West Sussex, Maljamar, and Reservoir D Systems

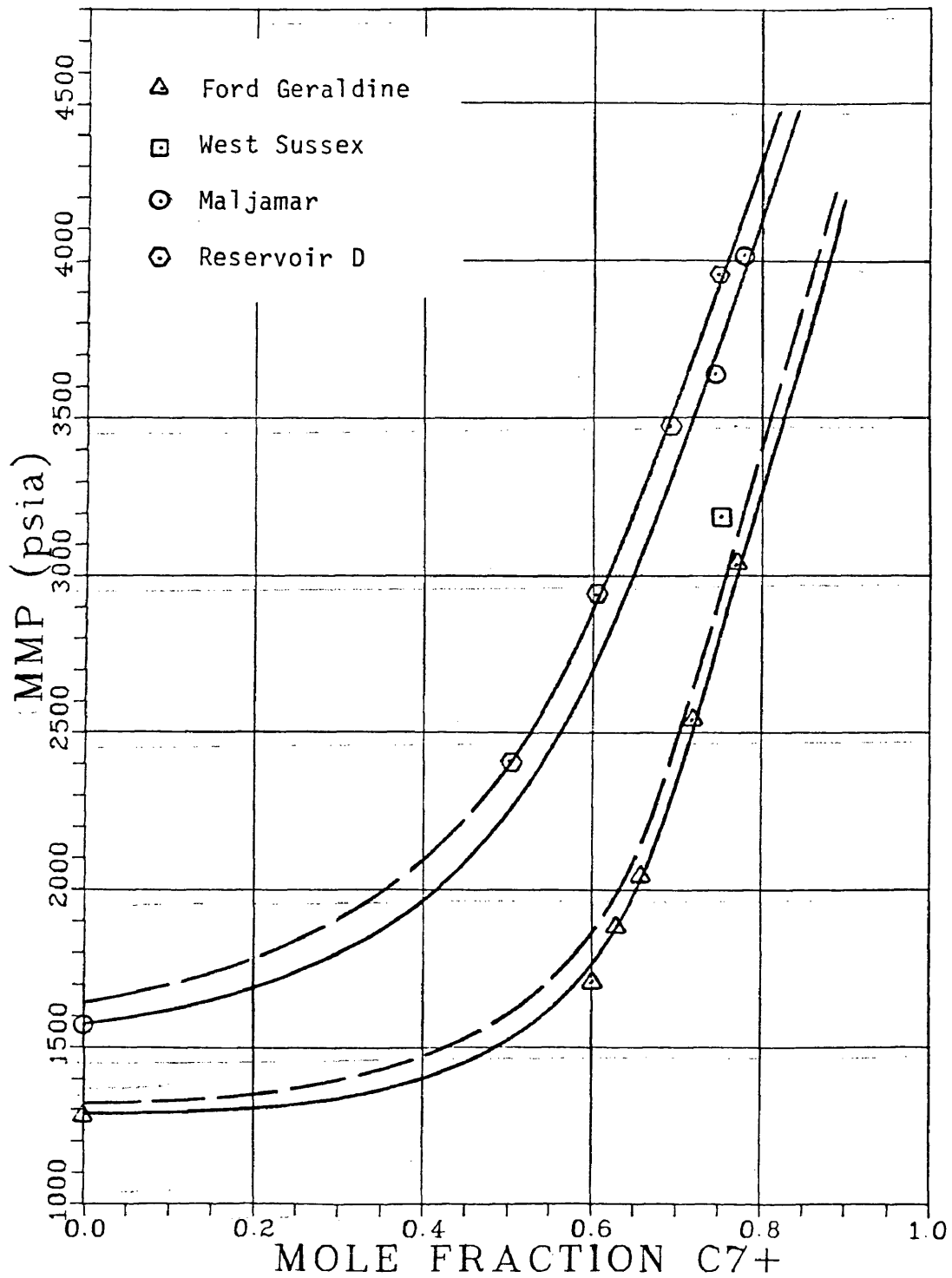


Figure 56. Calculated Miscibility Conditions at 150°F: Ford Geraldine, West Sussex, Maljamar, and Reservoir D Systems

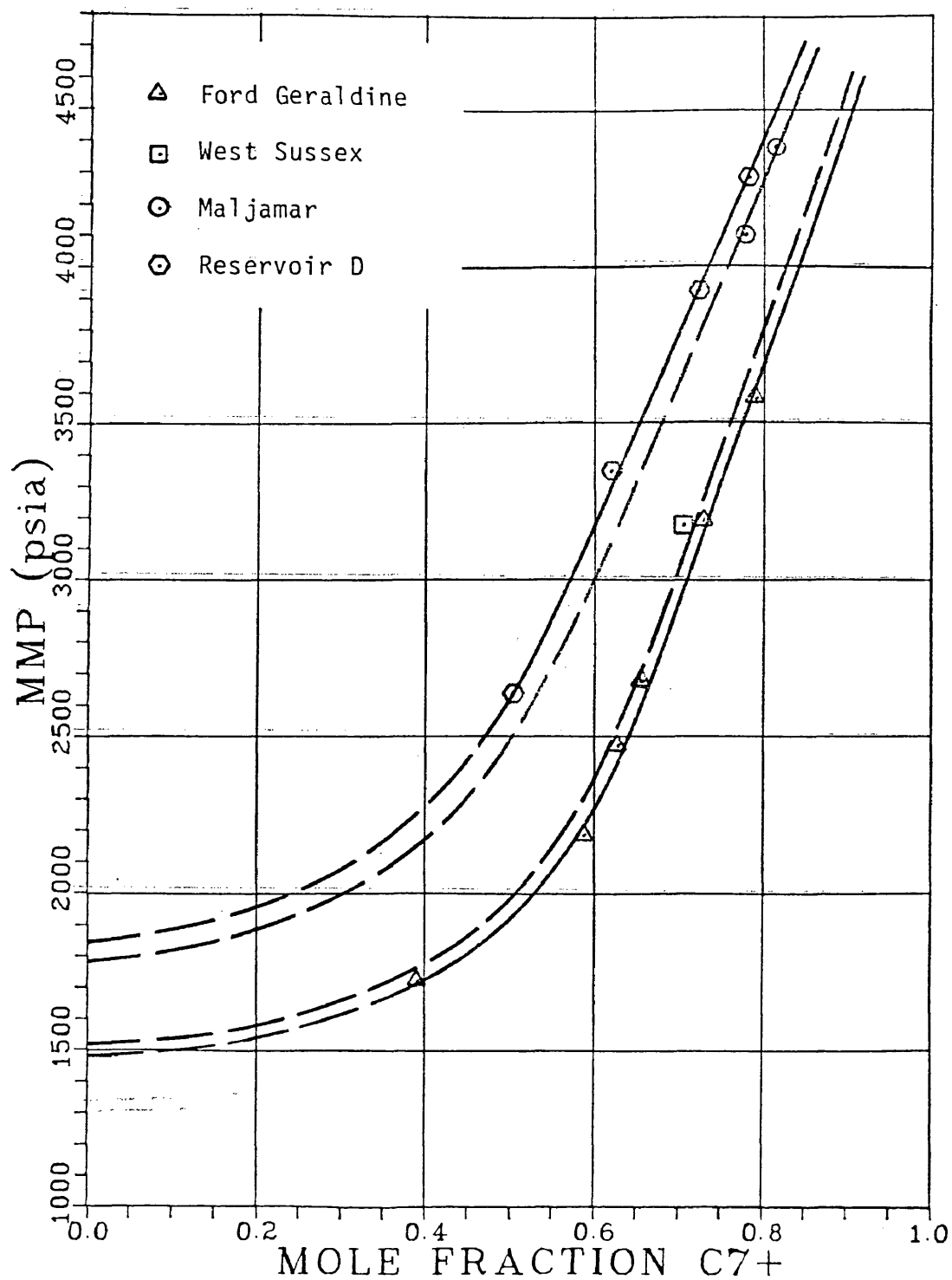


Figure 57. Calculated Miscibility Conditions at 200°F: Ford Geraldine, West Sussex, Maljamar, and Reservoir D Systems

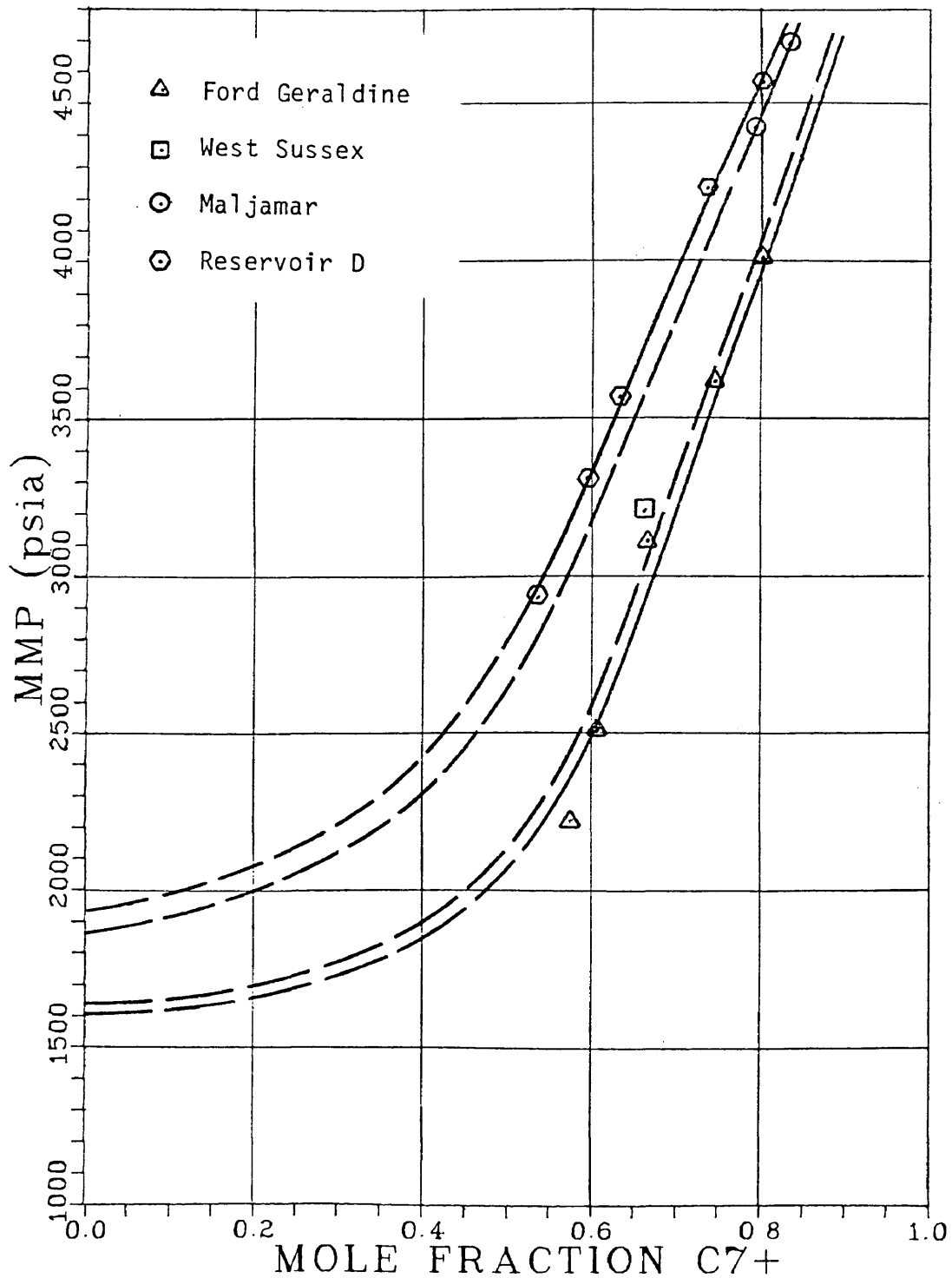


Figure 58. Calculated Miscibility Conditions at 250°F: Ford Geraldine, West Sussex, Maljamar, and Reservoir D Systems

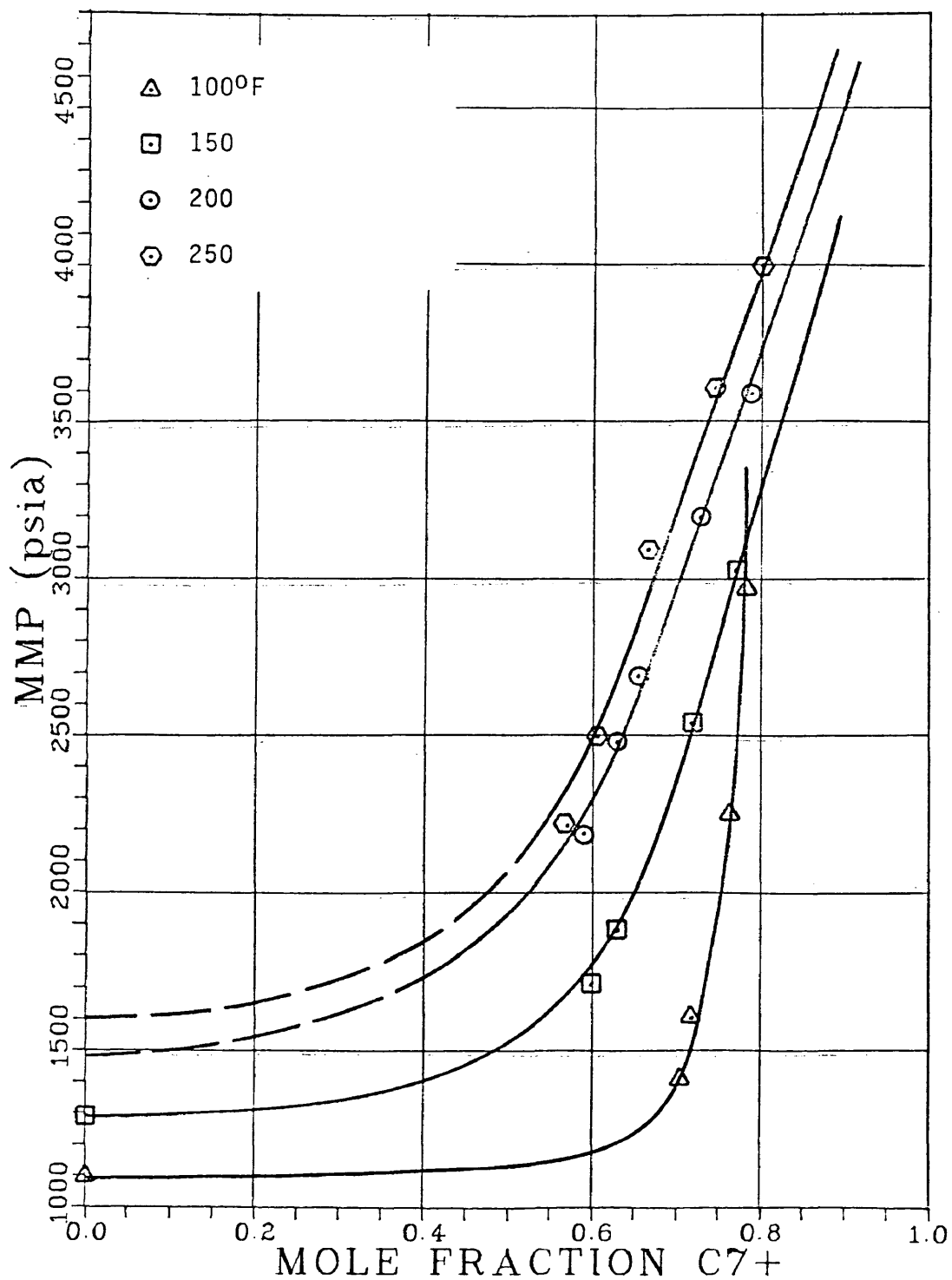


Figure 59. Calculated Miscibility Conditions for Ford Geraldine System at 100, 150, 200, 250°F

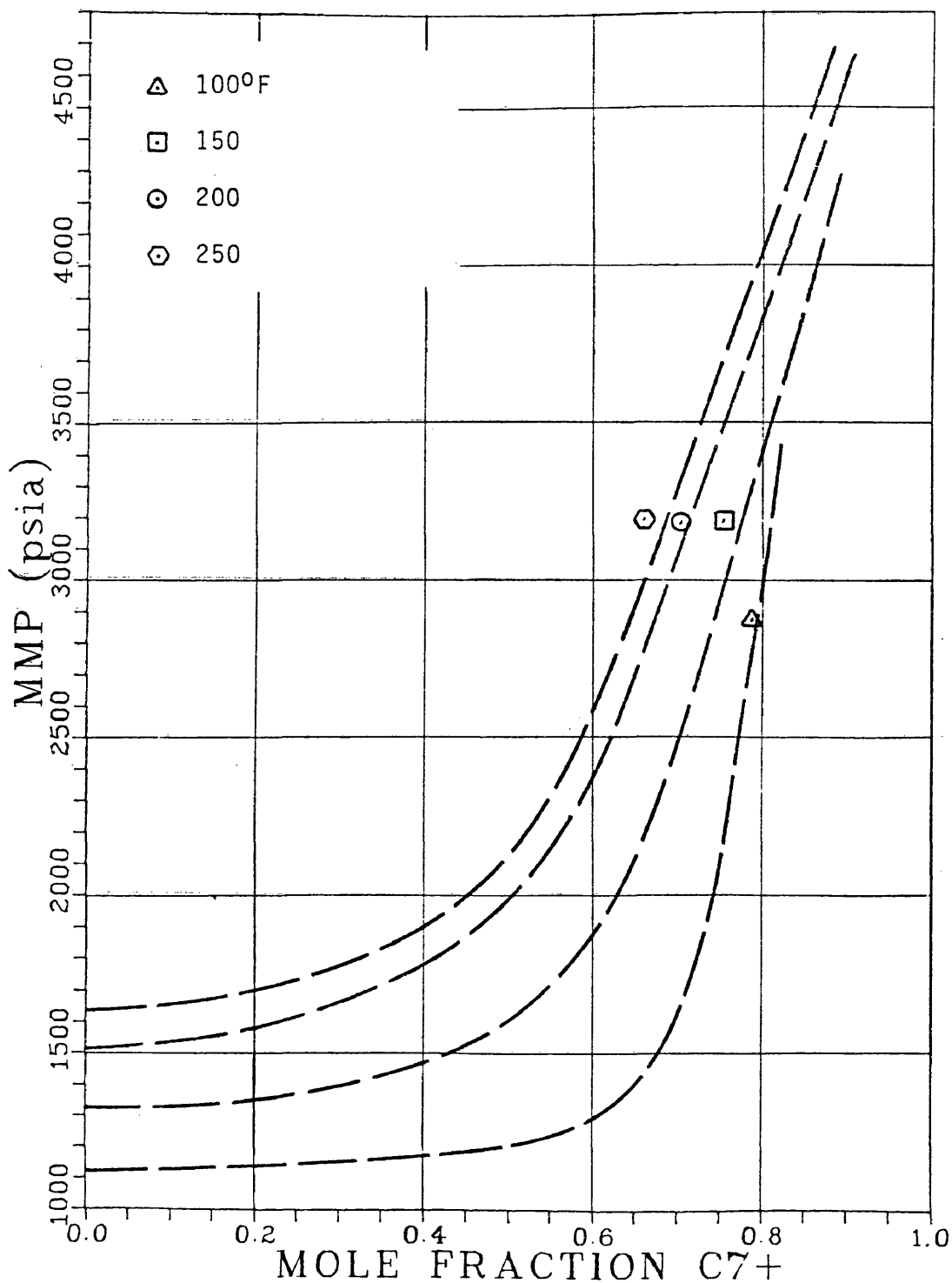


Figure 60. Calculated Miscibility Conditions for West Sussex System at 100, 150, 200, 250°F

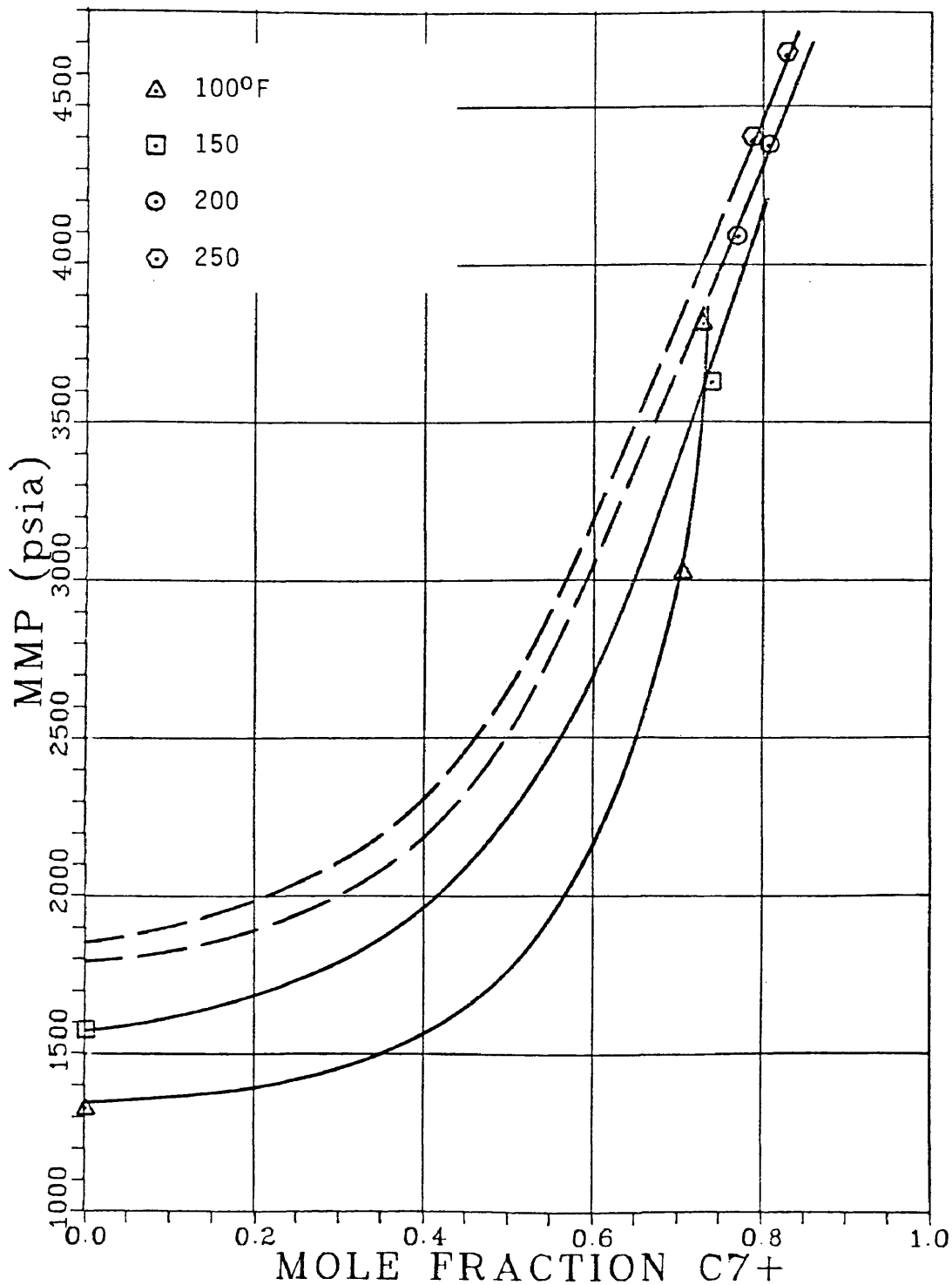


Figure 61. Calculated Miscibility Conditions for Maljamar System at 100, 150, 200, 250°F

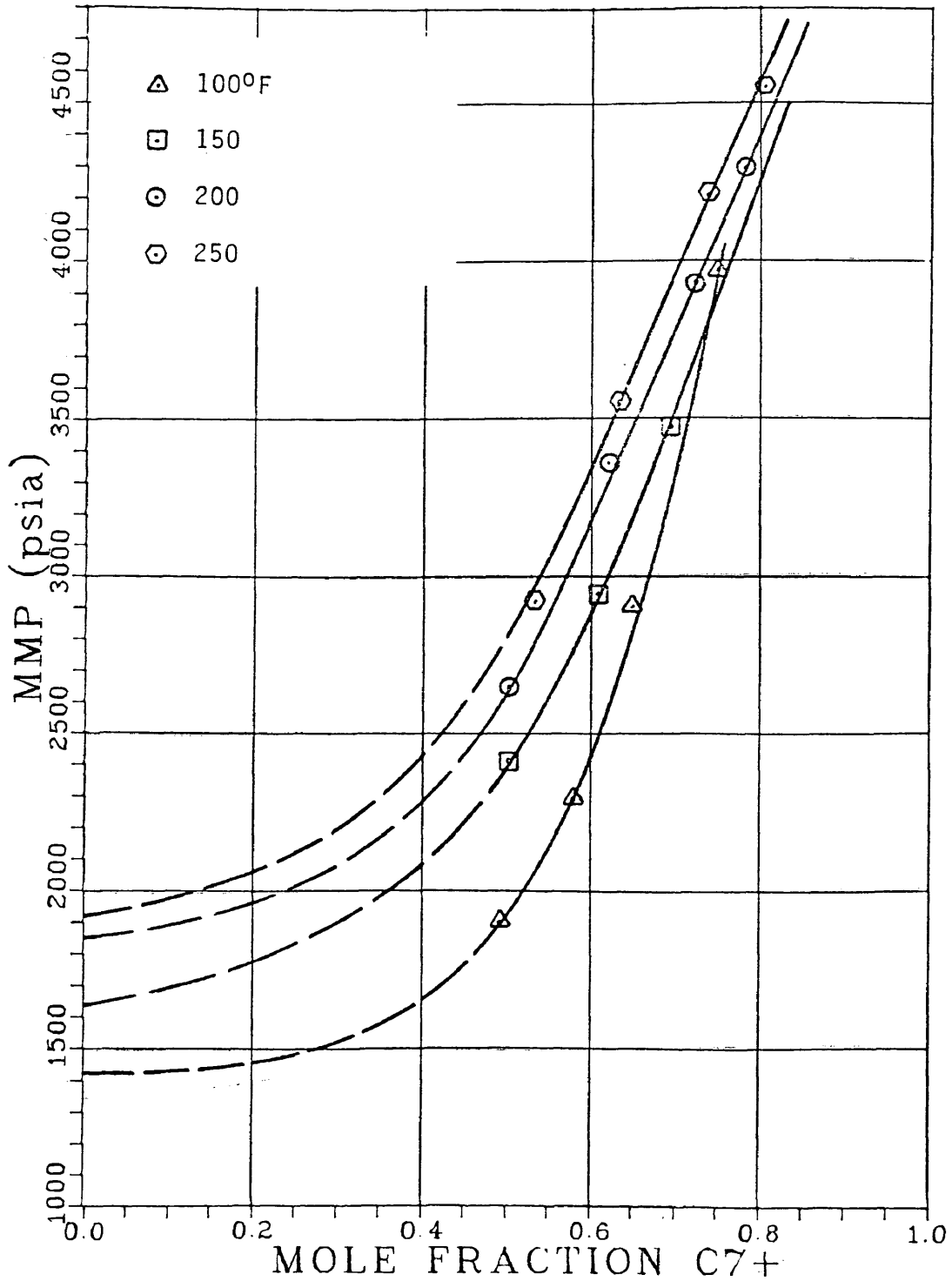


Figure 62. Calculated Miscibility Conditions for Reservoir D System at 100, 150, 200, 250°F

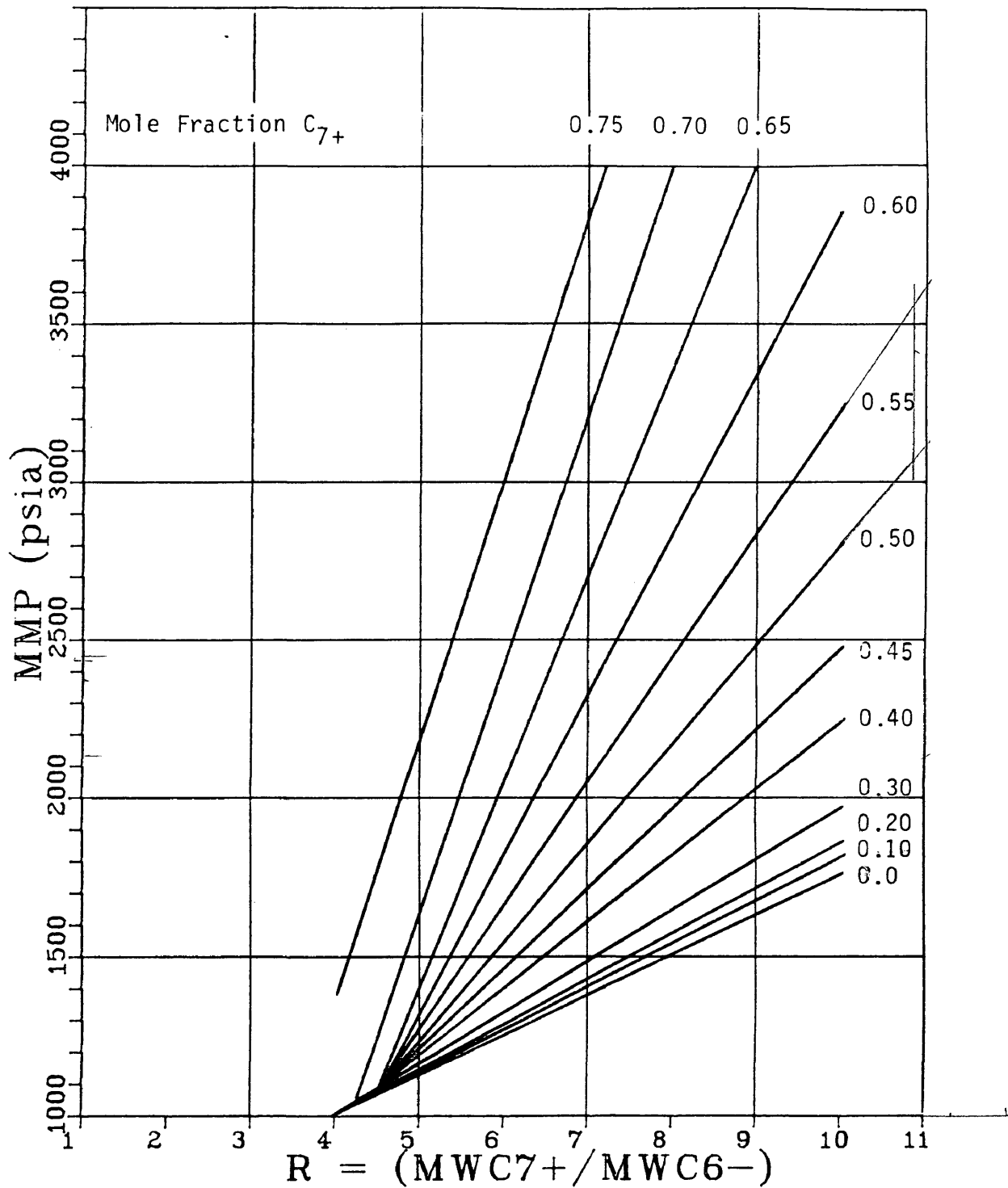


Figure 63. Relationship Between MMP and Crude Molecular Weight Ratio at 100 °F

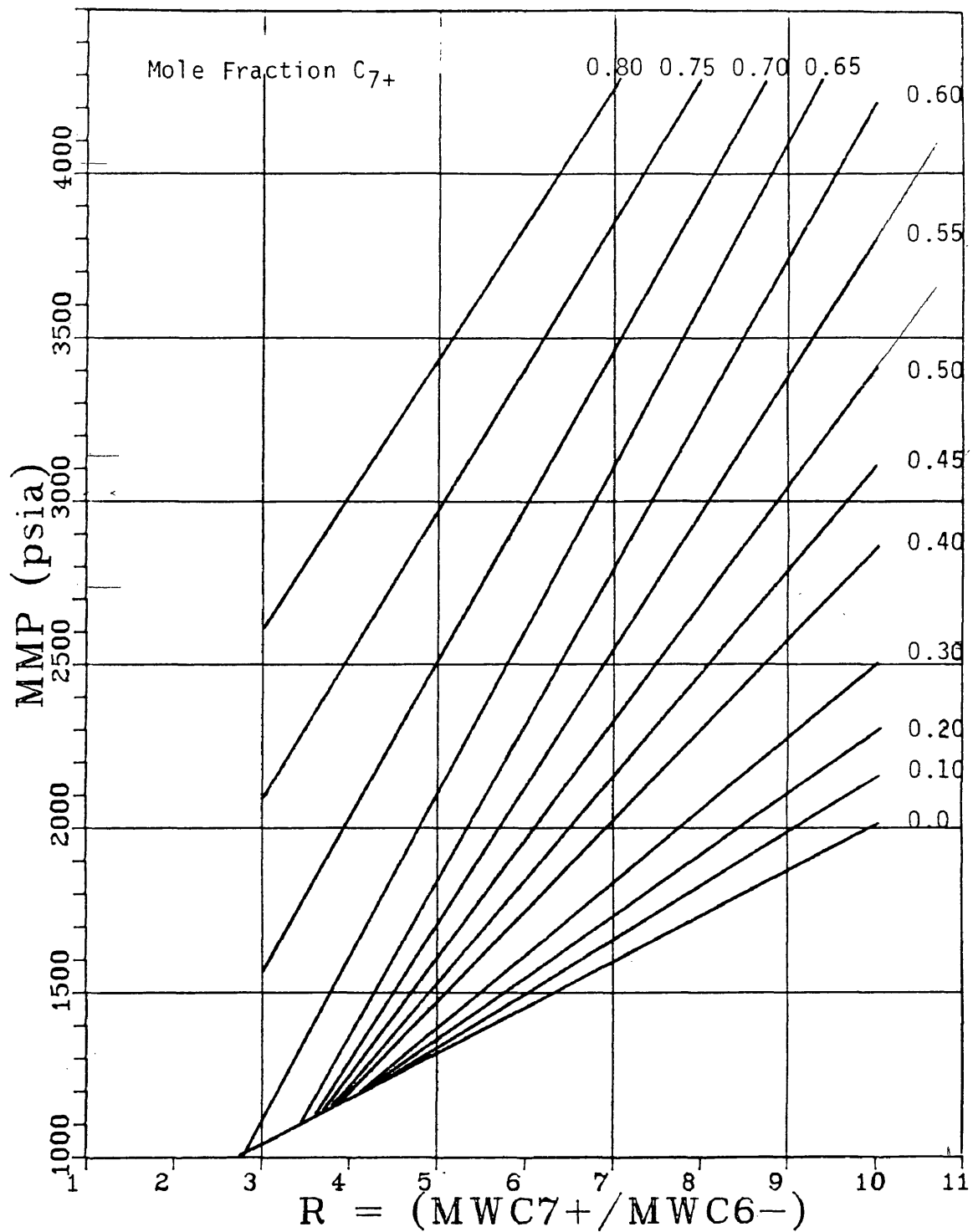


Figure 64. Relationship Between MMP and Crude Molecular Weight Ratio at 150 °F

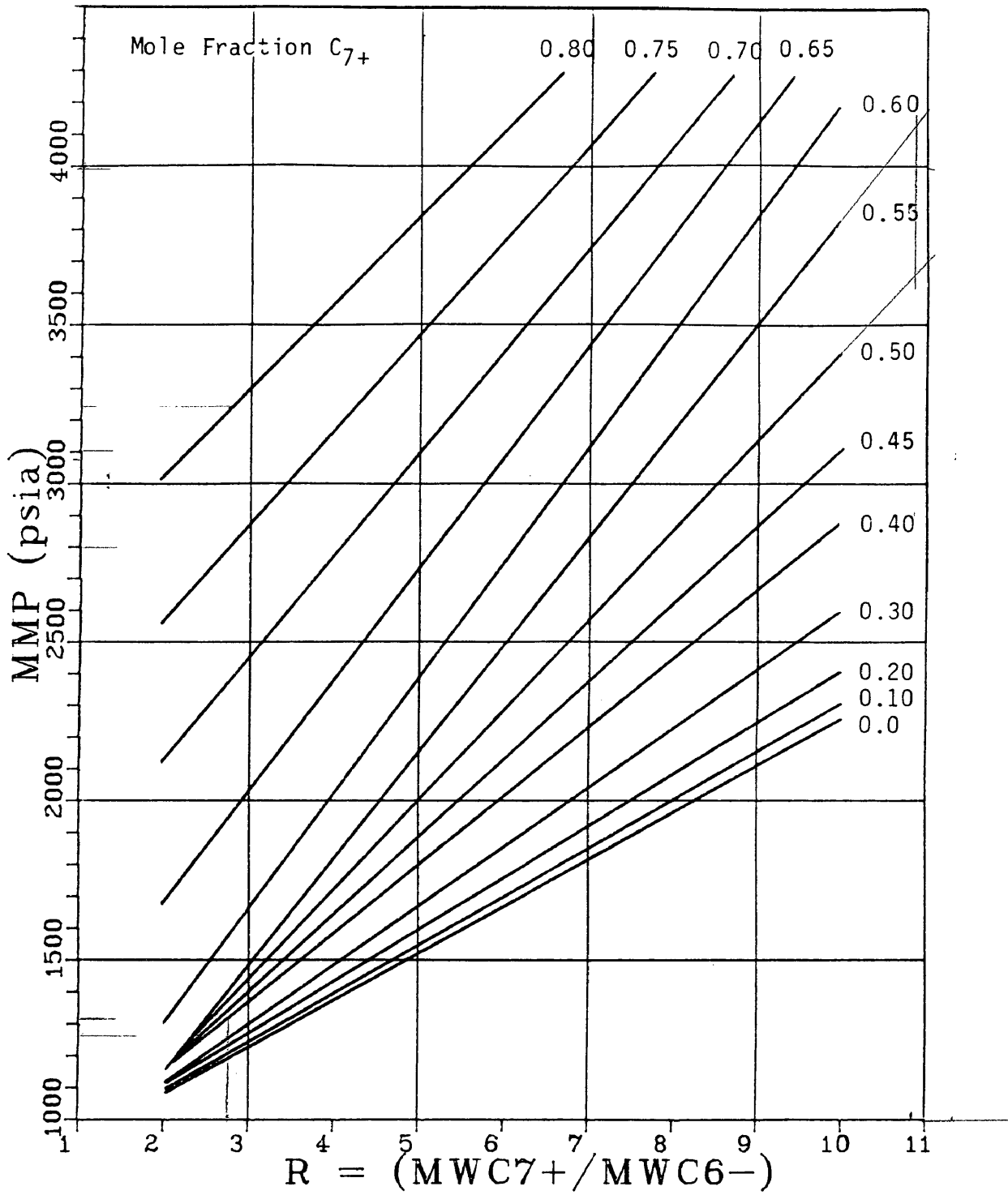


Figure 65. Relationship Between MMP and Crude Molecular Weight Ratio at 200 °F

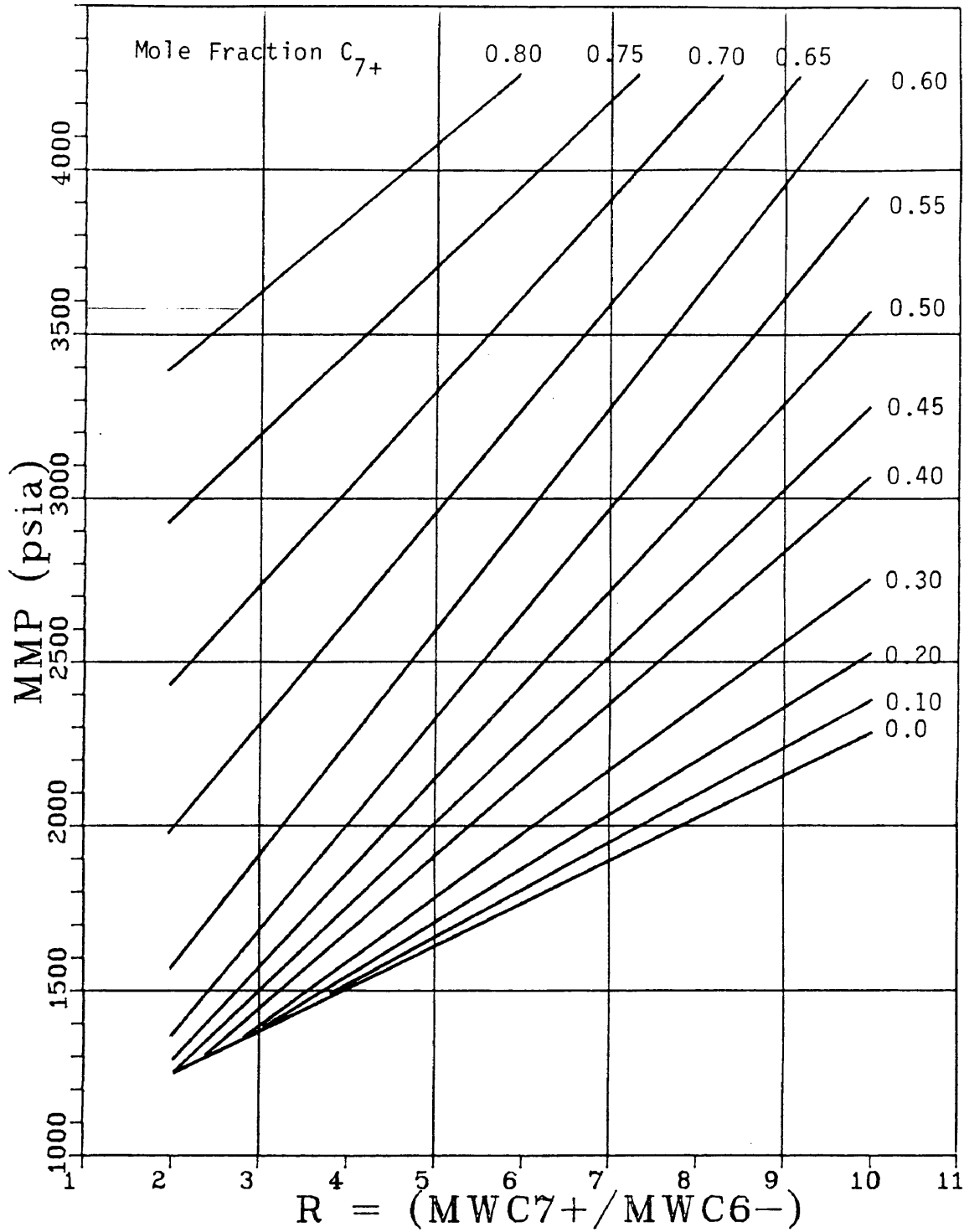


Figure 66. Relationship Between MMP and Crude Molecular Weight Ratio at 250 °F

Table 24. Molecular Weight of C₆₋ and C₇₊ Fractions and Molecular Weight Ratio R of Original Reservoir Fluids

Crude	MW _{C6-}	MW _{C7+}	R
Ford Geraldine	42.89	201.46	4.697
West Sussex	43.72	216.39	4.949
Maljamar	32.83	219.51	6.686
Reservoir D	35.70	255.77	7.164

appropriate temperatures, the critical pressure was plotted in Figures 55-62 at $X_{C7+} = 0$. While the critical pressures of the CO_2-C_6- systems are not directly related to the dynamic miscibility process, they are a logical endpoint for the curves and yield good results. The calculated critical pressures are shown in Table 25. The maximum critical temperature of both the Maljamar and Reservoir D pseudo-binary systems is less than $200^\circ F$, and while there is a critical pressure at $200^\circ F$ for the Ford Geraldine system it is lower than the critical pressure at $150^\circ F$. There is nothing to suggest that the MMP at $200^\circ F$ is lower than the MMP at $150^\circ F$, however, so this point was omitted.

Similarly, the Reservoir D data was not used because the critical pressure of this system at $100^\circ F$ is lower than the critical pressure of the Maljamar system and at $150^\circ F$ it is lower than the critical pressure of the Maljamar and Ford Geraldine systems. However, there is no reason to suspect the same behavior in MMP data so the Reservoir D critical pressures were not used.

The West Sussex curves in Figures 55-58 and Figure 60 were plotted merely to indicate where the calculated data for this system would have to lie in order to be consistent with the rest of the data. Of the 12 points that were calculated for this system, only one point at each temperature is relatively close to the curve.

Table 25. Critical Temperature and Pressure of pseudobinary Mixtures of Crude C₆- Fractions with CO₂

Temperature (°F)	Critical Pressure (psia)		
	Ford Geraldine	Maljamar	Reservoir D
100	1098.2	1320.0	1156.5
150	1287.5	1581.4	1262.9
200	1258.2	--	--
250	--	--	--

In the early stages of this work it was recognized that the proposed correlation could be conveniently displayed in a form similar to the Benham et al.(28) correlation for condensing gas drive MMP (refer to Figure 16). Based on the properties of the crudes used in this study, it was decided that C_{6-} molecular weights of 30 to 50, and C_{7+} molecular weights of 180 to 260 represent reasonable limits for this correlation. The final correlation is shown in Figures 67-78 which were plotted by taking points from Figures 63-66 at values of R corresponding to even molecular weight intervals within the recommended limits. To use the correlation it is necessary to calculate the C_{6-} and C_{7+} molecular weights of the reservoir fluid being considered. The CO_2 MMP is then determined from the appropriate charts by interpolating where necessary between molecular weight and reservoir temperature.

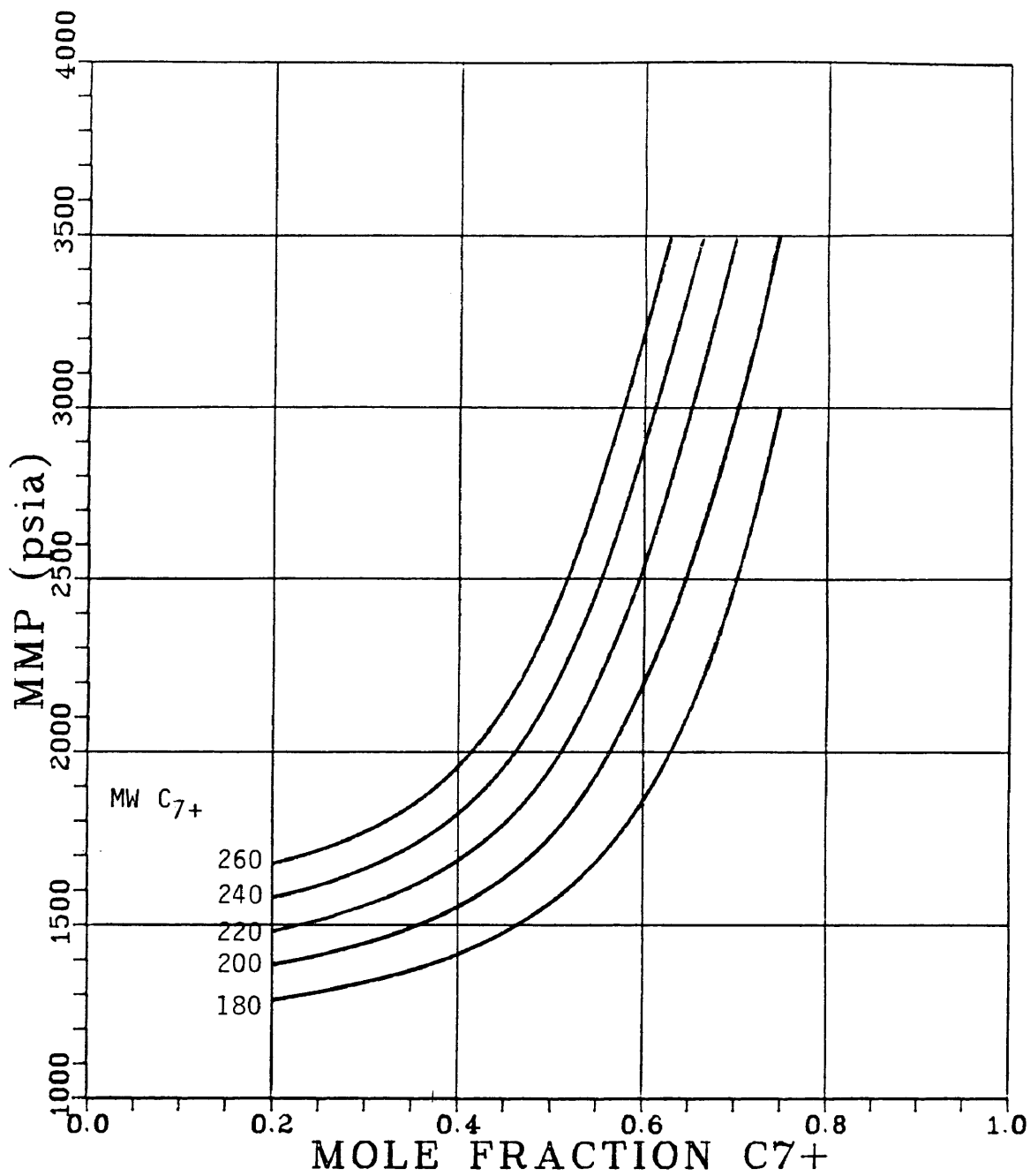


Figure 67. CO₂ MMP Correlation: Crude C₆₋ MW= 30
 Temperature= 100 °F

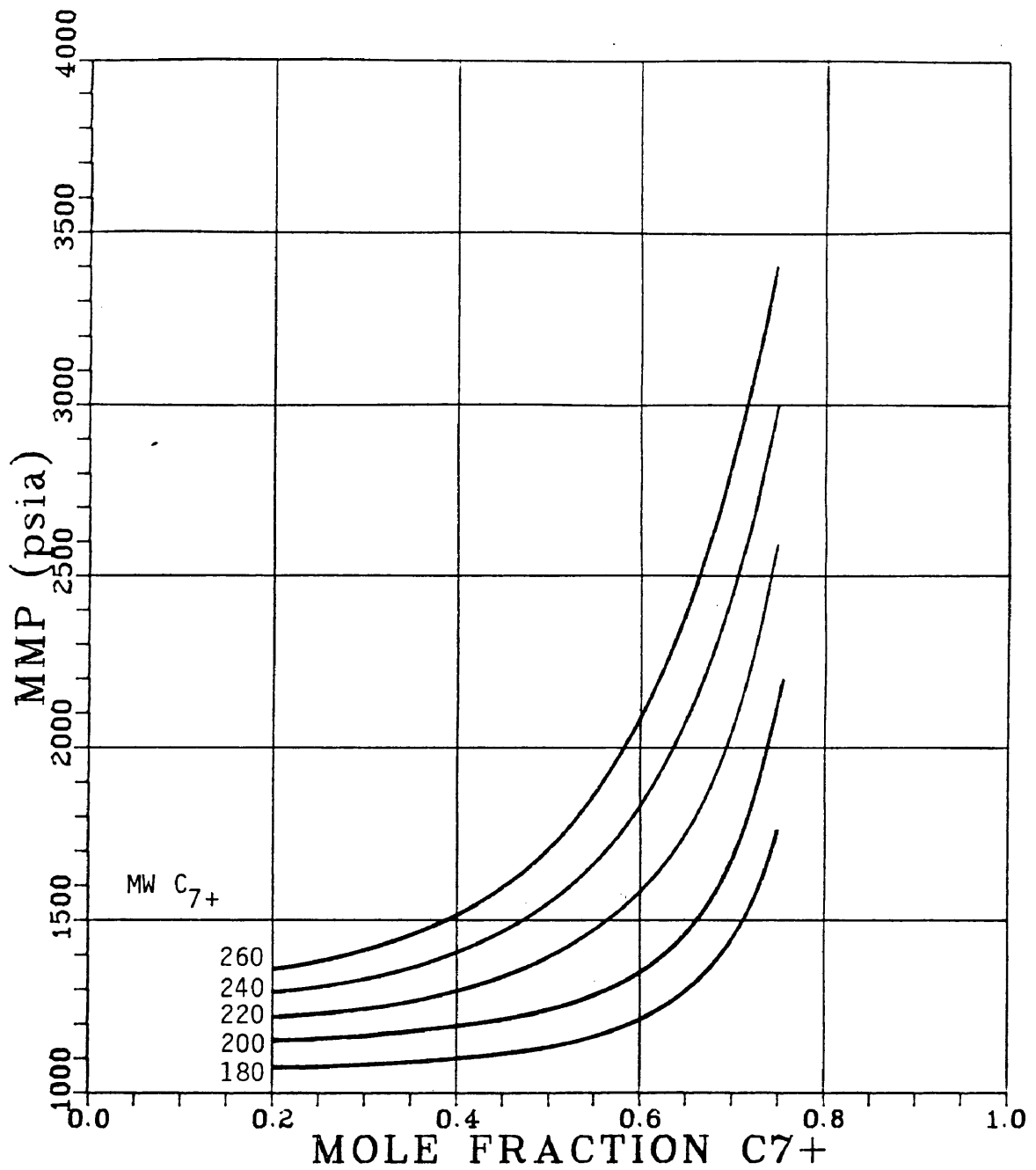


Figure 68. CO₂ MMP Correlation: Crude C₆₋ MW= 40
Temperature= 100 °F

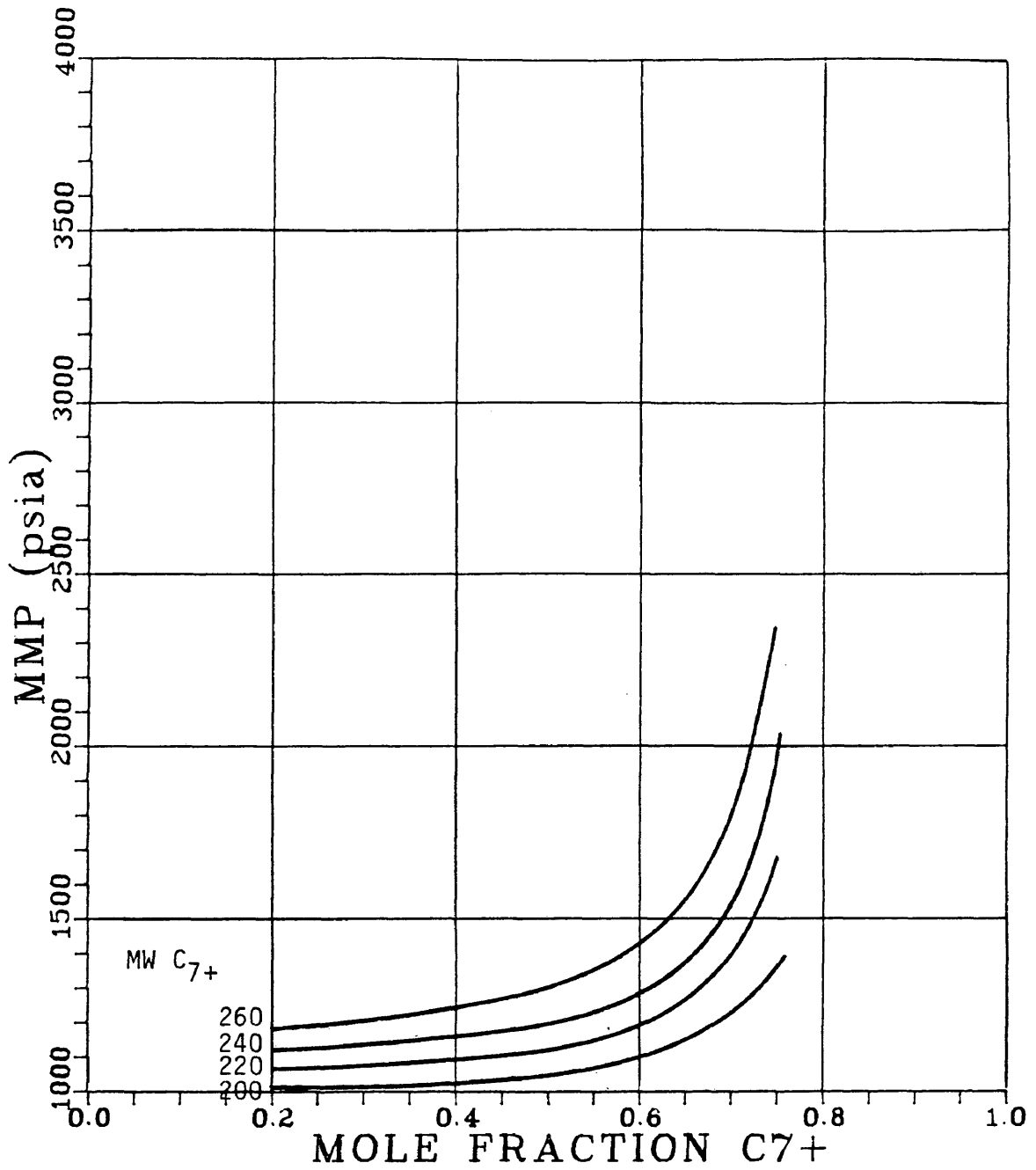


Figure 69. CO₂ MMP Correlation: Crude C₆₋ MW= 50
Temperature= 100 °F

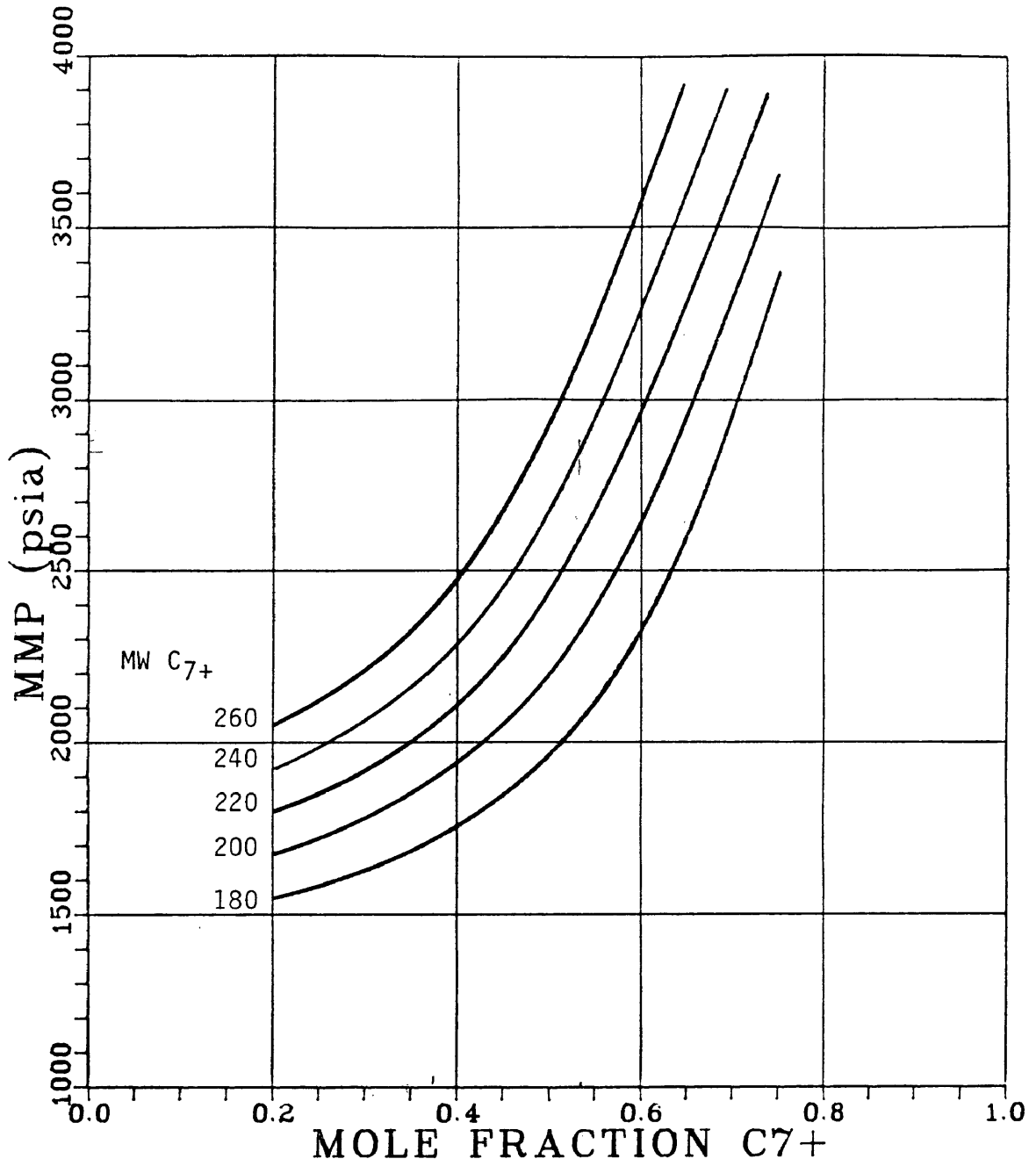


Figure 70. CO₂ MMP Correlation: Crude C₆₋ MW= 30
Temperature= 150 °F

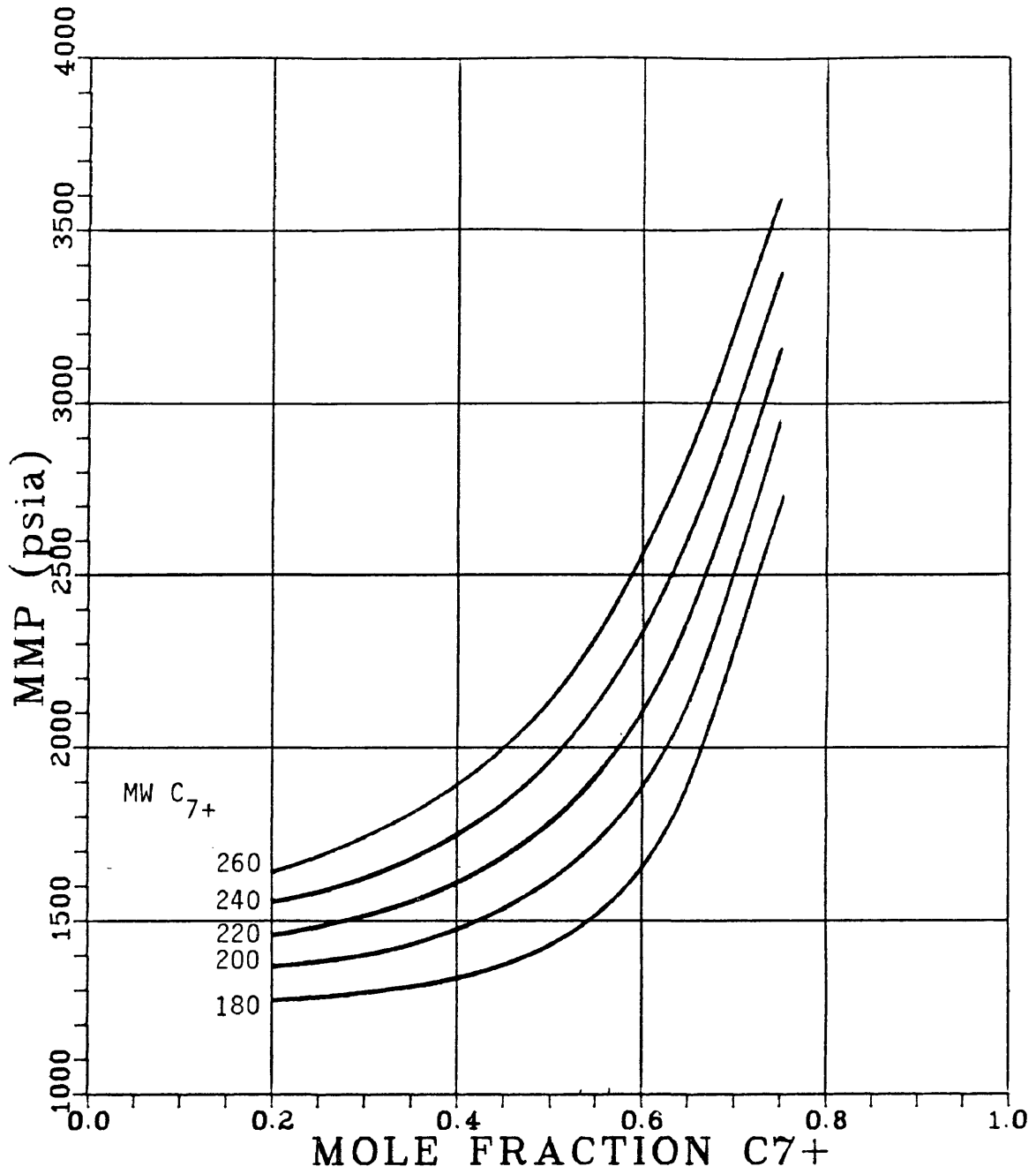


Figure 71. CO₂ MMP Correlation: Crude C₆₋ MW= 40
Temperature= 150 °F

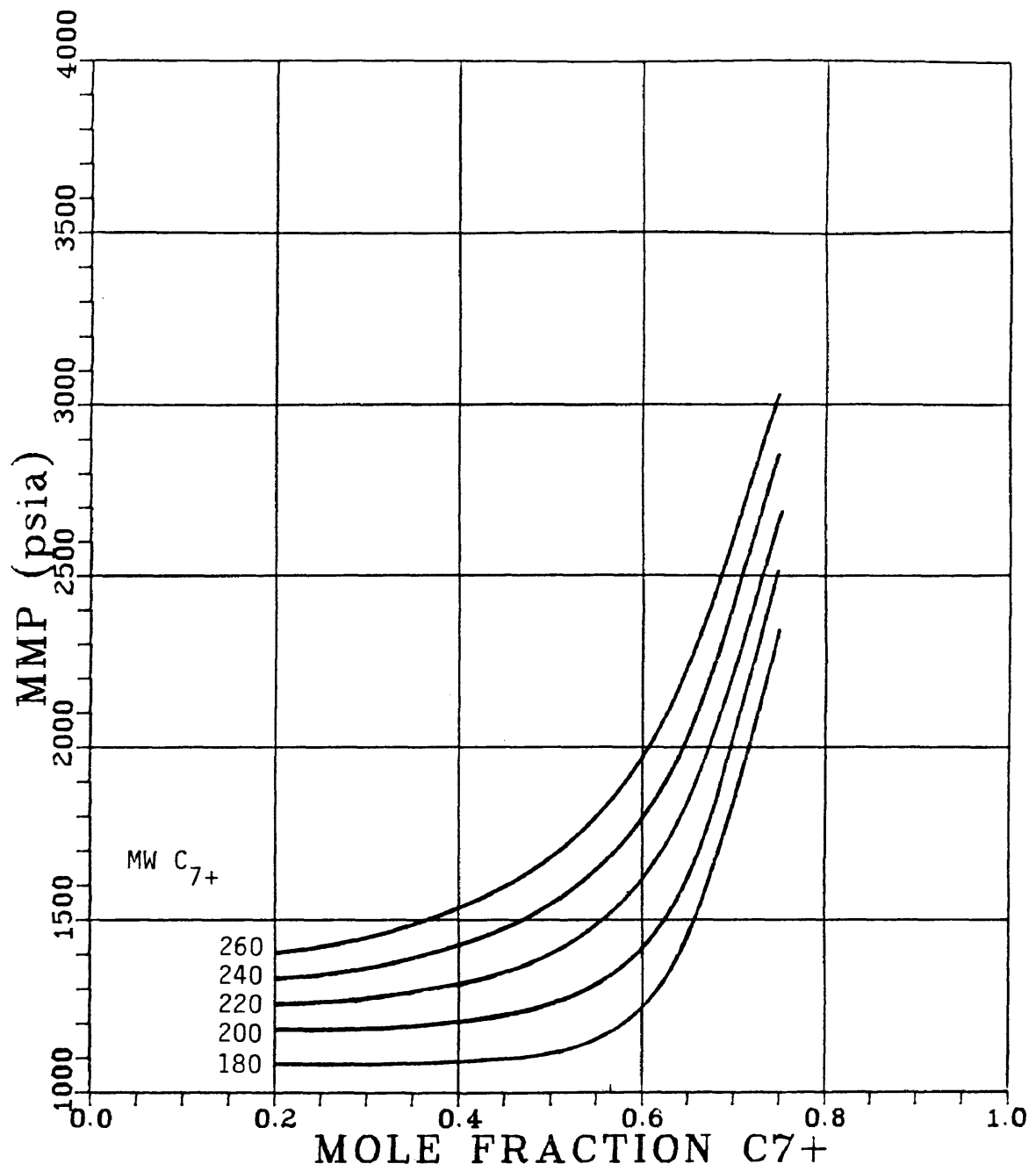


Figure 72. CO₂ MMP Correlation: Crude C₆₋ MW= 50
 Temperature= 150 °F

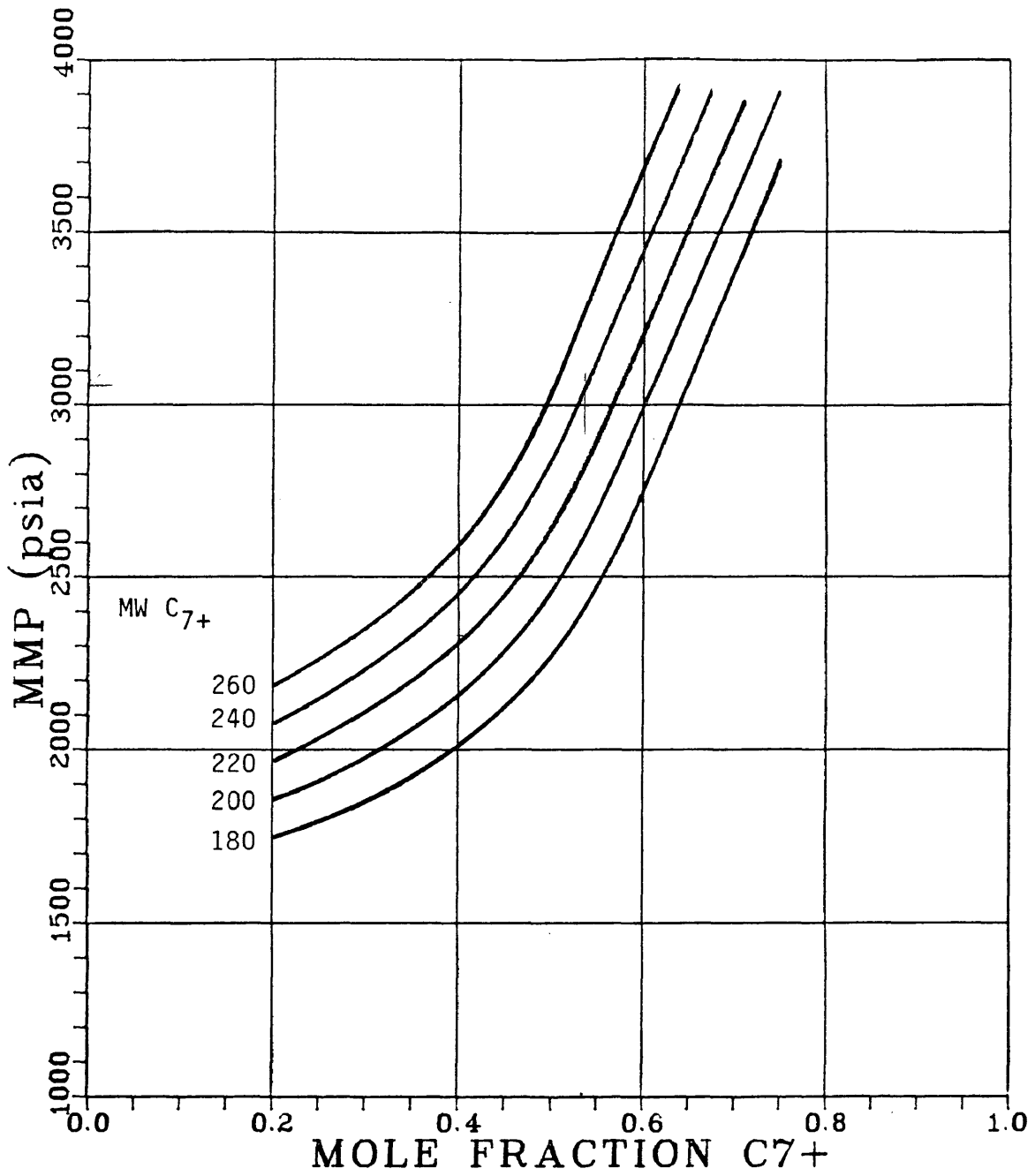


Figure 73. CO₂ MMP Correlation: Crude C₆₋ MW= 30
 Temperature= 200 °F

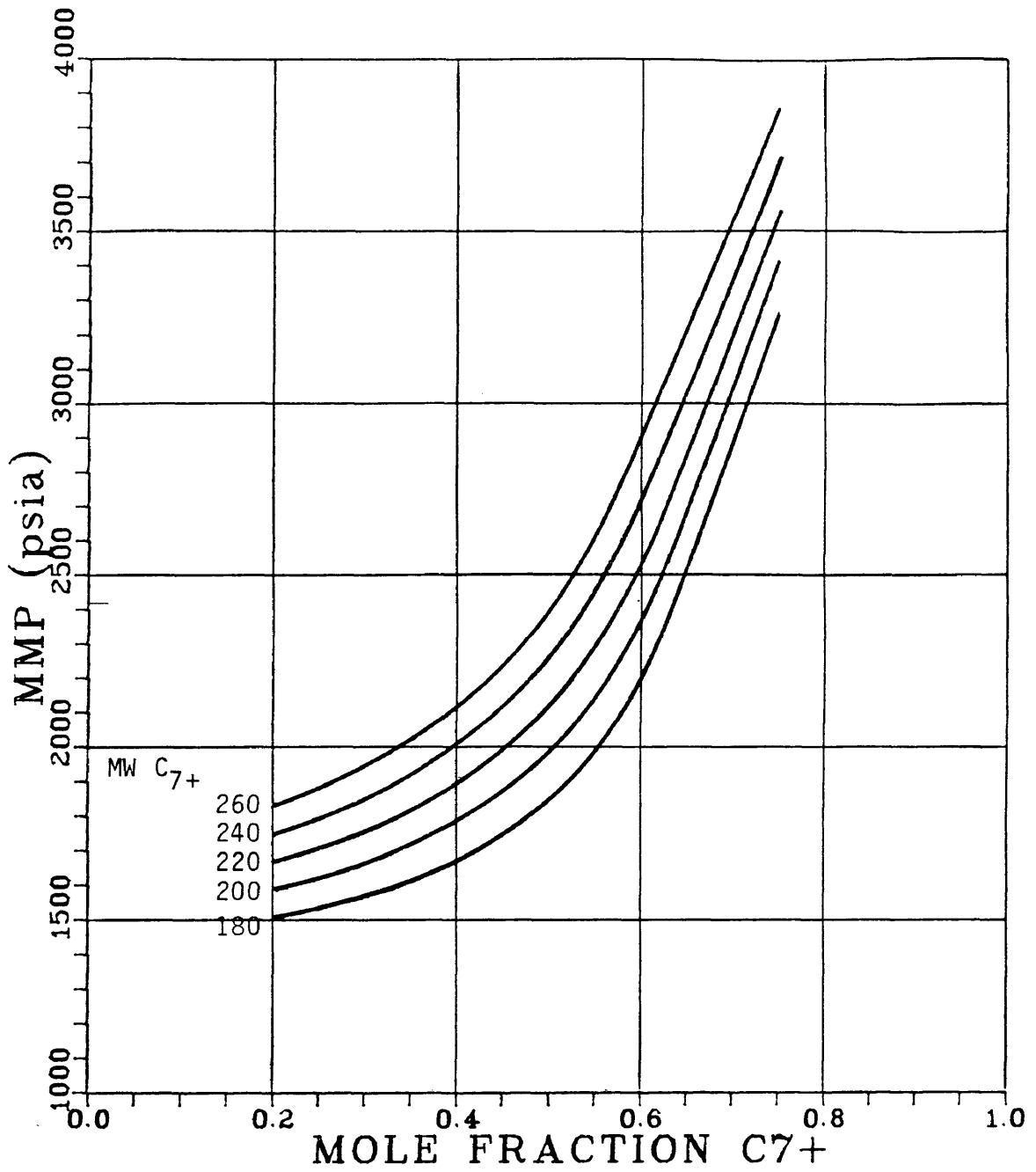


Figure 74. CO₂ MMP Correlation: Crude C₆₋ MW= 40
 Temperature= 200 °F

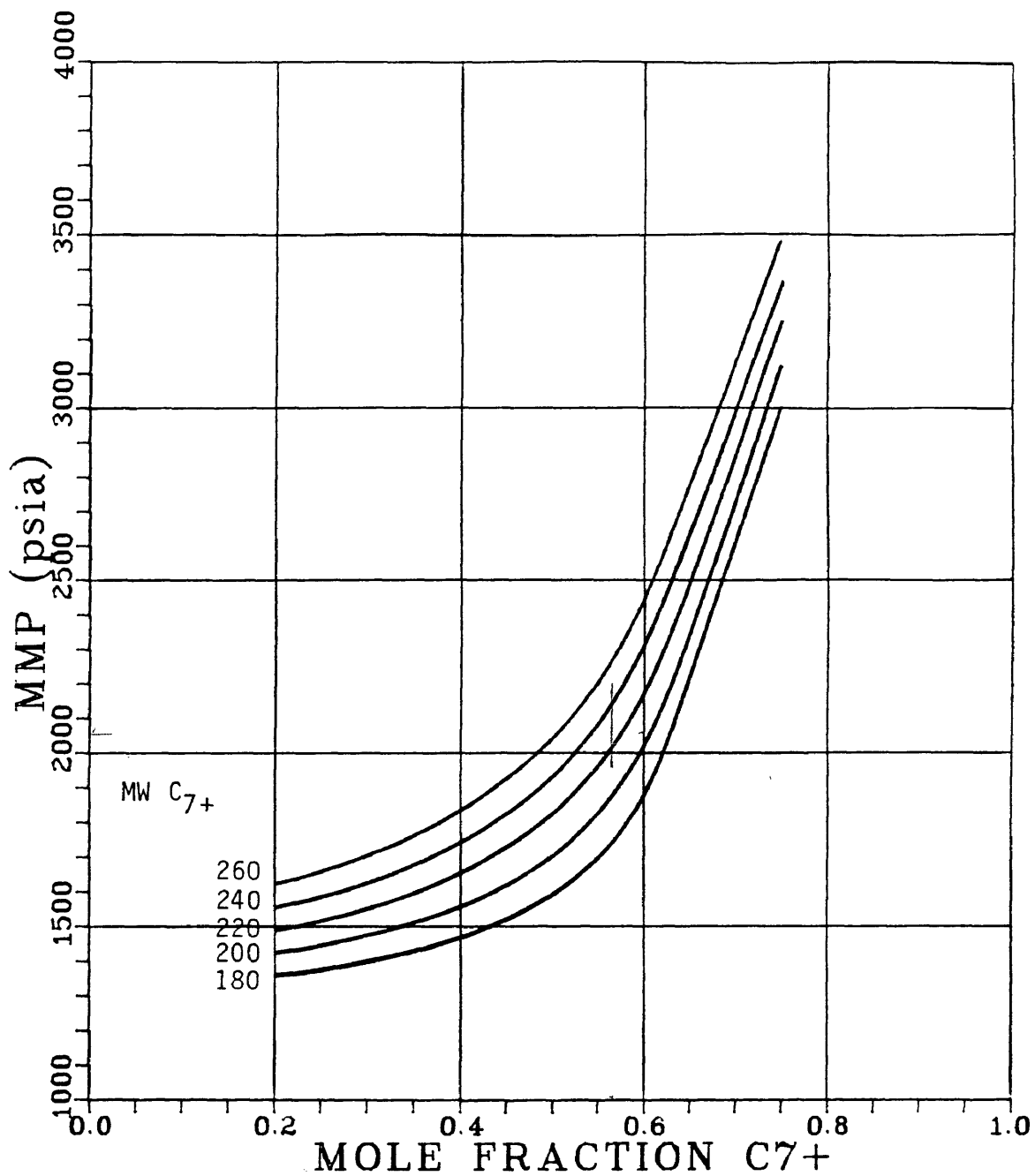


Figure 75. CO₂ MMP Correlation: Crude C₆₋ MW= 50
 Temperature= 200 °F

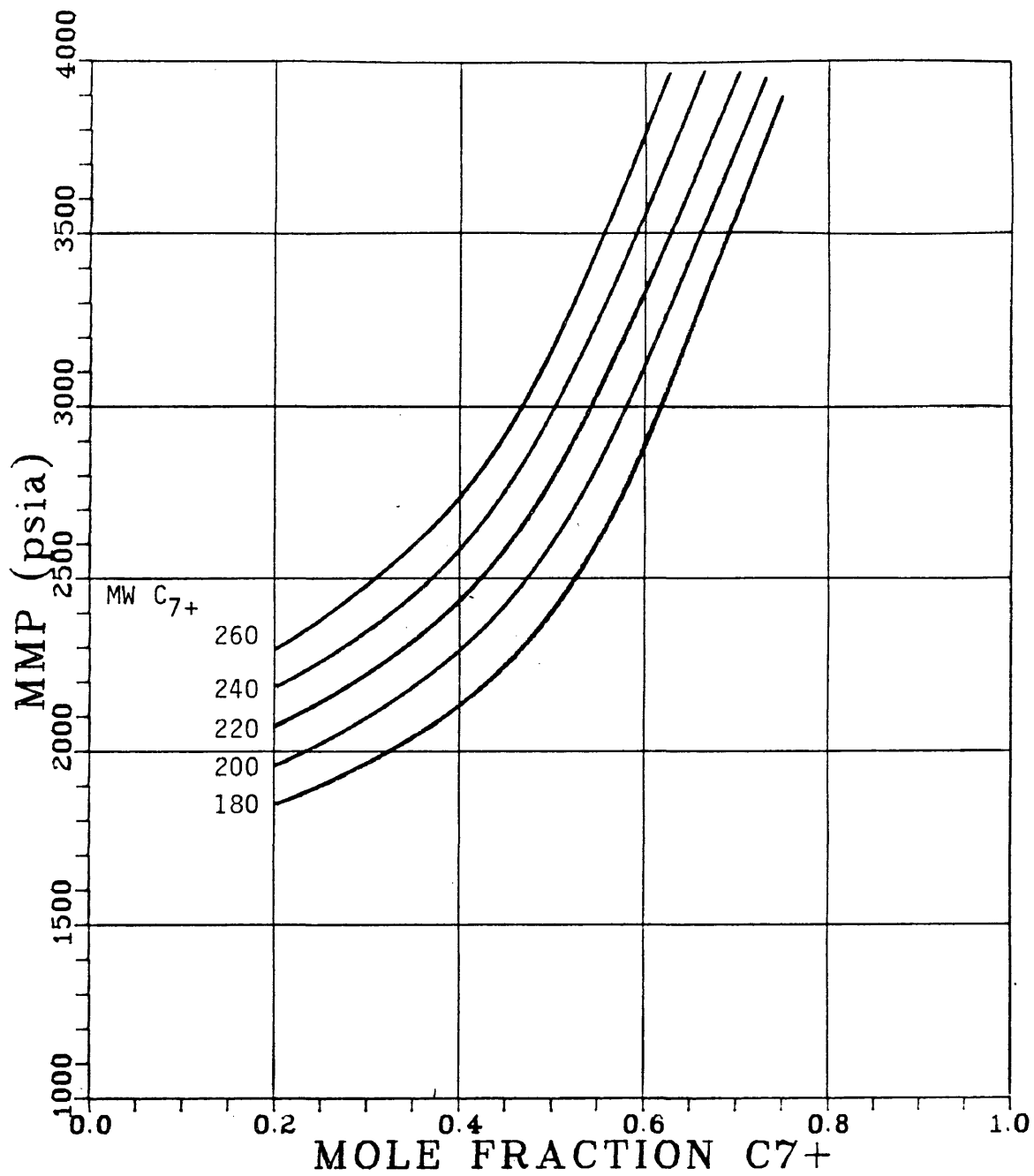


Figure 76. CO₂ MMP Correlation: Crude C₆₋ MW= 30
 Temperature= 250 °F

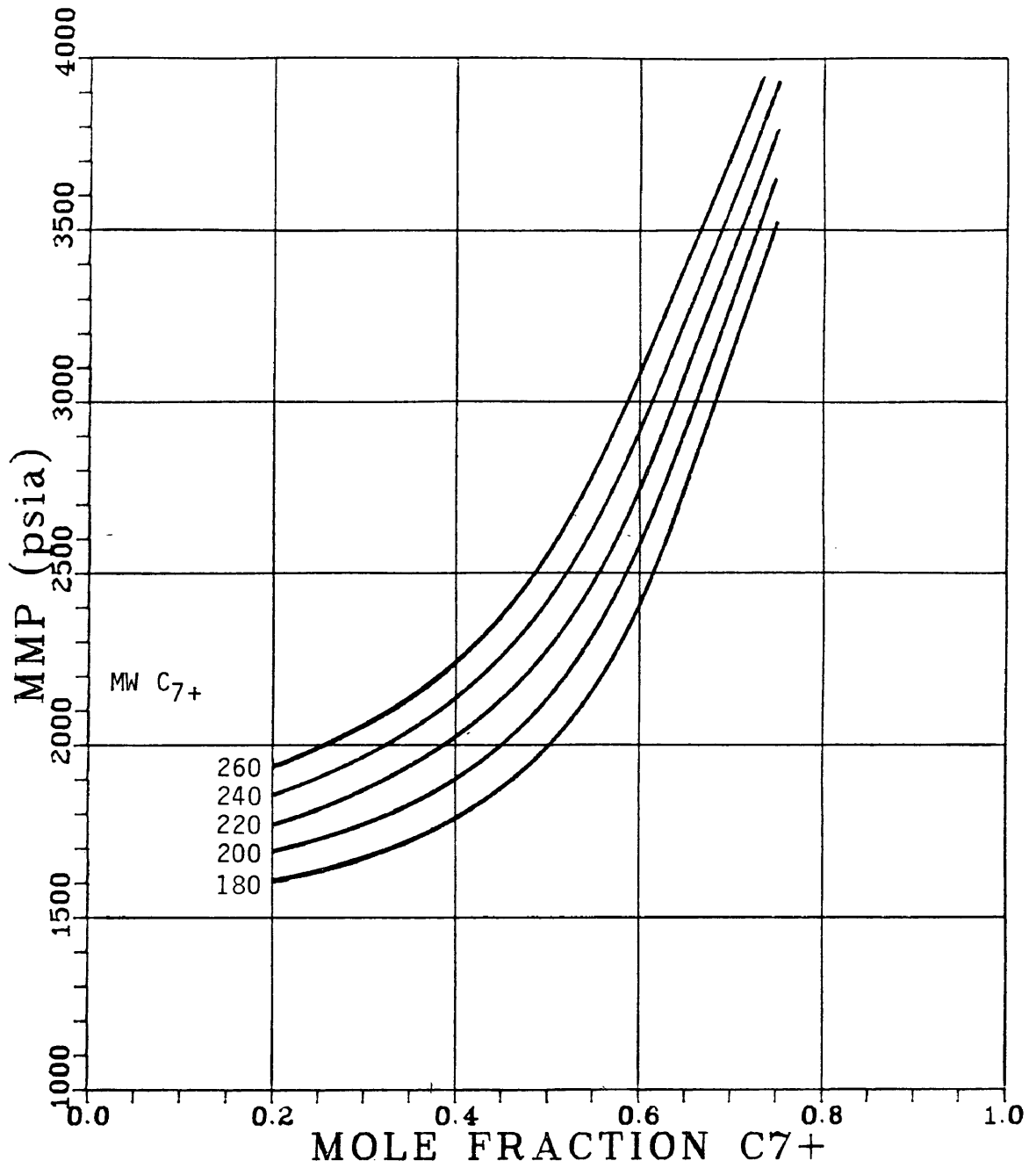


Figure 77. CO₂ MMP Correlation: Crude C₆₋ MW= 40
Temperature= 250 °F

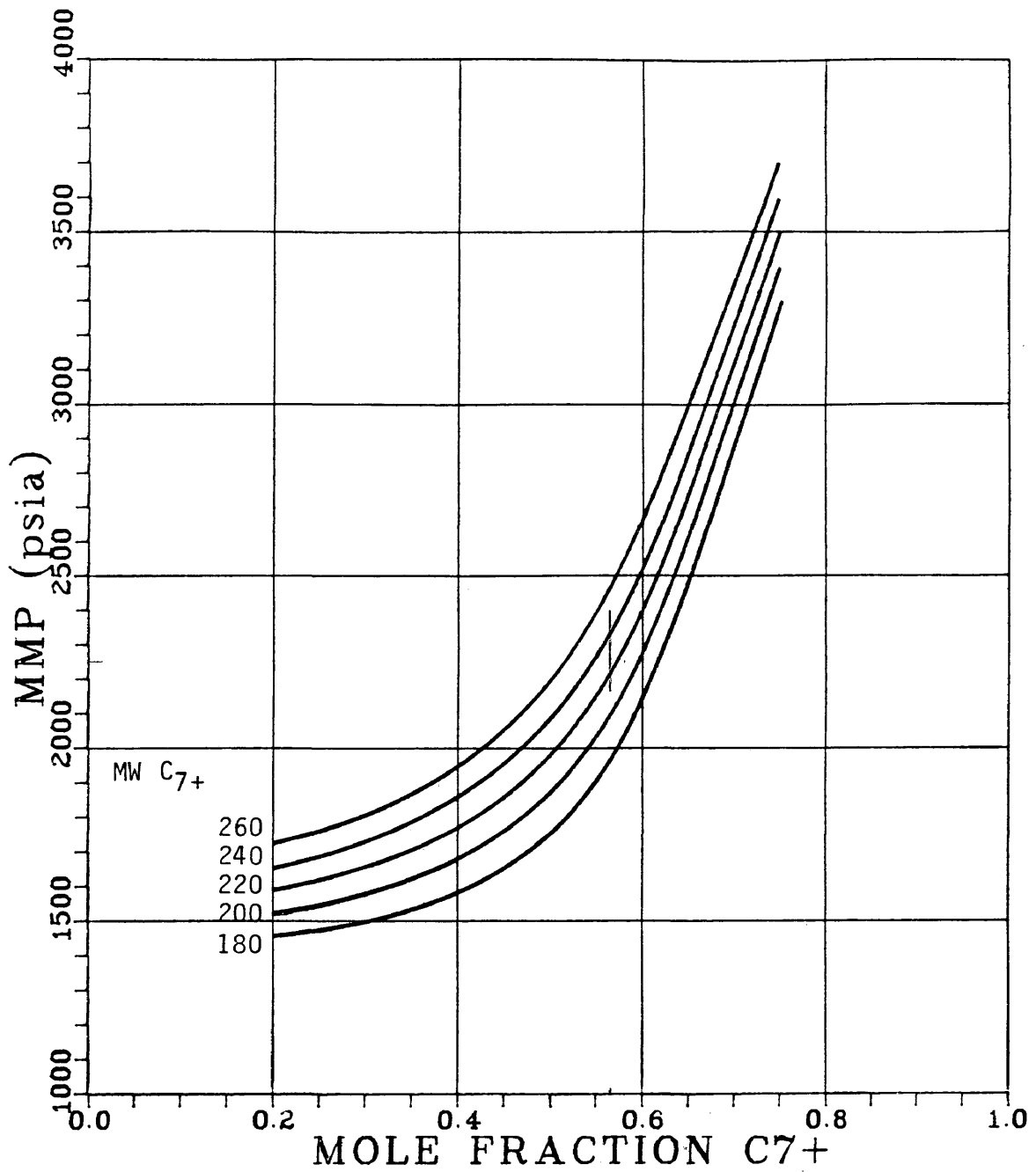


Figure 78. CO₂ MMP Correlation: Crude C₆₋ MW= 50
Temperature= 250 °F

ACCURACY OF CORRELATION

The accuracy of the correlation was tested by comparing the predicted MMP with the experimental MMP of 17 oils reported in the literature. The data is divided into two groups. Group A consists of ten displacement tests from six different sources and Group B consists of seven tests performed by Yellig and Metcalfe.⁽¹⁷⁾ The properties of the oils in both groups and the predicted and measured MMPs are shown in Table 26. The comparison is also shown in Figure 79. For the 17 oils, the average error in the predictions is 150 psi. The maximum error for both groups is 490 psi and the standard deviation of the ratios of predicted MMP to measured MMP is 12.6%. This agreement is probably as good as can be expected when it is considered that the precision of slim tube MMPs is no greater than 50-100 psi and that the literature data is not necessarily consistent since different laboratories have different techniques for conducting slim tube tests and interpreting the results. In addition, defining MMP in terms of slim tube oil recovery is not strictly consistent with the phase behavior definition. Of course, the pseudoternary model itself is a simplified description of the dynamic miscibility process and as such has a quantitative limit.

Table 26. Properties of Literature Oils and Experimental and Predicted CO₂ MMP

Oil No.	Temp (°F)	MWC ₆₋	MWC ₇₊	X _{C7+}	MMP _{exp}	MMP _{corr}	Ref. No.
Group A							
1	109	40.18	222	0.5410	1500	1553	13
2	103	34.26	223	0.4213	2000	1569	13
3	135	30.87	197	0.5661	2000	2244	14
4	130	36.01	197	0.3015	1600	1407	63
5	109	39.70	221	0.4432	1540	1413	11
6	105	48.13	206	0.6448	1200	1269	16
7	135	48.13	206	0.6448	1700	1569	16
8	120	30.06	200	0.3841	1600	1675	16
9	150	30.06	200	0.3841	1950	1906	16
10	160	54.86	228	0.7067	2250	2296	10
Group B							
1	95	34.02	201	0.5700	1150	1102	17
2	118	34.02	201	0.5700	1375	1865	17
3	150	34.02	201	0.5700	1875	2172	17
4	192	34.02	201	0.5700	2350	2479	17
5	95	43.84	201	0.5700	1150	1171	17
6	118	43.84	201	0.5700	1300	1351	17
7	150	43.84	201	0.5700	1700	1601	17

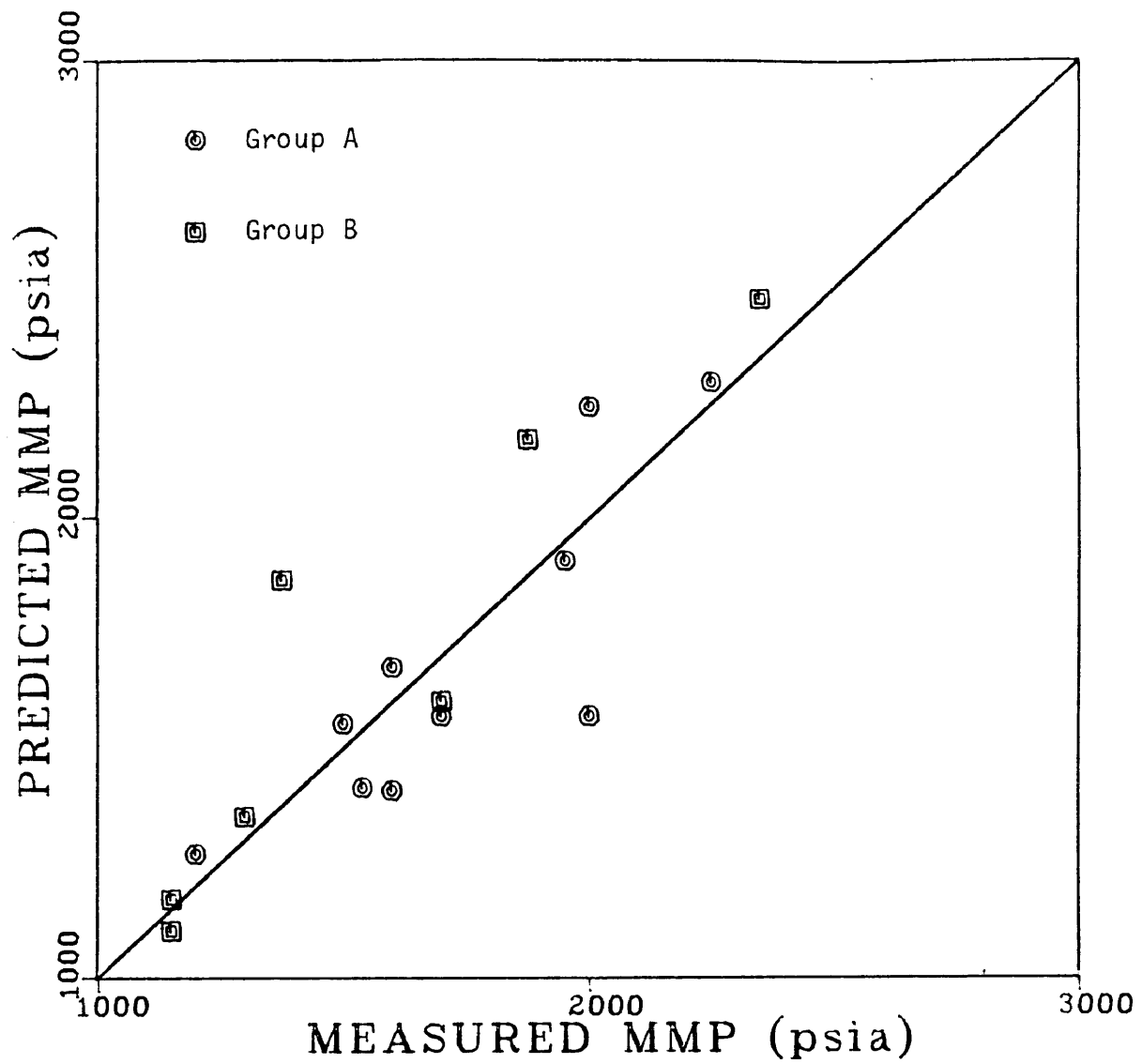


Figure 79. Accuracy of Proposed Correlation for Predicting CO₂ MMP of Group A and Group B Oils

The proposed correlation was also compared for accuracy to the correlations of Alston et al.⁽¹⁵⁾ and Holm and Josendal⁽¹⁴⁾. For this comparison, only the ten oils in Group A were used since there was not enough compositional data reported for the Group B oils to apply the other correlations. The measured MMPs and the values predicted by each of the correlations are shown in Table 27 and Figures 80-82. Based on this limited set of data, the performance of all three correlations is about equal, although the Holm and Josendal⁽¹⁴⁾ correlation predicted too high an MMP for eight of the ten oils.

The proposed correlation appears to satisfactorily predict the CO₂ minimum miscibility pressure of crude oils within the recommended molecular weight limits. It should be emphasized, however, that a more extensive testing of the correlation is necessary, particularly in the range of higher temperatures and higher C₇₊ molecular weights.

Table 27. Comparison of Accuracy of Proposed Correlation with Correlations of Alston et al. and Holm and Josendal for Group A Oils

Oil No.	Temp (°F)	Measured MMP	Predicted MMP		
			Proposed	Alston	Holm & Josendal
1	109	1500	1553	1594	1625
2	103	2000	1569	1540	1550
3	135	2000	2244	2289	1940
4	130	1600	1407	1431	1850
5	109	1540	1413	1486	1575
6	105	1200	1269	1303	1570
7	135	1700	1569	1701	1940
8	120	1600	1675	1647	1750
9	150	1950	1906	2086	2160
10	160	2250	2296	2177	2400
Largest Error:			431	460	450
Average Error:			141	143	204
Std. Dev.	$\frac{\text{Predicted MMP}}{\text{Measured MMP}}$		10.04%	10.76%	13.77%

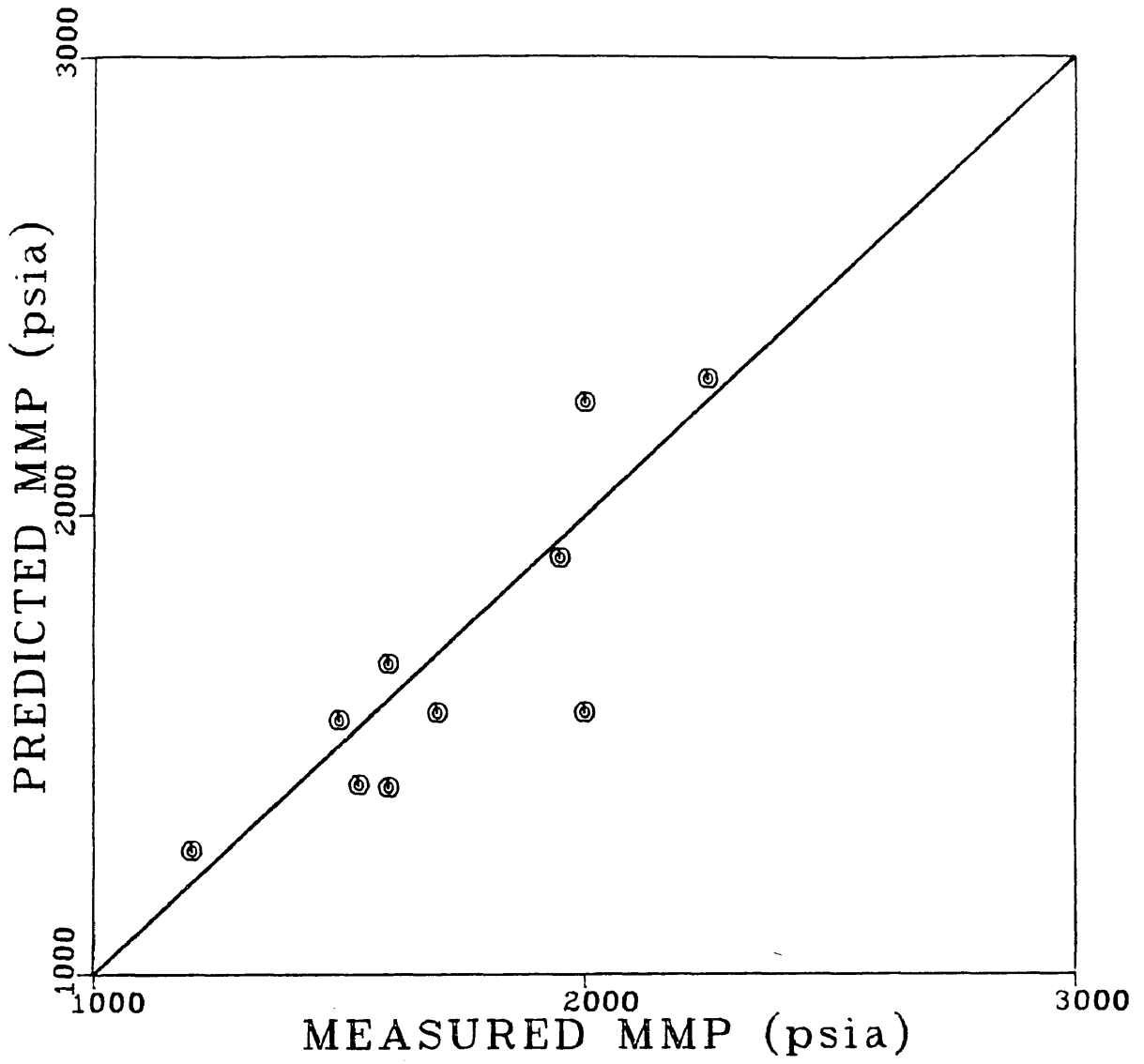


Figure 80. Accuracy of Proposed Correlation for Predicting CO₂ MMP of Group A Oils

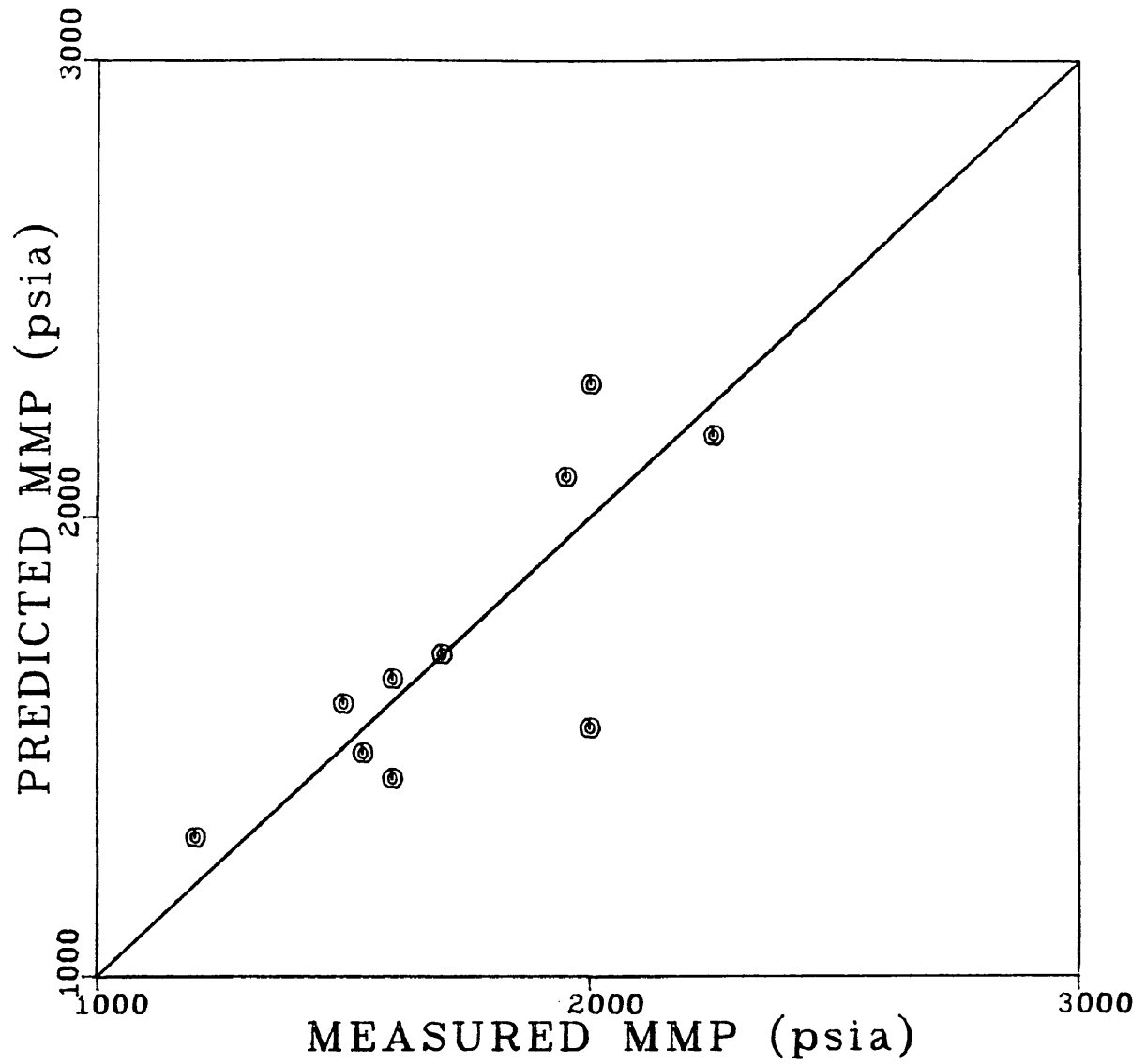


Figure 81. Accuracy of Alston et al. Correlation for Predicting CO₂ MMP of Group A Oils

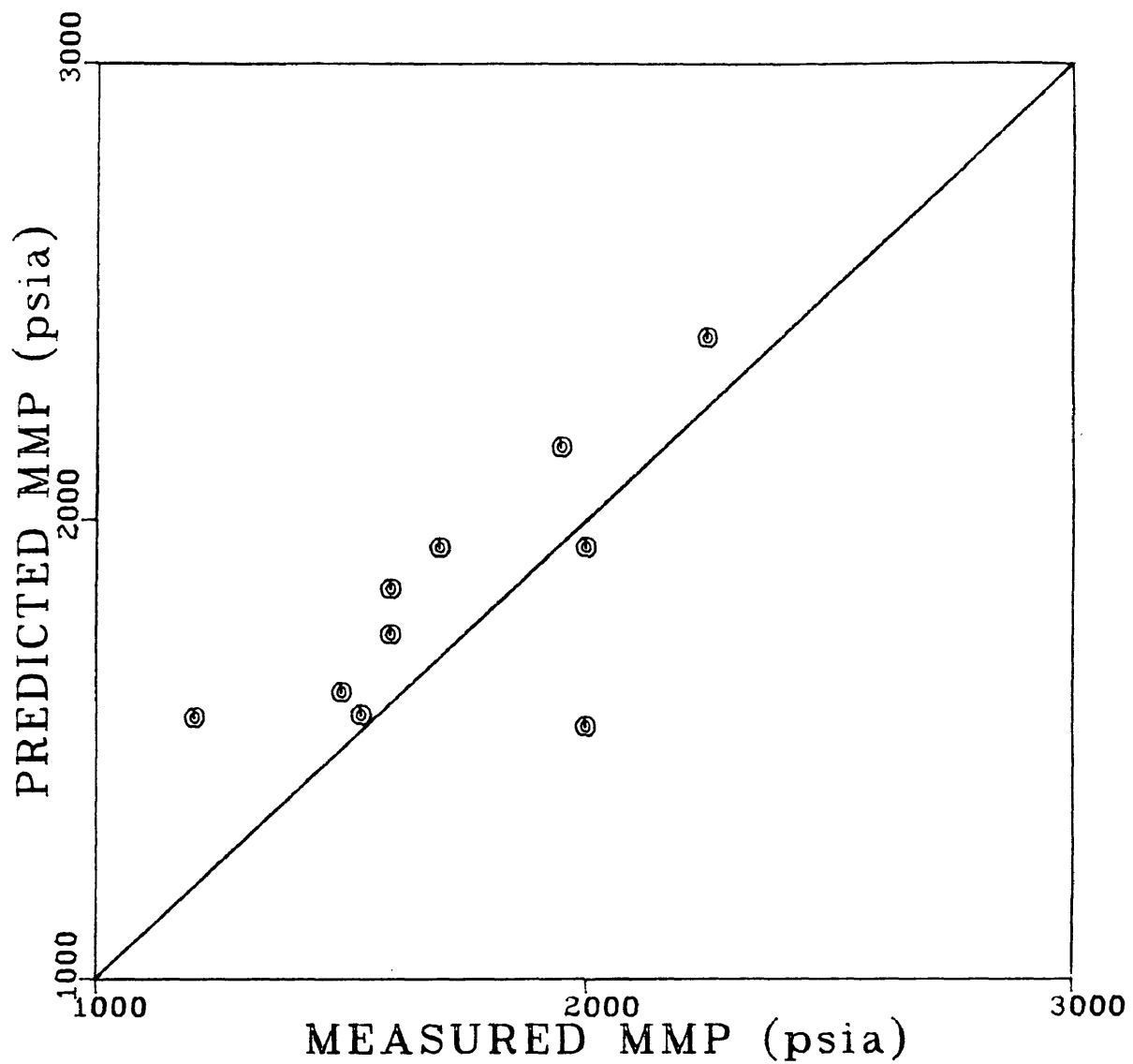


Figure 82. Accuracy of Holm and Josendal Correlation for Predicting CO₂ MMP of Group A Oils

It was stated earlier that it is important for the user of a correlation to understand what the correlation is based upon and, in particular, how this may differ from the actual case or process. The assumptions and simplifications which were made in the development of the proposed correlation and which may affect its accuracy are summarized below.

- 1) It is assumed that the dynamic miscibility process is quantitatively described by the pseudoternary model. In fact, representing the phase behavior of multi-component systems on a pseudoternary diagram is not thermodynamically rigorous and the model ignores any effects flow through porous media has on the process.
- 2) For the purposes of EOS calculations, crude oil systems which contain hundreds of components are represented by a small number of pseudocomponents. The properties of these pseudocomponents are calculated from empirical correlations using data from a GC/MS analysis of each crude. Also, binary interaction coefficients are obtained from empirical relationships and assumed to be independent of temperature, pressure, and composition.
- 3) The calculated miscibility conditions are heavily dependent on the accuracy of critical points and tie

lines calculated with the PR EOS, however, it is generally difficult to obtain solutions of two constant equations of state in the critical region.

- 4) The generalized correlation is derived from miscibility conditions calculated for only three crude oil systems. Calculations made for a fourth system did not correlate and were not used.
- 5) Although there is no unique method of characterizing a reservoir oil or hydrocarbon fraction, it is assumed that C_{7+} concentration and the molecular weight of the C_{6-} and C_{7+} fractions are sufficient parameters to account for the effect of oil composition on CO_2 MMP.

CONCLUSIONS

- 1) The Peng-Robinson equation of state was calibrated to accurately predict the phase behavior of four reservoir oil-CO₂ systems using a small number of hydrocarbon pseudocomponents. The specific combination of single carbon number groups within the pseudocomponents and the hydrocarbon binary interaction coefficients were both found to have an effect on the predicted phase behavior.
- 2) A reliable procedure for calculating pseudoternary phase diagrams for CO₂-crude oil mixtures with the Peng-Robinson equation of state was developed. The method allows precise calculation of the critical point and the calculation of tie lines very near the critical point. The procedure also provides a convenient means of extrapolating the tie line data to the critical point to determine the limiting tie line.
- 3) Pseudoternary diagrams were generated at several temperatures and pressures for each of the four reservoir oil-CO₂ systems and the limiting tie line was used to define the minimum miscibility pressure (MMP) and the maximum miscibility composition (MMC) for each set of conditions. The calculated miscibility data for three

of these systems was used to develop a generalized correlation for CO₂ MMP. The data from the fourth system did not correlate, however, the reason for this was not clear. The correlation accounts for the effects of temperature, crude composition in terms of C₇₊ concentration, and the molecular weight of the C₆₋ and C₇₊ fractions.

- 4) A preliminary test of the accuracy of the correlation was performed with 17 oils reported in the literature. The average error of the predictions was 150 psi and the standard deviation of the predicted MMP/experimental MMP was 12.6%. The largest error was 490 psi. The correlation was also compared to two published correlations using 10 of the 17 oils. All three correlations were found to perform equally well. For final design purposes, however, MMP should be determined in the lab.

RECOMMENDATIONS

- 1) A more extensive test of the correlation accuracy should be performed. It would be advantageous to use a set of slim tube data where the experimental technique and interpretation of results were consistent. This would help to identify any bias or limitations of the correlation.
- 2) The quantitative limits of the pseudoternary model should be examined, possibly by comparing it to more complex models such as a pseudoquaternary representation or simple compositional simulators. If it is found that the pseudoternary representation of the CO₂ miscible process is sufficiently accurate, the calculation of additional data using different reservoir fluids may improve the accuracy of the correlation.
- 3) In general, further research needs to be done in the area of calibrating equations of state to accurately predict complex CO₂-crude phase behavior. Regression based equation of state models may lead to better predictions as would better experimental data such as compositional data measured during CO₂ displacement tests.

NOMENCLATURE

a	Constant in Peng-Robinson normal boiling point temperature correlation
a(T)	Temperature dependent parameter of Peng-Robinson equation of state
A	Parameter of Peng-Robinson equation of state
b	Parameter of Peng-Robinson equation of state
B	Parameter of Peng-Robinson equation of state
C	Constant used to determine oil characterization index of Johnson and Pollin
EOS	Equation of state
EVP	Extrapolated vapor pressure
f	Fugacity
F	Correlating parameter of Silva et al
GC/MS	Gas chromatography/mass spectrometry
I	Oil characterization index of Johnson and Pollin
IOC	Initial oil composition
K	Equilibrium ratio
m	Slope or characterization factor in Peng-Robinson equation of state
M	Molecular weight of injection gas
MMC	Maximum miscibility composition, mole fraction C ₇₊
MMP	Minimum miscibility pressure, psia
MW	Molecular weight
MWC ₅₊	Molecular weight of crude C ₅₊ fraction
n	Number of components or carbon number

P	Pressure, psia or atm
P_c	Critical pressure, atm
P-T	Pressure-temperature
PNA	Paraffin, naphthene, aromatic
PR EOS	Peng-Robinson equation of state
PV	Pore volume
P-X	Pressure-composition
R	Gas constant
RBA	Rising bubble apparatus
S	Correction factor in Peng-Robinson critical temperature correlation or proportionality variable for determining binary interaction coefficients
T	Temperature, °F or °K
T_b	Normal boiling point temperature, °K
T_c	Critical temperature, °K
T_r	Reduced temperature
v	Molar volume
x	Mole fraction (not specifically liquid phase)
X	Mole fraction (not specifically liquid phase)
Z	Compressibility factor

Greek Letters

α	Scaling factor in Peng-Robinson equation of state or injection gas characterization parameter of Johnson and Pollin
δ_{ij}	Binary interaction coefficient
ΔX_{CO_2}	Difference in CO ₂ concentration between composition of mixture flashed and critical point composition
ρ	Density, g/cc
ϕ	Fugacity coefficient
ω	Acentric factor

Subscripts

B	Bisector of initial tie line
C	Critical point
C1	Methane
Cn	Hydrocarbon with n carbon atoms
H	Heavier hydrocarbon
i	Component identification
j	Component identification
LL	Lower liquid/phase
LTL	Limiting tie line
M	Mixture on line connecting critical point and tie line bisector
TL	Tie line
UL	Upper liquid/phase

REFERENCES CITED

1. Stalkup, F.I.: Miscible Displacement, SPE Monograph Volume 8, Dallas (1983)
2. Stalkup, F.I.: "Carbon Dioxide Flooding: Past, Present, and Outlook for the Future," J. Pet. Tech. (August 1978) pp. 1102-12
3. Peng, D.Y. and Robinson, D.B.: "A New Two Constant Equation of State," Ind. Eng. Chem. Fund., 15 (1976) pp. 59-64
4. Simon, R., Rosman, A., and Zana, E.: "Phase Behavior Properties of CO₂-Reservoir Oil Systems," Soc. Pet. Eng. J. (February 1978) pp. 20-26
5. Orr, F.M. and Jensen, C.M.: "Interpretation of Pressure Composition Phase Diagrams for CO₂-Crude Oil Systems," SPE 11125 (1982)
6. Hutchinson, C.A. and Braun, P.H.: "Phase Relations of Miscible Displacement in Oil Recovery," AIChE Journal Vol 7, No. 1 (March 1961) pp. 64-72
7. Holm, L.W.: "Carbon Dioxide Flooding for Increased Oil Recovery," Transactions AIME , 216, (1959) pp. 225-231
8. Metcalfe, R.S. and Yarborough, L.: "The Effect of Phase Equilibria on the CO₂ Displacement Mechanism," Soc. Pet. Eng. J. (August 1979) pp. 242-252
9. Orr, F.M., Yu, A.D., and Lien, C.L.: "Phase Behavior of CO₂ and Crude Oil in Low Temperature Reservoirs," Soc. Pet. Eng. J. (August 1981) pp. 480-492
10. Graue, D.J. and Zana, E.: "Study of a Possible CO₂ Flood in the Rangely Field, Colorado," SPE 7060 (1978)
11. Gardner, J.W., Orr, F.M., and Patel, P.D.: "The Effect of Phase Behavior on CO₂ Flood Displacement Efficiency," SPE 8367 (1979)

12. Huang, E.T. and Tracht, J.H.: "The Displacement of Residual Oil by Carbon Dioxide," SPE 4735 (1974)
13. Rathmell, J.J., Stalkup, F.I., and Hassinger, R.C.: "A Laboratory Investigation of Miscible Displacement by Carbon Dioxide," SPE 3483 (1971)
14. Holm, L.W. and Josendal, V.A.: "Mechanisms of Oil Displacement by Carbon Dioxide," J. Pet. Tech. (December 1974) pp. 1427-38
15. Alston, R.B., Kokolis, G.P., and James, C.F.: "CO₂ Minimum Miscibility Pressure: A Correlation for Impure CO₂ Streams and Live Oil Systems," SPE 11959 (1983)
16. Metcalfe, R.S.: "Effects of Impurities on Minimum Miscibility Pressures and Minimum Enrichment Levels for CO₂ and Rich Gas Displacement," SPE 9230 (1980)
17. Yellig, W.F. and Metcalfe, R.S.: "Determination of CO₂ Minimum Miscibility Pressures," J. Pet. Tech. (January 1980) pp.160-168
18. Holm, L.W. and Josendal, V.A.: "Effect of Oil Composition on Miscible-Type Displacement by Carbon Dioxide," Soc. Pet. Eng. J. (February 1982) pp. 87-98
19. Orr, F.M., Silva, M.K., and Lien, C.L.: "Equilibrium Phase Compositions of CO₂-Crude Oil Mixtures: Comparison of Continuous Multiple Contact and Slim Tube Displacement Tests," SPE/DOE 10725 (1982)
20. Monger, T.G.: "The Impact of Oil Aromaticity on Carbon Dioxide Flooding," SPE/DOE 12708 (1984)
21. Cramer, H.C. and Swift, G.W.: "Phase Behavior of Carbon Dioxide in Admixture with n-Butane, N-Decane, n-Butylcyclohexane, and n-Butylbenzene at 344 K and 9600 kPa," J. Chem. Eng. Data Vol 30, No. 1 (1985) pp. 63-66
22. Silva, M.K., Taber, J.J., and Orr, F.M.: "Minimum Miscibility Pressure: Effects of Crude Oil Composition," Presented at International Energy Agency EOR Workshop, Trondheim, Norway (October 5, 1984)

23. Yellig, W.F.: "Carbon Dioxide Displacement of a West Texas Reservoir Oil," Soc. Pet. Eng. J. (December 1982) pp.805-815
24. Mungan, N.: "Carbon Dioxide Flooding--Fundamentals," J. Can. Pet. Tech. (January-March 1981) pp. 87-92
25. Johnson, J.P. and Pollin, J.S.: "Measurement and Correlation of CO₂ Miscibility Pressures," SPE/DOE 9790 (1981)
26. Taber, J.J.: "Technical and Economic Criteria for Selecting Methods and Materials for Enhanced Oil Recovery," Presented to Enhanced Recovery Committee IOCC, Sante Fe, NM, (December 4, 1984)
27. Christiansen, R.L. and Kim, H.: "Rapid Measurement of Minimum Miscibility Pressure Using the Rising Bubble Apparatus," SPE 13114 (1984)
28. Benham, A.L., Dowden, W.E., and Kunzman, W.J.: "Miscible Fluid Displacement--Prediction of Miscibility," Transactions AIME, 219, (1960) pp. 229-237
29. "Enhanced Oil Recovery--An Analysis of the Potential for Enhanced Oil Recovery from Known Fields in the United States--1976 to 2000," National Petroleum Council, Washington, D.C. (1976)
30. Cronquist, C.: "Carbon Dioxide Dynamic Miscibility With Light Reservoir Oils," Fourth Annual US DOE Symposium, Tulsa, OK, (August 28-30, 1978)
31. Sebastian, H.M., Wenger, R.S., and Renner, T.A.: "Correlation of Minimum Miscibility Pressure for Impure CO₂ Streams," SPE/DOE 12648 (1984)
32. Glaso, O.: "Generalized Minimum Miscibility Pressure Correlation," SPE 12893 (1984)
33. Enick, R.M., Holder, G.D., and Morsi, B.I.: "A Thermodynamic Correlation for the Minimum Miscibility Pressure in CO₂ Flooding of Petroleum Reservoirs," Presented at the AIChE National Meeting, Houston, TX (March 24-25, 1985)

34. Dumyuskin, I.I. and Namiot, A.Y.: "Mixing Conditions of Oil with Carbon Dioxide," Neft. Khozyaistvo (March 1978) pp. 59-61
35. Lee, J.I.: "Effectiveness of Carbon Dioxide Displacement Under Miscible and Immiscible Conditions," Petroleum Recovery Institute Research Report RR-40 (March 1979)
36. Contracts for EOR and Improved Drilling Technology, US DOE Progress Review No. 37, BERC, Bartlesville, OK (December 1983)
37. Metcalfe, R.S., Fussell, D.D., and Shelton, J.L.: "A Multicell Equilibrium Separation Model for the Study of Multiple Contact Miscibility in Rich-Gas Drives," Soc. Pet. Eng. J. (June 1973) pp. 147-155
38. Firoozabadi, A. and Aziz, K.: "Analysis and Correlation of Nitrogen and Lean Gas Miscibility Pressure," Presented at SPE California Regional Meeting, (1984)
39. Katz, D.L. and Firoozabadi, A.: "Predicting Phase Behavior of Condensate/Crude Oil Systems Using Methane Interaction Coefficients," J. Pet. Tech. (November 1978) pp. 1649-55
40. Williams, C.A., Zana, E.A., and Humphrys, G.E.: "Use of the Peng-Robinson Equation of State to Predict Hydrocarbon Phase Behavior and Miscibility for Fluid Displacement," SPE 8817 (1980)
41. Wu, R.S., Batycky, J.P., Harker, B., and Rancier, D.: "Enriched Gas Displacement: Design of Solvent Compositions," Petroleum Society of CIM 84-35-111, (1984)
42. Hagoort, J. and Dumore, J.M.: "Determination of Minimum Miscibility Pressures With an Equation of State Program," Proceedings Third European EOR Conference Vol. 1, Rome, Italy (April 16-18, 1985)
43. University of Kansas: "Development of a Method for Evaluating Carbon Dioxide Miscible Flooding Prospects, Final Report," DOE/BC/10122-50 (March 1985)

44. Whitson, C.H.: "Effect of Physical Properties Estimation on Equation of State Predictions," SPE 11200 (1982)
45. Kessler, M.G. and Lee, B.I.: "Improved Predictions of Enthalpy of Fractions," Hydro. Proc. (March 1977) pp. 153-158
46. Kuo, S.S.: "Prediction of Miscibility for the Enriched Gas Drive Process," SPE 14152 (September 1985)
47. Grigg, R.B. and Lingane, P.J.: "Predicting Phase Behavior of Mixtures of Reservoir Fluids With Carbon Dioxide," SPE 11960 (1983)
48. Hong, K.C.: "Lumped-Component Characterization of Crude Oils for Compositional Simulation," SPE/DOE 10691 (1982)
49. Robinson, D.B. and Peng, D.Y.: "The Characterization of the Heptanes and Heavier Fractions for the GPA Peng-Robinson Programs," Research Report RR-28, Gas Processors Assoc., Tulsa (1978)
50. Lydersen, A.L.: "Estimation of Critical Properties of Organic Compounds," Univ. of Wisconsin, Eng. Experiments Station Report 3, Madison, Wisconsin (April 1955)
51. Edmister, W.C.: "Applied Hydrocarbon Thermodynamics Part 4: Compressibility Factors and Equations of State," Pet. Refiner, 7 (1981) pp. 173-179
52. GPSA Engineering Data Book, 9th edition, GPSA, Tulsa (1981)
53. Kato, K.: "Generalized Interaction Parameters for the Peng-Robinson Equation of State: Carbon Dioxide-n-Paraffin Binary Systems," Fluid Phase Equilibria, 7 (1981) pp. 219-231
54. Lin, H.M.: "Peng-Robinson Equation of State for Vapor-Liquid Equilibrium Calculations for Carbon Dioxide + Hydrocarbon Mixtures," Fluid Phase Equilibria, 16 (1984) pp. 151-169

5. Varotsis, N., Stewart, G., Todd, A.C., and Clancy, M.: "The Phase Behavior of Systems Comprising North Sea Reservoir Fluids and Injection Gases," SPE/DOE 12647 (1984)
56. Mehra, R.K., Heidemann, R.A., and Aziz, K.: "A Statistical Approach for Combining Reservoir Fluids Into Pseudo Components for Compositional Model Studies," SPE 11201 (1982)
57. Whitson, C.H.: "Characterizing Hydrocarbon Plus Fractions," Soc. Pet. Eng. J. (August 1983) pp. 683-694
58. Li, Y.K. and Nghiem, L.X.: "Phase Behavior Computation for Reservoir Fluid: Effects of Pseudo Component on Phase Diagrams and Simulation Results," Petroleum Society of CIM 84-35-19 (1984)
59. Orr, F.M., Lien, C.L., and Pelletier, M.T.: "Liquid-Liquid Phase Behavior in CO₂-Hydrocarbon Systems," Symposium on Chemistry of Enhanced Oil Recovery, ACS Atlanta Meeting (March 29 - April 3, 1981) pp. 132-145
60. Coats, K.H. and Smart, G.T.: "Application of a Regression-Based EOS PVT Program to Laboratory Data," SPE 11197 (1982)
61. Peng, D.Y. and Robinson, D.B.: "A Rigorous Method for Predicting the Critical Properties of Multicomponent Systems from an Equation of State," AIChE Journal Vol. 23, No. 2 (March 1977) pp. 137-144
62. Heidemann, R.A. and Khalil, A.M.: "The Calculation of Critical Points," AIChE Journal Vol. 26, No. 5 (September 1980) pp. 769-779
63. Dicharry, R.M., Perryman, T.L., and Ronquille, J.D.: "Evaluation and Design of a CO₂ Miscible Flood Project--SACROC Unit, Kelly Snider Field," J. Pet. Tech. (November 1973) p. 1309

APPENDIX A
Sample Calculations

This section shows the procedure and PR EOS program output for the calculation of the miscibility conditions of a Ford Geraldine mixture at 150°F. The arbitrarily selected IOC is 70 mole percent C₆₋ and 30 mole percent C₇₊. A series of bubble point pressure and retrograde dewpoint pressure calculations were made for mixtures of this oil and CO₂. The predicted P-X diagram saturation boundary is shown in Figure A-1. It was determined that the critical CO₂ concentration is 65.0 mole percent, where the predicted bubble point pressure is 2534.9 psia and the predicted dewpoint pressure is 2535.0 psia. The critical pressure is taken as 2534.9 psia. The PR EOS program output for the saturation pressure calculations at X_{CO₂} = 0.65 and 150°F is shown in Data Sheets A-1 and A-2. The pseudoternary critical point composition is given below:

$$X_{\text{CO}_2, \text{c}} = 0.6500$$

$$X_{\text{C}_{6-}, \text{c}} = 0.2450$$

$$X_{\text{C}_{7+}, \text{c}} = 0.1050$$

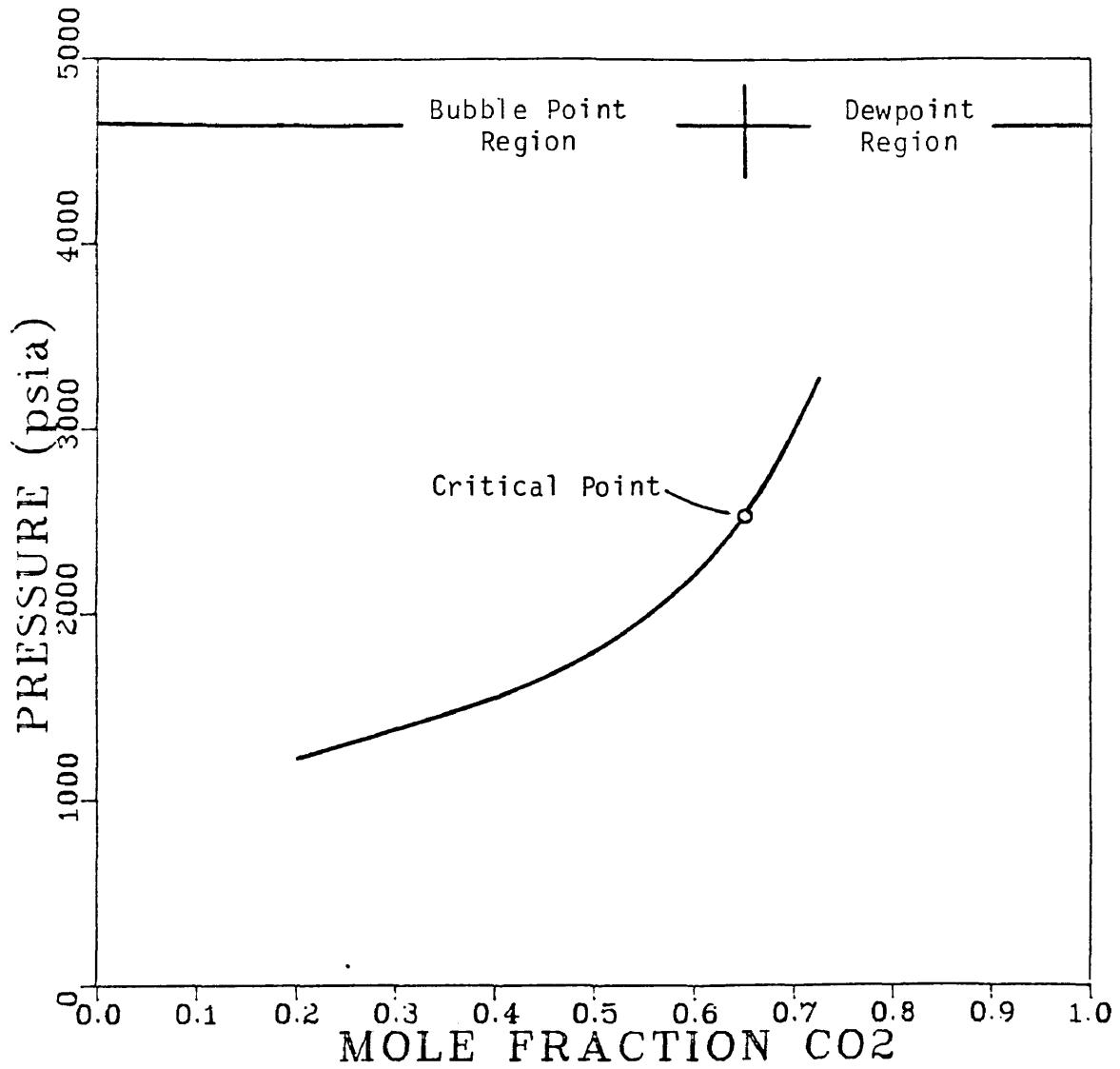


Figure A-1. Predicted Saturation Boundary: Ford Geraldine System IOC = 70/30 Temperature = 150°F

Data Sheet A-1
Bubble Point Pressure Calculation

Project: FORD GERALDINE TEST

Bubble Point Pressure Prediction at 150.00 F
 Initial Value was 2447.4 psia Predicted Value was 2534.9 psia

Component	Composition, Mole Fraction			K-Factor
	Feed	Liquid	Vapor	
CO2	.6500D+00	.6500D+00	.6509D+00	.1001D+01
C1	.5715D-01	.5715D-01	.5729D-01	.1002D+01
C2-3	.1097D+00	.1097D+00	.1097D+00	.1000D+01
C4-6	.7816D-01	.7816D-01	.7799D-01	.9979D+00
C7-10	.5088D-01	.5088D-01	.5066D-01	.9957D+00
C11-24	.4183D-01	.4183D-01	.4146D-01	.9913D+00
C26+	.1230D-01	.1230D-01	.1203D-01	.9782D+00

Project: FORD GERALDINE TEST

Bubble Point Pressure Prediction at 150.00 F
 Initial Value was 2447.4 psia Predicted Value was 2534.9 psia

Fluid Properties	Feed	Liquid	Vapor
Z=PV/RT		.5500	.5485
Viscosity, Centipoise		.0867	.0864
MW lb/lb-mole	60.2711	60.2711	60.0602
Cp BTU/lb-mole-F	217.6426	217.6426	216.9359
H BTU/lb-mole	67362.7886	67362.7886	67134.7428
J-T Coef F/psi	.0001	.0001	.0002
S BTU/lb-mole-F	540.9151	540.9151	538.9907
V cu ft/lb-mole	1.4197	1.4197	1.4158
D=MW/V lb/cu ft	42.4544	42.4544	42.4228
Volume %	100.0000	100.0000	.0000
Mole %	100.0000	100.0000	.0000
Total Moles	1.0000	1.0000	.0000
Total H, k BTU	67.3629	67.3629	.0000
V(H-T) cu ft/lb-mole		1.2827	

Data Sheet A-2
Retrograde Dewpoint Pressure Calculation

Project: FORD GERALDINE TEST

Dew Point Pressure Prediction at 150.00 F
 Initial Value was 2534.9 psia Predicted Value was 2535.0 psia

Component	Composition, Mole Fraction			K-Factor
	Feed	Liquid	Vapor	
CO2	.6500D+00	.6488D+00	.6500D+00	.1002D+01
C1	.5715D-01	.5698D-01	.5715D-01	.1003D+01
C2-3	.1097D+00	.1097D+00	.1097D+00	.1000D+01
C4-6	.7816D-01	.7837D-01	.7816D-01	.9973D+00
C7-10	.5088D-01	.5116D-01	.5088D-01	.9945D+00
C11-24	.4183D-01	.4230D-01	.4183D-01	.9889D+00
C26+	.1230D-01	.1265D-01	.1230D-01	.9721D+00

Project: FORD GERALDINE TEST

Dew Point Pressure Prediction at 150.00 F
 Initial Value was 2534.9 psia Predicted Value was 2535.0 psia

Fluid Properties	Feed	Liquid	Vapor
Z=PV/RT		.5520	.5500
Viscosity, Centipoise		.0870	.0867
MW lb/lb-mole	60.2734	60.5489	60.2734
Cp BTU/lb-mole-F	217.6502	218.5743	217.6502
H BTU/lb-mole	67365.2907	67663.2650	67365.2907
J-T Coef F/psi	.0001	.0001	.0001
S BTU/lb-mole-F	540.9363	543.4504	540.9363
V cu ft/lb-mole	1.4197	1.4248	1.4197
D=MW/V lb/cu ft	42.4549	42.4951	42.4549
Volume %	100.0000	.0000	100.0000
Mole %	100.0000	.0000	100.0000
Total Moles	1.0000	.0000	1.0000
Total H, k BTU	67.3666	.0000	67.3666
V(H-T) cu ft/lb-mole		1.2845	

A flash calculation was performed for an arbitrarily selected mixture at 150°F and 2534.9 psia. The pseudoternary composition of this mixture is given below:

$$X_{CO_2} = 0.72$$

$$X_{C6-} = 0.15$$

$$X_{C7+} = 0.13$$

The program output for this calculation is shown in Data Sheet A-3. The pseudoternary composition of the upper and lower phases are:

$$X_{CO_2,UL} = 0.7793 \quad X_{CO_2,LL} = 0.6892$$

$$X_{C6-,UL} = 0.1454 \quad X_{C6-,LL} = 0.1524$$

$$X_{C7+,UL} = 0.0753 \quad X_{C7+,LL} = 0.1584$$

The bisector B of the tie line connecting these mixtures on a pseudoternary diagram can be specified by an (x,y) coordinate pair where the x coordinate is mole fraction C₆₋ and the y coordinate is mole fraction CO₂. These coordinates are calculated as follows:

$$X_{CO_2,B} = \frac{X_{CO_2,UL} + X_{CO_2,LL}}{2} = 0.7343$$

$$X_{C6-,B} = \frac{X_{C6-,UL} + X_{C6-,LL}}{2} = 0.1489$$

Data Sheet A-3
Initial Flash Calculation

	Feed	Liquid 1	Liquid 2	Vapor
C02	.7200D+00	.6892D+00	.7793D+00	.0000D+00
C1	.3499D-01	.3274D-01	.3932D-01	.0000D+00
C2-3	.6716D-01	.6801D-01	.6551D-01	.0000D+00
C4-6	.4785D-01	.5164D-01	.4054D-01	.0000D+00
C7-10	.6299D-01	.7200D-01	.4562D-01	.0000D+00
C11-24	.5179D-01	.6463D-01	.2702D-01	.0000D+00
C26+	.1522D-01	.2174D-01	.2666D-02	.0000D+00

Component	K-Factor	
	K1=Y/X1	K2=Y/X2
C02	.1000D+01	.8844D+00
C1	.1000D+01	.8327D+00
C2-3	.1000D+01	.1038D+01
C4-6	.1000D+01	.1274D+01
C7-10	.1000D+01	.1578D+01
C11-24	.1000D+01	.2392D+01
C26+	.1000D+01	.8152D+01

Project: FORD GERALDINE TEST

L1-L2 Flash Calculation at 2534.9 psia 150.00 F

Fluid Properties	Feed	Liquid 1	Liquid 2
Z=PV/RT		.6073	.4851
Viscosity, Centipoise		.0968	.0444
MW lb/lb-mole	64.3124	70.3494	52.6744
Cp BTU/lb-mole-F	232.0262	252.0421	193.4393
H BTU/lb-mole	71902.0599	78427.9803	59821.3541
dT/dP F/psi	.0001	-.0002	.0009
S BTU/lb-mole-F	577.5090	632.6357	471.2356
V cu ft/lb-mole	1.4598	1.5675	1.2521
D=MW/V lb/cu ft	44.0554	44.8789	42.0630
Volume %	100.0000	70.7039	29.2961
Mole %	100.0000	65.8447	34.1553
Total Moles	1.0000	.6584	.3416
Total H, k BTU	71.9021	51.6407	20.2614
V(H-T) cu ft/lb-mole		1.3137	n.a.

The slope of the line connecting the initial tie line bisector B and the critical point C is given by:

$$m_{BC} = \frac{X_{CO_2,B} - X_{CO_2,C}}{X_{C6-,B} - X_{C6-,C}} = -0.8772$$

The pseudoternary composition of a mixture M which lies on the line BC can be calculated from the following expressions if the CO₂ concentration X_{CO₂,M} is specified:

$$\begin{aligned} X_{C6-,M} &= \frac{X_{CO_2,M} - X_{CO_2,B}}{m_{BC}} + X_{C6-,B} \\ &= \frac{X_{CO_2,M} - 0.7343}{-0.8772} + 0.1489 \end{aligned}$$

$$X_{C7+,M} = 1 - X_{CO_2,M} - X_{C6-,M}$$

Five mixtures which lie on the line BC were flashed to define tie lines in the vicinity of the critical point. These mixtures correspond to values of ΔX_{CO₂} of 0.08, 0.06, 0.04, 0.02, and 0.01. (ΔX_{CO₂} measures the departure of a mixture M from the critical point composition in terms of mole fraction CO₂.) The pseudoternary composition of these mixtures, calculated from the above expressions, is shown in Table A-1. The PR EOS program output for the flash calculations is shown in data sheets A-4 through A-8.

Table A-1: Pseudoternary Composition of Mixtures Flashed to define Tie Lines

ΔX_{CO_2}	X_{CO_2}	X_{C6-}	X_{C7+}
0.08	0.7300	0.1537	0.1163
0.06	0.7100	0.1765	0.1136
0.04	0.6900	0.1994	0.1106
0.02	0.6700	0.2222	0.1078
0.01	0.6600	0.2336	0.1064

Data Sheet A-4
Flash Calculation for Mixture M1

	Feed	Liquid 1	Liquid 2	Vapor
CO2	.7300D+00	.6820D+00	.7790D+00	.0000D+00
C1	.3586D-01	.3230D-01	.3949D-01	.0000D+00
C2-3	.6883D-01	.7011D-01	.6752D-01	.0000D+00
C4-6	.4904D-01	.5526D-01	.4270D-01	.0000D+00
C7-10	.5634D-01	.6966D-01	.4276D-01	.0000D+00
C11-24	.4632D-01	.6624D-01	.2600D-01	.0000D+00
C26+	.1362D-01	.2447D-01	.2546D-02	.0000D+00

Component	K-Factor	
	K1=Y/X1	K2=Y/X2
CO2	.1000D+01	.8754D+00
C1	.1000D+01	.8180D+00
C2-3	.1000D+01	.1038D+01
C4-6	.1000D+01	.1294D+01
C7-10	.1000D+01	.1629D+01
C11-24	.1000D+01	.2548D+01
C26+	.1000D+01	.9609D+01

Project: FORD GERALDINE TEST

L1-L2 Flash Calculation at 2534.9 psia 150.00 F

Fluid Properties	Feed	Liquid 1	Liquid 2
Z=PV/RT		.6212	.4844
Viscosity, Centipoise		.0971	.0436
MW lb/lb-mole	62.1466	71.8253	52.2770
Cp BTU/lb-mole-F	224.9508	257.1007	192.1669
H BTU/lb-mole	69562.0690	80026.7644	58890.9694
dT/dP F/psi	.0003	-.0002	.0010
S BTU/lb-mole-F	557.7430	646.1197	467.6232
V cu ft/lb-mole	1.4287	1.6035	1.2503
D=MW/V lb/cu ft	43.5001	44.7922	41.8104
Volume %	100.0000	56.6681	43.3319
Mole %	100.0000	50.4883	49.5117
Total Moles	1.0000	.5049	.4951
Total H, k BTU	69.5621	40.4041	29.1579
V(H-T) cu ft/lb-mole		1.3298	n.a.

Data Sheet A-5
Flash Calculation for Mixture M2

	Feed	Liquid 1	Liquid 2	Vapor
C02	.7100D+00	.6712D+00	.7514D+00	.0000D+00
C1	.4118D-01	.3769D-01	.4491D-01	.0000D+00
C2-3	.7904D-01	.8000D-01	.7803D-01	.0000D+00
C4-6	.5632D-01	.6198D-01	.5029D-01	.0000D+00
C7-10	.5497D-01	.6544D-01	.4382D-01	.0000D+00
C11-24	.4519D-01	.6117D-01	.2817D-01	.0000D+00
C26+	.1329D-01	.2256D-01	.3404D-02	.0000D+00

Component	K-Factor	
	K1=Y/X1	K2=Y/X2
C02	.1000D+01	.8933D+00
C1	.1000D+01	.8391D+00
C2-3	.1000D+01	.1025D+01
C4-6	.1000D+01	.1232D+01
C7-10	.1000D+01	.1493D+01
C11-24	.1000D+01	.2171D+01
C26+	.1000D+01	.6626D+01

Project: FORD GERALDINE TEST

L1-L2 Flash Calculation at 2534.9 psia 150.00 F

Fluid Properties	Feed	Liquid 1	Liquid 2
Z=PV/RT		.6090	.4923
Viscosity, Centipoise		.0954	.0455
MW lb/lb-mole	61.6773	69.7236	53.1035
Cp BTU/lb-mole-F	223.0927	249.8680	194.5621
H BTU/lb-mole	69013.1014	77711.3773	59744.5906
dT/dP F/psi	.0002	-.0002	.0008
S BTU/lb-mole-F	553.5433	627.0049	475.2657
V cu ft/lb-mole	1.4261	1.5719	1.2708
D=MW/V lb/cu ft	43.2483	44.3562	41.7880
Volume %	100.0000	56.8602	43.1398
Mole %	100.0000	51.5869	48.4131
Total Moles	1.0000	.5159	.4841
Total H, k BTU	69.0131	40.0889	28.9242
V(H-T) cu ft/lb-mole		1.3218	1.0694

Data Sheet A-6
Flash Calculation for Mixture M3

	Feed	Liquid 1	Liquid 2	Vapor
CO2	.6900D+00	.6606D+00	.7227D+00	.0000D+00
C1	.4651D-01	.4333D-01	.5004D-01	.0000D+00
C2-3	.8926D-01	.8986D-01	.8860D-01	.0000D+00
C4-6	.6360D-01	.6834D-01	.5833D-01	.0000D+00
C7-10	.5361D-01	.6132D-01	.4503D-01	.0000D+00
C11-24	.4407D-01	.5610D-01	.3070D-01	.0000D+00
C26+	.1296D-01	.2045D-01	.4631D-02	.0000D+00

Component	K-Factor	
	K1=Y/X1	K2=Y/X2
CO2	.1000D+01	.9141D+00
C1	.1000D+01	.8660D+00
C2-3	.1000D+01	.1014D+01
C4-6	.1000D+01	.1172D+01
C7-10	.1000D+01	.1362D+01
C11-24	.1000D+01	.1828D+01
C26+	.1000D+01	.4415D+01

Project: FORD GERALDINE TEST

L1-L2 Flash Calculation at 2534.9 psia 150.00 F

Fluid Properties	Feed	Liquid 1	Liquid 2
Z=Pv/RT		.5961	.5021
Viscosity, Centipoise		.0936	.0477
MW lb/lb-mole	61.2079	67.5198	54.1933
Cp BTU/lb-mole-F	221.2539	242.2997	197.8649
H BTU/lb-mole	68463.0253	75286.1167	60880.2496
dT/dP F/psi	.0002	-.0001	.0007
S BTU/lb-mole-F	549.3349	606.9544	485.3000
V cu ft/lb-mole	1.4237	1.5386	1.2960
D=MW/V lb/cu ft	42.9918	43.8835	41.8153
Volume %	100.0000	56.8848	43.1152
Mole %	100.0000	52.6367	47.3633
Total Moles	1.0000	.5264	.4736
Total H, k BTU	68.4630	39.6281	28.8349
V(H-T) cu ft/lb-mole		1.3139	1.2204

Data Sheet A-7
Flash Calculation for Mixture M4

	Feed	Liquid 1	Liquid 2	Vapor
C02	.6700D+00	.6514D+00	.6928D+00	.0000D+00
C1	.5183D-01	.4945D-01	.5476D-01	.0000D+00
C2-3	.9948D-01	.9975D-01	.9914D-01	.0000D+00
C4-6	.7088D-01	.7417D-01	.6683D-01	.0000D+00
C7-10	.5224D-01	.5699D-01	.4638D-01	.0000D+00
C11-24	.4295D-01	.5051D-01	.3363D-01	.0000D+00
C26+	.1262D-01	.1767D-01	.6420D-02	.0000D+00

Component	K-Factor	
	K1=Y/X1	K2=Y/X2
C02	.1000D+01	.9403D+00
C1	.1000D+01	.9031D+00
C2-3	.1000D+01	.1006D+01
C4-6	.1000D+01	.1110D+01
C7-10	.1000D+01	.1229D+01
C11-24	.1000D+01	.1502D+01
C26+	.1000D+01	.2752D+01

Project: FORD GERALDINE TEST

L1-L2 Flash Calculation at 2534.9 psia 150.00 F

Fluid Properties	Feed	Liquid 1	Liquid 2
Z=PV/RT		.5800	.5147
Viscosity, Centipoise		.0913	.0505
MW lb/lb-mole	60.7387	64.8743	55.6480
Cp BTU/lb-mole-F	219.4351	233.2479	202.4324
H BTU/lb-mole	67912.3234	72382.8734	62409.3589
dT/dP F/psi	.0002	-.0001	.0005
S BTU/lb-mole-F	545.1208	582.8693	498.6547
V cu ft/lb-mole	1.4215	1.4970	1.3286
D=MW/V lb/cu ft	42.7279	43.3348	41.8861
Volume %	100.0000	58.1073	41.8927
Mole %	100.0000	55.1758	44.8242
Total Moles	1.0000	.5518	.4482
Total H, k BTU	67.9124	39.9379	27.9745
V(H-T) cu ft/lb-mole		1.3037	1.2468

Data Sheet A-8
Flash Calculation for Mixture M5

	Feed	Liquid 1	Liquid 2	Vapor
C02	.6600D+00	.6502D+00	.6786D+00	.0000D+00
C1	.5449D-01	.5312D-01	.5708D-01	.0000D+00
C2-3	.1046D+00	.1047D+00	.1043D+00	.0000D+00
C4-6	.7452D-01	.7637D-01	.7101D-01	.0000D+00
C7-10	.5156D-01	.5407D-01	.4679D-01	.0000D+00
C11-24	.4238D-01	.4638D-01	.3482D-01	.0000D+00
C26+	.1246D-01	.1513D-01	.7410D-02	.0000D+00

Component	K-Factor	
	K1=Y/X1	K2=Y/X2
C02	.1000D+01	.9582D+00
C1	.1000D+01	.9307D+00
C2-3	.1000D+01	.1004D+01
C4-6	.1000D+01	.1076D+01
C7-10	.1000D+01	.1156D+01
C11-24	.1000D+01	.1332D+01
C26+	.1000D+01	.2042D+01

Project: FORD GERALDINE TEST

L1-L2 Flash Calculation at 2534.9 psia 150.00 F

Fluid Properties	Feed	Liquid 1	Liquid 2
Z=Pv/RT		.5656	.5212
Viscosity, Centipoise		.0893	.0518
MW lb/lb-mole	60.5036	62.6966	56.3530
Cp BTU/lb-mole-F	218.5270	225.8441	204.6783
H BTU/lb-mole	67636.0976	70005.8234	63151.0235
dT/dP F/psi	.0002	.0000	.0004
S BTU/lb-mole-F	543.0070	563.0225	505.1247
V cu ft/lb-mole	1.4204	1.4600	1.3454
D=MW/V lb/cu ft	42.5962	42.9425	41.8850
Volume %	100.0000	67.2545	32.7455
Mole %	100.0000	65.4297	34.5703
Total Moles	1.0000	.6543	.3457
Total H, k BTU	67.6360	45.8045	21.8315
V(H-T) cu ft/lb-mole		1.2930	1.2563

The pseudoternary composition of the upper and lower phases for each of the five tie lines was calculated from the detailed phase compositions in Data Sheets A-4 through A-8. This data was used with the following expressions to calculate the slope of each tie line, and the MMC that would result if each tie line were extended through the critical point. The results are summarized in Table A-2. (For the pseudoternary compositions of the upper and lower phases refer to Data Sheet B-8 in Appendix B.)

$$m_{TL} = \frac{X_{CO_2,UL} - X_{CO_2,LL}}{X_{C6-,UL} - X_{C6-,LL}}$$

where UL and LL now denote the upper and lower phases that define this particular tie line

$$\begin{aligned} MMC &= 1 - X_{C6-,C} + \frac{X_{CO_2,C}}{m_{TL}} \\ &= 1 - 0.2450 + \frac{0.6500}{m_{TL}} \end{aligned}$$

A second degree polynomial was fit to the MMC versus ΔX_{CO_2} data. The equation of this polynomial is shown below:

$$MMC = 0.7179 - 0.3228(\Delta X_{CO_2}) + 1.4287(\Delta X_{CO_2})^2$$

Thus, the true MMC which corresponds to $\Delta X_{CO_2} = 0$ is 0.7179

Table A-2. Tie Line Slopes and Calculated MMC Data

ΔX_{CO_2}	Tie Line Slope	MMC (X_{C7+})
0.08	-12.1859	0.7017
0.06	-12.4534	0.7028
0.04	-13.6184	0.7073
0.02	-15.6818	0.7135
0.01	-15.7778	0.7138

APPENDIX B

Summary of EOS Calculations

Data Sheet B-1

Reservoir Fluid: Ford Geraldine
 Critical Conditions: 100°F 1414.3 psia
 MMC (XC7+): 0.7038

IOC: XC6- = 0.7300 XC7+ = 0.2700
 Critical CO2 Conc.: XC02 = 0.5900
 Critical Point Comp.: XC02 = 0.5900 XC6- = 0.2993 XC7+ = 0.1107

Calculated Tie Line Data (Equilibrium Compositions)

dXC02	Overall Mixture			Upper Phase			Lower Phase			Calc. MMC XC7+
	XC02	XC6-	XC7+	XC02	XC6-	XC7+	XC02	XC6-	XC7+	
0.08	0.6700	0.2140	0.1160	0.7278	0.2080	0.0642	0.6271	0.2184	0.1545	0.6399
0.06	0.6500	0.2353	0.1147	0.6991	0.2309	0.0700	0.6164	0.2383	0.1453	0.6477
0.04	0.6300	0.2566	0.1134	0.6684	0.2541	0.0775	0.6054	0.2583	0.1363	0.6618
0.02	0.6100	0.2780	0.1120	0.6363	0.2771	0.0866	0.5951	0.2785	0.1264	0.6811
0.01	0.6000	0.2886	0.1114	0.6195	0.2884	0.0921	0.5912	0.2888	0.1200	0.6909
Initial	0.7200	0.1500	0.1200	0.8039	0.1412	0.0549	0.6583	0.1565	0.1852	---
CO2-C7+	0.9000	0.0000	0.1000	0.9608	0.0000	0.0392	0.7072	0.0000	0.2928	---

Data Sheet B-2

Reservoir Fluid: Ford Geraldine
 Critical Conditions: 100°F 1610.1 psia
 MMC (XC7+): 0.7154

IOC: XC6- = 0.7000 XC7+ = 0.3000
 Critical CO2 Conc.: XC02 = 0.6200
 Critical Point Comp.: XC02 = 0.6200 XC6- = 0.2660 XC7+ = 0.1140

Calculated Tie Line Data (Equilibrium Compositions)

dXC02	Overall Mixture		Upper Phase		Lower Phase		Calc. MMC XC7+
	XC02	XC6- XC7+	XC02	XC6- XC7+	XC02	XC6- XC7+	
0.08	0.7000	0.1788 0.1212	0.7536	0.1736 0.0728	0.6508	0.1835 0.1657	0.6740
0.06	0.6800	0.2006 0.1194	0.7248	0.1967 0.0785	0.6407	0.2040 0.1553	0.6800
0.04	0.6600	0.2224 0.1176	0.6945	0.2200 0.0855	0.6304	0.2245 0.1451	0.6899
0.02	0.6400	0.2442 0.1158	0.6631	0.2431 0.0938	0.6211	0.2451 0.1338	0.7040
0.01	0.6300	0.2551 0.1149	0.6490	0.2543 0.0967	0.6202	0.2556 0.1242	0.7069
Initial	0.7200	0.1500 0.1200	0.7883	0.1433 0.0684	0.6657	0.1553 0.1790	--
CO2-C7+	0.9000	0.0000 0.1000	0.9564	0.0000 0.0436	0.7125	0.0000 0.2875	--

Data Sheet B-3

Reservoir Fluid: Ford Geraldine
 Critical Conditions: 100°F 2251.6 psia
 MMC (XC7+): 0.7599

IOC: XC6- = 0.6000 XC7+ = 0.4000
 Critical CO2 Conc.: XC02 = 0.6810
 Critical Point Comp.: XC02 = 0.6810 XC6- = 0.1914 XC7+ = 0.1276

Calculated Tie Line Data (Equilibrium Compositions)

dXC02	Overall Mixture		Upper Phase		Lower Phase		Calc. MMC XC7+			
	XC02	XC6- XC7+	XC02	XC6- XC7+	XC02	XC6- XC7+				
0.08	0.7610	0.0980	0.1410	0.0927	0.0811	0.7036	0.1027	0.1937	0.7529	
0.06	0.7410	0.1213	0.1377	0.7959	0.1166	0.0875	0.6950	0.1254	0.1796	0.7492
0.04	0.7210	0.1447	0.1343	0.7640	0.1410	0.0950	0.6864	0.1477	0.1659	0.7495
0.02	0.7010	0.1680	0.1310	0.7304	0.1657	0.1039	0.6791	0.1698	0.1511	0.7540
0.01	0.6910	0.1797	0.1293	0.7136	0.1780	0.1084	0.6783	0.1807	0.1410	0.7556
Initial	0.8000	0.0500	0.1500	0.8834	0.0456	0.0710	0.7210	0.0542	0.2248	---
CO2-C7+	0.9000	0.0000	0.1000	0.9493	0.0000	0.0507	0.7233	0.0000	0.2767	---

Data Sheet B-4

Reservoir Fluid: Ford Geraldine
 Critical Conditions: 100°F 2964.5 psia
 MMC (XC7+): 0.7809

IOC: XC6- = 0.5500 XC7+ = 0.4500
 Critical CO2 Conc.: XC02 = 0.7060
 Critical Point Comp.: XC02 = 0.7060 XC6- = 0.1617 XC7+ = 0.1323

Calculated Tie Line Data (Equilibrium Compositions)

dXC02	Overall Mixture		Upper Phase		Lower Phase		Calc. MMC XC7+
	XC02	XC6- XC7+	XC02	XC6- XC7+	XC02	XC6- XC7+	
0.08	0.7860	0.0687 0.1453	0.8523	0.0641 0.0836	0.7222	0.0731 0.2047	0.7893
0.06	0.7660	0.0919 0.1421	0.8217	0.0874 0.0909	0.7143	0.0961 0.1896	0.7810
0.04	0.7460	0.1152 0.1388	0.7898	0.1114 0.0988	0.7069	0.1186 0.1745	0.7772
0.02	0.7260	0.1384 0.1356	0.7557	0.1359 0.1084	0.7006	0.1406 0.1588	0.7781
0.01	0.7160	0.1500 0.1339	0.7381	0.1482 0.1137	0.7004	0.1514 0.1482	0.7780
Initial	0.8000	0.0500 0.1500	0.8752	0.0458 0.0790	0.7291	0.0539 0.2170	--
CO2-C7+	0.9000	0.0000 0.1000	0.9608	0.0000 0.0392	0.7292	0.0000 0.2708	--

Data Sheet B-5

Reservoir Fluid: Ford Geraldine
 Critical Conditions: 150°F 1705.2 psia
 MMC (XC7+): 0.6016

IOC: XC6- = 0.8600 XC7+ = 0.1400
 Critical CO2 Conc.: XC02 = 0.4300
 Critical Point Comp.: XC02 = 0.4300 XC6- = 0.4902 XC7+ = 0.0798

Calculated Tie Line Data (Equilibrium Compositions)

dXC02	Overall Mixture			Upper Phase			Lower Phase			Calc. MMC XC7+
	XC02	XC6-	XC7+	XC02	XC6-	XC7+	XC02	XC6-	XC7+	
0.08	0.5100	0.4104	0.0796	0.5769	0.3972	0.0259	0.4836	0.4155	0.1009	0.4257
0.06	0.4900	0.4303	0.0797	0.5514	0.4198	0.0288	0.4708	0.4336	0.0956	0.4362
0.04	0.4700	0.4503	0.0797	0.5213	0.4442	0.0345	0.4574	0.4518	0.0908	0.4585
0.02	0.4500	0.4702	0.0798	0.4751	0.4715	0.0534	0.4418	0.4699	0.0883	0.5305
0.01	0.4400	0.4802	0.0798	0.4584	0.4821	0.0595	0.4359	0.4798	0.0843	0.5538
Initial	0.5300	0.3500	0.1200	0.6514	0.3309	0.0177	0.5048	0.3540	0.1412	---
CO2-C7+	0.9000	0.0000	0.1000	0.9827	0.0000	0.0173	0.6787	0.0000	0.3213	---

Data Sheet B-6

Reservoir Fluid: Ford Geraldine
 Critical Conditions: 150°F 1881.7 psia
 MMC (XC7+): 0.6298

IOC: XC6- = 0.8300 XC7+ = 0.1700
 Critical CO2 Conc.: XC02 = 0.4900
 Critical Point Comp.: XC02 = 0.4900 XC6- = 0.4232 XC7+ = 0.0868

Calculated Tie Line Data (Equilibrium Compositions)

dXC02	Overall Mixture			Upper Phase			Lower Phase			Calc. MMC XC7+
	XC02	XC6-	XC7+	XC02	XC6-	XC7+	XC02	XC6-	XC7+	
0.08	0.5700	0.3501	0.0799	0.6080	0.3466	0.0454	0.5305	0.3537	0.1158	0.5316
0.06	0.5500	0.3684	0.0816	0.5833	0.3664	0.0503	0.5191	0.3702	0.1107	0.5481
0.04	0.5300	0.3867	0.0833	0.5570	0.3864	0.0566	0.5073	0.3869	0.1058	0.5725
0.02	0.5100	0.4049	0.0851	0.5294	0.4058	0.0648	0.4964	0.4043	0.0933	0.5986
0.01	0.5000	0.4141	0.0859	0.5150	0.4152	0.0698	0.4921	0.4135	0.0944	0.6134
Initial	0.5600	0.3500	0.0900	0.6101	0.3452	0.0447	0.5324	0.2865	0.1811	--
CO2-C7+	0.9000	0.0000	0.1000	0.9748	0.0000	0.0252	0.7017	0.0000	0.2983	--

Data Sheet B-7

Reservoir Fluid: Ford Geraldine
 Critical Conditions: 150°F 2046.7 psia
 MMC (XC7+): 0.6298

IOC: XC6- = 0.8000 XC7+ = 0.2000
 Critical CO2 Conc.: XC02 = 0.5400
 Critical Point Comp.: XC02 = 0.5400 XC6- = 0.3680 XC7+ = 0.0920

Calculated Tie Line Data (Equilibrium Compositions)

dXC02	Overall Mixture		Upper Phase		Lower Phase		Calc. MMC XC7+
	XC02	XC6- XC7+	XC02	XC6- XC7+	XC02	XC6- XC7+	
0.08	0.6200	0.2786 0.1014	0.6734	0.2737 0.0529	0.5866	0.2816 0.1318	0.5824
0.06	0.6000	0.3010 0.0990	0.6448	0.2977 0.0575	0.5738	0.3029 0.1233	0.5926
0.04	0.5800	0.3233 0.0967	0.6146	0.3218 0.0636	0.5608	0.3242 0.1150	0.6077
0.02	0.5600	0.3457 0.0943	0.5836	0.3455 0.0709	0.5484	0.3458 0.1058	0.6275
0.01	0.5500	0.3569 0.0931	0.5698	0.3569 0.0733	0.5444	0.3569 0.0987	0.6432
Initial	0.7200	0.1500 0.1300	0.8181	0.1410 0.0409	0.6546	0.1560 0.1894	---
CO2-C7+	0.9000	0.0000 0.1000	0.9673	0.0000 0.0327	0.7161	0.0000 0.2839	---

Data Sheet B-8

Reservoir Fluid: Ford Geraldine
 Critical Conditions: 150°F 2534.9 psia
 MMC (XC7+): 0.7179

IOC: XC6- = 0.7000 XC7+ = 0.3000
 Critical CO2 Conc.: XC02 = 0.6500
 Critical Point Comp.: XC02 = 0.6500 XC6- = 0.2450 XC7+ = 0.1050

Calculated Tie Line Data (Equilibrium Compositions)

dXC02	Overall Mixture		Upper Phase		Lower Phase		Calc. MMC XC7+
	XC02	XC6-	XC02	XC6-	XC02	XC6-	
0.08	0.7300	0.1537	0.7790	0.1497	0.6820	0.1577	0.7017
0.06	0.7100	0.1765	0.7514	0.1732	0.6712	0.1797	0.7028
0.04	0.6900	0.1994	0.7227	0.1970	0.6606	0.2015	0.7073
0.02	0.6700	0.2222	0.6928	0.2207	0.6514	0.2234	0.7135
0.01	0.6600	0.2336	0.6786	0.2324	0.6502	0.2342	0.7138
Initial	0.7200	0.1500	0.7793	0.1454	0.6892	0.1524	---
CO2-C7+	0.9000	0.0000	0.9521	0.0000	0.7408	0.0000	---

Data Sheet B-9

Reservoir Fluid: Ford Geraldine
 Critical Conditions: 150°F 3023.5 psia
 MMC (XC7+): 0.7728

IOC: XC6- = 0.6000 XC7+ = 0.4000
 Critical CO2 Conc.: XC02 = 0.7130
 Critical Point Comp.: XC02 = 0.7130 XC6- = 0.1722 XC7+ = 0.1148

Calculated Tie Line Data (Equilibrium Compositions)

dXC02	Overall Mixture		Upper Phase		Lower Phase		Calc. MMC XC7+
	XC02	XC6- XC7+	XC02	XC6- XC7+	XC02	XC6- XC7+	
0.08	0.7930	0.0745 0.1325	0.8492	0.0713 0.0795	0.7391	0.0776 0.1833	0.7866
0.06	0.7730	0.0989 0.1281	0.8203	0.0957 0.0840	0.7292	0.1019 0.1689	0.7794
0.04	0.7530	0.1234 0.1236	0.7902	0.1206 0.0892	0.7195	0.1258 0.1547	0.7752
0.02	0.7330	0.1478 0.1192	0.7585	0.1459 0.0956	0.7113	0.1494 0.1393	0.7739
0.01	0.7230	0.1600 0.1170	0.7426	0.1585 0.0989	0.7104	0.1610 0.1286	0.7720
Initial	0.8000	0.0500 0.1500	0.8734	0.0470 0.0796	0.7537	0.0519 0.1944	---
CO2-C7+	0.9000	0.0000 0.1000	0.9437	0.0000 0.0563	0.7545	0.0000 0.2455	---

Data Sheet B-10

Reservoir Fluid: Ford Geraldine
 Critical Conditions: 200°F 1727.0 psia
 MMC (XC7+): 0.3945

IOC: XC6- = 0.9000 XC7+ = 0.1000
 Critical CO2 Conc.: XC02 = 0.2280
 Critical Point Comp.: XC02 = 0.2280 XC6- = 0.6948 XC7+ = 0.0772

Calculated Tie Line Data (Equilibrium Compositions)

dXC02	Overall Mixture		Upper Phase		Lower Phase		Calc. MMC XC7+
	XC02	XC6- XC7+	XC02	XC6- XC7+	XC02	XC6- XC7+	
0.08	0.3080	0.6196 0.0724	0.3624	0.6159 0.0217	0.2882	0.6210 0.0908	0.2895
0.06	0.2880	0.6384 0.0736	0.3394	0.6376 0.0230	0.2741	0.6387 0.0872	0.3014
0.04	0.2680	0.6572 0.0748	0.3153	0.6599 0.0248	0.2595	0.6567 0.0838	0.3183
0.02	0.2480	0.6760 0.0760	0.2886	0.6828 0.0286	0.2444	0.6754 0.0802	0.3434
0.01	0.2380	0.6854 0.0766	0.2703	0.6953 0.0344	0.2366	0.6850 0.0784	0.3749
Initial	0.3200	0.5800 0.1000	0.4044	0.5771 0.0185	0.2983	0.5807 0.1210	---
CO2-C7+	0.9000	0.0000 0.1000	0.9841	0.0000 0.0159	0.5875	0.0000 0.4125	---

Data Sheet B-11

Reservoir Fluid: Ford Geraldine
 Critical Conditions: 200°F 2187.8 psia
 MMC (XC7+): 0.5903

IOC: XC6- = 0.8600 XC7+ = 0.1400
 Critical CO2 Conc.: XC02 = 0.3900
 Critical Point Comp.: XC02 = 0.3900 XC6- = 0.5247 XC7+ = 0.0853

Calculated Tie Line Data (Equilibrium Compositions)

dXC02	Overall Mixture		Upper Phase		Lower Phase		Calc. MMC XC7+
	XC02	XC6- XC7+	XC02	XC6- XC7+	XC02	XC6- XC7+	
0.08	0.4700	0.4398 0.0902	0.5150	0.4398 0.0452	0.4423	0.4398 0.1179	0.4756
0.06	0.4500	0.4610 0.0890	0.4876	0.4629 0.0495	0.4286	0.4599 0.1115	0.4951
0.04	0.4300	0.4822 0.0878	0.4590	0.4856 0.0554	0.4146	0.4805 0.1049	0.5201
0.02	0.4100	0.5035 0.0865	0.4296	0.5074 0.0630	0.4009	0.5017 0.0974	0.5528
0.01	0.4000	0.5141 0.0859	0.4145	0.5176 0.0679	0.3948	0.5128 0.0924	0.5703
Initial	0.5300	0.3500 0.1200	0.6211	0.3441 0.0348	0.4914	0.3525 0.1561	--
CO2-C7+	0.9000	0.0000 0.1000	0.9759	0.0000 0.0241	0.6669	0.0000 0.3331	--

Data Sheet B-12

Reservoir Fluid: Ford Geraldine
 Critical Conditions: 200°F 2475.1 psia
 MMC (XC7+): 0.6270

IOC: XC6- = 0.8300 XC7+ = 0.1700
 Critical CO2 Conc.: XC02 = 0.4800
 Critical Point Comp.: XC02 = 0.4800 XC6- = 0.4316 XC7+ = 0.0884

Calculated Tie Line Data (Equilibrium Compositions)

dXC02	Overall Mixture		Upper Phase		Lower Phase		Calc. MMC XC7+
	XC02	XC6-	XC02	XC6-	XC02	XC6-	
0.08	0.5600	0.3493	0.0907	0.3484	0.5229	0.3503	0.5561
0.06	0.5400	0.3699	0.0901	0.3700	0.5105	0.3698	0.5701
0.04	0.5200	0.3904	0.0896	0.3914	0.4980	0.3896	0.5876
0.02	0.5000	0.4110	0.0890	0.4124	0.4866	0.4100	0.6059
0.01	0.4900	0.4213	0.0887	0.4226	0.4815	0.4205	0.6162
Initial	0.5600	0.3500	0.0900	0.3491	0.5224	0.3510	---
CO2-C7+	0.9000	0.0000	0.1000	0.0000	0.7020	0.0000	0.2980

Data Sheet B-13

Reservoir Fluid: Ford Geraldine
 Critical Conditions: 200°F 2681.3 psia
 MMC (XC7+): 0.6496

IOC: XC6- = 0.8000 XC7+ = 0.2000
 Critical CO2 Conc.: XC02 = 0.5400
 Critical Point Comp.: XC02 = 0.5400 XC6- = 0.3680 XC7+ = 0.0920

Calculated Tie Line Data (Equilibrium Compositions)

dXC02	Overall Mixture		Upper Phase		Lower Phase		Calc. MMC XC7+
	XC02	XC6- XC7+	XC02	XC6- XC7+	XC02	XC6- XC7+	
0.08	0.6200	0.2761 0.1039	0.6655	0.2738 0.0607	0.5851	0.2779 0.1370	0.6046
0.06	0.6000	0.2991 0.1009	0.6378	0.2978 0.0644	0.5719	0.3000 0.1281	0.6138
0.04	0.5800	0.3221 0.0979	0.6093	0.3218 0.0689	0.5589	0.3224 0.1187	0.6255
0.02	0.5600	0.3451 0.0949	0.5802	0.3453 0.0745	0.5469	0.3449 0.1082	0.6391
0.01	0.5500	0.3566 0.0934	0.5666	0.3569 0.0765	0.5435	0.3565 0.1000	0.6423
Initial	0.7200	0.1500 0.1300	0.8062	0.1443 0.0495	0.6546	0.1544 0.1910	---
CO2-C7+	0.9000	0.0000 0.1000	0.9626	0.0000 0.0374	0.7215	0.0000 0.2785	---

Data Sheet B-14

Reservoir Fluid: Ford Geraldine
 Critical Conditions: 200°F 3182.8 psia
 MMC (XC7+): 0.7261

IOC: XC6- = 0.7000 XC7+ = 0.3000
 Critical CO2 Conc.: XC02 = 0.6600
 Critical Point Comp.: XC02 = 0.6600 XC6- = 0.2380 XC7+ = 0.1020

Calculated Tie Line Data (Equilibrium Compositions)

dXC02	Overall Mixture		Upper Phase		Lower Phase		Calc. MMC XC7+
	XC02	XC6-	XC02	XC6-	XC02	XC6-	
0.08	0.7400	0.1448	0.7863	0.1418	0.6941	0.1478	0.7194
0.06	0.7200	0.1681	0.7591	0.1656	0.6826	0.1705	0.7193
0.04	0.7000	0.1914	0.7310	0.1895	0.6714	0.1932	0.7219
0.02	0.6800	0.2147	0.7017	0.2135	0.6617	0.2157	0.7257
0.01	0.6700	0.2264	0.6874	0.2254	0.6601	0.2270	0.7238
Initial	0.7200	0.1500	0.7745	0.1467	0.6983	0.1513	---
CO2-C7+	0.9000	0.0000	0.9494	0.0000	0.7545	0.0000	0.2455

Data Sheet B-15

Reservoir Fluid: Ford Geraldine
 Critical Conditions: 200°F 3567.4 psia
 MMC (XC7+): 0.7878

IOC: XC6- = 0.6000 XC7+ = 0.4000
 Critical CO2 Conc.: XC02 = 0.7250
 Critical Point Comp.: XC02 = 0.7250 XC6- = 0.1650 XC7+ = 0.1100

Calculated Tie Line Data (Equilibrium Compositions)

dXC02	Overall Mixture		Upper Phase		Lower Phase		Calc. MMC XC7+		
	XC02	XC6-	XC02	XC6-	XC02	XC6-			
0.08	0.8050	0.0672	0.1278	0.0650	0.0784	0.7550	0.0695	0.1755	0.8035
0.06	0.7850	0.0917	0.1233	0.0821	0.0821	0.7441	0.0938	0.1621	0.7963
0.04	0.7650	0.1161	0.1189	0.0863	0.0863	0.7336	0.1180	0.1484	0.7917
0.02	0.7450	0.1406	0.1144	0.0918	0.0918	0.7247	0.1418	0.1335	0.7889
0.01	0.7350	0.1528	0.1122	0.0954	0.0954	0.7224	0.1536	0.1240	0.7879
Initial	0.8000	0.0500	0.1500	0.0478	0.0831	0.7701	0.0510	0.1789	---
C02-C7+	0.9000	0.0000	0.1000	0.0000	0.0585	0.7714	0.0000	0.2286	---

Data Sheet B-16

Reservoir Fluid: Ford Geraldine
 Critical Conditions: 250°F 2199.7 psia
 MMC (XC7+): 0.5761

IOC: XC6- = 0.8800 XC7+ = 0.1200
 Critical CO2 Conc.: XC02 = 0.2400
 Critical Point Comp.: XC02 = 0.2400 XC6- = 0.6688 XC7+ = 0.0912

Calculated Tie Line Data (Equilibrium Compositions)

dXC02	Overall Mixture		Upper Phase		Lower Phase		Calc. MMC XC7+
	XC02	XC6-	XC02	XC6-	XC02	XC6-	
0.08	0.3200	0.5888	0.3481	0.5994	0.2966	0.5799	0.4221
0.06	0.3000	0.6088	0.3228	0.6199	0.2821	0.6000	0.4486
0.04	0.2800	0.6288	0.2970	0.6397	0.2672	0.6207	0.4842
0.02	0.2600	0.6488	0.2712	0.6579	0.2525	0.6427	0.5263
0.01	0.2500	0.6588	0.2580	0.6661	0.2455	0.6547	0.5501
Initial	0.3500	0.5500	0.3932	0.5602	0.3209	0.5432	---
CO2-C7+	0.9000	0.0000	0.9745	0.0000	0.6050	0.0000	0.3950

Data Sheet B-17

Reservoir Fluid: Ford Geraldine
 Critical Conditions: 250°F 2491.2 psia
 MMC (XC7+): 0.6056

IOC: XC6- = 0.8600 XC7+ = 0.1400
 Critical CO2 Conc.: XC02 = 0.3400
 Critical Point Comp.: XC02 = 0.3400 XC6- = 0.5676 XC7+ = 0.0924

Calculated Tie Line Data (Equilibrium Compositions)

dXC02	Overall Mixture		Upper Phase		Lower Phase		Calc. MMC XC7+
	XC02	XC6-	XC02	XC6-	XC02	XC6-	
0.08	0.4200	0.4784	0.4572	0.4847	0.3941	0.4740	0.4901
0.06	0.4000	0.5007	0.4301	0.5076	0.3796	0.4961	0.5098
0.04	0.3800	0.5230	0.4027	0.5300	0.3651	0.5185	0.5364
0.02	0.3600	0.5453	0.3752	0.5513	0.3510	0.5418	0.5659
0.01	0.3500	0.5565	0.3606	0.5612	0.3443	0.5538	0.5868
Initial	0.4500	0.4000	0.5412	0.4085	0.4333	0.3985	---
CO2-C7+	0.9000	0.0000	0.9700	0.0000	0.6479	0.0000	0.3521

Data Sheet B-18

Reservoir Fluid: Ford Geraldine
 Critical Conditions: 250°F 3076.7 psia
 MMC (XC7+): 0.6653

IOC: XC6- = 0.8000 XC7+ = 0.2000
 Critical CO2 Conc.: XC02 = 0.5200
 Critical Point Comp.: XC02 = 0.5200 XC6- = 0.3840 XC7+ = 0.0960

Calculated Tie Line Data (Equilibrium Compositions)

dXC02	Overall Mixture		Upper Phase		Lower Phase		Calc. MMC XC7+
	XC02	XC6- XC7+	XC02	XC6- XC7+	XC02	XC6- XC7+	
0.08	0.6000	0.2908 0.1092	0.6416	0.2906 0.0678	0.5649	0.2911 0.1440	0.6127
0.06	0.5800	0.3141 0.1059	0.6143	0.3145 0.0712	0.5514	0.3137 0.1349	0.6223
0.04	0.5600	0.3374 0.1026	0.5865	0.3383 0.0752	0.5382	0.3366 0.1252	0.6350
0.02	0.5400	0.3607 0.0993	0.5580	0.3618 0.0802	0.5260	0.3598 0.1142	0.6482
0.01	0.5300	0.3723 0.0977	0.5423	0.3733 0.0844	0.5204	0.3716 0.1080	0.6571
Initial	0.7200	0.1500 0.1300	0.7982	0.1465 0.0553	0.6437	0.1534 0.2029	---
CO2-C7+	0.9000	0.0000 0.1000	0.9585	0.0000 0.0415	0.7142	0.0000 0.2858	---

Data Sheet B-19

Reservoir Fluid: Ford Geraldine
 Critical Conditions: 250°F 3580.0 psia
 MMC (XC7+): 0.7425

IOC: XC6- = 0.7000 XC7+ = 0.3000
 Critical CO2 Conc.: XC02 = 0.6500
 Critical Point Comp.: XC02 = 0.6500 XC6- = 0.2450 XC7+ = 0.1050

Calculated Tie Line Data (Equilibrium Compositions)

dXC02	Overall Mixture			Upper Phase			Lower Phase			Calc. MMC XC7+
	XC02	XC6-	XC7+	XC02	XC6-	XC7+	XC02	XC6-	XC7+	
0.08	0.7300	0.1521	0.1179	0.7752	0.1500	0.0748	0.6858	0.1541	0.1601	0.7251
0.06	0.7100	0.1753	0.1147	0.7484	0.1736	0.0780	0.6739	0.1769	0.1492	0.7265
0.04	0.6900	0.1986	0.1114	0.7208	0.1974	0.0818	0.6625	0.1966	0.1409	0.7295
0.02	0.6700	0.2218	0.1082	0.6918	0.2211	0.0871	0.6523	0.2223	0.1254	0.7344
0.01	0.6600	0.2334	0.1066	0.6754	0.2330	0.0916	0.6479	0.2337	0.1184	0.7387
Initial	0.7200	0.1500	0.1300	0.7731	0.1478	0.0792	0.6914	0.1512	0.1574	--
CO2-C7+	0.9000	0.0000	0.1000	0.9475	0.0000	0.0525	0.7538	0.0000	0.2462	--

Data Sheet B-20

Reservoir Fluid: Ford Geraldine
 Critical Conditions: 250°F 3963.3 psia
 MMC (XC7+): 0.8017

IOC: XC6- = 0.6000 XC7+ = 0.4000
 Critical CO2 Conc.: XC02 = 0.7250
 Critical Point Comp.: XC02 = 0.7250 XC6- = 0.1650 XC7+ = 0.1100

Calculated Tie Line Data (Equilibrium Compositions)

dXC02	Overall Mixture		Upper Phase		Lower Phase		Calc. MMC XC7+		
	XC02	XC6-	XC02	XC6-	XC02	XC6-			
0.08	0.8050	0.0675	0.1275	0.0659	0.0803	0.7574	0.0691	0.1735	0.8106
0.06	0.7850	0.0919	0.1231	0.0902	0.0834	0.7460	0.0935	0.1605	0.8052
0.04	0.7650	0.1162	0.1188	0.1148	0.0872	0.7349	0.1176	0.1475	0.8019
0.02	0.7450	0.1406	0.1144	0.1395	0.0927	0.7251	0.1416	0.1333	0.8005
0.01	0.7350	0.1528	0.1122	0.1521	0.0971	0.7211	0.1535	0.1254	0.8011
Initial	0.8000	0.0500	0.1500	0.0484	0.0856	0.7735	0.0507	0.1758	---
CO2-C7+	0.9000	0.0000	0.1000	0.0000	0.0603	0.7765	0.0000	0.2235	---

Data Sheet B-21

Reservoir Fluid: West Sussex
 Critical Conditions: 100°F 1817.0 psia
 MMC (XC7+): 0.7957

IOC: XC6- = 0.7300 XC7+ = 0.2700
 Critical CO2 Conc.: XC02 = 0.5370
 Critical Point Comp.: XC02 = 0.5370 XC6- = 0.3380 XC7+ = 0.1250

Calculated Tie Line Data (Equilibrium Compositions)

dXC02	Overall Mixture			Upper Phase			Lower Phase			Calc. MMC XC7+
	XC02	XC6-	XC7+	XC02	XC6-	XC7+	XC02	XC6-	XC7+	
0.08	0.6170	0.2625	0.1205	0.6567	0.2629	0.0804	0.5823	0.2622	0.1555	0.6674
0.06	0.5970	0.2814	0.1216	0.6296	0.2831	0.0873	0.5699	0.2799	0.1502	0.6914
0.04	0.5770	0.3002	0.1228	0.6018	0.3030	0.0952	0.5572	0.2980	0.1448	0.7218
0.02	0.5570	0.3191	0.1239	0.5744	0.3222	0.1034	0.5456	0.3171	0.1373	0.7558
0.01	0.5470	0.3285	0.1245	0.5595	0.3312	0.1093	0.5401	0.3271	0.1328	0.7752
Initial	0.6300	0.2400	0.1300	0.6835	0.2389	0.0776	0.5987	0.2407	0.1606	---
CO2-C7+	0.9000	0.0000	0.1000	0.9579	0.0000	0.0421	0.7040	0.0000	0.2960	---

Data Sheet B-22

Reservoir Fluid: West Sussex
 Critical Conditions: 100°F 2134.1 psia
 MMC (XC7+): 0.7864

IOC: XC6- = 0.7000 XC7+ = 0.3000
 Critical CO2 Conc.: XC02 = 0.5780
 Critical Point Comp.: XC02 = 0.5780 XC6- = 0.2954 XC7+ = 0.1266

Calculated Tie Line Data (Equilibrium Compositions)

dXC02	Overall Mixture			Upper Phase		Lower Phase		Calc. MMC XC7+		
	XC02	XC6-	XC7+	XC02	XC6-	XC7+	XC02		XC6-	XC7+
0.08	0.6580	0.2177	0.1243	0.6994	0.2165	0.0841	0.6161	0.2189	0.1650	0.6876
0.06	0.6380	0.2371	0.1249	0.6724	0.2372	0.0904	0.6050	0.2371	0.1579	0.7053
0.04	0.6180	0.2566	0.1254	0.6448	0.2577	0.0975	0.5937	0.2556	0.1507	0.7279
0.02	0.5980	0.2760	0.1260	0.6168	0.2777	0.1055	0.5835	0.2748	0.1417	0.7547
0.01	0.5880	0.2857	0.1263	0.6015	0.2873	0.1112	0.5789	0.2847	0.1364	0.7700
Initial	0.6300	0.2400	0.1300	0.6645	0.2404	0.0951	0.6055	0.2397	0.1548	---
CO2-C7+	0.9000	0.0000	0.1000	0.9552	0.0000	0.0448	0.7091	0.0000	0.2909	---

Data Sheet B-23

Reservoir Fluid: West Sussex
 Critical Conditions: 100°F 2859.9 psia
 MMC (XC7+): 0.7837

IOC: XC6- = 0.6500 XC7+ = 0.3500
 Critical CO2 Conc.: XC02 = 0.6280
 Critical Point Comp.: XC02 = 0.6280 XC6- = 0.2418 XC7+ = 0.1302

Calculated Tie Line Data (Equilibrium Compositions)

dXC02	Overall Mixture		Upper Phase		Lower Phase		Calc. MMC XC7+
	XC02	XC6-	XC02	XC6-	XC02	XC6-	
0.08	0.7080	0.1621	0.7538	0.1591	0.6561	0.1655	0.7174
0.06	0.6880	0.1820	0.7265	0.1802	0.6466	0.1840	0.7277
0.04	0.6680	0.2019	0.6983	0.2012	0.6372	0.2027	0.7426
0.02	0.6480	0.2219	0.6691	0.2220	0.6289	0.2218	0.7609
0.01	0.6380	0.2318	0.6532	0.2322	0.6258	0.2316	0.7720
Initial	0.7300	0.1600	0.7677	0.1571	0.6492	0.1662	---
CO2-C7+	0.9000	0.0000	0.9524	0.0000	0.7159	0.0000	0.2841

Data Sheet B-24

Reservoir Fluid: West Sussex
 Critical Conditions: 150°F 2214.7 psia
 MMC (XC7+): 0.7525

IOC: XC6- = 0.8200 XC7+ = 0.1800
 Critical CO2 Conc.: XC02 = 0.4400
 Critical Point Comp.: XC02 = 0.4400 XC6- = 0.4592 XC7+ = 0.1008

Calculated Tie Line Data (Equilibrium Compositions)

dXC02	Overall Mixture		Upper Phase		Lower Phase		Calc. MMC XC7+
	XC02	XC6- XC7+	XC02	XC6- XC7+	XC02	XC6- XC7+	
0.08	0.5200	0.3950 0.0850	0.5453	0.3976 0.0571	0.4896	0.3917 0.1187	0.5874
0.06	0.5000	0.4110 0.0890	0.5223	0.4149 0.0628	0.4767	0.4070 0.1163	0.6170
0.04	0.4800	0.4271 0.0929	0.4982	0.4318 0.0700	0.4633	0.4227 0.1140	0.6555
0.02	0.4600	0.4431 0.0969	0.4740	0.4481 0.0779	0.4508	0.4399 0.1093	0.6963
0.01	0.4500	0.4512 0.0988	0.4608	0.4557 0.0835	0.4447	0.4489 0.1064	0.7266
Initial	0.5000	0.4000 0.1000	0.5380	0.4041 0.0579	0.4862	0.3985 0.1153	---
CO2-C7+	0.9000	0.0000 0.1000	0.9645	0.0000 0.0355	0.7145	0.0000 0.2855	---

Data Sheet B-25

Reservoir Fluid: West Sussex
 Critical Conditions: 150°F 2413.7 psia
 MMC (XC7+): 0.7306

IOC: XC6- = 0.8000 XC7+ = 0.2000
 Critical CO2 Conc.: XC02 = 0.4950
 Critical Point Comp.: XC02 = 0.4950 XC6- = 0.4039 XC7+ = 0.1011

Calculated Tie Line Data (Equilibrium Compositions)

dXC02	Overall Mixture			Upper Phase			Lower Phase			Calc. MMC XC7+
	XC02	XC6-	XC7+	XC02	XC6-	XC7+	XC02	XC6-	XC7+	
0.08	0.5750	0.3219	0.1031	0.6125	0.3230	0.0645	0.5505	0.3213	0.1282	0.6098
0.06	0.5550	0.3424	0.1026	0.5859	0.3446	0.0695	0.5360	0.3410	0.1230	0.6317
0.04	0.5350	0.3629	0.1021	0.5587	0.3661	0.0752	0.5213	0.3611	0.1176	0.6623
0.02	0.5150	0.3834	0.1016	0.5322	0.3867	0.0811	0.5076	0.3820	0.1104	0.6907
0.01	0.5050	0.3936	0.1014	0.5172	0.3965	0.0863	0.5006	0.3926	0.1068	0.7124
Initial	0.6300	0.2400	0.1300	0.7078	0.2367	0.0555	0.6041	0.2411	0.1548	--
CO2-C7+	0.9000	0.0000	0.1000	0.9595	0.0000	0.0405	0.7237	0.0000	0.2763	--

Data Sheet B-26

Reservoir Fluid: West Sussex
 Critical Conditions: 150°F 3172.1 psia
 MMC (XC7+): 0.7544

IOC: XC6- = 0.7000 XC7+ = 0.3000
 Critical CO2 Conc.: XC02 = 0.6360
 Critical Point Comp.: XC02 = 0.6360 XC6- = 0.2548 XC7+ = 0.1092

Calculated Tie Line Data (Equilibrium Compositions)

dXC02	Overall Mixture		Upper Phase		Lower Phase		Calc. MMC XC7+
	XC02	XC6-	XC02	XC6-	XC02	XC6-	
0.08	0.7160	0.1668	0.7574	0.1644	0.6737	0.1693	0.7082
0.06	0.6960	0.1888	0.7308	0.1871	0.6621	0.1904	0.7148
0.04	0.6760	0.2108	0.7034	0.2099	0.6506	0.2116	0.7247
0.02	0.6560	0.2328	0.6754	0.2326	0.6404	0.2330	0.7372
0.01	0.6460	0.2438	0.6597	0.2438	0.6357	0.2438	0.7460
Initial	0.7300	0.1600	0.7694	0.1575	0.6740	0.1636	---
CO2-C7+	0.9000	0.0000	0.9487	0.0000	0.7453	0.0000	0.2547

Data Sheet B-27

Reservoir Fluid: West Sussex
 Critical Conditions: 200°F 2703.9 psia
 MMC (XC7+): 0.6743

IOC: XC6- = 0.8500 XC7+ = 0.1500
 Critical CO2 Conc.: XC02 = 0.4000
 Critical Point Comp.: XC02 = 0.4000 XC6- = 0.5100 XC7+ = 0.0900

Calculated Tie Line Data (Equilibrium Compositions)

dXC02	Overall Mixture		Upper Phase		Lower Phase		Calc. MMC XC7+
	XC02	XC6-	XC02	XC6-	XC02	XC6-	
0.08	0.4800	0.4323	0.0877	0.4360	0.4575	0.4249	0.5418
0.06	0.4600	0.4518	0.0882	0.4564	0.4426	0.4485	0.5663
0.04	0.4400	0.4712	0.0888	0.4763	0.4276	0.4678	0.5986
0.02	0.4200	0.4906	0.0894	0.4956	0.4132	0.4882	0.6316
0.01	0.4100	0.5003	0.0897	0.5046	0.4060	0.4987	0.6539
Initial	0.5000	0.4000	0.1000	0.4031	0.4792	0.3986	--
CO2-C7+	0.9000	0.0000	0.1000	0.0000	0.7128	0.0000	0.2872

Data Sheet B-28

Reservoir Fluid: West Sussex
 Critical Conditions: 200°F 3170.5 psia
 MMC (XC7+): 0.7013

IOC: XC6- = 0.8000 XC7+ = 0.2000
 Critical CO2 Conc.: XC02 = 0.5350
 Critical Point Comp.: XC02 = 0.5350 XC6- = 0.3720 XC7+ = 0.0930

Calculated Tie Line Data (Equilibrium Compositions)

dXC02	Overall Mixture		Upper Phase		Lower Phase		Calc. MMC XC7+
	XC02	XC6- XC7+	XC02	XC6- XC7+	XC02	XC6- XC7+	
0.08	0.6150	0.2835 0.1015	0.6499	0.2834 0.0667	0.5868	0.2835 0.1297	0.6270
0.06	0.5950	0.3056 0.0994	0.6241	0.3063 0.0696	0.5725	0.3051 0.1224	0.6412
0.04	0.5750	0.3277 0.0973	0.5977	0.3289 0.0734	0.5583	0.3269 0.1148	0.6558
0.02	0.5550	0.3499 0.0951	0.5708	0.3514 0.0778	0.5448	0.3489 0.1063	0.6794
0.01	0.5450	0.3609 0.0941	0.5560	0.3622 0.0818	0.5382	0.3602 0.1016	0.6881
Initial	0.6300	0.2400 0.1300	0.6929	0.2392 0.0679	0.6162	0.2402 0.1436	---
CO2-C7+	0.9000	0.0000 0.1000	0.9550	0.0000 0.0450	0.7422	0.0000 0.2578	---

Data Sheet B-29

Reservoir Fluid: West Sussex
 Critical Conditions: 200°F 3791.2 psia
 MMC (XC7+): 0.7543

IOC: XC6- = 0.7000 XC7+ = 0.3000
 Critical CO2 Conc.: XC02 = 0.6620
 Critical Point Comp.: XC02 = 0.6620 XC6- = 0.2366 XC7+ = 0.1014

Calculated Tie Line Data (Equilibrium Compositions)

dXC02	Overall Mixture			Upper Phase			Lower Phase			Calc. MMC XC7+
	XC02	XC6-	XC7+	XC02	XC6-	XC7+	XC02	XC6-	XC7+	
0.08	0.7420	0.1450	0.1130	0.7816	0.1429	0.0755	0.7012	0.1471	0.1517	0.7287
0.06	0.7220	0.1679	0.1101	0.7554	0.1663	0.0783	0.6889	0.1695	0.1416	0.7313
0.04	0.7020	0.1908	0.1072	0.7285	0.1897	0.0818	0.6769	0.1918	0.1313	0.7362
0.02	0.6820	0.2137	0.1043	0.7005	0.2132	0.0863	0.6659	0.2142	0.1199	0.7435
0.01	0.6720	0.2252	0.1029	0.6849	0.2249	0.0902	0.6610	0.2254	0.1136	0.7490
Initial	0.7300	0.1600	0.1100	0.7651	0.1582	0.0767	0.6926	0.1619	0.1455	--
C02-C7+	0.9000	0.0000	0.1000	0.9454	0.0000	0.0546	0.7670	0.0000	0.2330	--

Data Sheet B-30

Reservoir Fluid: West Sussex
 Critical Conditions: 250°F 3178.8 psia
 MMC (XC7+): 0.6605

IOC: XC6- = 0.8500 XC7+ = 0.1500
 Critical CO2 Conc.: XC02 = 0.4100
 Critical Point Comp.: XC02 = 0.4100 XC6- = 0.5015 XC7+ = 0.0885

Calculated Tie Line Data (Equilibrium Compositions)

dXC02	Overall Mixture			Upper Phase			Lower Phase			Calc. MMC XC7+
	XC02	XC6-	XC7+	XC02	XC6-	XC7+	XC02	XC6-	XC7+	
0.08	0.4900	0.4170	0.0930	0.5170	0.4208	0.0622	0.4655	0.4135	0.1210	0.5566
0.06	0.4700	0.4381	0.0919	0.4924	0.4423	0.0653	0.4506	0.4343	0.1151	0.5770
0.04	0.4500	0.4592	0.0908	0.4675	0.4635	0.0690	0.4356	0.4558	0.1086	0.5975
0.02	0.4300	0.4804	0.0896	0.4423	0.4842	0.0735	0.4213	0.4778	0.1009	0.6235
0.01	0.4200	0.4909	0.0891	0.4286	0.4940	0.0774	0.4143	0.4889	0.0968	0.6447
Initial	0.5000	0.4000	0.1000	0.5342	0.4040	0.0618	0.4768	0.3972	0.1260	---
CO2-C7+	0.9000	0.0000	0.1000	0.9602	0.0000	0.0398	0.7141	0.0000	0.2859	---

Data Sheet B-31

Reservoir Fluid: West Sussex
 Critical Conditions: 250°F 3625.3 psia
 MMC (XC7+): 0.6944

IOC: XC6- = 0.8000 XC7+ = 0.2000
 Critical CO2 Conc.: XC02 = 0.5400
 Critical Point Comp.: XC02 = 0.5400 XC6- = 0.3680 XC7+ = 0.0920

Calculated Tie Line Data (Equilibrium Compositions)

dXC02	Overall Mixture		Upper Phase		Lower Phase		Calc. MMC XC7+
	XC02	XC6- XC7+	XC02	XC6- XC7+	XC02	XC6- XC7+	
0.08	0.6200	0.2762 0.1038	0.6542	0.2765 0.0693	0.5911	0.2760 0.1329	0.6365
0.06	0.6000	0.2992 0.1008	0.6283	0.3000 0.0717	0.5765	0.2985 0.1250	0.6479
0.04	0.5800	0.3221 0.0979	0.6020	0.3233 0.0747	0.5621	0.3212 0.1167	0.6603
0.02	0.5600	0.3451 0.0949	0.5749	0.3463 0.0788	0.5484	0.3442 0.1074	0.6756
0.01	0.5500	0.3565 0.0935	0.5602	0.3575 0.0823	0.5420	0.3557 0.1023	0.6854
Initial	0.6300	0.2400 0.1300	0.6870	0.2404 0.0726	0.6159	0.2399 0.1442	---
CO2-C7+	0.9000	0.0000 0.1000	0.9522	0.0000 0.0478	0.7462	0.0000 0.2538	---

Data Sheet B-32

Reservoir Fluid: West Sussex
 Critical Conditions: 250°F 4177.2 psia
 MMC (XC7+): 0.7601

IOC: XC6- = 0.7000 XC7+ = 0.3000
 Critical CO2 Conc.: XC02 = 0.6670
 Critical Point Comp.: XC02 = 0.6670 XC6- = 0.2331 XC7+ = 0.0999

Calculated Tie Line Data (Equilibrium Compositions)

dXC02	Overall Mixture			Upper Phase			Lower Phase			Calc. MMC XC7+
	XC02	XC6-	XC7+	XC02	XC6-	XC7+	XC02	XC6-	XC7+	
0.08	0.7470	0.1408	0.1122	0.7852	0.1392	0.0756	0.7077	0.1424	0.1499	0.7401
0.06	0.7270	0.1639	0.1091	0.7594	0.1626	0.0780	0.6949	0.1651	0.1400	0.7420
0.04	0.7070	0.1869	0.1061	0.7329	0.1861	0.0810	0.6825	0.1877	0.1298	0.7457
0.02	0.6870	0.2100	0.1030	0.7050	0.2096	0.0854	0.6710	0.2104	0.1186	0.7514
0.01	0.6770	0.2216	0.1014	0.6896	0.2214	0.0890	0.6659	0.2217	0.1124	0.7559
Initial	0.7300	0.1600	0.1100	0.7635	0.1587	0.0778	0.6972	0.1612	0.1416	--
CO2-C7+	0.9000	0.0000	0.1000	0.9436	0.0000	0.0564	0.7755	0.0000	0.2245	--

Data Sheet B-33

Reservoir Fluid: Maljamar
 Critical Conditions: 100°F 2618.9 psia
 MMC (XC7+): 0.7685

IOC: XC6- = 0.9000 XC7+ = 0.1000
 Critical CO2 Conc.: XC02 = 0.4000
 Critical Point Comp.: XC02 = 0.4000 XC6- = 0.5400 XC7+ = 0.0600

Calculated Tie Line Data (Equilibrium Compositions)

dXC02	Overall Mixture			Upper Phase			Lower Phase			Calc. MMC XC7+
	XC02	XC6-	XC7+	XC02	XC6-	XC7+	XC02	XC6-	XC7+	
0.08	0.4800	0.4490	0.0710	0.4985	0.4557	0.0458	0.4713	0.4458	0.0829	0.6062
0.06	0.4600	0.4718	0.0682	0.4737	0.4779	0.0484	0.4509	0.4677	0.0814	0.6383
0.04	0.4400	0.4985	0.0655	0.4498	0.4999	0.0503	0.4325	0.4904	0.0711	0.6780
0.02	0.4200	0.5173	0.0627	0.4260	0.5211	0.0529	0.4144	0.5137	0.0719	0.7155
0.01	0.4100	0.5286	0.0614	0.4139	0.5314	0.0547	0.4058	0.5256	0.0686	0.7454
Initial	0.4500	0.4700	0.0800	0.4714	0.4807	0.0479	0.4447	0.4673	0.0880	--
CO2-C7+	0.9000	0.0000	0.1000	0.9679	0.0000	0.0321	0.7194	0.0000	0.2806	--

Data Sheet B-34

Reservoir Fluid: Maljamar
 Critical Conditions: 100°F 3003.9 psia
 MMC (XC7+): 0.7087

IOC: XC6- = 0.8000 XC7+ = 0.2000
 Critical CO2 Conc.: XC02 = 0.6170
 Critical Point Comp.: XC02 = 0.6170 XC6- = 0.3064 XC7+ = 0.0766

Calculated Tie Line Data (Equilibrium Compositions)

dXC02	Overall Mixture			Upper Phase			Lower Phase			Calc. MMC XC7+
	XC02	XC6-	XC7+	XC02	XC6-	XC7+	XC02	XC6-	XC7+	
0.08	0.6970	0.2073	0.0957	0.7424	0.2049	0.0527	0.6526	0.2097	0.1377	0.6602
0.06	0.6770	0.2321	0.0909	0.7141	0.2306	0.0553	0.6412	0.2336	0.1252	0.6681
0.04	0.6570	0.2568	0.0862	0.6853	0.2561	0.0586	0.6297	0.2575	0.1128	0.6787
0.02	0.6370	0.2816	0.0814	0.6553	0.2816	0.0631	0.6185	0.2817	0.0988	0.6921
0.01	0.6270	0.2940	0.0790	0.6391	0.2941	0.0668	0.6137	0.2939	0.0924	0.7002
Initial	0.6900	0.2100	0.1000	0.7383	0.2076	0.0541	0.6518	0.2119	0.1363	--
CO2-C7+	0.9000	0.0000	0.1000	0.9670	0.0000	0.0330	0.7276	0.0000	0.2724	--

Data Sheet B-35

Reservoir Fluid: **Maljamar**
 Critical Conditions: **100°F 3782.9 psia**
 MMC (XC7+): **0.7306**

IOC: **XC6- = 0.7000 XC7+ = 0.3000**
 Critical CO2 Conc.: **XC02 = 0.7130**
 Critical Point Comp.: **XC02 = 0.7130 XC6- = 0.2009 XC7+ = 0.0861**

Calculated Tie Line Data (Equilibrium Compositions)

dXC02	Overall Mixture		Upper Phase		Lower Phase		Calc. MMC XC7+
	XC02	XC6-	XC02	XC6-	XC02	XC6-	
0.08	0.7930	0.0924	0.8649	0.0870	0.7196	0.0981	0.7446
0.06	0.7730	0.1196	0.8339	0.1142	0.7127	0.1249	0.7360
0.04	0.7570	0.1467	0.8011	0.1421	0.7063	0.1512	0.7307
0.02	0.7370	0.1738	0.7656	0.1706	0.7015	0.1769	0.7288
0.01	0.7270	0.1874	0.7453	0.1852	0.7008	0.1895	0.7294
Initial	0.7800	0.1100	0.8450	0.1045	0.7151	0.1155	--
CO2-C7+	0.9000	0.0000	0.9661	0.0000	0.7393	0.0000	--

Data Sheet B-36

Reservoir Fluid: Maljamar
 Critical Conditions: 150°F 3232.2 psia
 MMC (XC7+): 0.7763

IOC: XC6- = 0.9000 XC7+ = 0.1000
 Critical CO2 Conc.: XC02 = 0.3600
 Critical Point Comp.: XC02 = 0.3600 XC6- = 0.5760 XC7+ = 0.0640

Calculated Tie Line Data (Equilibrium Compositions)

dXC02	Overall Mixture		Upper Phase		Lower Phase		Calc. MMC XC7+
	XC02	XC6- XC7+	XC02	XC6- XC7+	XC02	XC6- XC7+	
0.08	0.4400	0.4888 0.0712	0.4551	0.4970 0.0479	0.4287	0.4828 0.0885	0.6182
0.06	0.4200	0.5106 0.0694	0.4320	0.5182 0.0498	0.4103	0.5045 0.0852	0.6509
0.04	0.4000	0.5324 0.0676	0.4090	0.5390 0.0520	0.3923	0.5268 0.0809	0.6859
0.02	0.3800	0.5542 0.0658	0.3857	0.5591 0.0552	0.3746	0.5497 0.0757	0.7289
0.01	0.3700	0.5651 0.0649	0.3739	0.5687 0.0574	0.3660	0.5615 0.0725	0.7521
Initial	0.4500	0.4700 0.0800	0.4711	0.4808 0.0481	0.4388	0.4643 0.0969	--
CO2-C7+	0.9000	0.0000 0.1000	0.9633	0.0000 0.0367	0.7483	0.0000 0.2517	--

Data Sheet B-37

Reservoir Fluid: Maljamar
 Critical Conditions: 150°F 3615.9 psia
 MMC (XC7+): 0.7477

IOC: XC6- = 0.8000 XC7+ = 0.2000
 Critical CO2 Conc.: XC02 = 0.6150
 Critical Point Comp.: XC02 = 0.6150 XC6- = 0.3080 XC7+ = 0.0770

Calculated Tie Line Data (Equilibrium Compositions)

dXC02	Overall Mixture		Upper Phase			Lower Phase			Calc. MMC XC7+
	XC02	XC6-	XC02	XC6-	XC7+	XC02	XC6-	XC7+	
0.08	0.6950	0.2125	0.7307	0.2126	0.0567	0.6607	0.2124	0.1269	0.6932
0.06	0.6750	0.2364	0.7043	0.2369	0.0588	0.6470	0.2359	0.1171	0.7024
0.04	0.6550	0.2602	0.6774	0.2611	0.0615	0.6332	0.2594	0.1074	0.7165
0.02	0.6350	0.2841	0.6495	0.2850	0.0655	0.6198	0.2832	0.0970	0.7305
0.01	0.6250	0.2961	0.6347	0.2968	0.0685	0.6139	0.2952	0.0909	0.7387
Initial	0.6900	0.2100	0.7314	0.2102	0.0584	0.6627	0.2099	0.1274	---
CO2-C7+	0.9000	0.0000	0.9600	0.0000	0.0400	0.7636	0.0000	0.2364	---

Data Sheet B-38

Reservoir Fluid: Maljamar
 Critical Conditions: 150°F 3989.3 psia
 MMC (XC7+): 0.7814

IOC: XC6- = 0.7000 XC7+ = 0.3000
 Critical CO2 Conc.: XC02 = 0.7130
 Critical Point Comp.: XC02 = 0.7130 XC6- = 0.2009 XC7+ = 0.0861

Calculated Tie Line Data (Equilibrium Compositions)

dXC02	Overall Mixture		Upper Phase		Lower Phase		Calc. MMC XC7+			
	XC02	XC6-	XC02	XC6-	XC02	XC6-				
0.08	0.7930	0.0997	0.1073	0.8458	0.0975	0.0567	0.7403	0.1018	0.1579	0.7701
0.06	0.7730	0.1250	0.1020	0.8172	0.1231	0.0597	0.7297	0.1268	0.1435	0.7690
0.04	0.7530	0.1503	0.0967	0.7875	0.1489	0.0636	0.7193	0.1516	0.1291	0.7704
0.02	0.7330	0.1756	0.0914	0.7560	0.1748	0.0692	0.7099	0.1764	0.1137	0.7743
0.01	0.7230	0.1883	0.0887	0.7385	0.1878	0.0737	0.7064	0.1888	0.1048	0.7778
Initial	0.7800	0.1100	0.1100	0.8330	0.1079	0.0591	0.7370	0.1117	0.1513	--
CO2-C7+	0.9000	0.0000	0.1000	0.9573	0.0000	0.0427	0.7762	0.0000	0.2238	--

Data Sheet B-39

Reservoir Fluid: Maljamar
 Critical Conditions: 200°F 3626.2 psia
 MMC (XC7+): 0.7789

IOC: XC6- = 0.9000 XC7+ = 0.1000
 Critical CO2 Conc.: XC02 = 0.3000
 Critical Point Comp.: XC02 = 0.3000 XC6- = 0.6300 XC7+ = 0.0700

Calculated Tie Line Data (Equilibrium Compositions)

dXC02	Overall Mixture			Upper Phase			Lower Phase			Calc. MMC XC7+
	XC02	XC6-	XC7+	XC02	XC6-	XC7+	XC02	XC6-	XC7+	
0.08	0.3800	0.5395	0.0805	0.3967	0.5528	0.0505	0.3701	0.5316	0.0983	0.6094
0.06	0.3600	0.5621	0.0779	0.3728	0.5739	0.0533	0.3509	0.5537	0.0954	0.6467
0.04	0.3400	0.5847	0.0753	0.3494	0.5946	0.0560	0.3327	0.5769	0.0904	0.6880
0.02	0.3200	0.6074	0.0726	0.3259	0.6145	0.0596	0.3148	0.6012	0.0840	0.7295
0.01	0.3100	0.6187	0.0713	0.3139	0.6237	0.0624	0.3062	0.6138	0.0800	0.7577
Initial	0.3500	0.5600	0.0900	0.3684	0.5783	0.0533	0.3442	0.5543	0.1015	---
CO2-C7+	0.9000	0.0000	0.1000	0.9622	0.0000	0.0378	0.7541	0.0000	0.2459	---

Data Sheet B-40

Reservoir Fluid: Maljamar
 Critical Conditions: 200°F 4077.2 psia
 MMC (XC7+): 0.7782

IOC: XC6- = 0.8000 XC7+ = 0.2000
 Critical CO2 Conc.: XC02 = 0.5980
 Critical Point Comp.: XC02 = 0.5980 XC6- = 0.3216 XC7+ = 0.0804

Calculated Tie Line Data (Equilibrium Compositions)

dXC02	Overall Mixture		Upper Phase		Lower Phase		Calc. MMC XC7+
	XC02	XC6-	XC02	XC6-	XC02	XC6-	
0.08	0.6780	0.2296	0.7087	0.2313	0.6485	0.2278	0.7131
0.06	0.6580	0.2526	0.6834	0.2545	0.6336	0.2506	0.7255
0.04	0.6380	0.2756	0.6577	0.2777	0.6188	0.2736	0.7410
0.02	0.6180	0.2986	0.6310	0.3003	0.6045	0.2968	0.7574
0.01	0.6080	0.3101	0.6169	0.3114	0.5982	0.3086	0.7683
Initial	0.6900	0.2100	0.7283	0.2118	0.6613	0.2087	--
CO2-C7+	0.9000	0.0000	0.9555	0.0000	0.7813	0.0000	0.2187

Data Sheet B-41

Reservoir Fluid: Maljamar
 Critical Conditions: 200°F 4361.0 psia
 MMC (XC7+): 0.8130
 IOC: XC6- = 0.7000 XC7+ = 0.3000
 Critical CO2 Conc.: XC02 = 0.7070
 Critical Point Comp.: XC02 = 0.7070 XC6- = 0.2051 XC7+ = 0.0879

Calculated Tie Line Data (Equilibrium Compositions)

dXC02	Overall Mixture			Upper Phase			Lower Phase			Calc. MMC XC7+
	XC02	XC6-	XC7+	XC02	XC6-	XC7+	XC02	XC6-	XC7+	
0.08	0.7870	0.1089	0.1041	0.8296	0.1084	0.0620	0.7450	0.1094	0.1456	0.7865
0.06	0.7670	0.1329	0.1001	0.8026	0.1327	0.0647	0.7323	0.1332	0.1345	0.7898
0.04	0.7470	0.1570	0.0960	0.7749	0.1570	0.0681	0.7198	0.1570	0.1232	0.7954
0.02	0.7270	0.1811	0.0919	0.7457	0.1813	0.0730	0.7081	0.1808	0.1111	0.8033
0.01	0.7170	0.1931	0.0899	0.7297	0.1933	0.0770	0.7033	0.1929	0.1038	0.8077
Initial	0.7800	0.1100	0.1100	0.8264	0.1095	0.0641	0.7458	0.1103	0.1439	---
CO2-C7+	0.9000	0.0000	0.1000	0.9513	0.0000	0.0487	0.7966	0.0000	0.2034	---

Data Sheet B-42

Reservoir Fluid: Maljamar
 Critical Conditions: 250°F 3823.4 psia
 MMC (XC7+): 0.7697

IOC: XC6- = 0.9000 XC7+ = 0.1000
 Critical CO2 Conc.: XC02 = 0.2250
 Critical Point Comp.: XC02 = 0.2250 XC6- = 0.6975 XC7+ = 0.0775

Calculated Tie Line Data (Equilibrium Compositions)

dXC02	Overall Mixture			Upper Phase			Lower Phase			Calc. MMC XC7+
	XC02	XC6-	XC7+	XC02	XC6-	XC7+	XC02	XC6-	XC7+	
0.08	0.3050	0.6129	0.0821	0.3164	0.6270	0.0566	0.2938	0.5990	0.1072	0.5813
0.06	0.2850	0.6341	0.0809	0.2941	0.6469	0.0590	0.2759	0.6212	0.1029	0.6202
0.04	0.2650	0.6552	0.0798	0.2718	0.6662	0.0620	0.2580	0.6439	0.0981	0.6661
0.02	0.2450	0.6764	0.0786	0.2494	0.6844	0.0662	0.2404	0.6679	0.0917	0.7150
0.01	0.2350	0.6869	0.0781	0.2380	0.6928	0.0692	0.2317	0.6805	0.0878	0.7418
Initial	0.2800	0.6300	0.0900	0.2934	0.6492	0.0574	0.2741	0.6216	0.1043	---
CO2-C7+	0.9000	0.0000	0.1000	0.9624	0.0000	0.0376	0.7408	0.0000	0.2592	---

Data Sheet B-43

Reservoir Fluid: Maljamar
 Critical Conditions: 250°F 4370.9 psia
 MMC (XC7+): 0.7925

IOC: XC6- = 0.8000 XC7+ = 0.2000
 Critical CO2 Conc.: XC02 = 0.5700
 Critical Point Comp.: XC02 = 0.5700 XC6- = 0.3439 XC7+ = 0.0861

Calculated Tie Line Data (Equilibrium Compositions)

dXC02	Overall Mixture			Upper Phase			Lower Phase			Calc. MMC XC7+
	XC02	XC6-	XC7+	XC02	XC6-	XC7+	XC02	XC6-	XC7+	
0.08	0.6500	0.2541	0.0959	0.6787	0.2575	0.0638	0.6225	0.2508	0.1267	0.7234
0.06	0.6300	0.2766	0.0934	0.6538	0.2799	0.0663	0.6067	0.2732	0.1201	0.7370
0.04	0.6100	0.2990	0.0910	0.6286	0.3022	0.0692	0.5915	0.2959	0.1126	0.7529
0.02	0.5900	0.3215	0.0885	0.6025	0.3240	0.0735	0.5771	0.3189	0.1040	0.7714
0.01	0.5800	0.3327	0.0873	0.5887	0.3346	0.0767	0.5706	0.3306	0.0988	0.7817
Initial	0.6900	0.2100	0.1000	0.7266	0.2128	0.0606	0.6520	0.2071	0.1409	---
CO2-C7+	0.9000	0.0000	0.1000	0.9530	0.0000	0.0470	0.7831	0.0000	0.2169	---

Data Sheet B-44

Reservoir Fluid: Maljamar
 Critical Conditions: 250°F 4646.5 psia
 MMC (XC7+): 0.8321

IOC: XC6- = 0.7000 XC7+ = 0.3000
 Critical CO2 Conc.: XC02 = 0.6940
 Critical Point Comp.: XC02 = 0.6940 XC6- = 0.2142 XC7+ = 0.0918

Calculated Tie Line Data (Equilibrium Compositions)

dXC02	Overall Mixture			Upper Phase			Lower Phase			Calc. MMC XC7+
	XC02	XC6-	XC7+	XC02	XC6-	XC7+	XC02	XC6-	XC7+	
0.08	0.7740	0.1209	0.1051	0.8117	0.1215	0.0668	0.7367	0.1203	0.1430	0.7962
0.06	0.7540	0.1442	0.1018	0.7856	0.1450	0.0694	0.7229	0.1435	0.1336	0.8029
0.04	0.7340	0.1675	0.0985	0.7589	0.1685	0.0726	0.7093	0.1666	0.1241	0.8113
0.02	0.7140	0.1909	0.0951	0.6967	0.1900	0.1133	0.7307	0.1917	0.0776	0.8215
0.01	0.7040	0.2025	0.0935	0.7155	0.2032	0.0813	0.6914	0.2018	0.1068	0.8261
Initial	0.7800	0.1100	0.1100	0.8226	0.1105	0.0669	0.7440	0.1096	0.1464	--
CO2-C7+	0.9000	0.0000	0.1000	0.9473	0.0000	0.0527	0.8029	0.0000	0.1971	--

Data Sheet B-45

Reservoir Fluid: Reservoir D
 Critical Conditions: 100°F 1893.5 psia
 MMC (XC7+): 0.4947

IOC: XC6- = 0.9500 XC7+ = 0.0500
 Critical CO2 Conc.: XC02 = 0.3700
 Critical Point Comp.: XC02 = 0.3700 XC6- = 0.5985 XC7+ = 0.0315

Calculated Tie Line Data (Equilibrium Compositions)

dXC02	Overall Mixture		Upper Phase		Lower Phase		Calc. MMC XC7+
	XC02	XC6-	XC02	XC6-	XC02	XC6-	
0.08	0.4500	0.5033	0.4818	0.5065	0.4202	0.5002	0.4393
0.06	0.4300	0.5271	0.4562	0.5306	0.4052	0.5238	0.4508
0.04	0.4100	0.5509	0.4303	0.5542	0.3905	0.5477	0.4619
0.02	0.3900	0.5747	0.3891	0.5887	0.3704	0.5844	0.4866
0.01	0.7040	0.2025	0.7155	0.2032	0.6914	0.2018	0.8261
Initial	0.4500	0.5000	0.4853	0.5039	0.4197	0.4967	---
CO2-C7+	0.9000	0.0000	0.9901	0.0000	0.6858	0.0000	0.3142

Data Sheet B-46

Reservoir Fluid: Reservoir D
 Critical Conditions: 100°F 2281.7 psia
 MMC (XC7+): 0.5803

IOC: XC6- = 0.9000 XC7+ = 0.1000
 Critical CO2 Conc.: XC02 = 0.5380
 Critical Point Comp.: XC02 = 0.5380 XC6- = 0.4158 XC7+ = 0.0462

Calculated Tie Line Data (Equilibrium Compositions)

dXC02	Overall Mixture			Upper Phase			Lower Phase			Calc. MMC XC7+
	XC02	XC6-	XC7+	XC02	XC6-	XC7+	XC02	XC6-	XC7+	
0.08	0.6180	0.3157	0.0663	0.6658	0.3122	0.0220	0.5724	0.3191	0.1085	0.5445
0.06	0.5980	0.3407	0.0613	0.6379	0.3383	0.0283	0.5602	0.3430	0.0968	0.5517
0.04	0.5780	0.3658	0.0562	0.6094	0.3643	0.0263	0.5487	0.3671	0.0842	0.5594
0.02	0.5580	0.3908	0.0512	0.5789	0.3902	0.0309	0.5375	0.3914	0.0711	0.5686
0.01	0.5480	0.4033	0.0487	0.5622	0.4030	0.0348	0.5332	0.4035	0.0633	0.5749
Initial	0.6100	0.3200	0.0700	0.6621	0.3167	0.0212	0.5676	0.3226	0.1098	---
CO2-C7+	0.9000	0.0000	0.1000	0.9877	0.0000	0.0123	0.7010	0.0000	0.2990	---

Data Sheet B-47

Reservoir Fluid: Reservoir D
 Critical Conditions: 100°F 2889.6 psia
 MMC (XC7+): 0.6495

IOC: XC6- = 0.8000 XC7+ = 0.2000
 Critical CO2 Conc.: XC02 = 0.6810
 Critical Point Comp.: XC02 = 0.6810 XC6- = 0.2552 XC7+ = 0.0638

Calculated Tie Line Data (Equilibrium Compositions)

dXC02	Overall Mixture		Upper Phase		Lower Phase		Calc. MMC XC7+
	XC02	XC6- XC7+	XC02	XC6- XC7+	XC02	XC6- XC7+	
0.08	0.7610	0.1416 0.0974	0.8427	0.1321 0.0252	0.6818	0.1508 0.1674	0.6658
0.06	0.7410	0.1700 0.0890	0.8103	0.1612 0.0285	0.6750	0.1784 0.1466	0.6580
0.04	0.7210	0.1984 0.0806	0.7760	0.1909 0.0331	0.6690	0.2055 0.1255	0.6521
0.02	0.7010	0.2268 0.0722	0.7385	0.2215 0.0400	0.6652	0.2322 0.1026	0.6489
0.01	0.6910	0.2410 0.0680	0.7168	0.2374 0.0458	0.6654	0.2446 0.0900	0.6494
Initial	0.7200	0.1800 0.1000	0.8012	0.1702 0.0286	0.6693	0.1862 0.1445	--
CO2-C7+	0.9000	0.0000 0.1000	0.9853	0.0000 0.0147	0.7183	0.0000 0.2817	--

Data Sheet B-48

Reservoir Fluid: Reservoir D
 Critical Conditions: 100°F 3931.3 psia
 MMC (XC7+): 0.6993

IOC: XC6- = 0.7000 XC7+ = 0.3000
 Critical CO2 Conc.: XC02 = 0.7585
 Critical Point Comp.: XC02 = 0.7585 XC6- = 0.1691 XC7+ = 0.0724

Calculated Tie Line Data (Equilibrium Compositions)

dXC02	Overall Mixture			Upper Phase			Lower Phase			Calc. MMC XC7+
	XC02	XC6-	XC7+	XC02	XC6-	XC7+	XC02	XC6-	XC7+	
0.08	0.8385	0.0432	0.1183	0.9419	0.0371	0.0210	0.7309	0.0495	0.2196	0.7867
0.06	0.8185	0.0746	0.1669	0.9086	0.0661	0.0253	0.7275	0.0832	0.1893	0.7593
0.04	0.7985	0.1061	0.0954	0.8720	0.0969	0.0311	0.7259	0.1152	0.1589	0.7357
0.02	0.7785	0.1376	0.0839	0.8299	0.1298	0.0403	0.7281	0.1452	0.1267	0.7156
0.01	0.7685	0.1533	0.0782	0.8044	0.1475	0.0481	0.7328	0.1592	0.1080	0.7070
Initial	0.8200	0.0800	0.1000	0.9021	0.0717	0.0263	0.7274	0.0894	0.1832	---
CO2-C7+	0.9000	0.0000	0.1000	0.9834	0.0000	0.0166	0.7372	0.0000	0.2628	---

Data Sheet B-49

Reservoir Fluid: Reservoir D
 Critical Conditions: 150°F 2399.4 psia
 MMC (XC7+): 0.5046

IOC: XC6- = 0.9500 XC7+ = 0.0500
 Critical CO2 Conc.: XC02 = 0.2600
 Critical Point Comp.: XC02 = 0.2600 XC6- = 0.7030 XC7+ = 0.0370

Calculated Tie Line Data (Equilibrium Compositions)

dXC02	Overall Mixture			Upper Phase			Lower Phase			Calc. MMC XC7+
	XC02	XC6-	XC7+	XC02	XC6-	XC7+	XC02	XC6-	XC7+	
0.08	0.3400	0.6082	0.0518	0.3663	0.6199	0.0138	0.3165	0.5978	0.0857	0.4124
0.06	0.3200	0.6319	0.0481	0.3413	0.6429	0.0158	0.3006	0.6219	0.0775	0.4312
0.04	0.3000	0.6556	0.0444	0.3162	0.6652	0.0186	0.2850	0.6467	0.0683	0.4512
0.02	0.2800	0.6793	0.0407	0.2906	0.6866	0.0228	0.2699	0.6724	0.0577	0.4754
0.01	0.2700	0.6912	0.0388	0.2771	0.6964	0.0265	0.2630	0.6859	0.0511	0.4906
Initial	0.3500	0.5900	0.0600	0.3839	0.6046	0.0115	0.3240	0.5788	0.0972	---
CO2-C7+	0.9000	0.0000	0.1000	0.9921	0.0000	0.0079	0.6896	0.0000	0.3104	---

Data Sheet B-50

Reservoir Fluid: Reservoir D
 Critical Conditions: 150°F 2925.6 psia
 MMC (X_{C7+}): 0.6072

IOC: X_{C6-} = 0.9000 X_{C7+} = 0.1000
 Critical CO₂ Conc.: X_{CO2} = 0.5040
 Critical Point Comp.: X_{CO2} = 0.5040 X_{C6-} = 0.4464 X_{C7+} = 0.0496

Calculated Tie Line Data (Equilibrium Compositions)

dX _{CO2}	Overall Mixture		Upper Phase		Lower Phase		Calc. MMC X _{C7+}
	X _{CO2}	X _{C6-}	X _{CO2}	X _{C6-}	X _{CO2}	X _{C6-}	
0.08	0.5840	0.3512	0.6239	0.3517	0.5448	0.3507	0.5600
0.06	0.5640	0.3750	0.5973	0.3760	0.5312	0.3740	0.5689
0.04	0.5440	0.3988	0.5704	0.4002	0.5185	0.3976	0.5789
0.02	0.5240	0.4226	0.5416	0.4239	0.5060	0.4213	0.5904
0.01	0.5140	0.4345	0.5260	0.4356	0.5010	0.4333	0.6000
Initial	0.6100	0.3200	0.6581	0.3196	0.5624	0.3204	--
CO ₂ -C ₇₊	0.9000	0.0000	0.9858	0.0000	0.7261	0.0000	--

Data Sheet B-51

Reservoir Fluid: Reservoir D
 Critical Conditions: 150°F 3450.0 psia
 MMC (XC7+): 0.6921

IOC: XC6- = 0.8000 XC7+ = 0.2000
 Critical CO2 Conc.: XC02 = 0.6770
 Critical Point Comp.: XC02 = 0.6770 XC6- = 0.2584 XC7+ = 0.0646

Calculated Tie Line Data (Equilibrium Compositions)

dXC02	Overall Mixture		Upper Phase		Lower Phase		Calc. MMC XC7+
	XC02	XC6- XC7+	XC02	XC6- XC7+	XC02	XC6- XC7+	
0.08	0.7570	0.1521 0.0909	0.8228	0.1472 0.0300	0.6951	0.1568 0.1481	0.6943
0.06	0.7370	0.1787 0.0843	0.7926	0.1743 0.0331	0.6851	0.1828 0.1321	0.6879
0.04	0.7170	0.2053 0.0777	0.7611	0.2017 0.0372	0.6758	0.2086 0.1156	0.6874
0.02	0.6970	0.2318 0.0712	0.7270	0.2295 0.0435	0.6683	0.2341 0.0976	0.6886
0.01	0.6870	0.2451 0.0679	0.7076	0.2435 0.0489	0.6663	0.2467 0.0870	0.6891
Initial	0.7200	0.1800 0.1000	0.7936	0.1750 0.0314	0.6802	0.1827 0.1371	--
CO2-C7+	0.9000	0.0000 0.1000	0.9803	0.0000 0.0197	0.7530	0.0000 0.2470	--

Data Sheet B-52

Reservoir Fluid: Reservoir D
 Critical Conditions: 150°F 3927.8 psia
 MMC (X_{C7+}): 0.7514

IOC: X_{C6-} = 0.7000 X_{C7+} = 0.3000
 Critical CO₂ Conc.: X_{CO2} = 0.7555
 Critical Point Comp.: X_{CO2} = 0.7555 X_{C6-} = 0.1712 X_{C7+} = 0.0733

Calculated Tie Line Data (Equilibrium Compositions)

dX _{CO2}	Overall Mixture		Upper Phase		Lower Phase		Calc. MMC X _{C7+}
	X _{CO2}	X _{C6-} X _{C7+}	X _{CO2}	X _{C6-} X _{C7+}	X _{CO2}	X _{C6-} X _{C7+}	
0.08	0.8355	0.0594 0.1051	0.9144	0.0555 0.0301	0.7555	0.0634 0.1811	0.7910
0.06	0.8155	0.0873 0.0972	0.8832	0.0827 0.0060	0.7483	0.0919 0.1598	0.7774
0.04	0.7955	0.1153 0.0892	0.8499	0.1108 0.0393	0.7421	0.1197 0.1382	0.7661
0.02	0.7755	0.1432 0.0813	0.8131	0.1397 0.0472	0.7385	0.1467 0.1148	0.7575
0.01	0.7655	0.1572 0.0773	0.7916	0.1546 0.0538	0.7390	0.1598 0.1012	0.7542
Initial	0.8200	0.0800 0.1000	0.8916	0.0755 0.0329	0.7500	0.0844 0.1656	--
CO ₂ -C ₇₊	0.9000	0.0000 0.1000	0.9760	0.0000 0.0240	0.7725	0.0000 0.2275	--

Data Sheet B-53

Reservoir Fluid: Reservoir D
 Critical Conditions: 200°F 2631.7 psia
 MMC (X_{C7+}): 0.5053

IOC: X_{C6-} = 0.9500 X_{C7+} = 0.0500
 Critical CO₂ Concn.: X_{CO2} = 0.1250
 Critical Point Comp.: X_{CO2} = 0.1250 X_{C6-} = 0.8313 X_{C7+} = 0.0437

Calculated Tie Line Data (Equilibrium Compositions)

dX _{CO2}	Overall Mixture			Upper Phase			Lower Phase			Calc. MMC X _{C7+}
	X _{CO2}	X _{C6-}	X _{C7+}	X _{CO2}	X _{C6-}	X _{C7+}	X _{CO2}	X _{C6-}	X _{C7+}	
0.08	0.2050	0.7361	0.0589	0.2227	0.7601	0.0172	0.1894	0.7150	0.0956	0.3380
0.06	0.1850	0.7599	0.0551	0.1987	0.7817	0.0196	0.1727	0.7404	0.0869	0.3673
0.04	0.1650	0.7837	0.0513	0.1749	0.8023	0.0228	0.1559	0.7667	0.0774	0.4029
0.02	0.1450	0.8075	0.0475	0.1510	0.8211	0.0279	0.1393	0.7947	0.0660	0.4507
0.01	0.1350	0.8194	0.0456	0.1389	0.8290	0.0321	0.1311	0.8098	0.0591	0.4764
Initial	0.2200	0.7100	0.0700	0.2451	0.7410	0.0140	0.2017	0.6874	0.1109	--
CO ₂ -C ₇₊	0.9000	0.0000	0.1000	0.9942	0.0000	0.0058	0.6593	0.0000	0.3407	--

Data Sheet B-54

Reservoir Fluid: Reservoir D
 Critical Conditions: 200°F 3335.1 psia
 MMC (XC7+): 0.6208

IOC: XC6- = 0.9000 XC7+ = 0.1000
 Critical CO2 Conc.: XC02 = 0.4500
 Critical Point Comp.: XC02 = 0.4500 XC6- = 0.4950 XC7+ = 0.0550

Calculated Tie Line Data (Equilibrium Compositions)

dXC02	Overall Mixture		Upper Phase		Lower Phase		Calc. MMC XC7+
	XC02	XC6-	XC02	XC6-	XC02	XC6-	
0.08	0.5300	0.3987	0.5695	0.4038	0.4945	0.3942	0.5626
0.06	0.5100	0.4228	0.5428	0.4279	0.4800	0.4182	0.5745
0.04	0.4900	0.4469	0.5155	0.4516	0.4661	0.4425	0.5879
0.02	0.4700	0.4709	0.4870	0.4747	0.4533	0.4673	0.6038
0.01	0.4600	0.4830	0.4715	0.4857	0.4479	0.4801	0.6118
Initial	0.5200	0.4000	0.5679	0.4071	0.4881	0.3952	—
CO2-C7+	0.9000	0.0000	0.9857	0.0000	0.7273	0.0000	—

Data Sheet B-55

Reservoir Fluid: Reservoir D
 Critical Conditions: 200°F 3897.7 psia
 MMC (XC7+): 0.7211

IOC: XC6- = 0.8000 XC7+ = 0.2000
 Critical CO₂ Conc.: XC02 = 0.6625
 Critical Point Comp.: XC02 = 0.6625 XC6- = 0.2700 XC7+ = 0.0675

Calculated Tie Line Data (Equilibrium Compositions)

dXC02	Overall Mixture			Upper Phase			Lower Phase			Calc. MMC XC7+
	XC02	XC6-	XC7+	XC02	XC6-	XC7+	XC02	XC6-	XC7+	
0.08	0.7425	0.1691	0.0884	0.7992	0.1669	0.0339	0.6889	0.1712	0.1399	0.7042
0.06	0.7225	0.1943	0.0832	0.7704	0.1926	0.0370	0.6773	0.1960	0.1267	0.7057
0.04	0.7025	0.2195	0.0780	0.7405	0.2183	0.0412	0.6664	0.2207	0.1129	0.7087
0.02	0.6825	0.2448	0.0727	0.7083	0.2442	0.0475	0.6571	0.2454	0.0975	0.7145
0.01	0.6725	0.2574	0.0701	0.6902	0.2570	0.0528	0.6540	0.2577	0.0883	0.7172
Initial	0.7200	0.1800	0.1000	0.7883	0.1781	0.0337	0.6800	0.1812	0.1388	--
CO ₂ -C7+	0.9000	0.0000	0.1000	0.9772	0.0000	0.0228	0.7687	0.0000	0.2313	--

Data Sheet B-56

Reservoir Fluid: Reservoir D
 Critical Conditions: 200°F 4257.4 psia
 MMC (XC7+): 0.7831

IOC: XC6- = 0.7000 XC7+ = 0.3000
 Critical CO₂ Conc.: XC02 = 0.7500
 Critical Point Comp.: XC02 = 0.7500 XC6- = 0.1750 XC7+ = 0.0750

Calculated Tie Line Data (Equilibrium Compositions)

dXC02	Overall Mixture		Upper Phase		Lower Phase		Calc. MMC XC7+
	XC02	XC6-	XC02	XC6-	XC02	XC6-	
0.08	0.8300	0.0706	0.8960	0.0682	0.7640	0.0730	0.7979
0.06	0.8100	0.0967	0.8663	0.0942	0.7544	0.0992	0.7914
0.04	0.7900	0.1228	0.8351	0.1205	0.7457	0.1251	0.7867
0.02	0.7700	0.1489	0.8011	0.1472	0.7390	0.1506	0.7838
0.01	0.7600	0.1620	0.7815	0.1608	0.7376	0.1632	0.7833
Initial	0.8200	0.0800	0.8856	0.0775	0.7602	0.0823	---
CO ₂ -C7+	0.9000	0.0000	0.9712	0.0000	0.7916	0.0000	0.2084

Data Sheet B-57

Reservoir Fluid: Reservoir D
 Critical Conditions: 2500F 2900.1 psia
 MMC (XC7+): 0.5377

IOC: XC6- = 0.9400 XC7+ = 0.0600
 Critical CO2 Conc.: XC02 = 0.0850
 Critical Point Comp.: XC02 = 0.0850 XC6- = 0.8601 XC7+ = 0.0549

Calculated Tie Line Data (Equilibrium Compositions)

dXC02	Overall Mixture		Upper Phase		Lower Phase		Calc. MMC XC7+
	XC02	XC6- XC7+	XC02 XC6- XC7+	XC02 XC6- XC7+	XC02 XC6- XC7+	XC02 XC6- XC7+	
0.08	0.1650	0.7675 0.0675	0.1788 0.7957 0.0255	0.1520 0.7410 0.1070	0.3134		
0.06	0.1450	0.7907 0.0643	0.1554 0.8162 0.0284	0.1350 0.7662 0.0988	0.3482		
0.04	0.1250	0.8138 0.0612	0.1323 0.8355 0.0322	0.1179 0.7928 0.0893	0.3920		
0.02	0.1050	0.8370 0.0580	0.1093 0.8528 0.0379	0.1007 0.8211 0.0782	0.4532		
0.01	0.0950	0.8485 0.0565	0.0977 0.8599 0.0424	0.0922 0.8367 0.0711	0.4978		
Initial	0.1600	0.7700 0.0700	0.1743 0.8007 0.0250	0.1477 0.7436 0.1087	---		
CO2-C7+	0.9000	0.0000 0.1000	0.9928 0.0000 0.0072	0.6415 0.0000 0.3585	---		

Data Sheet B-58

Reservoir Fluid: Reservoir D
 Critical Conditions: 250°F 3273.2 psia
 MMC (XC7+): 0.5963

IOC: XC6- = 0.9200 XC7+ = 0.0800
 Critical CO2 Conc.: XC02 = 0.2600
 Critical Point Comp.: XC02 = 0.2600 XC6- = 0.6808 XC7+ = 0.0592

Calculated Tie Line Data (Equilibrium Compositions)

dXC02	Overall Mixture		Upper Phase		Lower Phase		Calc. MMC XC7+
	XC02	XC6- XC7+	XC02	XC6- XC7+	XC02	XC6- XC7+	
0.08	0.3400	0.5878 0.0722	0.3665	0.6046 0.0289	0.3155	0.5725 0.1120	0.4829
0.06	0.3200	0.6111 0.0689	0.3414	0.6264 0.0322	0.2996	0.5965 0.1039	0.5052
0.04	0.3000	0.6343 0.0657	0.3163	0.6477 0.0360	0.2843	0.6215 0.0942	0.5321
0.02	0.2800	0.6576 0.0624	0.2907	0.6675 0.0418	0.2694	0.6477 0.0829	0.5609
0.01	0.2700	0.6692 0.0608	0.2772	0.6764 0.0464	0.2625	0.6617 0.0758	0.5792
Initial	0.3500	0.5700 0.0800	0.3837	0.5901 0.0262	0.3234	0.5541 0.1225	--
CO2-C7+	0.9000	0.0000 0.1000	0.9890	0.0000 0.0110	0.6838	0.0000 0.3162	--

Data Sheet B-59

Reservoir Fluid: Reservoir D
 Critical Conditions: 250°F 3528.5 psia
 MMC (XC7+): 0.6324

IOC: XC6- = 0.9000 XC7+ = 0.1000
 Critical CO2 Conc.: XC02 = 0.3770
 Critical Point Comp.: XC02 = 0.3770 XC6- = 0.5607 XC7+ = 0.0623

Calculated Tie Line Data (Equilibrium Compositions)

dXC02	Overall Mixture		Upper Phase		Lower Phase		Calc. MMC XC7+
	XC02	XC6-	XC02	XC6-	XC02	XC6-	
0.08	0.4570	0.4656	0.4925	0.4762	0.4251	0.4561	0.5517
0.06	0.4370	0.4894	0.4662	0.4994	0.4100	0.4801	0.5688
0.04	0.4170	0.5132	0.4396	0.5220	0.3956	0.5048	0.5867
0.02	0.3970	0.5369	0.4120	0.5436	0.3822	0.5303	0.6076
0.01	0.3870	0.5488	0.3971	0.5537	0.3763	0.5437	0.6206
Initial	0.4600	0.4500	0.5078	0.4642	0.4285	0.4406	--
CO2-C7+	0.9000	0.0000	0.9858	0.0000	0.7099	0.0000	0.2901

Data Sheet B-60

Reservoir Fluid: Reservoir D
 Critical Conditions: 250°F 4176.9 psia
 MMC (XC7+): 0.7363

IOC: XC6- = 0.8000 XC7+ = 0.2000
 Critical CO2 Conc.: XC02 = 0.6360
 Critical Point Comp.: XC02 = 0.6360 XC6- = 0.2912 XC7+ = 0.0728

Calculated Tie Line Data (Equilibrium Compositions)

dXC02	Overall Mixture			Upper Phase			Lower Phase			Calc. MMC XC7+
	XC02	XC6-	XC7+	XC02	XC6-	XC7+	XC02	XC6-	XC7+	
0.08	0.7160	0.1942	0.0898	0.7673	0.1942	0.0385	0.6661	0.1942	0.1397	0.7093
0.06	0.6960	0.2185	0.0855	0.7394	0.2189	0.0417	0.6538	0.2181	0.1281	0.7149
0.04	0.6760	0.2427	0.0813	0.7105	0.2433	0.0462	0.6423	0.2421	0.1156	0.7201
0.02	0.6560	0.2669	0.0771	0.6795	0.2677	0.0528	0.6322	0.2662	0.1016	0.7290
0.01	0.6460	0.2791	0.0749	0.6622	0.2797	0.0581	0.6287	0.2785	0.0928	0.7316
Initial	0.7200	0.1800	0.1000	0.7838	0.1801	0.0361	0.6716	0.1799	0.1485	---
CO2-C7+	0.9000	0.0000	0.1000	0.9751	0.0000	0.0249	0.7688	0.0000	0.2312	---

Data Sheet B-61

Reservoir Fluid: Reservoir D
 Critical Conditions: 250°F 4517.0 psia
 MMC (X_{C7+}): 0.8033

IOC: X_{C6-}= 0.7000 X_{C7+}= 0.3000
 Critical CO₂ Conc.: X_{CO2}= 0.7370
 Critical Point Comp.: X_{CO2}= 0.7370 X_{C6-}= 0.1841 X_{C7+}= 0.0789

Calculated Tie Line Data (Equilibrium Compositions)

dX _{CO2}	Overall Mixture			Upper Phase			Lower Phase			Calc. MMC X _{C7+}
	X _{CO2}	X _{C6-}	X _{C7+}	X _{CO2}	X _{C6-}	X _{C7+}	X _{CO2}	X _{C6-}	X _{C7+}	
0.08	0.8170	0.0842	0.0988	0.8764	0.0829	0.0407	0.7577	0.0854	0.1569	0.8005
0.06	0.7970	0.1091	0.0939	0.8476	0.1080	0.0444	0.7469	0.1103	0.1428	0.7990
0.04	0.7770	0.1341	0.0889	0.8175	0.1332	0.0493	0.7369	0.1350	0.1281	0.7989
0.02	0.7570	0.1591	0.0839	0.7849	0.1585	0.0566	0.7287	0.1597	0.1116	0.8003
0.01	0.7470	0.1716	0.0814	0.7663	0.1712	0.0625	0.7265	0.1720	0.1015	0.8017
Initial	0.8200	0.0800	0.1000	0.8811	0.0788	0.0402	0.7596	0.0812	0.1592	--
CO ₂ -C ₇₊	0.9000	0.0000	0.1000	0.9678	0.0000	0.0322	0.7967	0.0000	0.2033	--